Institute of Physics

CLRC

SCMP
@
IoP

PCG

PCG
@
BCA

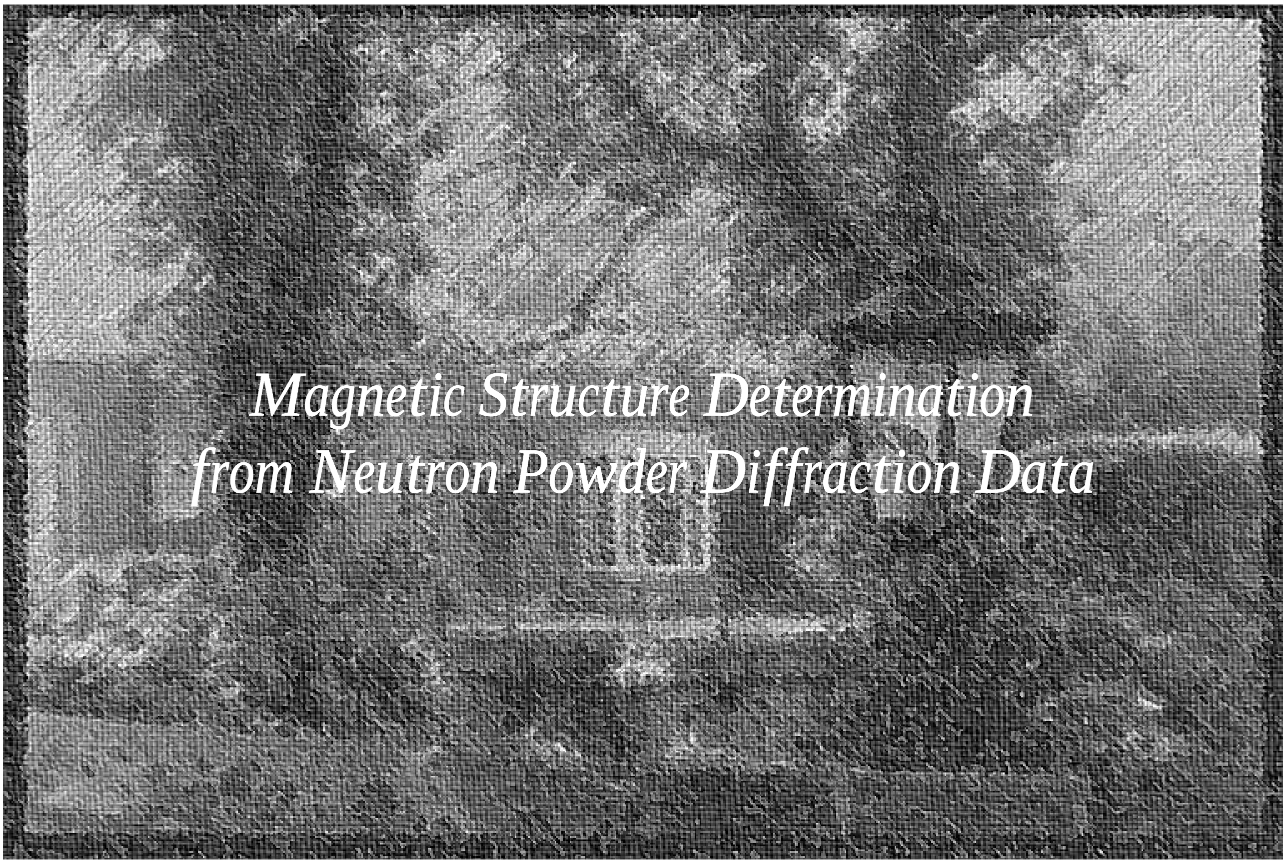

Magnetic Structure Determination from Neutron Powder Diffraction Data

The Cosener's House, Abingdon, 12-14 December 2002

Organiser: Paolo G. Radaelli (RAL-CLRC & UCL)
Tutors: Andrew S. Wills (UCL) &
Juan Rodriguez-Carvajal (LLB)

Programme

Thursday 12 December 2002

14:00 (PGR)	Welcome & Introduction
14:20 (PGR)	Magnetic SG Symmetry Shubnikov Groups.
15:10	Coffee Break
15:40 (PGR)	Generating magnetic structures from SG Defining a SG from a known magnetic structure. Additional topics in Shubnikov groups.
16:10	Break
16:20 (JRC)	What is a Magnetic Structure? Description of Magnetic Structures Propagation Vectors
17:10	Break
17:20 (JRC)	Examples of Common Magnetic Structures Additional topics
18:10	Close
19:00	Dinner
20:30 (All)	Problem-Solving Session with Tutors: Analysis and Description of Magnetic Structures
22:00	Close

Programme (cont'd)

Friday 13 December 2002

7:30	Breakfast
8:30 (ASW)	Symmetry of Magnetic Structures Representation Analysis
09:30	Break
09:40 (ASW)	Representation Analysis (con't)
10:30	Coffee Break
11:00 (ASW)	Introduction to Software for Symmetry Analysis: SARAH, etc.
11:50 (All)	Additional topics/discussion
12:15	Lunch
13:30 (All)	Training Session on Software for Symmetry Analysis
15:30	Coffee Break
15:50 (JRC)	Unpolarised Neutron Scattering - Powder Diffraction
16:40	Break
16:50 (PGR)	Software for magnetic PD: GSAS
17:40 (JRC)	Software for magnetic PD: FULLPROF
18:30	Close
19:00	Christmas Dinner
20:30 (All)	Training Session with Tutors: Refinements of Magnetic Structures
22:00	Close

Programme (cont’d)

Saturday 14 December 2002

7:30	Breakfast
08:30 (Tutors)	Additional software topics (if required)
09:00 (All)	Training Session with Tutors: Refinements of Magnetic Structures (cont'd)
10:00	Coffee Break
10:30 PGR	Powder Diffraction Instrumentation
11:10	Break
11:20 (JRC)	Additional Topics: Polarised Neutrons, etc.
12:15	Lunch & Close

Magnetic Symmetry - Shubnikov Groups

Paolo G. Radaelli

Objectives of this module

- To learn the relevance of time reversal for magnetic structures.
- To learn how PG and SG operators act on spins.
- To learn how magnetic groups can be constructed from subgroups of index 2.
- To learn how to find those on the International Tables for PG and SG.
- To learn about magnetic lattices.
- To be able to construct invariant spin arrangements for magnetic SG, with specific examples.
- To learn the relation between Shubnikov groups and representations.

Reference: W. Opechowski and R. Guccione, “Magnetic Symmetry”, in *Magnetism*, Vol II part A, ed. By G.T. Rado and H. Suhl. Academic Press (New York and London), 1965, pp 105-165.

Notation-1

Element of Space group $\{F\}$: $F=(R|\boldsymbol{\tau}(R)+\mathbf{t})$, where R is a proper or improper rotation, $\mathbf{t}$ is a primitive translation and $\boldsymbol{\tau}(R)$ is a non-primitive translation.

$\{R\}$ is the *point group* associated with $\{F\}$. If $\{(R|0)\}$ is a subgroup of $\{F\}$, then $\{F\}$ is called *symmorphic*.

Given a position $\boldsymbol{r}$ on the lattice, the subgroup $\{F(\boldsymbol{r})\}$ for which $(R|\boldsymbol{\tau}(R)+\mathbf{t})\,\boldsymbol{r} = \mathbf{t}' + \boldsymbol{r}$ is called *site space group*, and its point group $\{R(\boldsymbol{r})\}$.

We shall call $\{A\}=\{E, E'\}$ the 2-elements group of the *time identity* (E) and *time inversion* (E’). Because crystal structures are static, $\{F\}\otimes\{A\}$ is also a symmetry group of the crystal.

Notation-2

However, if we add spins (i.e., magnetic moments) to some of the atoms, time reversal will *switch* the direction of the spins. So $\{F\}\otimes\{A\}$ cannot be a symmetry group of the magnetic structure, and the magnetic symmetry group, $\{M\}$, *must* be a subgroup of $\{F\}\otimes\{A\}$. In particular, $(I|E')$ cannot belong to it.

Forward time   Backward time

Purpose of the study of magnetic symmetry is to generate systematically *all* the magnetic groups associated with a particular space group of the crystal structure.

Caveat

Magnetic space groups, also known as *Shubnikov* groups, are perhaps the most elegant description of magnetic structures. However, in the presence of magnetic ordering, the crystallographic space group is often *not known* a priori, because the symmetry subtly is lowered by magnetic ordering itself. One has therefore to lower the symmetry in a systematic way, which is the purpose of representation theory. The study of Shubnikov groups with therefore serve as an introduction to the more general methods to be described in the remainder of the workshop.

‘Coloured’ groups

We have just seen that the magnetic space group $\{M\}$ *must* be a subgroup of $\{F\}\otimes\{A\}$, and cannot contain (I|E’). However, it can contain elements of the form (F|E’), which will be called *primed* (F’). If *it does not*, it is called a *trivial* (or *colourless)* group. Trivial groups *can* describe magnetic structures. Groups of the type $\{F\}\otimes\{A\}$ are called *gray* or *paramagnetic* groups. All non-trivial subgroups of $\{F\}\otimes\{A\}$ are called *black and white* groups.

The original concepts and terminology were developed by Heesch (1930) and later by Belov and by Zamorzaev (~1955, including a complete list of the magnetic SG). The original aim was purely mathematical or crystallographic (study of coloured patterns on lattices, with A being colour inversion). The application to magnetism is due to Landau & Lifshitz (1958). These concept can be extended to *multicoloured* SG, which are also of some interest for magnetism. Aleksei Vasil'evich Shubnikov was the founder and first director of IC-RAS.

Colour vs. Spin

The analogy between colour and spin can be made by replacing the meaning of E’ from *time reversal* to *colour change*. However, colour and spin differ fundamentally in the way the regular *space group* operators act upon them. Colours are *scalars*, whereas spins are *axial vectors.*

It is important to remember that **an axial vector is left invariant by centering**. Therefore, *proper* rotations act on spins in the same way as on normal (*polar*) vectors, whereas for *mirror operations and centering* there is an additional *spin flip.*

On top of this, *priming* any operator will entail and additional *spin flip*.

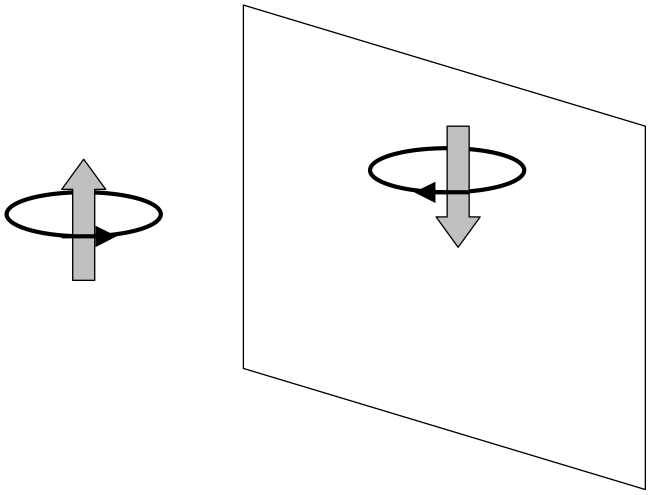

	m_x	2_z, 3_z, 4_z, 6_z	$\bar{1}$	1
Unprimed	Flip $s_y s_z$	Rotate s_x, s_y	No effect	No effect
Primed	Flip s_x	Rotate s_x, s_y Flip s_x, s_y, s_z	Flip s_x,s_y,s_z	Does not occur

Constructive theorem

We will give here the ‘fundamental lemma’ to construct magnetic groups. It will apply equally well to SG, PG or lattices. Let $\{G\}$ be a crystallographic group, $\{M\}$ a derived magnetic group (subgroup of $\{G\}\otimes\{A\}$) and $\{G_M\}$ the group of the elements of $\{G\}$ that are *unprimed* in $\{M\}$. It can be easily shown that

$$\{G\}= \{G_M\} +p\ \{G_M\}$$

where p *does* not belong to $\{G_M\}$, which is therefore a *subgroup of index 2* in $\{G\}$.

This simply has to do with the fact that the product of 2 primed elements must be unprimed.

Follows $\{M\}= \{(G_M|E)\} +p\ \{(G_M|E')\}$

So, the problem of finding *all* magnetic groups arising from a crystallographic group $\{G\}$ is reduced to that of finding all subgroups of index 2 of $\{G\}$.

Example: magnetic point groups

To apply this rule to magnetic point groups, one needs to look no further that page 781 of the International Tables (copied overleaf). Subgroups of index 2 are those that have exactly half the number of elements of the original group. Elements of the subgroup will be *unprimed*, all the remaining elements being *primed*.

Example 1: mmm

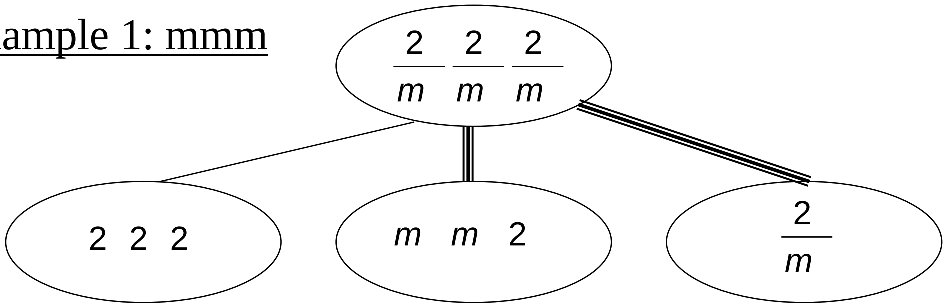

$\frac{2}{m}\,\frac{2}{m}\,\frac{2}{m}$

$2\;2\;2$ $\qquad m\;m\;2$ $\qquad \frac{2}{m}$

$\frac{2}{m'}\,\frac{2}{m'}\,\frac{2}{m'}$ $\qquad \frac{2'}{m}\,\frac{2'}{m}\,\frac{2}{m'}$ $\qquad \frac{2}{m}\,\frac{2'}{m'}\,\frac{2'}{m'}$

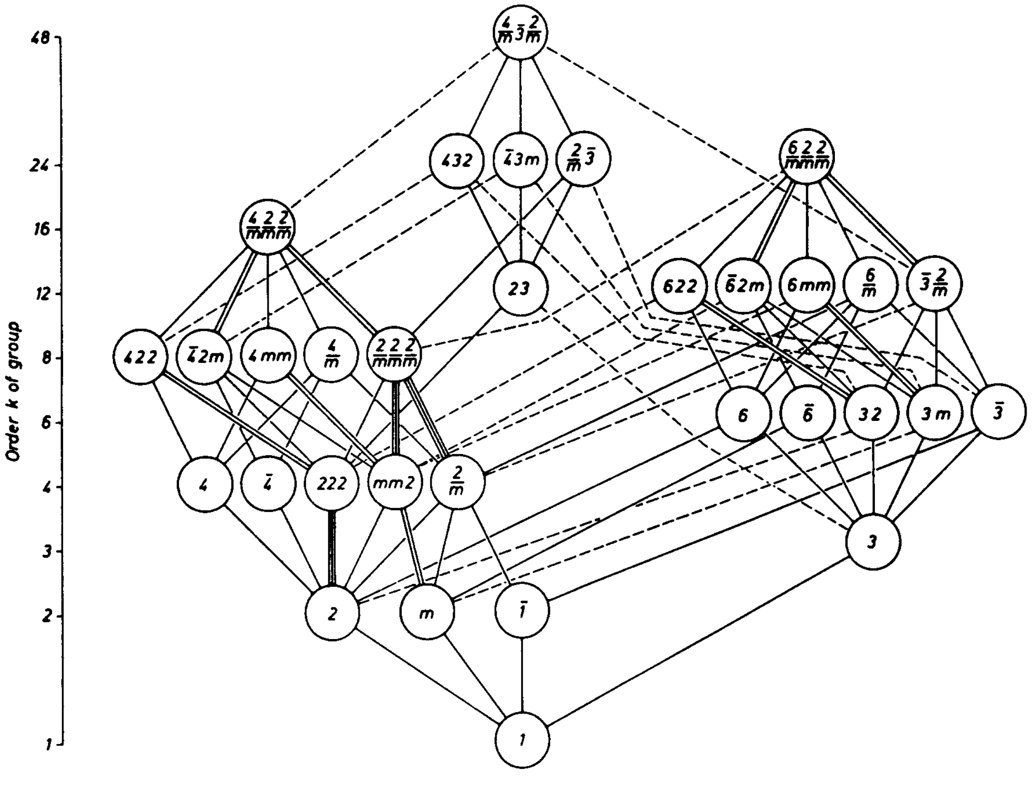

Fig. 10.3.2. Maximal subgroups and minimal supergroups of the three-dimensional crystallographic point groups. Solid lines indicate maximal normal subgroups; double or triple solid lines mean that there are two or three maximal normal subgroups with the same symbol. Dashed lines refer to sets of maximal conjugate subgroups. The group orders are given on the left. Full Hermann–Mauguin symbols are used.

781

Example 2: 4/m m m

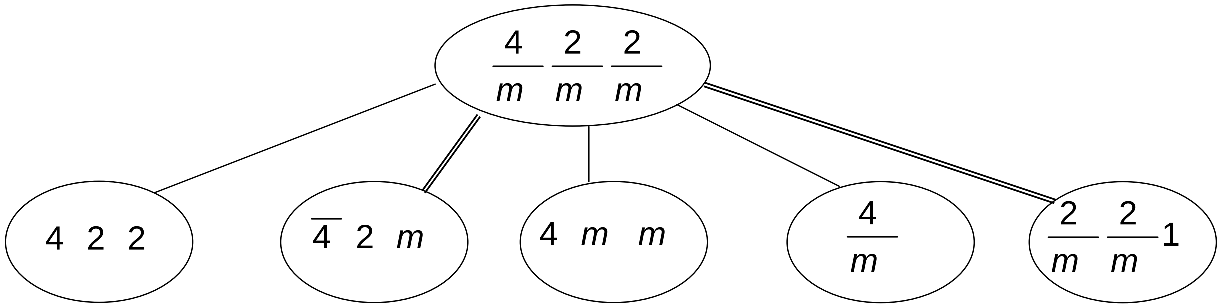

$\frac{4}{m'}\frac{2}{m'}\frac{2}{m'}$ $\frac{4'}{m'}\frac{2}{m'}\frac{2'}{m}$ $\frac{4}{m'}\frac{2'}{m}\frac{2'}{m}$ $\frac{4}{m}\frac{2'}{m'}\frac{2'}{m'}$ $\frac{4'}{m}\frac{2}{m}\frac{2'}{m'}$

Admissible magnetic point groups

A point group is called *admissible* if all its operators leave *at least one* spin component invariant. Admissible MPG are marked with an asterisk in OG, Table I.

As we shall see,admissible point groups (AMPG) have two very important applications.

- The site symmetry of a magnetic atom *must be* a AMPG.
- A *Ferromagnetic* MSG *must have* a AMPG as its MPG.

The second is a *necessary but not sufficient* condition for the MSP to support FM. The other condition is that its lattice is a trivial magnetic lattice (see below).

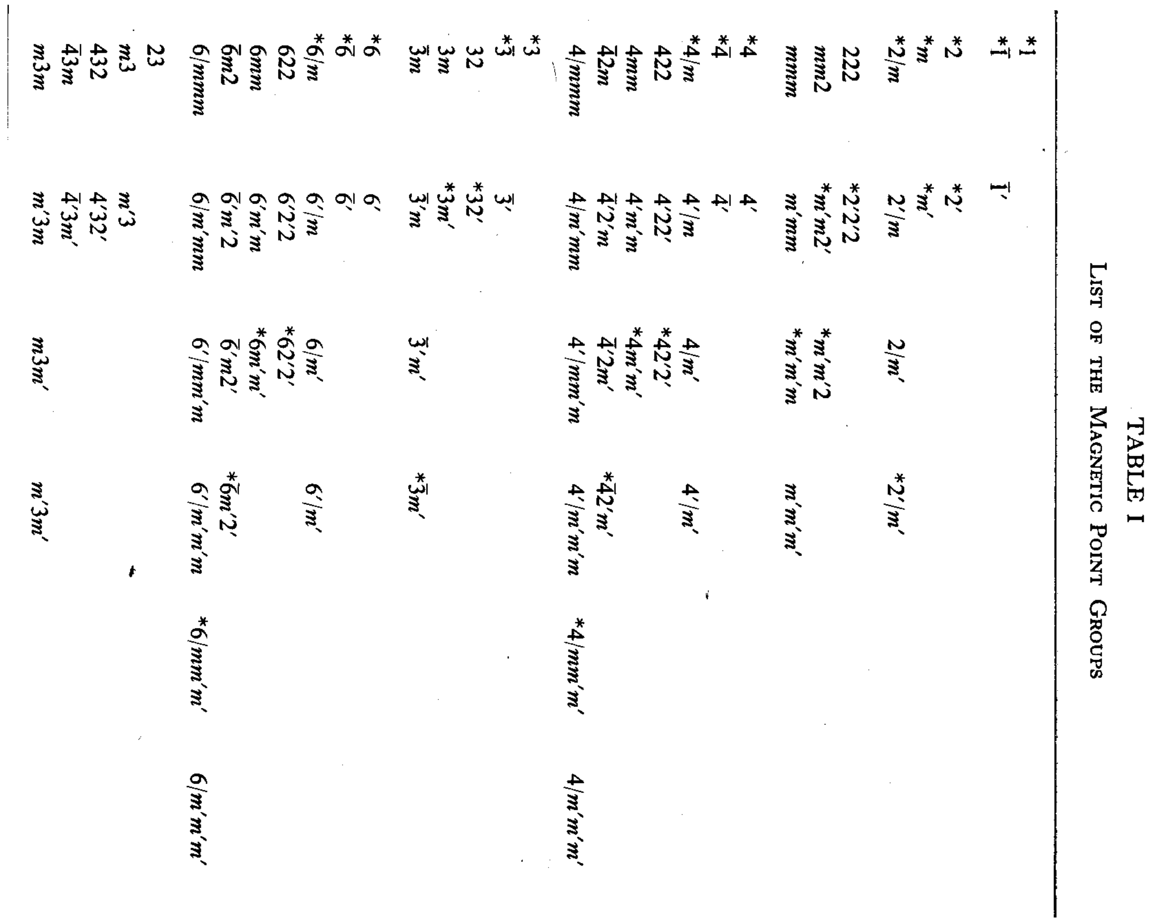

TABLE I

LIST OF THE MAGNETIC POINT GROUPS

^{*1}					
$^*\bar{1}$	$\bar{1}'$				
^{*2}	$^*2'$				
$^*m$	$^*m'$				
$^*2/m$	$2'/m$	$2/m'$	$^*2'/m'$		
222	$^*2'2'2$				
$mm2$	$^*m'm2'$	$^*m'm'2$			
mmm	$m'mm$	$^*m'm'm$	$m'm'm'$		
^{*4}	$4'$				
$^*\bar{4}$	$\bar{4}'$				
$^*4/m$	$4'/m$	$4/m'$	$4'/m'$		
422	$4'22'$	$^*42'2'$			
$4mm$	$4'm'm$	$^*4m'm'$			
$\bar{4}2m$	$\bar{4}'2'm$	$\bar{4}'2m'$	$^*\bar{4}2'm'$		
$4/mmm$	$4/m'mm$	$4'/mm'm$	$4'/m'm'm$	$^*4/mm'm'$	$4/m'm'm'$
^{*3}					
$^*\bar{3}$	$\bar{3}'$				
32	$^*32'$				
$3m$	$^*3m'$				
$\bar{3}m$	$\bar{3}'m$	$\bar{3}'m'$	$^*\bar{3}m'$		
^{*6}	$6'$				
$^*\bar{6}$	$\bar{6}'$				
$^*6/m$	$6'/m$	$6/m'$	$6'/m'$		
622	$6'2'2$	$^*62'2'$			
$6mm$	$6'm'm$	$^*6m'm'$			
$\bar{6}m2$	$\bar{6}'m'2$	$\bar{6}'m2'$	$^*\bar{6}m'2'$		
$6/mmm$	$6/m'mm$	$6'/mm'm$	$6'/m'm'm$	$^*6/mm'm'$	$6/m'm'm'$
23					
$m3$	$m'3$				
432	$4'32'$				
$\bar{4}3m$	$\bar{4}'3m'$				
$m3m$	$m'3m$	$m3m'$	$m'3m'$		

Examples of admissible PG

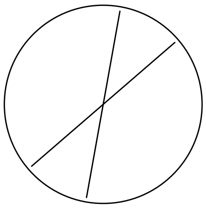

1^*

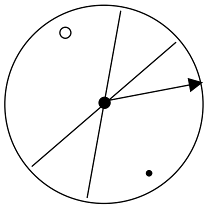

$\bar{1}^*$ (any direction)

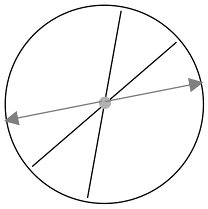

$\bar{1}'$

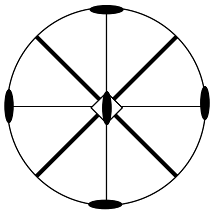

$\bar{4}2m$

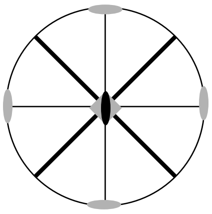

$\bar{4}'2'm$

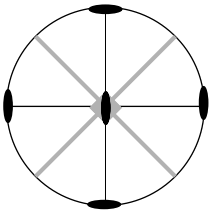

$\bar{4}'2m'$

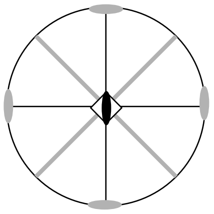

$\bar{4}2'm'^*$

Spin along z

Things to remark about the $\bar{4}2m$ example

- Spin must be parallel to the 4-fold axis (*always* true except for 2-fold axes).
- $\bar{4}$ *must be black*. In fact, for spins, $\bar{4} = 4$
- If a spin is in a plane, that plane *must be red*.
- If a spin is perpendicular to a 2-fold axis, that axis *must be red*.
- Note that the central 2-fold axis of $\bar{4}'$ or $4'$ *is always black*. This is because the product of two primed 45-degree rotations is an unprimed 90-degree rotation.

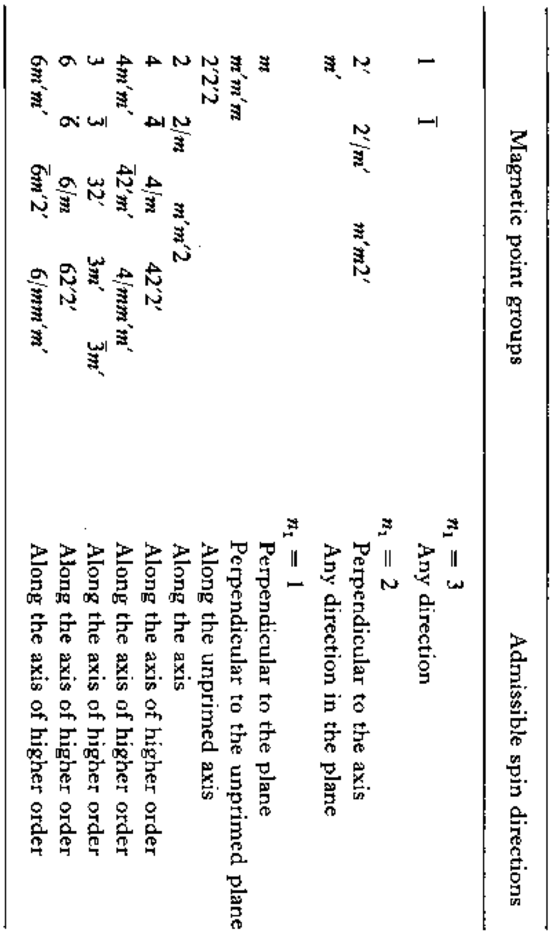

TABLE IV

LIST OF THE ADMISSIBLE MAGNETIC POINT GROUPS

Magnetic point groups	Admissible spin directions
	$n_1 = 3$
1 $\bar{1}$	Any direction
	$n_1 = 2$
$2'$ $2'/m'$ $m'm2'$	Perpendicular to the axis
m'	Any direction in the plane
	$n_1 = 1$
m	Perpendicular to the plane
$m'm'm$	Perpendicular to the unprimed plane
$2'2'2$	Along the unprimed axis
2 $2/m$ $m'm'2$	Along the axis
4 $\bar{4}$ $4/m$ $42'2'$	Along the axis of higher order
$4m'm'$ $\bar{4}2'm'$ $4/mm'm'$	Along the axis of higher order
3 $\bar{3}$ $32'$ $3m'$ $\bar{3}m'$	Along the axis of higher order
6 $\bar{6}$ $6/m$ $62'2'$	Along the axis of higher order
$6m'm'$ $\bar{6}m'2'$ $6/mm'm'$	Along the axis of higher order

Magnetic Bravais Lattices

The constructive theorem we have used to generate the magnetic point groups , based on the identification of subgroups of index 2, can be applied to generate magnetic lattices $\{T_M\}$ from Bravais lattices $\{T\}$.

In general, a group of lattice translations generated by a set of primitive vectors $\boldsymbol{a_1}, \boldsymbol{a_2}, \boldsymbol{a_3}$ has exactly *seven* subgroups of index 2. However, they do not always generate independent MBL, as some of them can be equivalent by interchange of the axes. Also, we are only interested in MBL that *belong to the same holoedry* of the original BL.

In fact, as we shall see in the remainder, MSG either share the *same lattice* with the original SG (trivial ML) or the same *point group* (and therefore, necessarily, the same holoedry).

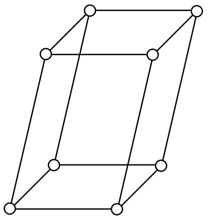

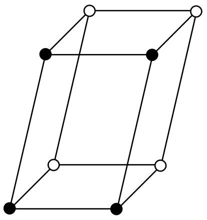

2a, b, c

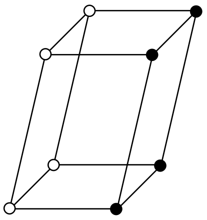

a, 2b, c

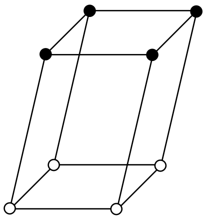

a, b, 2c

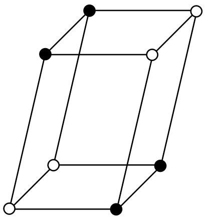

a, b+c, 2c

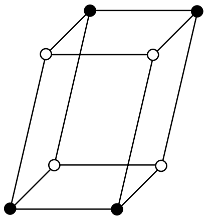

2a, b, a+c

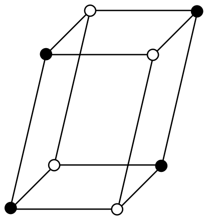

2a, a+b, c

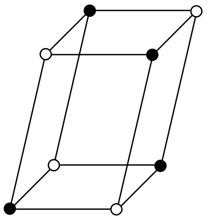

2a, a+b, a+c

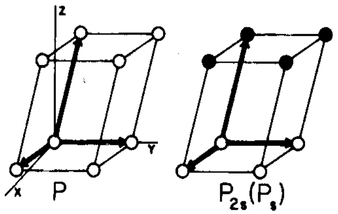

FIG. 1. Magnetic lattices of the triclinic system.

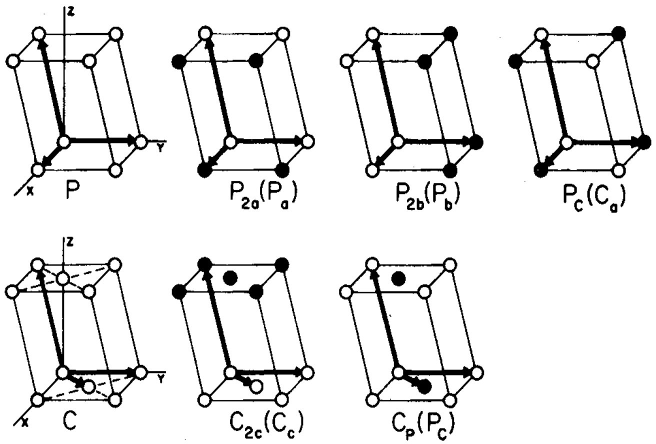

FIG. 2. Magnetic lattices of the monoclinic system (the twofold axis has been chosen as the y-axis).

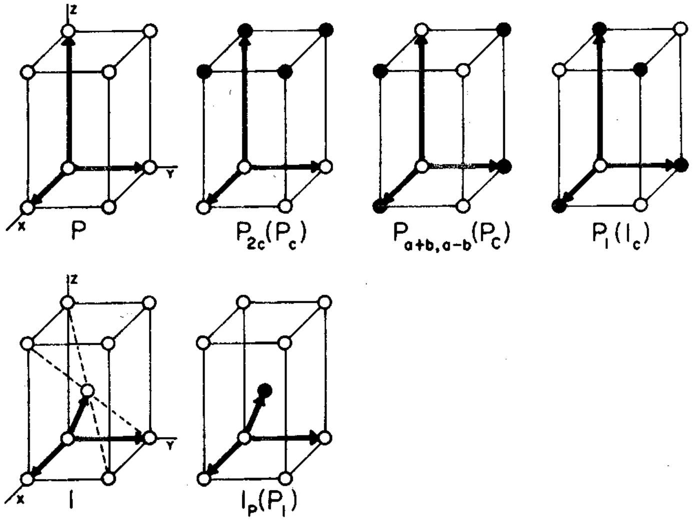

FIG. 4. Magnetic lattices of the tetragonal system.

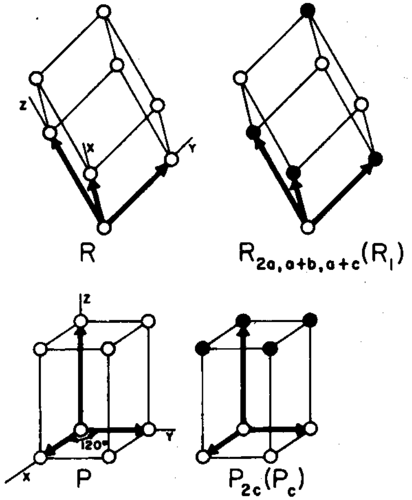

FIG. 5. Magnetic lattices of the trigonal and hexagonal systems.

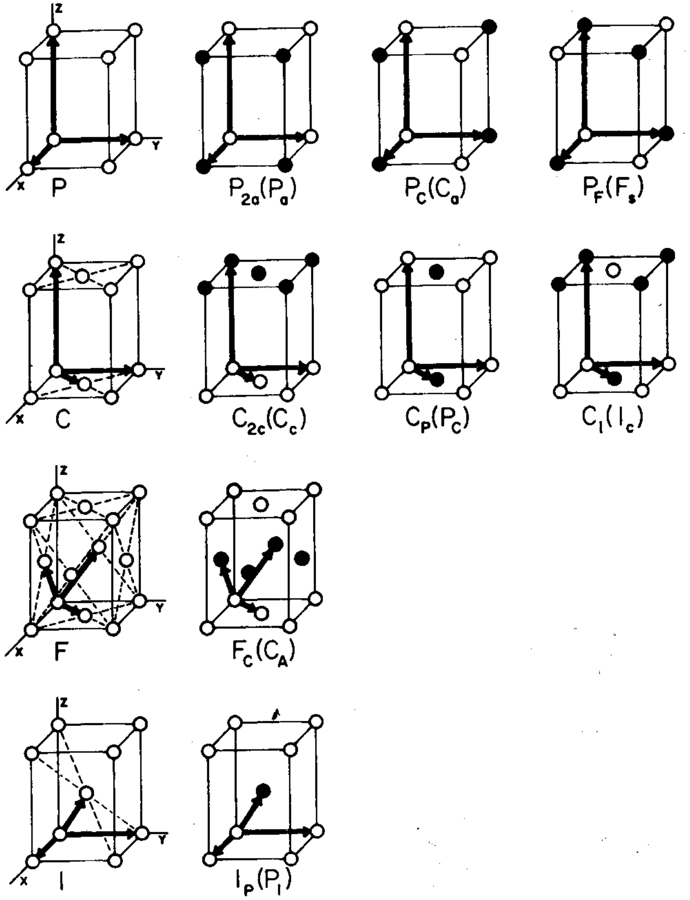

Fig. 3. Magnetic lattices of the orthorhombic system.

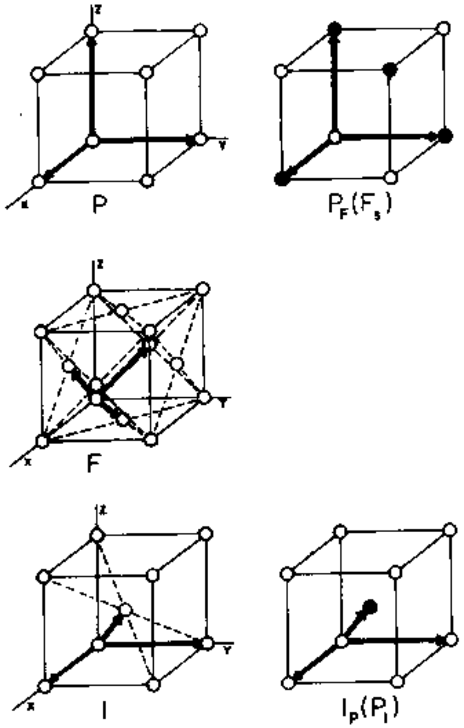

Fig. 6. Magnetic lattices of the cubic system.

Magnetic Space Groups

Once again, the constructive theorem, based on the identification of subgroups of index 2, can be applied to generate magnetic lattices $\{F_M\}$ from space groups $\{F\}$.

The method to generate all the MSG systematically is explained in OG. We will limit ourselves to use the International Tables volume A. In there, for each SG, there is a list of *minimal non-isomorphic subgroups* (Types I, IIa and IIb), and *minimal isomorphic subgroups of lowest index* (Type IIc). The index is indicated in brackets (e.g., [2]).

Therefore, each subgroup listed as [2] will generate a non-trivial magnetic space group. There are 1421 of them in total, 1191 of which are non-trivial. All SG except F23 and P$2_1$3 generate at least 1 non-trivial MSG.

Rules to construct Magnetic Space Groups

1. Identify the subgroups of type I. They share the same lattice (trivial MBL) but have different PG, so they correspond to all the subgroups of index [2] of the associated PG (with multiplicity). For these, it is sufficient to prime the generators that correspond to missing operators.
2. Identify all the other subgroups of index 2 (IIa, IIb and III, no distinction). Then
   - Identify the MBL based on the supercell, and write its symbol.
   - For the Belov symbol (right column in OG), one simply need to complete the H-M symbol with that of the subgroup.
   - For the OG symbol, the modified operators with respect to the original symbol will be primed (e.g. m->n=m’)

TABLE III

List of Magnetic Space Groups[a]

Triclinic system	
1	
$*P1$	
$P_{2s}1$	P_s1
$\bar{1}$	
$*P\bar{1}$	
$P\bar{1}'$	
$P_{2s}\bar{1}$	$P_s\bar{1}$
Monoclinic system	
2	
$*P2$	
$*P2'$	
$P_{2a}2$	P_a2
$P_{2b}2$	P_b2
P_C2	C_a2
$P_{2b}2'$	P_b2_1
$*P2_1$	
$*P2'_1$	
$P_{2a}2_1$	P_a2_1
$*C2$	
$*C2'$	
$C_{2c}2$	C_c2
C_P2	P_C2
C_P2'	P_C2_1
m	
$*Pm$	
$*Pm'$	
$P_{2a}m$	P_am
$P_{2b}m$	P_bm
P_Cm	C_am
$P_{2c}m'$	P_cc
$*Pc$	
$*Pc'$	
$P_{2a}c$	P_ac
$P_{2b}c$	P_bc
P_Cc	C_ac
$*Cm$	
$*Cm'$	
$C_{2c}m$	C_cm
C_Pm	P_Cm
$C_{2c}m'$	C_cc
C_Pm'	P_Ac
$*Cc$	
$*Cc'$	
C_Pc	P_Cc
$2/m$	
$*P2/m$	
$P2'/m$	
$P2/m'$	
$*P2'/m'$	
$P_{2a}2/m$	P_a2/m
$P_{2b}2/m$	P_b2/m
P_C2/m	C_a2/m
$P_{2b}2'/m$	P_b2_1/m
$P_{2c}2/m'$	P_c2/c
$*P2_1/m$	
$P2'_1/m$	
$P2_1/m'$	
$*P2'_1/m'$	
$P_{2a}2_1/m$	P_a2_1/m
$P_{2c}2_1/m'$	P_c2_1/c
$*C2/m$	
$C2'/m$	
$C2/m'$	
$*C2'/m'$	
$C_{2c}2/m$	C_c2/m
C_P2/m	P_C2/m
$C_{2c}2/m'$	C_c2/c
C_P2'/m	P_C2_1/m
C_P2/m'	P_A2/c
C_P2'/m'	P_A2_1/c
$*P2/c$	
$P2'/c$	
$P2/c'$	
$*P2'/c'$	
$P_{2a}2/c$	P_a2/c
$P_{2b}2/c$	P_b2/c
P_C2/c	C_a2/c
$P_{2b}2'/c$	P_b2_1/c
$*P2_1/c$	
$P2'_1/c$	
$P2_1/c'$	
$*P2'_1/c'$	
$P_{2a}2_1/c$	P_a2_1/c
$*C2/c$	
$C2'/c$	
$C2/c'$	

---

[a] Every page of Table III should be read first from the top to the bottom of the left-hand double column, then from the top to the bottom of the middle double column, and finally from the top to the bottom of the right-hand double column.

TABLE III (*continued*)

Monoclinic system	
$*C2/c$	
$*C2'/c'$	
C_P2/c	P_C2/c
C_P2'/c	P_C2_1/c
Orthorhombic system	
222	
$P222$	
$*P2'2'2$	
$P_{2a}222$	P_a222
P_C222	C_a222
P_F222	F_s222
$P_{2c}22'2'$	P_c222_1
$P222_1$	
$*P2'2'2_1$	
$*P22'2'_1$	
$P_{2a}222_1$	P_a222_1
P_C222_1	C_a222_1
$P_{2a}2'2'2_1$	$P_a2_12_12$
$P2_12_12$	
$*P2'_12'_12$	
$*P2_12'_12'$	
$P_{2c}2_12_12$	$P_c2_12_12$
$P_{2c}2_12'_12'$	$P_a2_12_12_1$
$P2_12_12_1$	
$*P2'_12'_12_1$	
$C222_1$	
$*C2'2'2_1$	
$*C22'2'_1$	
C_P222_1	P_C222_1
$C_P2'2'2_1$	$P_C2_12_12_1$
$C_P22'2'_1$	$P_A2_12_12$
$C222$	
$*C2'2'2$	
$*C22'2'$	
$C_{2c}222$	C_c222
C_P222	P_C222
C_I222	I_c222
$C_{2c}22'2'$	C_c222_1
$C_P2'2'2$	$P_C2_12_12$
$C_P22'2'$	P_A222_1
$C_I2'22'$	$I_c2_12_12_1$
$F222$	
$*F2'2'2$	
F_C222	C_A222
$F_C22'2'$	C_A222_1
$I222$	
$*I2'2'2$	
I_P222	P_I222
$I_P2'2'2$	$P_I2_12_12$
$I2_12_12_1$	
$*I2'_12'_12_1$	
$I_P2_12_12_1$	$P_I2_12_12_1$
$I_P2'_12'_12_1$	P_I222_1
$mm2$	
$Pmm2$	
$*Pm'm2'$	
$*Pm'm'2$	
$P_{2c}mm2$	P_cmm2
$P_{2a}mm2$	P_amm2
P_Cmm2	C_amm2
P_Amm2	A_amm2
P_Fmm2	F_smm2
$P_{2c}mm'2'$	P_cmc2_1
$P_{2c}m'm'2$	P_ccc2
$P_{2a}m'm'2$	P_ama2
$P_Am'm'2$	A_cbm2
$Pmc2_1$	
$*Pm'c2'_1$	
$*Pmc'2'_1$	
$*Pm'c'2_1$	
$P_{2a}mc2_1$	P_amc2_1
$P_{2b}mc2_1$	P_bmc2_1
P_Cmc2_1	C_amc2_1
$P_{2a}mc'2'_1$	P_amn2_1
$P_{2b}m'c'2_1$	P_aca2_1
$Pcc2$	
$*Pc'c2'$	
$*Pc'c'2$	
$P_{2a}cc2$	P_acc2
P_Ccc2	C_acc2
$P_{2b}c'c2'$	P_bnc2
$Pma2$	
$*Pm'a2'$	
$*Pma'2'$	
$*Pm'a'2$	
$P_{2b}ma2$	P_bma2
$P_{2c}ma2$	P_cma2
P_Ama2	A_cma2
$P_{2b}m'a2'$	P_aba2
$P_{2c}m'a2'$	P_cca2_1
$P_{2c}ma'2'$	P_cmn2_1
$P_{2c}m'a'2$	P_cnc2
$P_Am'a'2$	A_cba2
$Pca2_1$	
$*Pc'a2'_1$	
$*Pca'2'_1$	

TABLE III (*continued*)

Orthorhombic system	
$Pca2_1$	
*$Pc'a'2_1$	
$P_{2b}ca2_1$	P_bca2_1
$P_{2b}c'a'2_1$	P_bna2_1
$Pnc2$	
*$Pn'c2'$	
*$Pnc'2'$	
*$Pn'c'2$	
$P_{2a}nc2$	P_anc2
$P_{2a}nc'2'$	P_ann2
$Pmn2_1$	
*$Pm'n2_1'$	
*$Pmn'2_1'$	
*$Pm'n'2_1$	
$P_{2b}mn2_1$	P_bmn2_1
$P_{2b}m'n2_1'$	P_ana2_1
$Pba2$	
*$Pb'a2'$	
*$Pb'a'2$	
$P_{2c}ba2$	P_cba2
$P_{2c}b'a2'$	P_cna2_1
$P_{2c}b'a'2$	P_cnn2
$Pna2_1$	
*$Pn'a2_1'$	
*$Pna'2_1'$	
*$Pn'a'2_1$	
$Pnn2$	
*$Pn'n2'$	
*$Pn'n'2$	
P_Fnn2	F_sdd2
$Cmm2$	
*$Cm'm2'$	
*$Cm'm'2$	
$C_{2c}mm2$	C_cmm2
C_Pmm2	P_Cmm2
C_Imm2	I_cmm2
$C_{2c}m'm2'$	C_cmc2_1
$C_{2c}m'm'2$	C_ccc2
$C_Pm'm2'$	P_Cma2
$C_Pm'm'2$	P_Cba2
$C_Im'm2'$	I_cma2
$C_Im'm'2$	I_cba2
$Cmc2_1$	
*$Cm'c2_1'$	
*$Cmc'2_1'$	
*$Cm'c'2_1$	
C_Pmc2_1	P_Cmc2_1
$C_Pm'c2_1'$	P_Cca2_1
$C_Pmc'2_1'$	P_Cmn2_1
$C_Pm'c'2_1$	P_Cna2_1
$Ccc2$	
*$Cc'c2'$	
*$Cc'c'2$	
C_Pcc2	P_Ccc2
$C_Pc'c2'$	P_Cnc2
$C_Pc'c'2$	P_Cnn2
$Amm2$	
*$Am'm2'$	
*$Amm'2'$	
*$Am'm'2$	
$A_{2a}mm2$	A_amm2
A_Pmm2	P_Amm2
A_Imm2	I_amm2
$A_{2a}mm'2'$	A_ama2
$A_Pm'm2'$	P_Bmn2_1
$A_Pmm'2'$	P_Amc2_1
$A_Pm'm'2$	P_Anc2
$A_Im'm'2$	I_ama2
$Abm2$	
*$Ab'm2'$	
*$Abm'2'$	
*$Ab'm'2$	
$A_{2a}bm2$	A_abm2
A_Pbm2	P_Bma2
A_Ibm2	B_Ima2
$A_{2a}b'm'2$	A_aba2
$A_Pb'm2'$	P_Bmc2_1
$A_Pbm'2'$	P_Bca2_1
$A_Pb'm'2$	P_Acc2
$A_Ib'm'2$	I_aba2
$Ama2$	
*$Am'a2'$	
*$Ama'2'$	
*$Am'a'2$	
A_Pma2	P_Ama2
$A_Pm'a2'$	P_Ana2_1
$A_Pma'2'$	P_Amn2_1
$A_Pm'a'2$	P_Ann2
$Aba2$	
*$Ab'a2'$	
*$Aba'2'$	
*$Ab'a'2$	
A_Pba2	P_Aba2
$A_Pb'a2'$	P_Aca2_1
$A_Pba'2'$	P_Bna2_1
$A_Pb'a'2$	P_Bnc2
$Fmm2$	
*$Fm'm2'$	
*$Fm'm'2$	

TABLE III (*continued*)

Orthorhombic system	
$Fmm2$	
F_Cmm2	C_Amm2
F_Amm2	A_Cmm2
$F_Cmm'2'$	C_Amc2_1
$F_Cm'm'2$	C_Acc2
$F_Am'm2'$	A_Cbm2
$F_Amm'2'$	A_Cma2
$F_Am'm'2$	A_Cba2
$Fdd2$	
*$Fd'd2'$	
*$Fd d'2$	
$Imm2$	
*$Im'm2'$	
*$Im'm'2$	
I_Pmm2	P_Imm2
$I_Pmm'2'$	P_Imn2_1
$I_Pm'm'2$	P_Inn2
$Iba2$	
*$Ib'a2'$	
*$Ib'a'2$	
I_Pba2	P_Icc2
$I_Pba'2'$	P_Ica2_1
$I_Pb'a'2$	P_Iba2
$Ima2$	
*$Im'a2'$	
*$Ima'2'$	
*$Im'a'2$	
I_Pma2	P_Ima2
$I_Pm'a2'$	P_Ina2_1
$I_Pma'2'$	P_Imc2_1
$I_Pm'a'2$	P_Inc2
mmm	
$Pmmm$	
$Pm'mm$	
*$Pm'm'm$	
$Pm'm'm'$	
$P_{2a}mmm$	P_ammm
P_Cmmm	C_ammm
P_Fmmm	F_smmm
$P_{2a}mmm'$	P_amma
$P_{2a}m'm'm$	P_cccm
P_Cmmm'	C_amma
$Pnnn$	
$Pn'nn$	
*$Pn'n'n$	
$Pn'n'n'$	
P_Fnnn	F_sddd
$Pccm$	
$Pc'cm$	
$Pccm'$	
*$Pc'c'm$	
*$Pc'cm'$	
$Pc'c'm'$	
$P_{2a}ccm$	P_accm
P_Cccm	C_accm
$P_{2a}ccm'$	P_acca
$P_{2a}c'c'm$	P_cmna
$P_{2a}c'c'm'$	P_aban
P_Cccm'	C_acca
$Pban$	
$Pb'an$	
$Pban'$	
*$Pb'a'n$	
*$Pb'an'$	
$Pb'a'n'$	
$P_{2c}ban$	P_cban
$P_{2c}b'an$	P_bnna
$P_{2c}b'a'n$	P_cnnn
$Pmma$	
$Pm'ma$	
$Pmm'a$	
$Pmma'$	
*$Pm'm'a$	
*$Pmm'a'$	
*$Pm'ma'$	
$Pm'm'a'$	
$P_{2b}mma$	P_bmma
$P_{2c}mma$	P_cmma
P_Amma	C_amcm
$P_{2b}m'ma$	P_bbcm
$P_{2b}mma'$	P_ammn
$P_{2b}m'ma'$	P_amna
$P_{2c}m'ma$	P_abam
$P_{2c}mm'a$	P_cbcm
$P_{2c}m'm'a$	P_ccca
$P_Am'ma$	C_amca
$Pnna$	
$Pn'na$	
$Pnn'a$	
$Pnna'$	
*$Pn'n'a$	
*$Pnn'a'$	
*$Pn'na'$	
$Pn'n'a'$	
$Pmna$	
$Pm'na$	
$Pmn'a$	
$Pmna'$	
*$Pm'n'a$	
*$Pmn'a'$	

TABLE III (*continued*)

Orthorhombic system	
$Pmna$	
$*Pm'na'$	
$Pm'n'a'$	
$P_{2b}mna$	$P_{b}mna$
$P_{2b}m'na$	$P_{c}bcn$
$P_{2b}mna'$	$P_{a}nnm$
$P_{2b}m'na'$	$P_{a}nna$
$Pcca$	
$Pc'ca$	
$Pcc'a$	
$Pcca'$	
$*Pc'c'a$	
$*Pcc'a'$	
$*Pc'ca'$	
$Pc'c'a'$	
$P_{2b}cca$	$P_{b}cca$
$P_{2b}c'ca$	$P_{a}bcn$
$P_{2b}cca'$	$P_{a}ccn$
$P_{2b}c'ca$	$P_{c}nna$
$Pbam$	
$Pb'am$	
$Pbam'$	
$*Pb'a'm$	
$*Pb'am'$	
$Pb'a'm'$	
$P_{2c}bam$	$P_{c}bam$
$P_{2c}b'am$	$P_{b}nma$
$P_{2c}b'a'm$	$P_{c}nnm$
$Pccn$	
$Pc'cn$	
$Pccn'$	
$*Pc'c'n$	
$*Pc'cn'$	
$Pc'c'n'$	

$Pbcm$	
$Pb'cm$	
$Pbc'm$	
$Pbcm'$	
$*Pb'c'm$	
$*Pbc'm'$	
$*Pb'cm'$	
$Pb'c'm'$	
$P_{2a}bcm$	$P_{a}bcm$
$P_{2a}bc'm$	$P_{c}nma$
$P_{2a}bcm'$	$P_{a}bca$
$P_{2a}bc'm'$	$P_{b}bcn$
$Pnnm$	
$Pn'nm$	
$Pnnm'$	
$*Pn'n'm$	
$*Pnn'm'$	
$Pn'n'm'$	
$Pmmn$	
$Pm'mn$	
$Pmmn'$	
$*Pm'm'n$	
$*Pmm'n'$	
$Pm'm'n'$	
$P_{2c}mmn$	$P_{c}mmn$
$P_{2c}m'mn$	$P_{a}nma$
$P_{2c}m'm'n$	$P_{c}ccn$
$Pbcn$	
$Pb'cn$	
$Pbc'n$	
$Pbcn'$	
$*Pb'c'n$	
$*Pbc'n'$	
$*Pb'cn'$	
$Pb'c'n'$	

$Pbca$	
$Pb'ca$	
$*Pb'c'a$	
$Pb'c'a'$	
$Pnma$	
$Pn'ma$	
$Pnm'a$	
$Pnma'$	
$*Pn'm'a$	
$*Pnm'a'$	
$*Pn'ma'$	
$Pn'm'a'$	
$Cmcm$	
$Cm'cm$	
$Cmc'm$	
$Cmcm'$	
$*Cm'c'm$	
$*Cmc'm'$	
$*Cm'cm'$	
$Cm'c'm'$	
$C_{P}mcm$	$P_{A}mma$
$C_{P}m'cm$	$P_{C}bcm$
$C_{P}mc'm$	$P_{C}mmn$
$C_{P}mcm'$	$P_{B}nma$
$C_{P}m'c'm$	$P_{C}nma$
$C_{P}mc'm'$	$P_{C}nnm$
$C_{P}m'cm'$	$P_{C}bcn$
$C_{P}m'c'm'$	$P_{C}nna$
$Cmca$	
$Cm'ca$	
$Cmc'a$	
$Cmca'$	
$*Cm'c'a$	
$*Cmc'a'$	

TABLE III (*continued*)

Orthorhombic system	
$Cmca$	
$*Cm'ca'$	
$Cm'c'a'$	
$C_{P}mca$	$P_{C}bam$
$C_{P}m'ca$	$P_{C}cca$
$C_{P}mc'a$	$P_{C}nma$
$C_{P}mca'$	$P_{C}bcm$
$C_{P}m'c'a$	$P_{C}ccn$
$C_{P}mc'a'$	$P_{C}mna$
$C_{P}m'ca'$	$P_{C}bca$
$C_{P}m'c'a'$	$P_{C}bcn$
$Cmmm$	
$Cm'mm$	
$Cmmm'$	
$*Cm'm'm$	
$*Cmm'm'$	
$Cm'm'm'$	
$C_{2c}mmm$	$C_{c}mmm$
$C_{P}mmm$	$P_{C}mmm$
$C_{I}mmm$	$I_{c}mmm$
$C_{2c}m'm'm$	$C_{c}ccm$
$C_{2c}mm'm'$	$C_{c}mcm$
$C_{P}m'mm$	$P_{C}mma$
$C_{P}mmm'$	$P_{C}mmn$
$C_{P}m'm'm$	$P_{C}bam$
$C_{P}mm'm'$	$P_{C}mna$
$C_{P}m'm'm'$	$P_{C}ban$
$C_{I}m'mm$	$I_{c}mma$
$C_{I}m'm'm$	$I_{c}bam$
$Cccm$	
$Cc'cm$	
$Cccm'$	
$*Cc'c'm$	
$*Ccc'm'$	
$Cc'c'm'$	

$C_{P}ccm$	$P_{C}ccm$
$C_{P}c'cm$	$P_{C}mna$
$C_{P}ccm'$	$P_{C}ccn$
$C_{P}c'c'm$	$P_{C}nnm$
$C_{P}cc'm'$	$P_{C}nna$
$C_{P}c'c'm'$	$P_{C}nnn$
$Cmma$	
$Cm'ma$	
$Cmma'$	
$*Cm'm'a$	
$*Cmm'a'$	
$Cm'm'a'$	
$C_{2c}mma$	$C_{c}mma$
$C_{P}mma$	$P_{C}ccm$
$C_{I}mma$	$I_{c}bam$
$C_{2c}m'ma$	$C_{c}mca$
$C_{2c}m'm'a$	$C_{c}cca$
$C_{P}m'ma$	$P_{C}cca$
$C_{P}mm'a$	$P_{C}mma$
$C_{P}mma'$	$P_{C}bcm$
$C_{I}mm'a$	$I_{c}mma$
$C_{I}m'm'a'$	$I_{c}bca$
$Ccca$	
$Cc'ca$	
$Ccca'$	
$*Cc'c'a$	
$*Ccc'a'$	
$Cc'c'a'$	
$C_{P}cca$	$P_{C}ban$
$C_{P}c'ca$	$P_{C}cca$
$C_{P}cca'$	$P_{C}bcn$
$C_{P}cc'a'$	$P_{C}nna$
$Fmmm$	
$Fm'mm$	
$*Fm'm'm$	

$Fm'm'm'$	
$F_{C}mmm$	$C_{A}mmm$
$F_{C}m'mm$	$C_{A}mcm$
$F_{C}mmm'$	$C_{A}mma$
$F_{C}m'm'm$	$C_{A}ccm$
$F_{C}mm'm'$	$C_{A}mca$
$F_{C}m'm'm'$	$C_{A}cca$
$Fddd$	
$Fd'dd$	
$*Fd'd'd$	
$Fd'd'd'$	
$Immm$	
$Im'mm$	
$*Im'm'm$	
$Im'm'm'$	
$I_{P}mmm$	$P_{I}mmm$
$I_{P}m'mm$	$P_{I}mmn$
$I_{P}m'm'm$	$P_{I}nnm$
$I_{P}m'm'm'$	$P_{I}nnn$
$Ibam$	
$Ib'am$	
$Ibam'$	
$*Ib'a'm$	
$*Iba'm'$	
$Ib'a'm'$	
$I_{P}bam$	$P_{I}ccm$
$I_{P}b'am$	$P_{I}bcm$
$I_{P}bam'$	$P_{I}ccn$
$I_{P}b'a'm$	$P_{I}bam$
$I_{P}b'am'$	$P_{I}bcn$
$I_{P}b'a'm'$	$P_{I}ban$
$Ibca$	
$Ib'ca$	
$*Ib'c'a$	

TABLE III (*continued*)

Orthorhombic system	
$Ibca$	
$Ib'c'a'$	
I_Pbca	P_Ibca
$I_Pb'ca$	P_Icca
$Imma$	
$Im'ma$	
$Imma'$	
$*Im'm'a$	
$*Imm'a'$	
$Im'm'a'$	
I_Pmma	P_Imma
$I_Pm'm'a$	P_Inna
$I_Pmm'a'$	P_Imna
$I_Pm'ma'$	P_Inma
Tetragonal system	
4	
$*P4$	
$P4'$	
$P_{2c}4$	P_c4
P_P4	P_C4
P_I4	I_c4
$P_{2c}4'$	P_c4_2
$*P4_1$	
$P4'_1$	
P_P4_1	P_C4_1
$*P4_3$	
$P4'_3$	
$P_{2c}4_3$	P_c4_1
P_P4_3	P_C4_3
P_I4_3	I_c4_1
$P_{2c}4'_3$	P_c4_3

$*P4_3$	
$P4'_3$	
P_P4_3	P_C4_3
$*I4$	
$I4'$	
I_P4	P_I4
I_P4'	P_I4_2
$*I4_1$	
$I4'_1$	
I_P4_1	P_I4_1
$I_P4'_1$	P_I4_3
$\bar{4}$	
$*P\bar{4}$	
$P\bar{4}'$	
$P_{2c}\bar{4}$	$P_c\bar{4}$
$P_P\bar{4}$	$P_C\bar{4}$
$P_I\bar{4}$	$I_c\bar{4}$
$*I\bar{4}$	
$I\bar{4}'$	
$I_P\bar{4}$	$P_I\bar{4}$
$4/m$	
$*P4/m$	
$P4'/m$	
$P4/m'$	
$P4'/m'$	
$P_{2c}4/m$	P_c4/m
P_P4/m	P_C4/m
P_I4/m	I_c4/m
$P_{2c}4'/m$	P_c4_2/m
P_P4/m'	P_C4/n

$*P4_2/m$	
$P4'_2/m$	
$P4_2/m'$	
$P4'_2/m'$	
P_P4_2/m	P_C4_2/m
P_P4_2/m'	P_C4_2/n
$*P4/n$	
$P4'/n$	
$P4/n'$	
$P4'/n'$	
$P_{2c}4/n$	P_c4/n
$P_{2c}4'/n$	P_c4_2/n
$*P4_2/n$	
$P4'_2/n$	
$P4_2/n'$	
$P4'_2/n'$	
P_I4_2/n	I_c4_1/a
$*I4/m$	
$I4'/m$	
$I4/m'$	
$I4'/m'$	
I_P4/m	P_I4/m
I_P4'/m	P_I4_2/m
I_P4/m'	P_I4/n
I_P4'/m'	P_I4_2/n
$*I4_1/a$	
$I4'_1/a$	
$I4_1/a'$	
$I4'_1/a'$	
422	
$P422$	
$P4'22'$	
$*P42'2'$	

TABLE III (*continued*)

Tetragonal system	
$P422$	
$P4'2'2$	
$P_{2c}422$	P_c422
P_P422	P_C422
P_I422	I_c422
$P_{2c}4'22'$	P_c4_222
$P_P4'22'$	P_C42_12
$P42_12$	
$P4'2_12'$	
$*P42'_12'$	
$P4'2'_12$	
$P_{2c}42_12$	P_c42_12
$P_{2c}4'2'_12$	$P_c4_22_12$
$P4_122$	
$P4'_122'$	
$*P4_12'2'$	
$P4'_12'2$	
P_P4_122	P_C4_122
$P_P4'_122'$	$P_C4_12_12$
$P4_12_12$	
$P4'_12_12'$	
$*P4_12'_12'$	
$P4'_12'_12$	
$P4_222$	
$P4'_222'$	
$*P4_22'2'$	
$P4'_22'2$	
$P_{2c}4_222$	P_c4_122
P_P4_222	P_C4_222
P_I4_222	I_c4_122
$P_{2c}4'_222'$	P_c4_322
$P_P4'_222'$	$P_C4_22_12$

$P4_22_12$	
$P4'_22_12'$	
$*P4_22'_12'$	
$P4'_22'_12$	
$P_{2c}4_22_12$	$P_c4_12_12$
$P_{2c}4'_22'_12$	$P_c4_32_12$
$P4_322$	
$P4'_322'$	
$*P4_32'2'$	
$P4'_32'2$	
P_P4_322	P_C4_322
$P_P4'_322'$	$P_C4_32_12$
$P4_32_12$	
$P4'_32_12'$	
$*P4_32'_12'$	
$P4'_32'_12$	
$I422$	
$I4'22'$	
$*I42'2'$	
$I4'2'2$	
I_P422	P_I422
$I_P4'22'$	P_I4_222
$I_P42'2'$	P_I42_12
$I_P4'2'2$	$P_I4_22_12$
$I4_122$	
$I4'_122'$	
$*I4_12'2'$	
$I4'_12'2$	
I_P4_122	P_I4_122
$I_P4'_122'$	P_I4_322
$I_P4_12'2'$	$P_I4_12_12$
$I_P4'_12'2$	$P_I4_32_12$

$4mm$	
$P4mm$	
$P4'm'm$	
$P4'mm'$	
$*P4m'm'$	
$P_{2c}4mm$	P_c4mm
P_P4mm	P_C4mm
P_I4mm	I_c4mm
$P_{2c}4'm'm$	P_c4_2cm
$P_{2c}4'mm'$	P_c4_2mc
$P_{2c}4m'm'$	P_c4cc
$P_P4'mm'$	P_C4bm
$P_I4m'm'$	I_c4cm
$P4bm$	
$P4'b'm$	
$P4'bm'$	
$*P4b'm'$	
$P_{2c}4bm$	P_c4bm
$P_{2c}4'b'm$	P_c4_2nm
$P_{2c}4'bm'$	P_c4_2bc
$P_{2c}4b'm'$	P_c4nc
$P4_2cm$	
$P4'_2c'm$	
$P4'_2cm'$	
$*P4_2c'm'$	
P_P4_2cm	P_C4_2mc
$P_P4'_2cm'$	P_C4_2bc
$P4_2nm$	
$P4'_2n'm$	
$P4'_2nm'$	
$*P4_2n'm'$	
P_I4_2nm	I_c4_1md
$P_I4_2n'm'$	I_c4_1cd

TABLE III (*continued*)

Tetragonal system

$\underline{P4cc}$

$P4'c'c$
$P4'cc'$
$*P4c'c'$
P_P4cc P_C4cc
$P_P4'cc'$ P_C4nc

$\underline{P4nc}$

$P4'n'c$
$P4'nc'$
$*P4n'c'$

$\underline{P4_2mc}$

$P4'_2m'c$
$P4'_2mc'$
$*P4_2m'c'$
P_P4_2mc P_C4_2cm
$P_P4'_2mc'$ P_C4_2nm

$\underline{P4_2bc}$

$P4'_2b'c$
$P4'_2bc'$
$*P4_2b'c'$

$\underline{I4mm}$

$I4'm'm$
$I4'mm'$
$*I4m'm'$
I_P4mm P_I4mm
$I_P4'm'm$ P_I4_2nm
$I_P4'mm'$ P_I4_2mc
$I_P4m'm'$ P_I4nc

$\underline{I4cm}$

$I4'c'm$
$I4'cm'$
$*I4c'm'$
I_P4cm P_I4bm
$I_P4'c'm$ P_I4_2cm
$I4'cm'$ P_I4_2bc
$I4c'm'$ P_I4cc

$\underline{I4_1md}$

$I4'_1m'd$
$I4'_1md'$
$*I4_1m'd'$

$\underline{I4_1cd}$

$I4'_1c'd$
$I4'_1cd'$
$*I4_1c'd'$

$\bar{4}2m$

$\underline{P\bar{4}2m}$

$P\bar{4}'2'm$
$P\bar{4}'2m'$
$*P\bar{4}2'm'$
$P_{2c}\bar{4}2m$ $P_c\bar{4}2m$
$P_P\bar{4}2m$ $P_C\bar{4}m2$
$P_I\bar{4}2m$ $I_c\bar{4}m2$
$P_{2c}\bar{4}2'm'$ $P_c\bar{4}2c$
$P_P\bar{4}'2m'$ $P_C\bar{4}b2$
$P_I\bar{4}'2m'$ $I_c\bar{4}c2$

$\underline{P\bar{4}2c}$

$P\bar{4}'2'c$
$P\bar{4}'2c'$
$*P\bar{4}2'c'$
$P_P\bar{4}2c$ $P_C\bar{4}c2$
$P_P\bar{4}'2c'$ $P_C\bar{4}n2$

$\underline{P\bar{4}2_1m}$

$P\bar{4}'2'_1m$
$P\bar{4}'2_1m'$
$*P\bar{4}2'_1m'$
$P_{2c}\bar{4}2_1m$ $P_c\bar{4}2_1m$
$P_{2c}\bar{4}'2_1m'$ $P_c\bar{4}2_1c$

$\underline{P\bar{4}2_1c}$

$P\bar{4}'2'_1c$
$P\bar{4}'2_1c'$
$*P\bar{4}2'_1c'$

$\underline{P\bar{4}m2}$

$P\bar{4}'m'2$
$P\bar{4}'m2'$
$*P\bar{4}m'2'$
$P_{2c}\bar{4}m2$ $P_c\bar{4}m2$
$P_P\bar{4}m2$ $P_C\bar{4}2m$
$P_I\bar{4}m2$ $I_c\bar{4}2m$
$P_{2c}\bar{4}'m'2$ $P_c\bar{4}c2$
$P_P\bar{4}'m2'$ $P_C\bar{4}2_1m$

$\underline{P\bar{4}c2}$

$P\bar{4}'c'2$
$P\bar{4}'c2'$
$*P\bar{4}c'2'$
$P_P\bar{4}c2$ $P_C\bar{4}2c$
$P_P\bar{4}'c2'$ $P_C\bar{4}2_1c$

$\underline{P\bar{4}b2}$

$P\bar{4}'b'2$
$P\bar{4}'b2'$
$*P\bar{4}b'2'$
$P_{2c}\bar{4}b2$ $P_c\bar{4}b2$
$P_{2c}\bar{4}'b'2$ $P_c\bar{4}n2$

$\underline{P\bar{4}n2}$

$P\bar{4}'n'2$
$P\bar{4}'n2'$
$*P\bar{4}n'2'$
$P_I\bar{4}n2$ $I_c\bar{4}2d$

TABLE III (*continued*)

Tetragonal system

$\underline{I\bar{4}m2}$

$I\bar{4}'m'2$
$I\bar{4}'m2'$
$*I\bar{4}m'2'$
$I_P\bar{4}m2$ $P_I\bar{4}m2$
$I_P\bar{4}'m'2$ $P_I\bar{4}n2$

$\underline{I\bar{4}c2}$

$I\bar{4}'c'2$
$I\bar{4}'c2'$
$*I\bar{4}c'2'$
$I_P\bar{4}c2$ $P_I\bar{4}c2$
$I_P\bar{4}c'2'$ $P_I\bar{4}b2$

$\underline{I\bar{4}2m}$

$I\bar{4}'2'm$
$I\bar{4}'2m'$
$*I\bar{4}2'm'$
$I_P\bar{4}2m$ $P_I\bar{4}2m$
$I_P\bar{4}'2'm$ $P_I\bar{4}2_1m$
$I_P\bar{4}'2m'$ $P_I\bar{4}2c$
$I_P\bar{4}2'm'$ $P_I\bar{4}2_1c$

$\underline{I\bar{4}2d}$

$I\bar{4}'2'd$
$I\bar{4}'2d'$
$*I\bar{4}2'd'$

$4/mmm$

$\underline{P4/mmm}$

$P4/m'mm$
$P4'/mm'm$
$P4'/mmm'$
$P4'/m'm'm$
$*P4/mm'm'$
$P4'/m'mm'$
$P4/m'm'm'$
$P_{2c}4/mmm$ P_c4/mmm
P_P4/mmm P_C4/mmm
P_I4/mmm I_c4/mmm
$P_{2c}4'/mm'm$ P_c4_2/mcm
$P_{2c}4'/mmm'$ P_c4_2/mmc
$P_{2c}4/mm'm'$ P_c4/mcc
$P_P4/m'mm$ P_C4/nmm
P_P4'/mmm' P_C4/mbm
$P_P4'/m'mm'$ P_C4/nbm
$P_I4/mm'm'$ I_c4/mcm

$\underline{P4/mcr}$

$P4/m'cc$
$P4'/mc'c$
$P4'/mcc'$
$P4'/m'c'c$
$*P4/mc'c'$
$P4'/m'cc'$
$P4/m'c'c'$
P_P4/mcc P_C4/mcc
$P_P4/m'cc$ P_C4/ncc
P_P4'/mcc' P_C4/mnc
$P_P4'/m'cc'$ P_C4/nnc

$\underline{P4/nbm}$

$P4/n'bm$
$P4'/nb'm$
$P4'/nbm'$
$P4'/n'b'm$
$*P4/nb'm'$
$P4'/n'bm'$
$P4/n'b'm'$
$P_{2c}4/nbm$ P_c4/nbm
$P_{2c}4'/nb'm$ P_c4_2/nnm
$P_{2c}4'/nbm'$ P_c4_2/nbc
$P_{2c}4/nb'm'$ P_c4/nnc

$\underline{P4/nnc}$

$P4/n'nc$
$P4'/nn'c$
$P4'/nnc'$
$P4'/n'n'c$
$*P4/nn'c'$
$P4'/n'nc'$
$P4/n'n'c'$

$\underline{P4/mbm}$

$P4/m'bm$
$P4'/mb'm$
$P4'/mbm'$
$P4'/m'b'm$
$*P4/mb'm'$
$P4'/m'bm'$
$P4/m'b'm'$
$P_{2c}4/mbm$ P_c4/mbm
$P_{2c}4'/mb'm$ P_c4_2/mnm
$P_{2c}4'/mbm'$ P_c4_2/mbc
$P_{2c}4/mb'm'$ P_c4/mnc

$\underline{P4/mnc}$

$P4/m'nc$
$P4'/mn'c$
$P4'/mnc'$
$P4'/m'n'c$
$*P4/mn'c'$
$P4'/m'nc'$
$P4/m'n'c'$

$\underline{P4/nmm}$

$P4/n'mm$
$P4'/nm'm$
$P4'/nmm'$
$P4'/n'm'm$
$*P4/nm'm'$
$P4'/n'mm'$
$P4/n'm'm'$
$P_{2c}4/nmm$ P_c4/nmm

TABLE III (*continued*)

Tetragonal system

$P4/nmm$

$P_{2c}4'/nm'm$ P_c4_2/ncm
$P_{2c}4'/nmm'$ P_c4_2/nmc
$P_{2c}4/nm'm'$ P_c4/ncc

$P4/ncc$

$P4/n'cc$
$P4'/nc'c$
$P4'/ncc'$
$P4'/n'c'c$
$*P4/nc'c'$
$P4'/n'cc'$
$P4/n'c'c'$

$P4_2/mmc$

$P4_2/m'mc$
$P4'_2/mm'c$
$P4'_2/mmc'$
$P4'_2/m'm'c$
$*P4_2/mm'c'$
$P4'_2/m'mc'$
$P4_2/m'm'c'$
P_P4_2/mmc P_C4_2/mcm
$P_P4_2/m'mc$ P_C4_2/ncm
$P_P4_2/mm'c'$ P_C4_2/mnm
$P_P4'_2/m'mc$ P_C4_2/nnm

$P4_2/mcm$

$P4_2/m'cm$
$P4'_2/mc'm$
$P4_2/mcm'$
$P4'_2/m'c'm$
$*P4_2/mc'm'$
$P4'_2/m'cm'$
$P4_2/m'c'm'$
P_P4_2/mcm P_C4_2/mmc

$P_P4_2/m'cm$ P_C4_2/nmc
$P_P4'_2/mcm'$ P_C4_2/mbc
$P_P4'_2/m'cm'$ P_C4_2/nbc

$P4_2/nbc$

$P4_2/n'bc$
$P4'_2/nb'c$
$P4'_2/nbc'$
$P4'_2/n'b'c$
$*P4_2/nb'c'$
$P4'_2/n'bc'$
$P4_2/n'b'c'$

$P4_2/nnm$

$P4_2/n'nm$
$P4'_2/nn'm$
$P4'_2/nnm'$
$P4'_2/n'n'm$
$*P4_2/nn'm'$
$P4'_2/n'nm'$
$P4_2/n'n'm'$
P_I4_2/nnm I_c4_1/amd
$P_I4_2/nn'm'$ I_c4_1/acd

$P4_2/mbc$

$P4_2/m'bc$
$P4'_2/mb'c$
$P4'_2/mbc'$
$P4'_2/m'b'c$
$*P4_2/mb'c'$
$P4'_2/m'bc'$
$P4_2/m'b'c'$

$P4_2/mnm$

$P4_2/m'nm$
$P4'_2/mn'm$
$P4'_2/mnm'$
$P4'_2/m'n'm$

$*P4_2/mn'm'$
$P4'_2/m'nm'$
$P4_2/m'n'm'$

$P4_2/nmc$

$P4_2/n'mc$
$P4'_2/nm'c$
$P4'_2/nmc'$
$P4'_2/n'm'c$
$*P4_2/nm'c'$
$P4'_2/n'mc'$
$P4_2/n'm'c'$

$P4_2/ncm$

$P4_2/n'cm$
$P4'_2/nc'm$
$P4'_2/ncm'$
$P4'_2/n'c'm$
$*P4_2/nc'm'$
$P4'_2/n'cm'$
$P4_2/n'c'm'$

$I4/mmm$

$I4/m'mm$
$I4'/mm'm$
$I4'/mmm'$
$I4'/m'm'm$
$*I4/mm'm'$
$I4'/m'mm'$
$I4/m'm'm'$
I_P4/mmm P_I4/mmm
$I_P4/m'mm$ P_I4/nmm
$I_P4'/mm'm$ P_I4_2/mnm
I_P4'/mmm' P_I4_2/mmc
$I_P4'/m'm'm$ P_I4_2/nnm
$I_P4/mm'm'$ P_I4/mnc
$I_P4'/m'mm'$ P_I4_2/nmc
$I_P4/m'm'm'$ P_I4/nnc

TABLE III (*continued*)

Tetragonal system

$I4/mcm$

$I4/m'cm$
$I4'/mc'm$
$I4'/mcm'$
$I4'/m'c'm$
$*I4/mc'm'$
$I4'/m'cm'$
$I4/m'c'm'$
I_P4/mcm P_I4/mcc
$I_P4/m'cm$ P_I4/ncc
$I_P4'/mc'm$ P_I4_2/mbc
I_P4'/mcm' P_I4_2/mcm
$I_P4'/m'c'm$ P_I4_2/nbc
$I_P4/mc'm'$ P_I4/mbm
$I_P4'/m'cm'$ P_I4_2/ncm
$I_P4/m'c'm'$ P_I4/nbm

$I4_1/amd$

$I4_1/a'md$
$I4'_1/am'd$
$I4'_1/amd'$
$I4'_1/a'm'd$
$*I4_1/am'd'$
$I4'_1/a'md'$
$I4_1/a'm'd'$

$I4_1/acd$

$I4_1/a'cd$
$I4'_1/ac'd$
$I4_1/acd'$

$I4'_1/a'c'd$
$*I4_1/ac'd'$
$I4'_1/a'cd'$
$I4_1/a'c'd'$

Trigonal system

3

$*P3$

$P_{2c}3$ P_c3

$*P3_1$

$P_{2c}3_2$ P_c3_2

$*P3_2$

$P_{2c}3_1$ P_c3_1

$*R3$

R_R3

$\bar{3}$

$*P\bar{3}$

$P\bar{3}'$
$P_{2c}\bar{3}$ $P_c\bar{3}$

$*R\bar{3}$

$R\bar{3}'$
$R_R\bar{3}$

32

$P312$

$*P312'$
$P_{2c}312$ P_c312

$P321$

$*P32'1$
$P_{2c}321$ P_c321

$P3_112$

$*P3_112'$
$P_{2c}3_212$ P_c3_212

$P3_121$

$*P3_12'1$
$P_{2c}3_221$ P_c3_221

$P3_212$

$*P3_212'$
$P_{2c}3_112$ P_c3_112

$P3_221$

$*P3_22'1$
$P_{2c}3_121$ P_c3_121

$R32$

$*R32'$
R_R32

$3m$

$P3m1$

$*P3m'1$
$P_{2c}3m1$ P_c3m1
$P_{2c}3m'1$ P_c3c1

$P31m$

$*P31m'$
$P_{2c}31m$ P_c31m
$P_{2c}31m'$ P_c31c

$P3c1$

$*P3c'1$

$P31c$

$*P31c'$

$R3m$

$*R3m'$

TABLE III (*continued*)

Trigonal system	
$\underline{R3m}$	
R_R3m	
R_R3m'	R_I3c
$\underline{R3c}$	
$*R3c'$	
$\bar{3}m$	
$\underline{P\bar{3}1m}$	
$P\bar{3}'1m$	
$P\bar{3}'1m'$	
$*P\bar{3}1m'$	
$P_{2c}\bar{3}1m$	$P_c\bar{3}1m$
$P_{2c}\bar{3}1m'$	$P_c\bar{3}1c$
$\underline{P\bar{3}1c}$	
$P\bar{3}'1c$	
$P\bar{3}'1c'$	
$*P\bar{3}1c'$	
$\underline{P\bar{3}m1}$	
$P\bar{3}'m1$	
$P\bar{3}'m'1$	
$*P\bar{3}m'1$	
$P_{2c}\bar{3}m1$	$P_c\bar{3}m1$
$P_{2c}\bar{3}m'1$	$P_c\bar{3}c1$
$\underline{P\bar{3}c1}$	
$P\bar{3}'c1$	
$P\bar{3}'c'1$	
$*P\bar{3}c'1$	
$\underline{R\bar{3}m}$	
$R\bar{3}'m$	
$R\bar{3}'m'$	
$*R\bar{3}m'$	

$R_R\bar{3}m$	
$R_R\bar{3}m'$	$R_I\bar{3}c$
$\underline{R\bar{3}c}$	
$R\bar{3}'c$	
$R\bar{3}'c'$	
$*R\bar{3}c'$	
Hexagonal system	
6	
$\underline{*P6}$	
$P6'$	
$P_{2c}6$	P_c6
$P_{2c}6'$	P_c6_3
$\underline{*P6_1}$	
$P6_1'$	
$\underline{*P6_5}$	
$P6_5'$	
$\underline{*P6_2}$	
$P6_2'$	
$P_{2c}6_2$	P_c6_1
$P_{2c}6_2'$	P_c6_4
$\underline{*P6_4}$	
$P6_4'$	
$P_{2c}6_4$	P_c6_2
$P_{2c}6_4'$	P_c6_5
$\underline{*P6_3}$	
$P6_3'$	
$\bar{6}$	
$\underline{*P\bar{6}}$	
$P\bar{6}'$	
$P_{2c}\bar{6}$	$P_c\bar{6}$

$6/m$	
$\underline{*P6/m}$	
$P6'/m$	
$P6/m'$	
$P6'/m'$	
$P_{2c}6/m$	P_c6/m
$P_{2c}6'/m$	P_c6_3/m
$\underline{*P6_3/m}$	
$P6_3'/m$	
$P6_3/m'$	
$P6_3'/m'$	
622	
$\underline{P622}$	
$P6'2'2$	
$P6'22'$	
$*P62'2'$	
$P_{2c}622$	P_c622
$P_{2c}6'22$	P_c6_322
$\underline{P6_122}$	
$P6_1'2'2$	
$P6_1'22'$	
$*P6_12'2'$	
$\underline{P6_522}$	
$P6_5'2'2$	
$P6_5'22'$	
$*P6_52'2'$	
$\underline{P6_222}$	
$P6_2'2'2$	
$P6_2'22'$	
$*P6_22'2'$	
$P_{2c}6_222$	P_c6_122
$P_{2c}6_2'22$	P_c6_422

TABLE III (*continued*)

Hexagonal system	
$\underline{P6_422}$	
$P6_4'2'2$	
$P6_4'22'$	
$*P6_42'2'$	
$P_{2c}6_422$	P_c6_222
$P_{2c}6_4'2'2$	P_c6_522
$\underline{P6_322}$	
$P6_3'2'2$	
$P6_3'22'$	
$*P6_32'2'$	
$6mm$	
$\underline{P6mm}$	
$P6'm'm$	
$P6'mm'$	
$*P6m'm'$	
$P_{2c}6mm$	P_c6mm
$P_{2c}6'm'm$	P_c6_3cm
$P_{2c}6'mm'$	P_c6_3mc
$P_{2c}6m'm'$	P_c6cc
$\underline{P6cc}$	
$P6'c'c$	
$P6'cc'$	
$*P6c'c'$	
$\underline{P6_3cm}$	
$P6_3'c'm$	
$P6_3'cm'$	
$*P6_3c'm'$	
$\underline{P6_3mc}$	
$P6_3'm'c$	
$P6_3'mc'$	
$*P6_3m'c'$	

$\bar{6}m2$	
$\underline{P\bar{6}m2}$	
$P\bar{6}'m'2$	
$P\bar{6}'m2'$	
$*P\bar{6}m'2'$	
$P_{2c}\bar{6}m2$	$P_c\bar{6}m2$
$P_{2c}\bar{6}'m'2$	$P_c\bar{6}c2$
$\underline{P\bar{6}c2}$	
$P\bar{6}'c'2$	
$P\bar{6}'c2'$	
$*P\bar{6}c'2'$	
$\underline{P\bar{6}2m}$	
$P\bar{6}'2'm$	
$P\bar{6}'2m'$	
$*P\bar{6}2'm'$	
$P_{2c}\bar{6}2m$	$P_c\bar{6}2m$
$P_{2c}\bar{6}'2m'$	$P_c\bar{6}2c$
$\underline{P\bar{6}2c}$	
$P\bar{6}'2'c$	
$P\bar{6}'2c'$	
$*P\bar{6}2'c'$	
$6/mmm$	
$\underline{P6/mmm}$	
$P6/m'mm$	
$P6'/mm'm$	
$P6'/mmm'$	
$P6'/m'm'm$	
$P6'/m'mm'$	
$*P6/mm'm'$	
$P6/m'm'm'$	
$P_{2c}6/mmm$	P_c6/mmm
$P_{2c}6'/mm'm$	P_c6_3/mcm
$P_{2c}6'/mmm'$	P_c6_3/mmc
$P_{2c}6/mm'm'$	P_c6/mcc

$\underline{P6/mcc}$	
$P6/m'cc$	
$P6'/mc'c$	
$P6'/mcc'$	
$P6'/m'c'c$	
$P6'/m'cc'$	
$*P6/mc'c'$	
$P6/m'c'c'$	
$\underline{P6_3/mcm}$	
$P6_3/m'cm$	
$P6_3'/mc'm$	
$P6_3'/mcm'$	
$P6_3'/m'c'm$	
$P6_3'/m'cm'$	
$*P6_3/mc'm'$	
$P6_3/m'c'm'$	
$\underline{P6_3/mmc}$	
$P6_3/m'mc$	
$P6_3'/mm'c$	
$P6_3'/mmc'$	
$P6_3'/m'm'c$	
$P6_3'/m'mc'$	
$*P6_3/mm'c'$	
$P6_3/m'm'c'$	
Cubic system	
23	
$\underline{P23}$	
P_F23	F_s23
$\underline{F23}$	
$\underline{I23}$	
I_P23	P_I23

TABLE III (*continued*)

Cubic system	
$\underline{P2_13}$	
$\underline{I2_13}$	
I_P2_13	P_I2_13
$m3$	
$\underline{Pm3}$	
$Pm'3$	
P_Fm3	F_sm3
$\underline{Pn3}$	
$Pn'3$	
P_Fn3	F_sd3
$\underline{Fm3}$	
$Fm'3$	
$\underline{Fd3}$	
$Fd'3$	
$\underline{Im3}$	
$Im'3$	
I_Pm3	P_Im3
$I_Pm'3$	P_In3
$\underline{Pa3}$	
$Pa'3$	
$\underline{Ia3}$	
$Ia'3$	
I_Pa3	P_Ia3
432	
$\underline{P432}$	
$P4'32'$	
P_F432	F_s432
$\underline{P4_232}$	
$P4_2'32'$	
P_F4_232	F_s4_132
$\underline{F432}$	
$F4'32'$	
$\underline{F4_132}$	
$F4_1'32'$	
$\underline{I432}$	
$I4'32'$	
I_P432	P_I432
$I_P4'32'$	P_I4_232
$\underline{P4_332}$	
$P4_3'32'$	
$\underline{P4_132}$	
$P4_1'32'$	
$\underline{I4_132}$	
$I4_1'32'$	
I_P4_132	P_I4_332
$I_P4_1'32'$	P_I4_132
$\bar{4}3m$	
$\underline{P\bar{4}3m}$	
$P\bar{4}'3m'$	
$P_F\bar{4}3m$	$F_s\bar{4}3m$
$P_F\bar{4}'3m'$	$F_s\bar{4}3c$
$\underline{F\bar{4}3m}$	
$F\bar{4}'3m'$	
$\underline{I\bar{4}3m}$	
$I\bar{4}'3m'$	
$I_P\bar{4}3m$	$P_I\bar{4}3m$
$I_P\bar{4}'3m'$	$P_I\bar{4}3n$
$\underline{P\bar{4}3n}$	
$P\bar{4}'3n'$	
$\underline{F\bar{4}3c}$	
$F\bar{4}'3c'$	
$\underline{I\bar{4}3d}$	
$I\bar{4}'3d'$	
$m3m$	
$\underline{Pm3m}$	
$Pm'3m$	
$Pm3m'$	
$Pm'3m'$	
P_Fm3m	F_sm3m
P_Fm3m'	F_sm3c
$\underline{Pn3n}$	
$Pn'3n$	
$Pn3n'$	
$Pn'3n'$	
$\underline{Pm3n}$	
$Pm'3n$	
$Pm3n'$	
$Pm'3n'$	
$\underline{Pn3m}$	
$Pn'3m$	
$Pn3m'$	
$Pn'3m'$	

TABLE III (*continued*)

Cubic system	
$\underline{Pn3m}$	
P_Fn3m	F_sd3m
P_Fn3m'	F_sd3c
$\underline{Fm3m}$	
$Fm'3m$	
$Fm3m'$	
$Fm'3m'$	
$\underline{Fm3c}$	
$Fm'3c$	
$Fm3c'$	
$Fm'3c'$	
$\underline{Fd3m}$	
$Fd'3m$	
$Fd3m'$	
$Fd'3m'$	
$\underline{Fd3c}$	
$Fd'3c$	
$Fd3c'$	
$Fd'3c'$	
$\underline{Im3m}$	
$Im'3m$	
$Im3m'$	
$Im'3m'$	
I_Pm3m	P_Im3m
$I_Pm'3m$	P_In3m
I_Pm3m'	P_Im3n
$I_Pm'3m'$	P_In3n
$\underline{Ia3d}$	
$Ia'3d$	
$Ia3d'$	
$Ia'3d'$	

Rules to construct invariant spin arrangements

- Define a magnetic space group generated by the SG of the crystal structure.
- Identify the magnetic site, and define its magnetic point symmetry. A *graphic* representation of the MG is useful.
- Check that the site MPG is *admissible* for at least one spin component. Otherwise, the MSG does not support any magnetic structure on that site.
- Pick one admissible component, and apply in turn all the MSG operators on that component, propagating it to all equivalent sites.

Rules to determine the MSG from a given structure

- Check that the magnetic structure Γ is Shubnikov-compatible. This is easily done by applying the operators of the *crystal* space group $\{F\}$ upon Γ (including lattice doublings). Γ is Shubnikov-compatible if and only if, the structure is either invariant ($\times$ 1) or reversed ($\times$ -1) for each and every F in $\{F\}$.
- Prime all the operators in $\{F\}$ for which Γ is reversed, and identify the new primitive translations. This completes the process.

Shubnikov groups and representations

To make a link with the more powerful representation analysis, we can simply think of how a magnetic structure Γ, which is invariant under a particular magnetic groups $\{F_M\}$, will transform under the 'parent' space group $\{F\}$. It is apparent that Γ will be invariant ($\times$ 1) under the operators which are *unprimed* in $\{F_M\}$, whereas all the spins will be switched ($\times -1$) for the operators that are *primed* in $\{F_M\}$. In other words, the set of numbers 1 or –1 is a *representation* of $\{F\}$ onto the linear space generated by Γ. We can easily prove that the reverse is also true.

We can conclude the Shubnikov groups are *equivalent to 1-dimensional real representations* of $\{F\}$, with the invariant Γ being their basis sets. In general, if we relax the requirement for invariance of the crystal structure, there is no reason to prefer these to all the (infinite) others, whence the need for extending the analysis to the *full expansion in irreducible representations*.

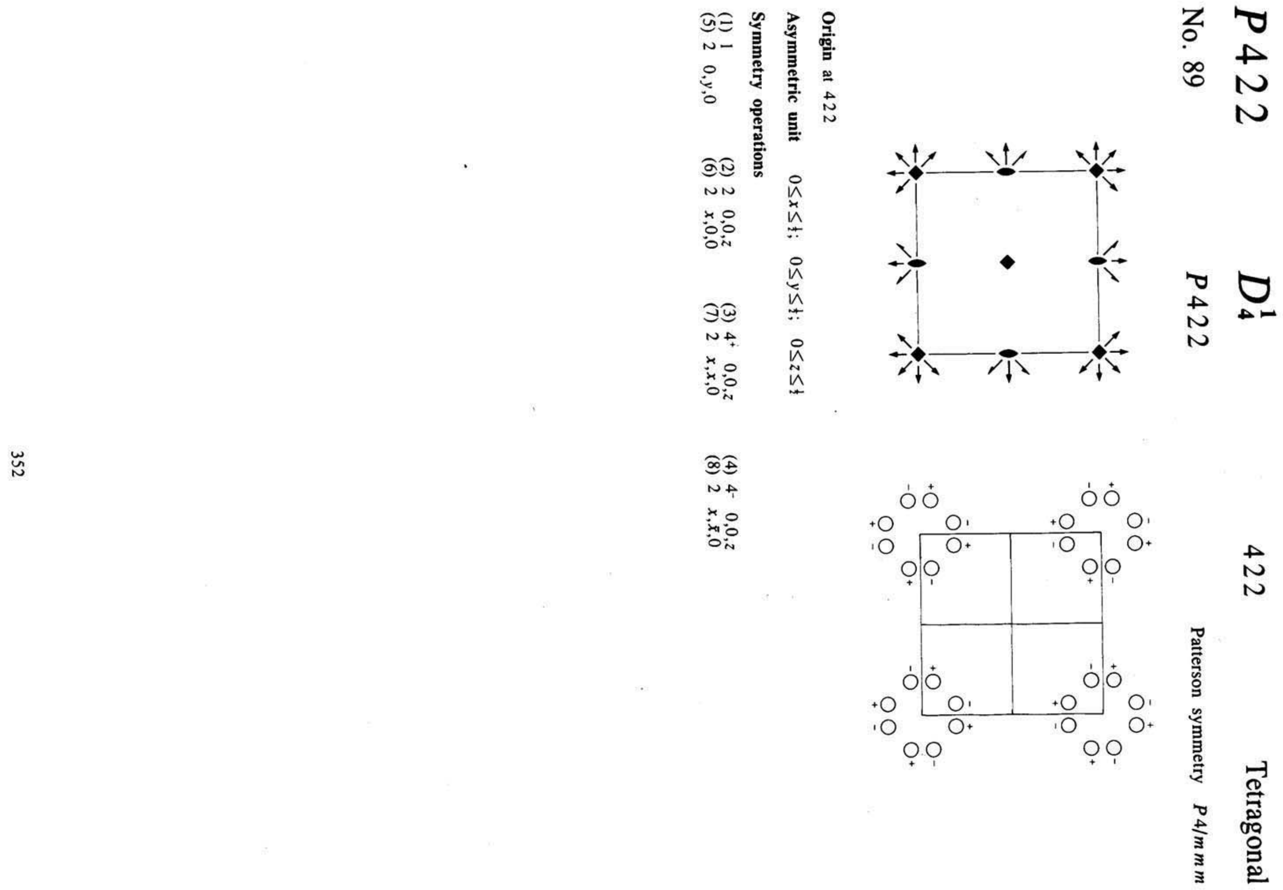

$P\,4\,2\,2$ $\qquad D_4^1$ $\qquad 4\,2\,2$ $\qquad$ Tetragonal

No. 89 $\qquad P\,4\,2\,2$ $\qquad$ Patterson symmetry $P\,4/m\,m\,m$

Origin at 422

Asymmetric unit $0\le x\le \tfrac{1}{2};\ 0\le y\le \tfrac{1}{2};\ 0\le z\le \tfrac{1}{2}$

Symmetry operations

(1) 1	(2) 2 $0,0,z$	(3) 4^+ $0,0,z$	(4) 4^- $0,0,z$
(5) 2 $0,y,0$	(6) 2 $x,0,0$	(7) 2 $x,x,0$	(8) 2 $x,\bar{x},0$

352

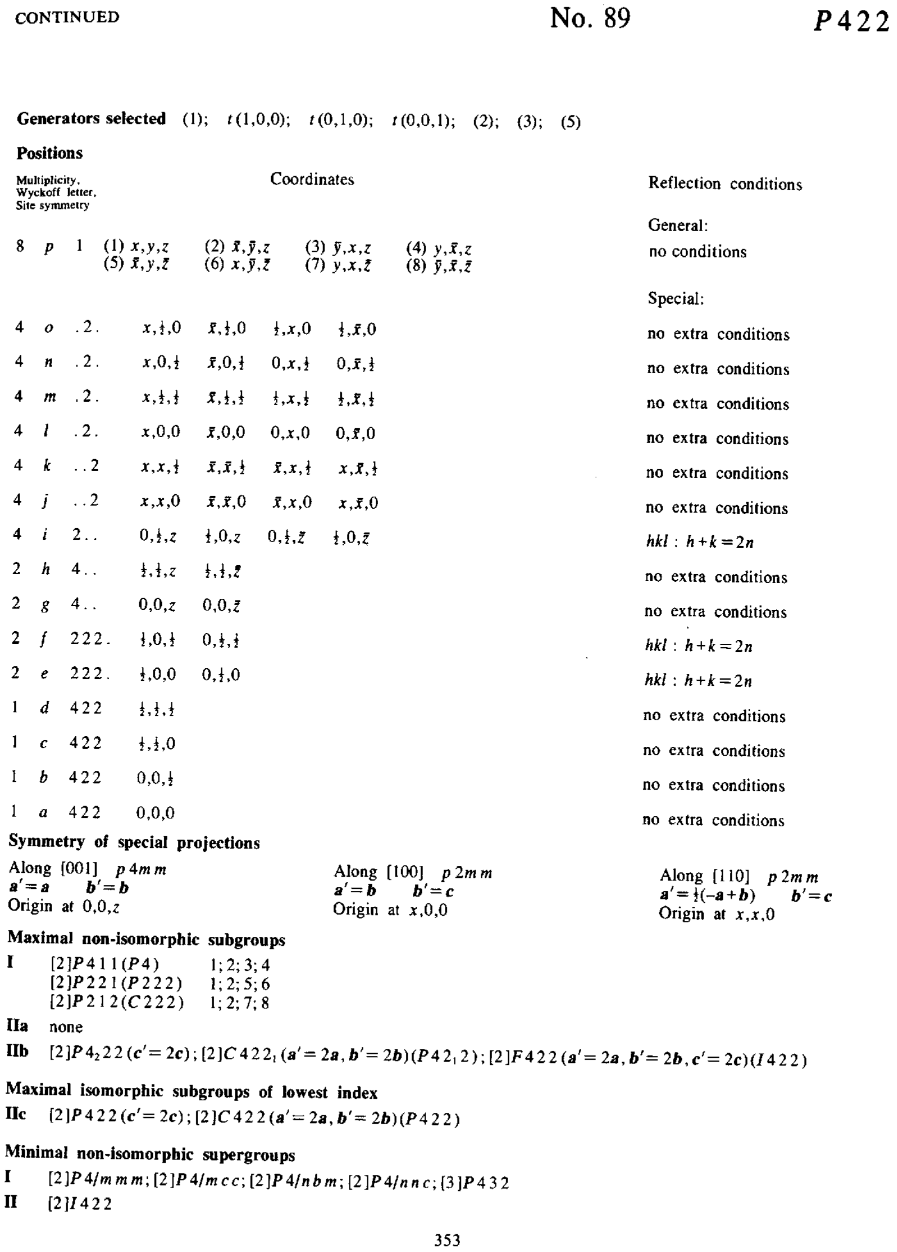

CONTINUED No. 89 *P*422

Generators selected (1); $t(1,0,0)$; $t(0,1,0)$; $t(0,0,1)$; (2); (3); (5)

Positions

Multiplicity, Wyckoff letter, Site symmetry			Coordinates				Reflection conditions
							General:
8	*p*	1	(1) x,y,z (5) $\bar{x},y,\bar{z}$	(2) $\bar{x},\bar{y},z$ (6) $x,\bar{y},\bar{z}$	(3) $\bar{y},x,z$ (7) $y,x,\bar{z}$	(4) $y,\bar{x},z$ (8) $\bar{y},\bar{x},\bar{z}$	no conditions
							Special:
4	*o*	.2.	$x,\frac{1}{2},0$	$\bar{x},\frac{1}{2},0$	$\frac{1}{2},x,0$	$\frac{1}{2},\bar{x},0$	no extra conditions
4	*n*	.2.	$x,0,\frac{1}{2}$	$\bar{x},0,\frac{1}{2}$	$0,x,\frac{1}{2}$	$0,\bar{x},\frac{1}{2}$	no extra conditions
4	*m*	.2.	$x,\frac{1}{2},\frac{1}{2}$	$\bar{x},\frac{1}{2},\frac{1}{2}$	$\frac{1}{2},x,\frac{1}{2}$	$\frac{1}{2},\bar{x},\frac{1}{2}$	no extra conditions
4	*l*	.2.	$x,0,0$	$\bar{x},0,0$	$0,x,0$	$0,\bar{x},0$	no extra conditions
4	*k*	..2	$x,x,\frac{1}{2}$	$\bar{x},\bar{x},\frac{1}{2}$	$\bar{x},x,\frac{1}{2}$	$x,\bar{x},\frac{1}{2}$	no extra conditions
4	*j*	..2	$x,x,0$	$\bar{x},\bar{x},0$	$\bar{x},x,0$	$x,\bar{x},0$	no extra conditions
4	*i*	2..	$0,\frac{1}{2},z$	$\frac{1}{2},0,z$	$0,\frac{1}{2},\bar{z}$	$\frac{1}{2},0,\bar{z}$	$hkl: h+k=2n$
2	*h*	4..	$\frac{1}{2},\frac{1}{2},z$	$\frac{1}{2},\frac{1}{2},\bar{z}$			no extra conditions
2	*g*	4..	$0,0,z$	$0,0,\bar{z}$			no extra conditions
2	*f*	222.	$\frac{1}{2},0,\frac{1}{2}$	$0,\frac{1}{2},\frac{1}{2}$			$hkl: h+k=2n$
2	*e*	222.	$\frac{1}{2},0,0$	$0,\frac{1}{2},0$			$hkl: h+k=2n$
1	*d*	422	$\frac{1}{2},\frac{1}{2},\frac{1}{2}$				no extra conditions
1	*c*	422	$\frac{1}{2},\frac{1}{2},0$				no extra conditions
1	*b*	422	$0,0,\frac{1}{2}$				no extra conditions
1	*a*	422	$0,0,0$				no extra conditions

Symmetry of special projections

Along [001] *p*4*mm*	Along [100] *p*2*mm*	Along [110] *p*2*mm*
$\mathbf{a}'=\mathbf{a}$ $\mathbf{b}'=\mathbf{b}$	$\mathbf{a}'=\mathbf{b}$ $\mathbf{b}'=\mathbf{c}$	$\mathbf{a}'=\frac{1}{2}(-\mathbf{a}+\mathbf{b})$ $\mathbf{b}'=\mathbf{c}$
Origin at $0,0,z$	Origin at $x,0,0$	Origin at $x,x,0$

Maximal non-isomorphic subgroups

I	[2]*P*411(*P*4)	1; 2; 3; 4
	[2]*P*221(*P*222)	1; 2; 5; 6
	[2]*P*212(*C*222)	1; 2; 7; 8

IIa none

IIb [2]$P4_222$ $(\mathbf{c}'=2\mathbf{c})$; [2]$C422_1$ $(\mathbf{a}'=2\mathbf{a}, \mathbf{b}'=2\mathbf{b})$($P42_12$); [2]$F422$ $(\mathbf{a}'=2\mathbf{a}, \mathbf{b}'=2\mathbf{b}, \mathbf{c}'=2\mathbf{c})$($I422$)

Maximal isomorphic subgroups of lowest index

IIc [2]$P422$ $(\mathbf{c}'=2\mathbf{c})$; [2]$C422$ $(\mathbf{a}'=2\mathbf{a}, \mathbf{b}'=2\mathbf{b})$($P422$)

Minimal non-isomorphic supergroups

I [2]*P*4/*mmm*; [2]*P*4/*mcc*; [2]*P*4/*nbm*; [2]*P*4/*nnc*; [3]*P*432

II [2]*I*422

353

P422 (No 89)

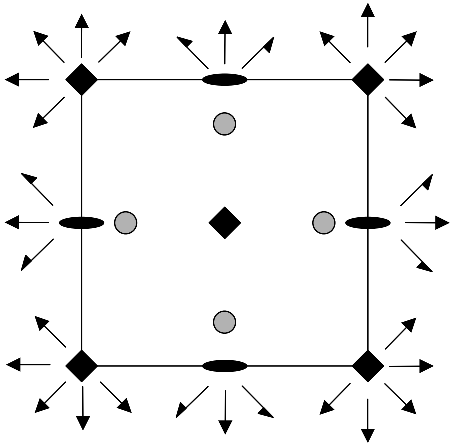

Special position: 4o [.2.] x, ½, 0

P42’2’

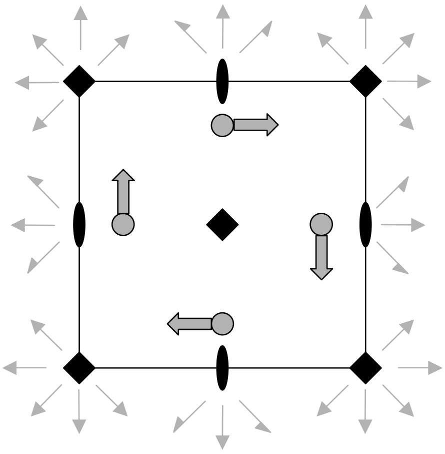

Special position: 4o [.2.] x, ½, 0

P_P422

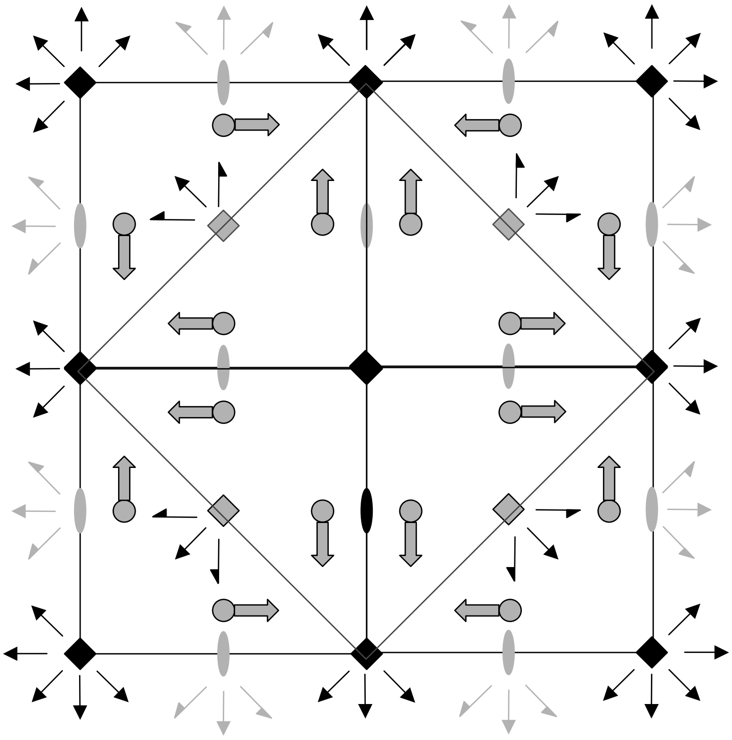

$Pnma$ D_{2h}^{16} mmm Orthorhombic

No. 62 $P\,2_1/n\,2_1/m\,2_1/a$ Patterson symmetry $Pmmm$

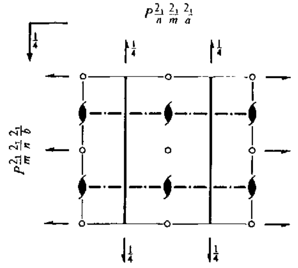

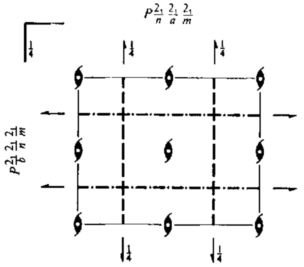

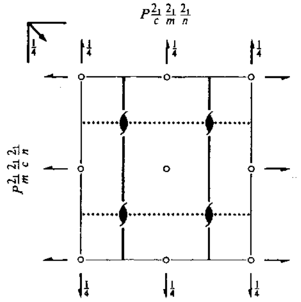

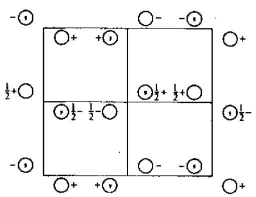

Origin at $\bar{1}$ on $1\,2_1\,1$

Asymmetric unit $0\leq x\leq\frac{1}{2};\quad 0\leq y\leq\frac{1}{4};\quad 0\leq z\leq 1$

Symmetry operations

(1) 1	(2) $2(0,0,\frac{1}{2})\ \ \frac{1}{4},0,z$	(3) $2(0,\frac{1}{2},0)\ \ 0,y,0$	(4) $2(\frac{1}{2},0,0)\ \ x,\frac{1}{4},\frac{1}{4}$
(5) $\bar{1}$ 0,0,0	(6) $a\ \ x,y,\frac{1}{4}$	(7) $m\ \ x,\frac{1}{4},z$	(8) $n(0,\frac{1}{2},\frac{1}{2})\ \ \frac{1}{4},y,z$

Generators selected (1); $t(1,0,0)$; $t(0,1,0)$; $t(0,0,1)$; (2); (3); (5)

Positions

Multiplicity, Wyckoff letter, Site symmetry			Coordinates				Reflection conditions
8	d	1	(1) x,y,z (5) $\bar{x},\bar{y},\bar{z}$	(2) $\bar{x}+\frac{1}{2},\bar{y},z+\frac{1}{2}$ (6) $x+\frac{1}{2},y,\bar{z}+\frac{1}{2}$	(3) $\bar{x},y+\frac{1}{2},\bar{z}$ (7) $x,\bar{y}+\frac{1}{2},z$	(4) $x+\frac{1}{2},\bar{y}+\frac{1}{2},\bar{z}+\frac{1}{2}$ (8) $\bar{x}+\frac{1}{2},y+\frac{1}{2},z+\frac{1}{2}$	General: $0kl: k+l=2n$ $hk0: h=2n$ $h00: h=2n$ $0k0: k=2n$ $00l: l=2n$ Special: as above, plus
4	c	$.m.$	$x,\frac{1}{4},z$	$\bar{x}+\frac{1}{2},\frac{3}{4},z+\frac{1}{2}$	$\bar{x},\frac{3}{4},\bar{z}$	$x+\frac{1}{2},\frac{1}{4},\bar{z}+\frac{1}{2}$	no extra conditions
4	b	$\bar{1}$	$0,0,\frac{1}{2}$	$\frac{1}{2},0,0$	$0,\frac{1}{2},\frac{1}{2}$	$\frac{1}{2},\frac{1}{2},0$	$hkl: h+l,k=2n$
4	a	$\bar{1}$	$0,0,0$	$\frac{1}{2},0,\frac{1}{2}$	$0,\frac{1}{2},0$	$\frac{1}{2},\frac{1}{2},\frac{1}{2}$	$hkl: h+l,k=2n$

Symmetry of special projections

Along [001] $p2gm$	Along [100] $c2mm$	Along [010] $p2gg$
$\mathbf{a}'=\frac{1}{2}\mathbf{a}$ $\mathbf{b}'=\mathbf{b}$	$\mathbf{a}'=\mathbf{b}$ $\mathbf{b}'=\mathbf{c}$	$\mathbf{a}'=\mathbf{c}$ $\mathbf{b}'=\mathbf{a}$
Origin at $0,0,z$	Origin at $x,\frac{1}{4},\frac{1}{4}$	Origin at $0,y,0$

Maximal non-isomorphic subgroups

I	$[2]P2_12_12_1$	1; 2; 3; 4
	$[2]P112_1/a\,(P2_1/c)$	1; 2; 5; 6
	$[2]P12_1/m1\,(P2_1/m)$	1; 3; 5; 7
	$[2]P2_1/n11\,(P2_1/c)$	1; 4; 5; 8
	$[2]Pnm2_1\,(Pmn2_1)$	1; 2; 7; 8
	$[2]Pn2_1a\,(Pna2_1)$	1; 3; 6; 8
	$[2]P2_1ma\,(Pmc2_1)$	1; 4; 6; 7
IIa	none	
IIb	none	

Maximal isomorphic subgroups of lowest index

IIc $[3]Pnma(\mathbf{a}'=3\mathbf{a})$; $[3]Pnma(\mathbf{b}'=3\mathbf{b})$; $[3]Pnma(\mathbf{c}'=3\mathbf{c})$

Minimal non-isomorphic supergroups

I none

II $[2]Amma(Cmcm)$; $[2]Bbmm(Cmcm)$; $[2]Ccmb(Cmca)$; $[2]Imma$; $[2]Pnmm(2\mathbf{a}'=\mathbf{a})(Pmmn)$; $[2]Pcma(2\mathbf{b}'=\mathbf{b})(Pbam)$; $[2]Pbma(2\mathbf{c}'=\mathbf{c})(Pbcm)$

Pnma (Pbnm)

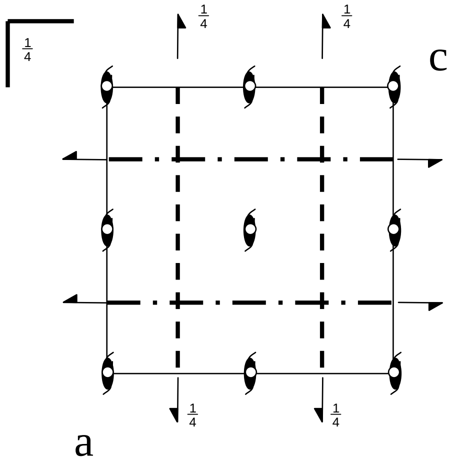

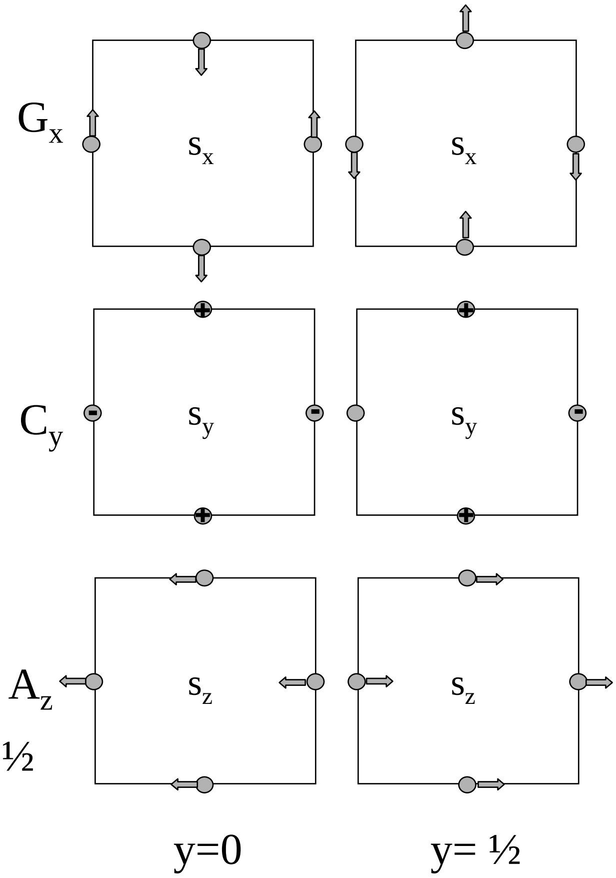

Special position: 4b [$\bar{1}$] 0,0, ½

Pn’m’a’ (Pb’n’m’)

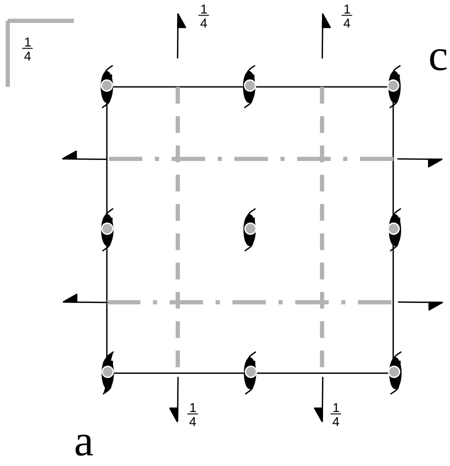

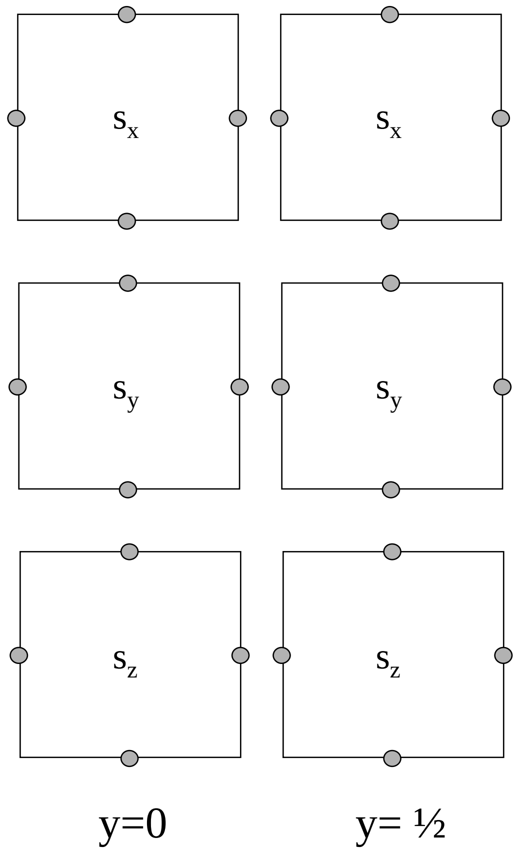

Special position: 4b [$\bar{1}$] 0,0, ½

Pn’m’a (Pb n’m’)

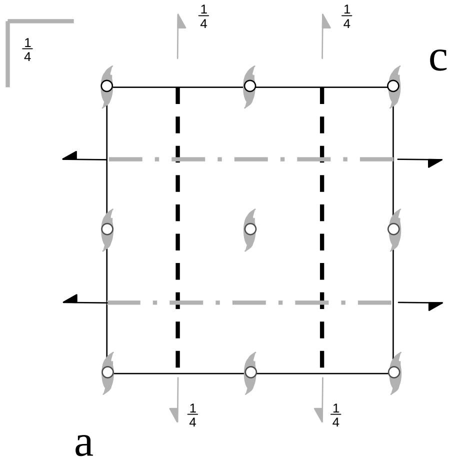

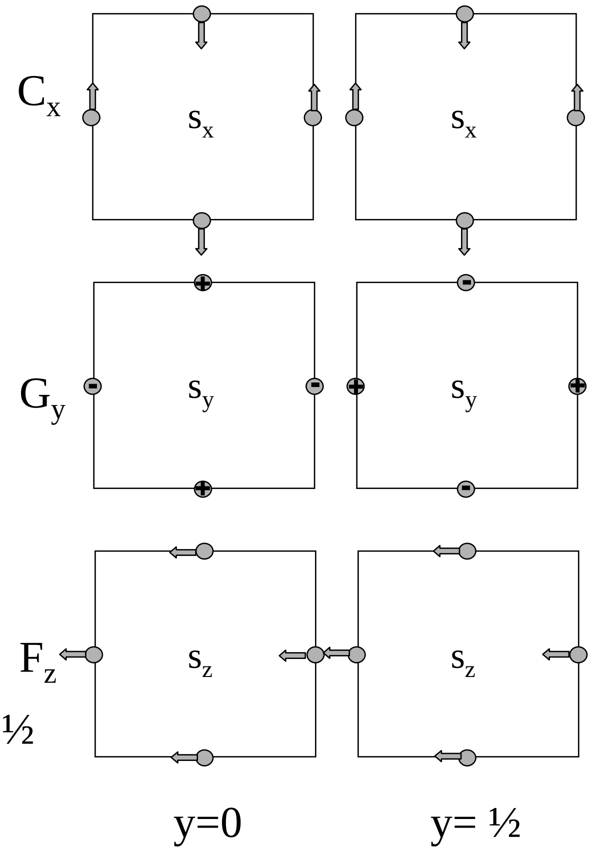

Special position: 4b [$\bar{1}$] 0,0, ½

Pn’ma’ (Pb’ n’m)

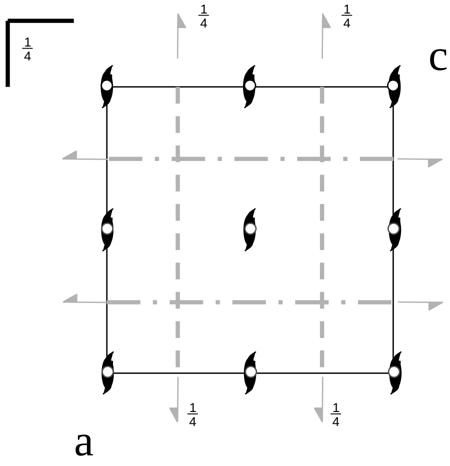

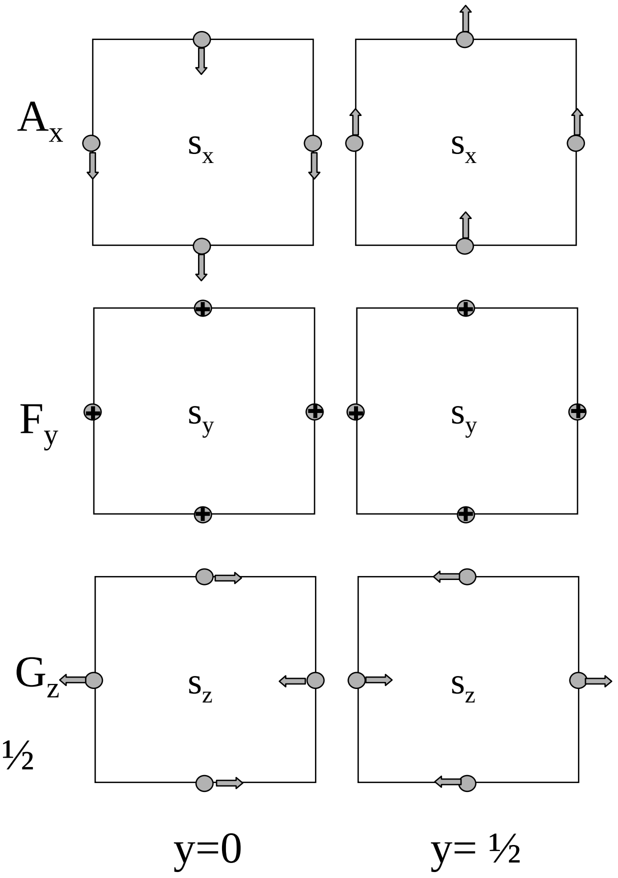

Special position: 4b [$\bar{1}$] 0,0, ½

Pnm’a’ (Pb’nm’)

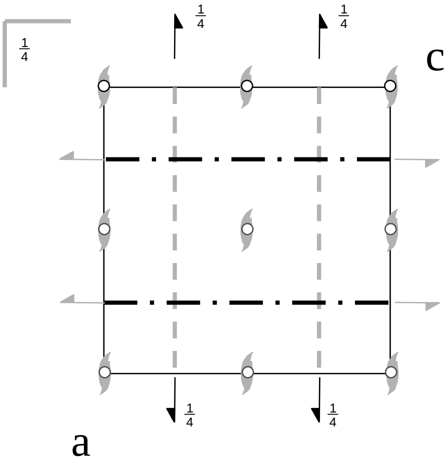

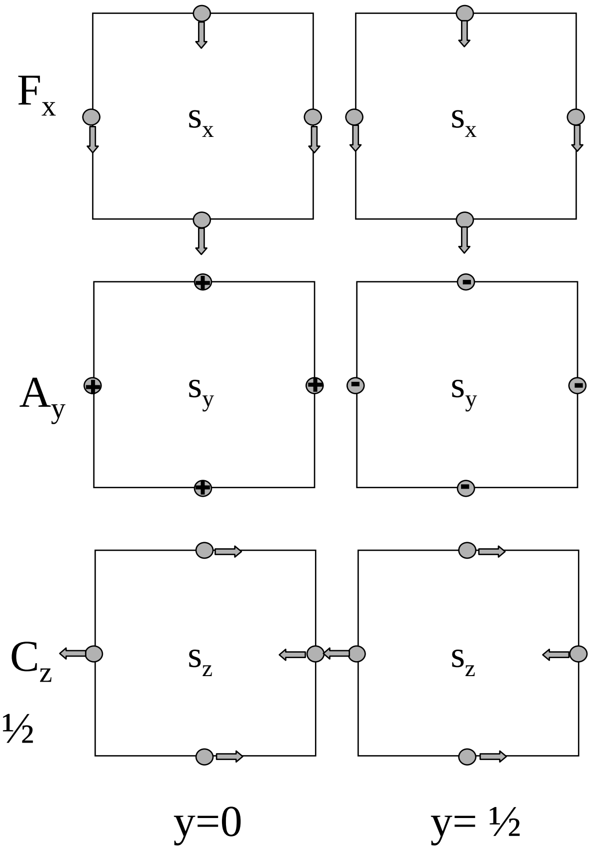

Special position: 4b [$\bar{1}$] 0,0, ½

Pnma’ (Pb’nm)

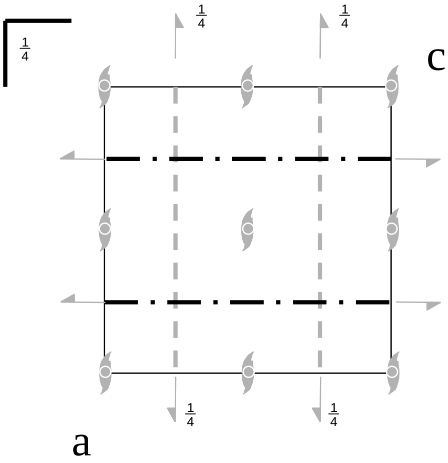

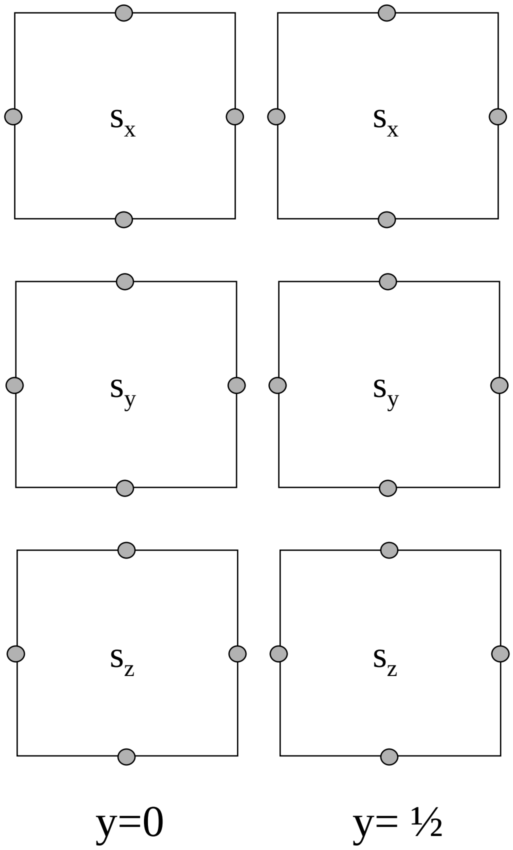

Special position: 4b [$\bar{1}$] 0,0, ½

Pnm'a (Pbnm')

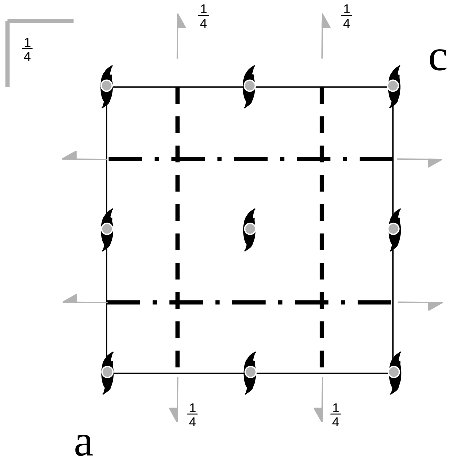

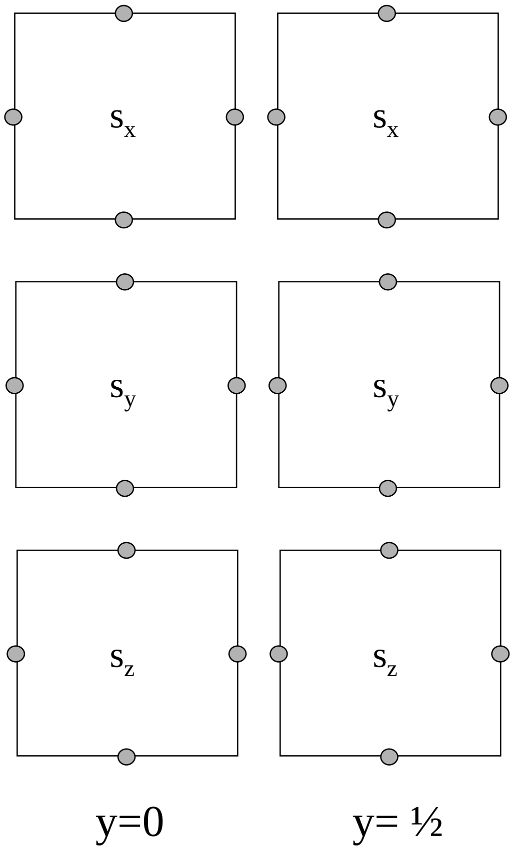

Special position: 4b [$\bar{1}$] 0,0, ½

Pn'ma (Pbn'm)

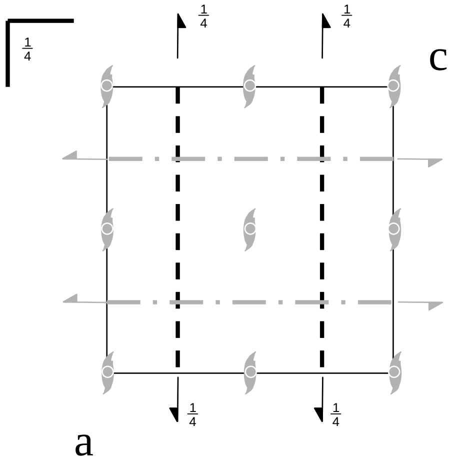

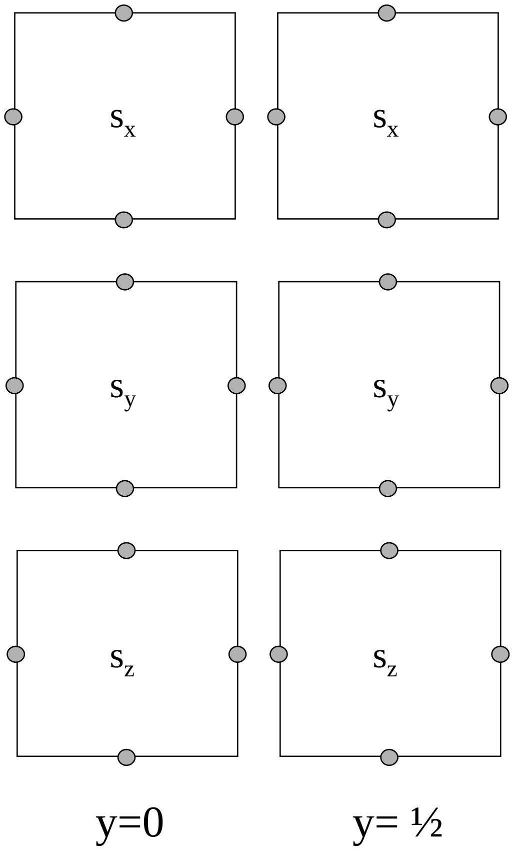

Special position: 4b [$\bar{1}$] 0,0, ½

Magnetic Structure Determination

Juan Rodriguez-Carvajal

Magnetic Structure Determination. What can we learn from a magnetic structure refined from neutron powder diffraction?
(Tutorial, overview, ...)

Juan Rodríguez-Carvajal
Laboratoire Léon Brillouin (CEA-CNRS)
DRECAM-CEA/Saclay, France
&
Service de Physique Statistique,
Magnétisme et Supraconductivité
DRFMC-CEA/Grenoble, France

Content:

- What's and why magnetic structures
- Formalism to describe magnetic structures
- The Rietveld method
- Magnetic neutron scattering
- Magnetic structure determination:

Indexing:	***SuperCell***
Symmetry Analysis:	***BasIreps***
Simulated Annealing:	***FullProf***

- Examples
- SIMBO and ENERMAG: programs to analyze exchange interactions.

Ions with intrinsic magnetic moments

Atoms/ions with unpaired electrons

Intra-atomic electron correlation
Hund's rule: maximum S

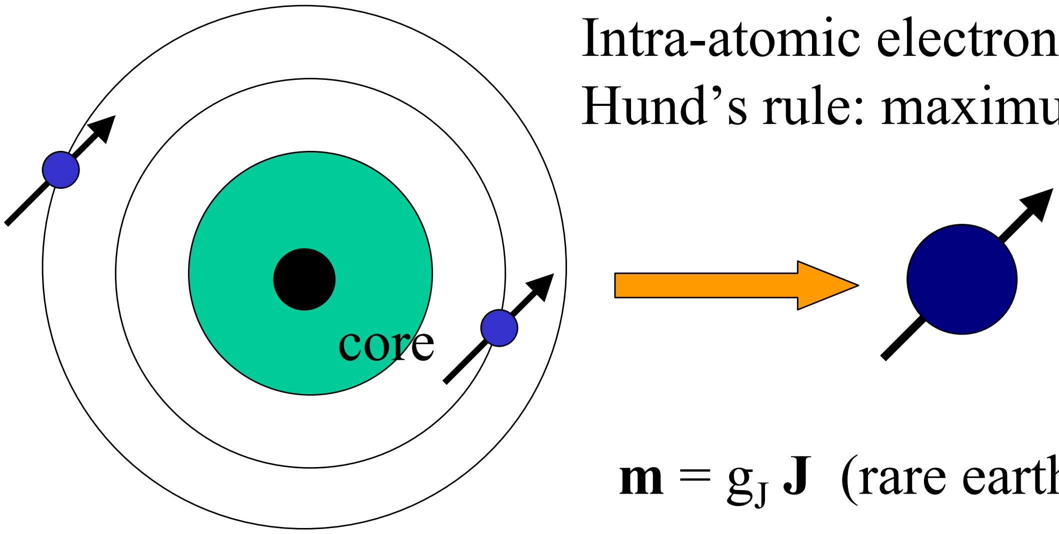

Ni^{2+}

$\mathbf{m} = g_J \, \mathbf{J}$ (rare earths)

$\mathbf{m} = g_S \, \mathbf{S}$ (transition metals)

What is a magnetic structure? (1)

Paramagnetic state:
Snapshot of magnetic moment configuration

$$E_{ij} = -J_{ij} \, \mathbf{S}_i \cdot \mathbf{S}_j$$

$$\langle \mathbf{S}_i \rangle = 0$$

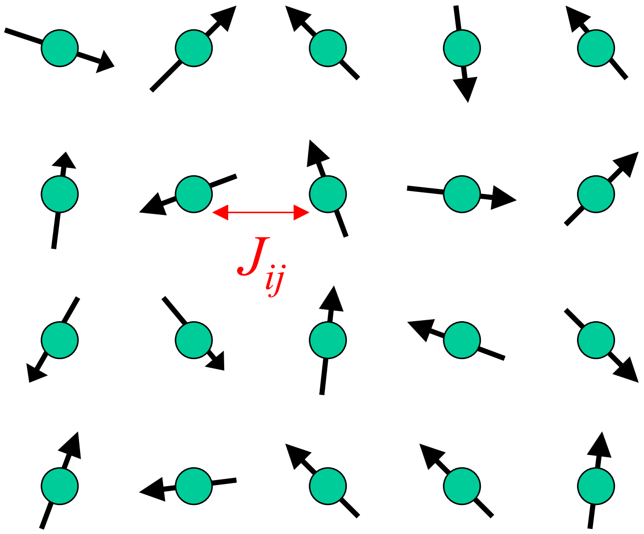

What is a magnetic structure? (2)

Ordered state: Anti-ferromagnetic
Small fluctuations (spin waves) of the static configuration

$$E_{ij} = -J_{ij}\ \mathbf{S}_i \cdot \mathbf{S}_j$$

$$\langle \mathbf{S}_i \rangle \neq 0$$

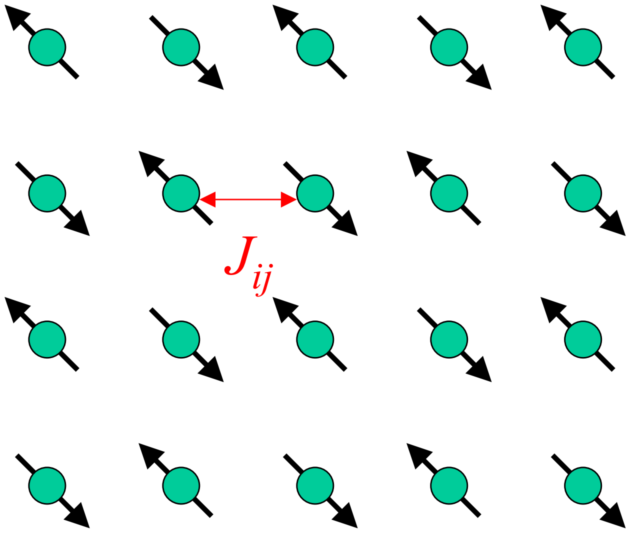

Magnetic structure:
Quasi-static configuration of magnetic moments

Magnetic structures for what?

- **Fundamental properties of condensed matter. Exchange interactions related to the electronic structure.**
- **The first step for determining the exchange interactions by inelastic neutron scattering**
- **Permanent magnet industry. Chemical substitutions controlling single ion anisotropy, strength of effective interactions, canting angles, etc: NdFeB materials, $SmCo_5$, hexaferrites, spinel ferrites.**
- **Spin electronics, thin films and mutilayers**

Formalism to describe magnetic structures

Geometric relation between magnetic moments of crystallographically equivalent atoms

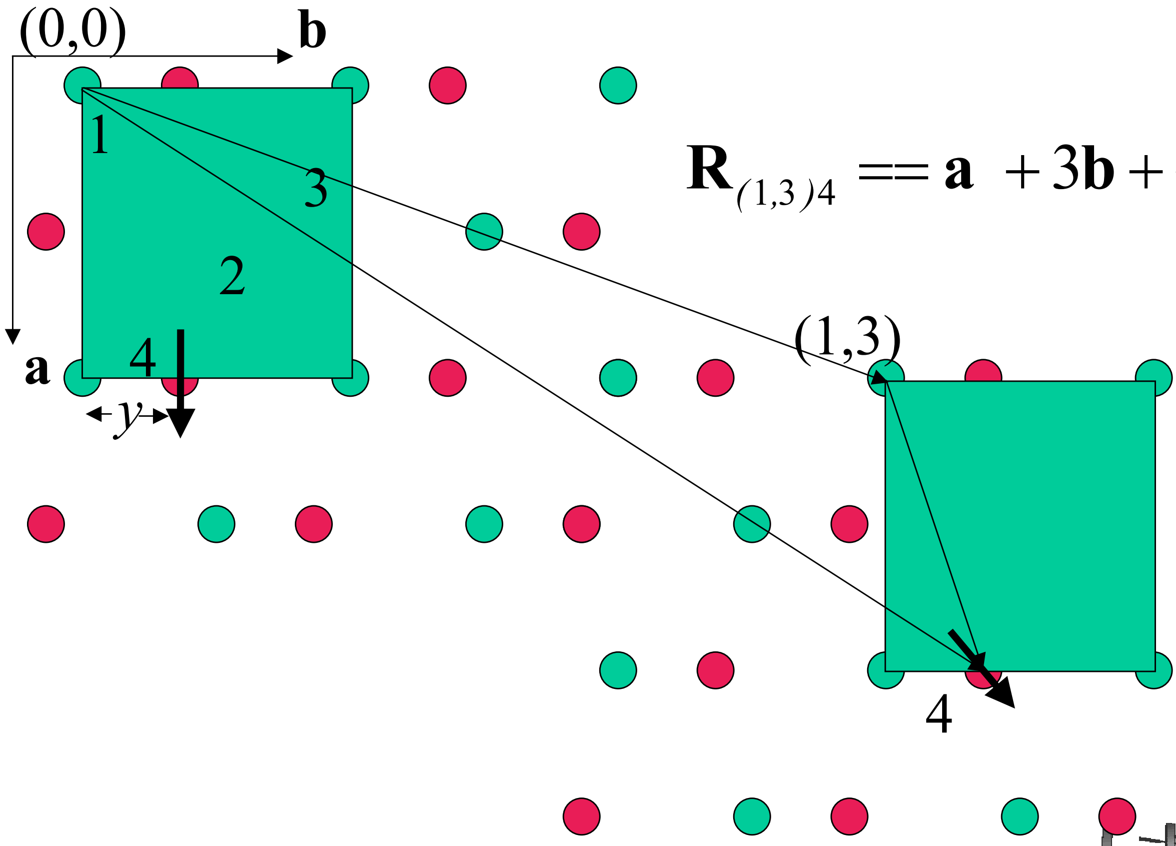

$$\mathbf{R}_{(1,3)4} == \mathbf{a} + 3\mathbf{b} + \frac{1}{2}\mathbf{a} + y\mathbf{b}$$

Magnetic structures
Magnetic moment of each atom: Fourier series

$$\mathbf{m}_{lj} = \sum_{\{\mathbf{k}\}} \mathbf{S}_{\mathbf{k}j}\ exp\{-2\pi\, i\mathbf{k}\mathbf{R}_l\}$$

Necessary condition for real $\mathbf{m}_{lj} \Rightarrow\ \mathbf{S}_{-\mathbf{k}j} = \mathbf{S}_{\mathbf{k}j}{}^{*}$

Position vector of atom "*j*" in the unit cell "*l*"

$$\mathbf{R}_{lj} = \mathbf{R}_l + \mathbf{r}_j = l_1\mathbf{a} + l_2\mathbf{b} + l_3\mathbf{c} + x_j\mathbf{a} + y_j\mathbf{b} + z_j\mathbf{c}$$

Examples of Fourier coefficients for simple magnetic structures
The simplest case:
Single propagation vector
$\mathbf{k} = (0,0,0)$

$$\mathbf{m}_{lj} = \sum_{\{\mathbf{k}\}} \mathbf{S}_{\mathbf{k}j}\ \ exp\{-2\pi i\mathbf{k}\mathbf{R}_l\} = \mathbf{S}_{\mathbf{k}j}$$

- The magnetic structure may be described within the crystallographic unit cell
- Magnetic symmetry: conventional crystallography plus time reversal operator: crystallographic magnetic groups

Examples of Fourier coefficients for simple magnetic structures

Single propagation vector

k=1/2 **H**

$$\mathbf{m}_{lj} = \sum_{\{\mathbf{k}\}} \mathbf{S}_{\mathbf{k}j}\; exp\{-2\pi i\,\mathbf{k}\mathbf{R}_l\} = \mathbf{S}_{\mathbf{k}j}\left(-1\right)^{n(l)}$$

REAL Fourier coefficients ≡ magnetic moments
The magnetic symmetry may also be described using crystallographic magnetic space groups

---

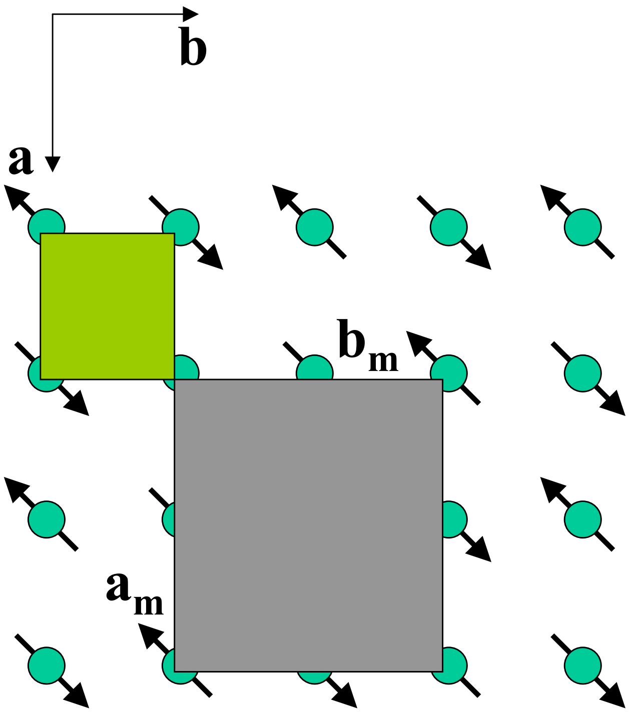

k= (1/2, 1/2)

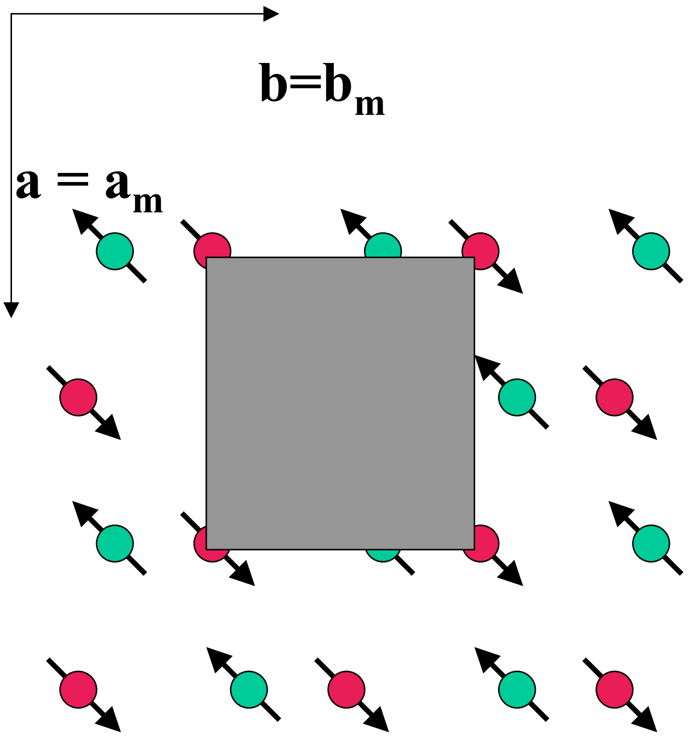

k= (0, 0)

Fourier coefficients of sinusoidal structures
k interior of the Brillouin zone (pair **k**, **-k**)
Real $\mathbf{S}_\mathbf{k}$, or imaginary component in the same direction as the real one

$$\mathbf{m}_{lj} = \mathbf{S}_{\mathbf{k}j}\ exp(-2\pi i\mathbf{k}\mathbf{R}_l) + \mathbf{S}_{-\mathbf{k}j}\ exp(2\pi i\mathbf{k}\mathbf{R}_l)$$

$$\mathbf{S}_{\mathbf{k}j} = \frac{1}{2} m_j \mathbf{u}_j exp(-2\pi i\phi_{\mathbf{k}j})$$

$$\mathbf{m}_{lj} = m_j \mathbf{u}_j \cos 2\pi(\mathbf{k}\mathbf{R}_l + \phi_{\mathbf{k}j})$$

Sinusoidal magnetic structure

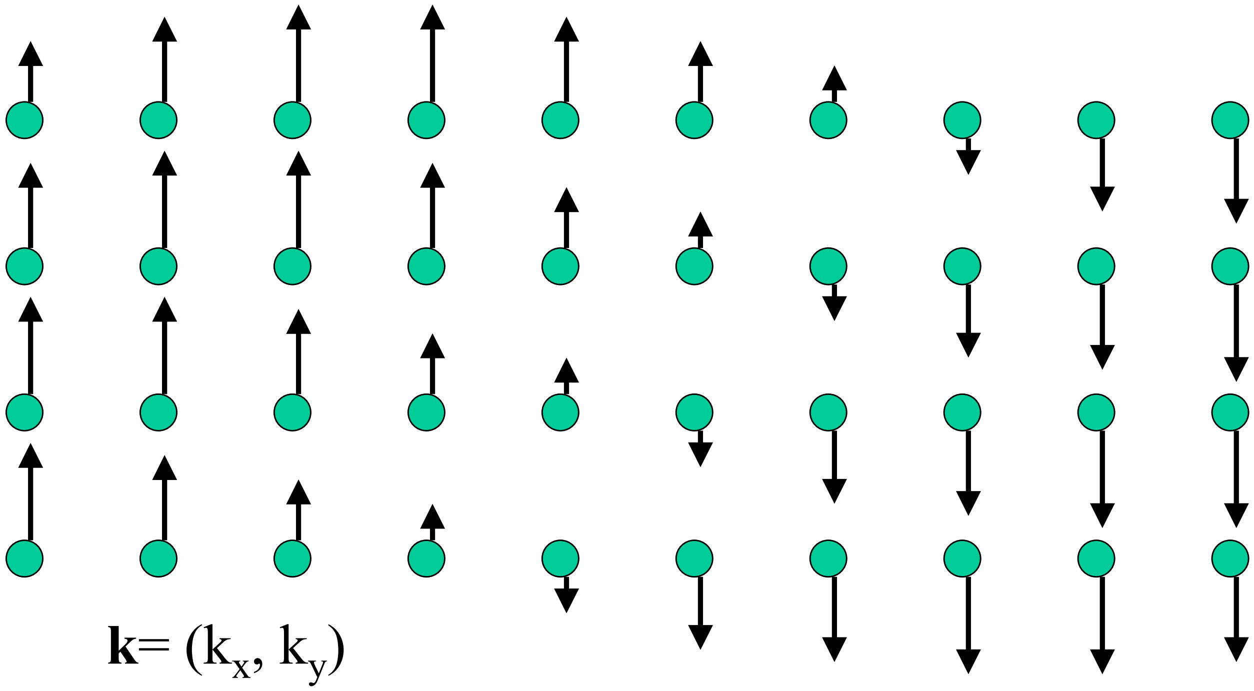

Fourier coefficients of helical structures **k** interior of the Brillouin zone Real component of $\mathbf{S}_{\mathbf{k}}$ perpendicular to the imaginary component

$$\mathbf{S}_{\mathbf{k}j} = \frac{1}{2}\left[m_{uj}\mathbf{u}_j + i m_{vj}\mathbf{v}_j \right] \ exp(-2\pi i\phi_{\mathbf{k}j})$$

$$\mathbf{m}_{lj} = m_{uj}\mathbf{u}_j \cos 2\pi(\mathbf{k}\mathbf{R}_l + \phi_{\mathbf{k}j}) + m_{vj}\mathbf{v}_j \sin 2\pi(\mathbf{k}\mathbf{R}_l + \phi_{\mathbf{k}j})$$

The Rietveld Method

A powder diffraction pattern can be recorded in numerical form for a discrete set of scattering angles, times of flight or energies. We will refer to this scattering variable as : T. The experimental powder diffraction pattern is usually given as two or three arrays :

$$\left\{T_i, y_i, \sigma_i\right\}_{i=1,\ldots,n}$$

The profile can be modelled using the calculated counts: y_{ci} at the *i*th step by summing the contribution from neighbouring Bragg reflections plus the background.

Powder diffraction profile:
scattering variable *T*: 2θ, TOF, Energy

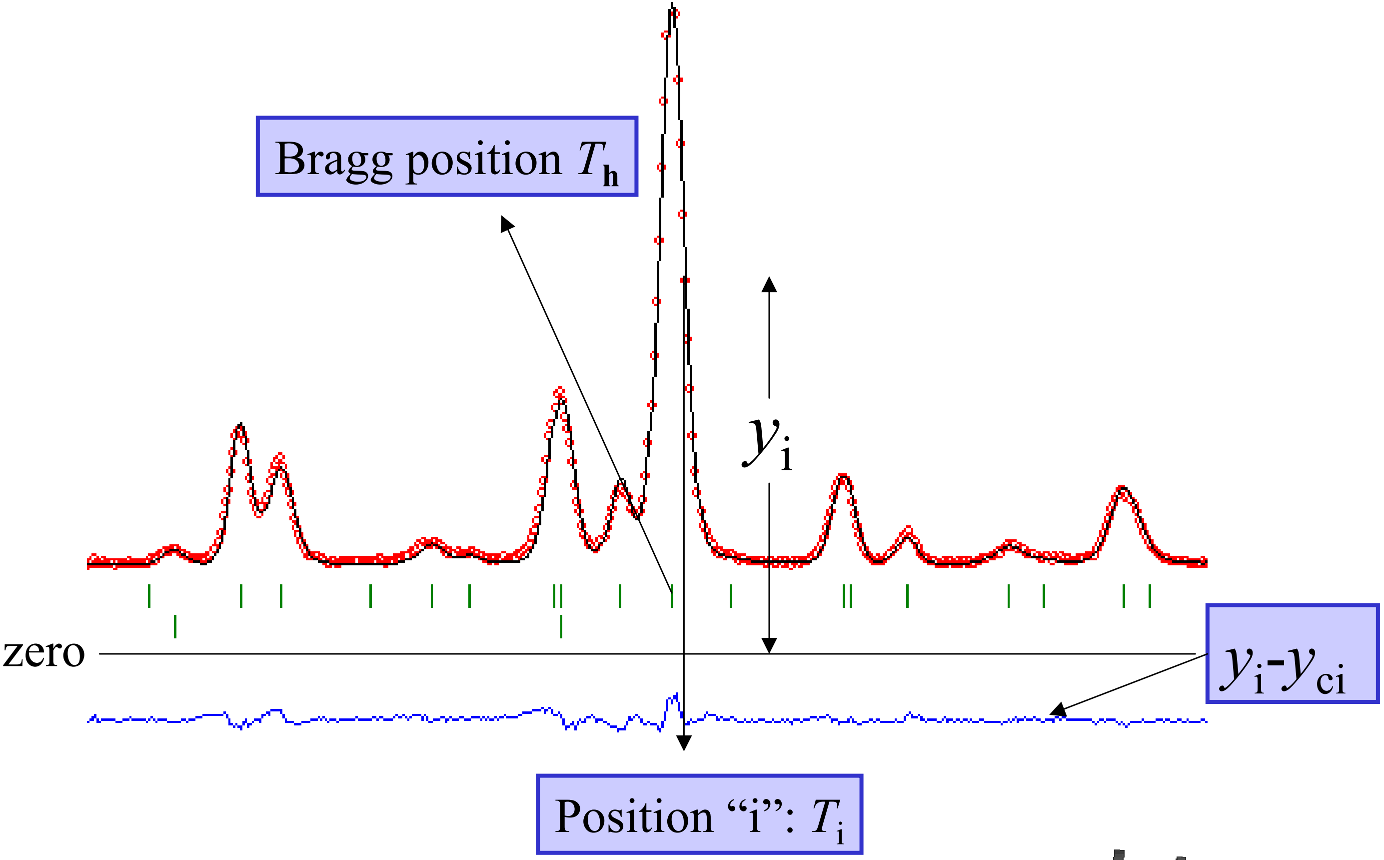

Bragg position $T_\mathbf{h}$

y_i

zero

y_i-y_ci

Position “i”: T_i

The profile of powder diffraction patterns

The model to calculate a powder diffraction pattern is:

$$y_{ci} = \sum_{\mathbf{h}} I_{\mathbf{h}} \Omega(T_i - T_{\mathbf{h}}) + b_i$$

$$\int_{-\infty}^{+\infty} \Omega(x)dx = 1$$

Profile function characterized by its full width at half maximum (FWHM=*H*) and *shape* parameters (η, m, ...)

$$\Omega(x) = g(x) \otimes f(x) = instrumental \otimes intrinsic\, profile$$

The profile of powder diffraction patterns

$$\boxed{y_{ci} = \sum_{\mathbf{h}} I_{\mathbf{h}} \Omega(T_i - T_{\mathbf{h}}) + b_i}$$

$$I_{\mathbf{h}} = I_{\mathbf{h}}\left(\beta_s\right)$$

Contains structural information: atom positions, magnetic moments, etc

$$\Omega = \Omega(x_{\mathbf{h}i}, \beta_m)$$

Contains micro-structural information: inst. resolution, defects, crystallite size, ...

$$b_i = b_i\left(\beta_b\right)$$

Background: noise, diffuse scattering, ...

The Rietveld Method consist of refining a crystal (and/or magnetic) structure by minimising the weighted squared difference between the observed and the calculated pattern against the parameter vector: β

$$\boxed{\chi^2 = \sum_{i=1}^{n} w_i \left\{ y_i - y_{ci}(\beta) \right\}^2}$$

$$\boxed{w_i = \frac{1}{\sigma_i^2}}$$

σ_i^2: **is the variance of the "observation" y_i**

Magnetic neutron scattering

Diffraction pattern of incommensurate magnetic structures

Portion of reciprocal space

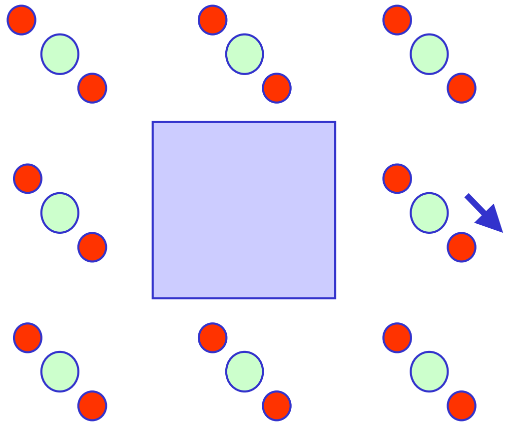

● Magnetic reflections

○ Nuclear reflections

h = H+k

Magnetic reflections: indexed by a set of propagation vectors {**k**}

H is a reciprocal vector of the crystallographic structure

k is one of the propagation vectors of the magnetic structure

(**k** is reduced to the Brillouin zone)

Setting up of magnetic ordering in a Tb-Pd-Sn compound

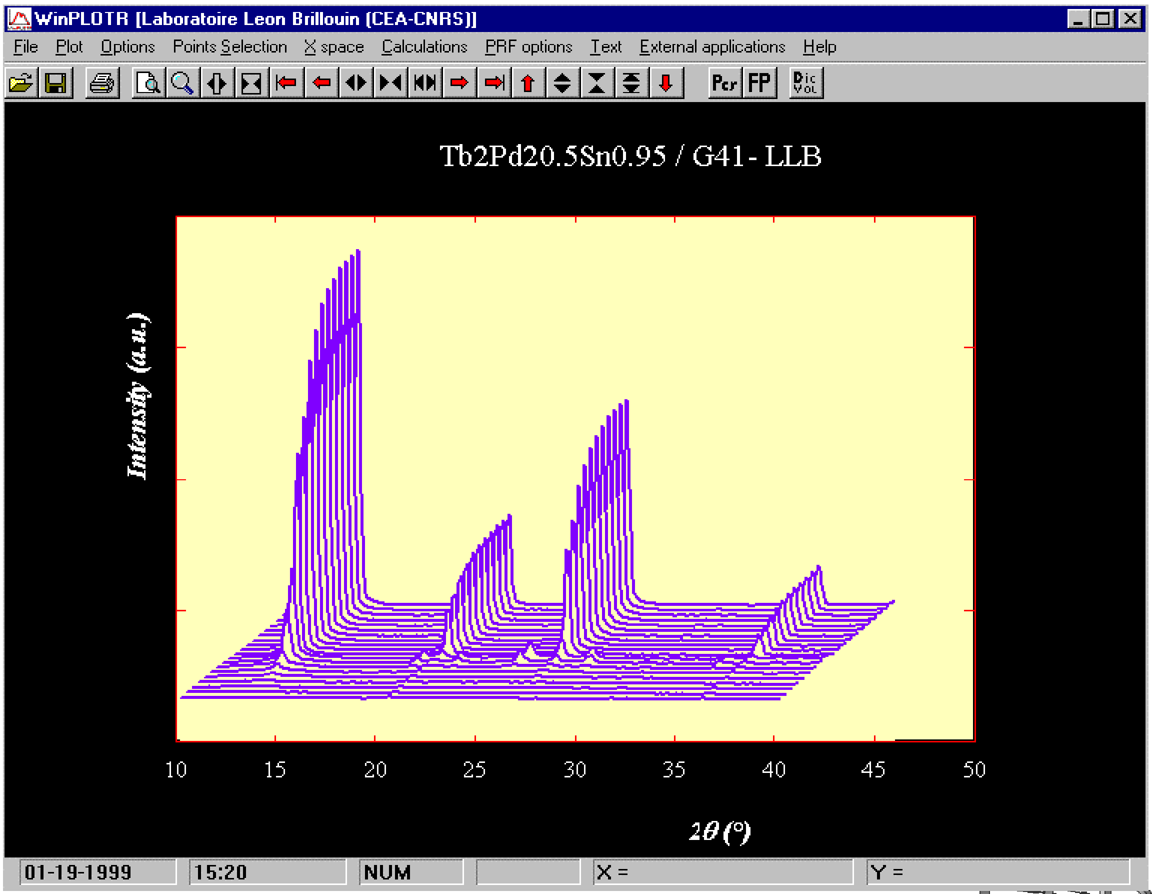

Magnetic structure of $DyMn_6Ge_6$

Conical structure with two propagation vectors

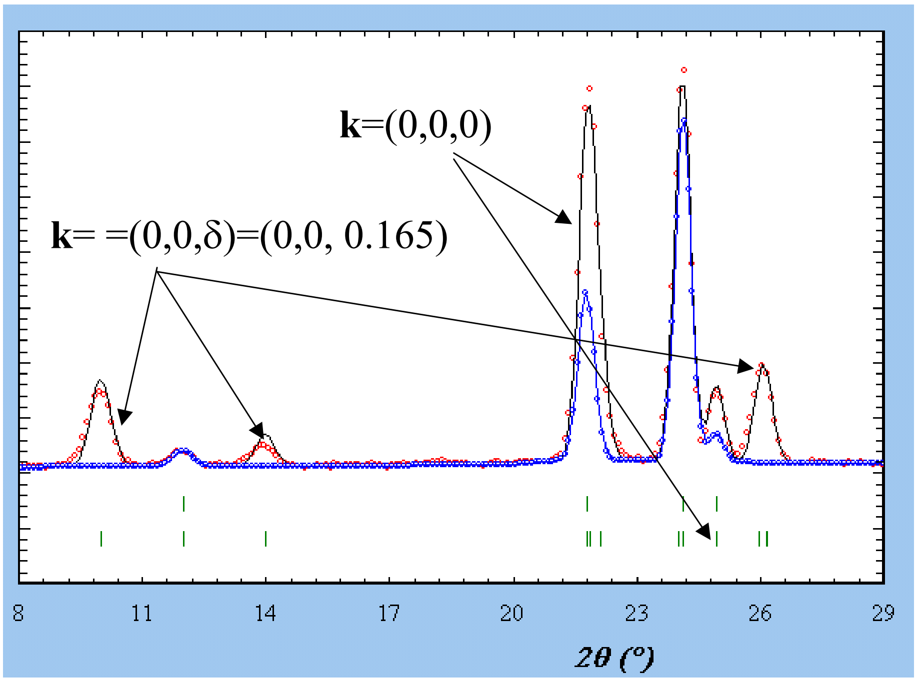

Nuclear contribution in blue

Magnetic scattering of neutrons

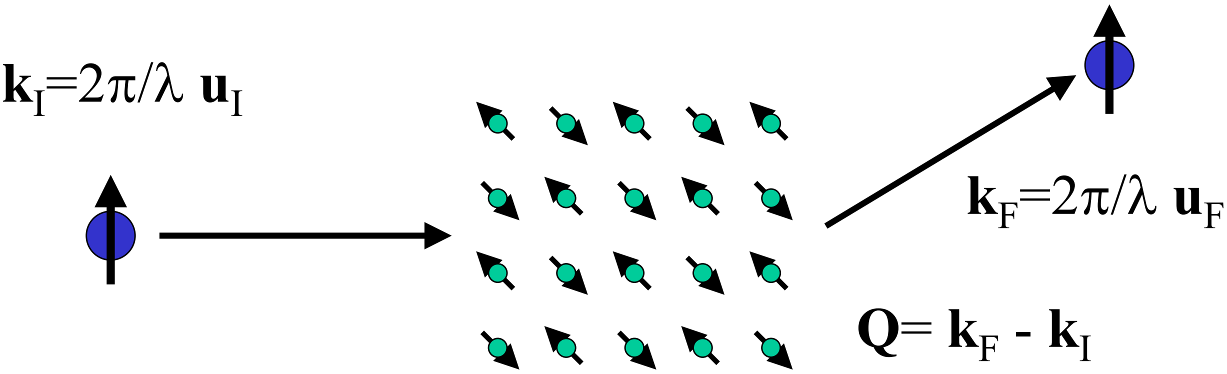

$\mathbf{k}_I = 2\pi/\lambda\ \mathbf{u}_I$

$\mathbf{k}_F = 2\pi/\lambda\ \mathbf{u}_F$

$\mathbf{Q} = \mathbf{k}_F - \mathbf{k}_I$

Dipolar interaction (μ_n , $\mathbf{m}$): vector scattering amplitude

$$\mathbf{a}_M(\mathbf{Q}) = \frac{1}{2} r_e \gamma f(\mathbf{Q}) \left\{ \mathbf{m} - \frac{\mathbf{Q}\ (\mathbf{m}\ \mathbf{Q})}{Q^2} \right\}$$

Magnetic scattering of neutrons

$$\mathbf{a}_M(\mathbf{Q}) = \frac{1}{2} r_e \gamma f(\mathbf{Q}) \left\{ \mathbf{m} - \frac{\mathbf{Q}\,(\mathbf{m}\,\mathbf{Q})}{Q^2} \right\} = p\, f(\mathbf{Q})\, \mathbf{m}_\perp$$

p=0.2696 10^{-12} cm

$$\boxed{f(\mathbf{Q}) = \int \rho_m(\mathbf{r}) \exp(i\,\mathbf{Q}\,\mathbf{r})\, d^3\mathbf{r}}$$

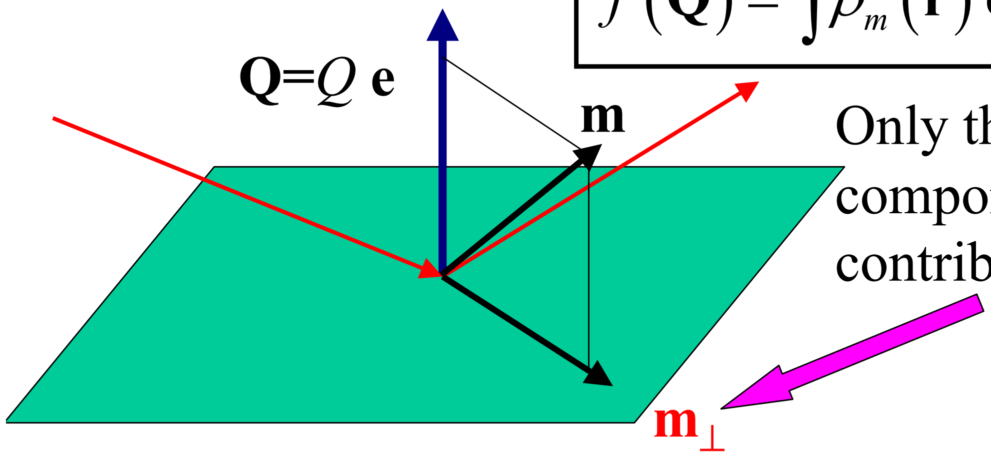

Only the perpendicular component of **m** to **Q**=2π**h** contributes to scattering

Magnetic Bragg scattering

Intensity (non-polarised neutrons)

$$I_{\mathbf{h}} = N_{\mathbf{h}} N^*_{\mathbf{h}} + \mathbf{M}_{\perp\mathbf{h}} \cdot \mathbf{M}^*_{\perp\mathbf{h}}$$

Magnetic interaction vector

$$\mathbf{M}_{\perp\mathbf{h}} = \mathbf{e} \times \mathbf{M}(\mathbf{h}) \times \mathbf{e} = \mathbf{M}(\mathbf{h}) - \mathbf{e}\,(\mathbf{e} \cdot \mathbf{M}(\mathbf{h}))$$

$\mathbf{h} = \mathbf{H} + \mathbf{k}$ ⇐ **Scattering vector** $\mathbf{e} = \dfrac{\mathbf{h}}{h}$

The magnetic structure factor:

$$\mathbf{M}(\mathbf{h}) = p\sum_{j=1}^{n} O_j\, f_j(\mathbf{h})\, T_j \sum_{s} \mathbf{S}_{\mathbf{k}js}\, exp\left\{2\pi i\left[(\mathbf{H}+\mathbf{k})\{S|\mathbf{t}\}_s \mathbf{r}_j - \Phi_{\mathbf{k}j}\right]\right\}$$

⬇

$$\mathbf{S}_{\mathbf{k}js} = \sum_{n\lambda} C^{\nu}_{n\lambda} \mathbf{S}^{\mathbf{k}\,\nu}_{n\lambda}(js)$$

$$\mathbf{M}(\mathbf{h}) = p\sum_{j=1}^{n} O_j\, f_j(\mathbf{h})\, T_j \sum_{n\lambda} C^{\nu}_{n\lambda} \sum_{s} \mathbf{S}^{\mathbf{k}\,\nu}_{n\lambda}(js)\, exp\left\{2\pi i\left[\mathbf{h}_s \mathbf{r}_j - \Phi_{\mathbf{k}j}\right]\right\}$$

Magnetic structure determination

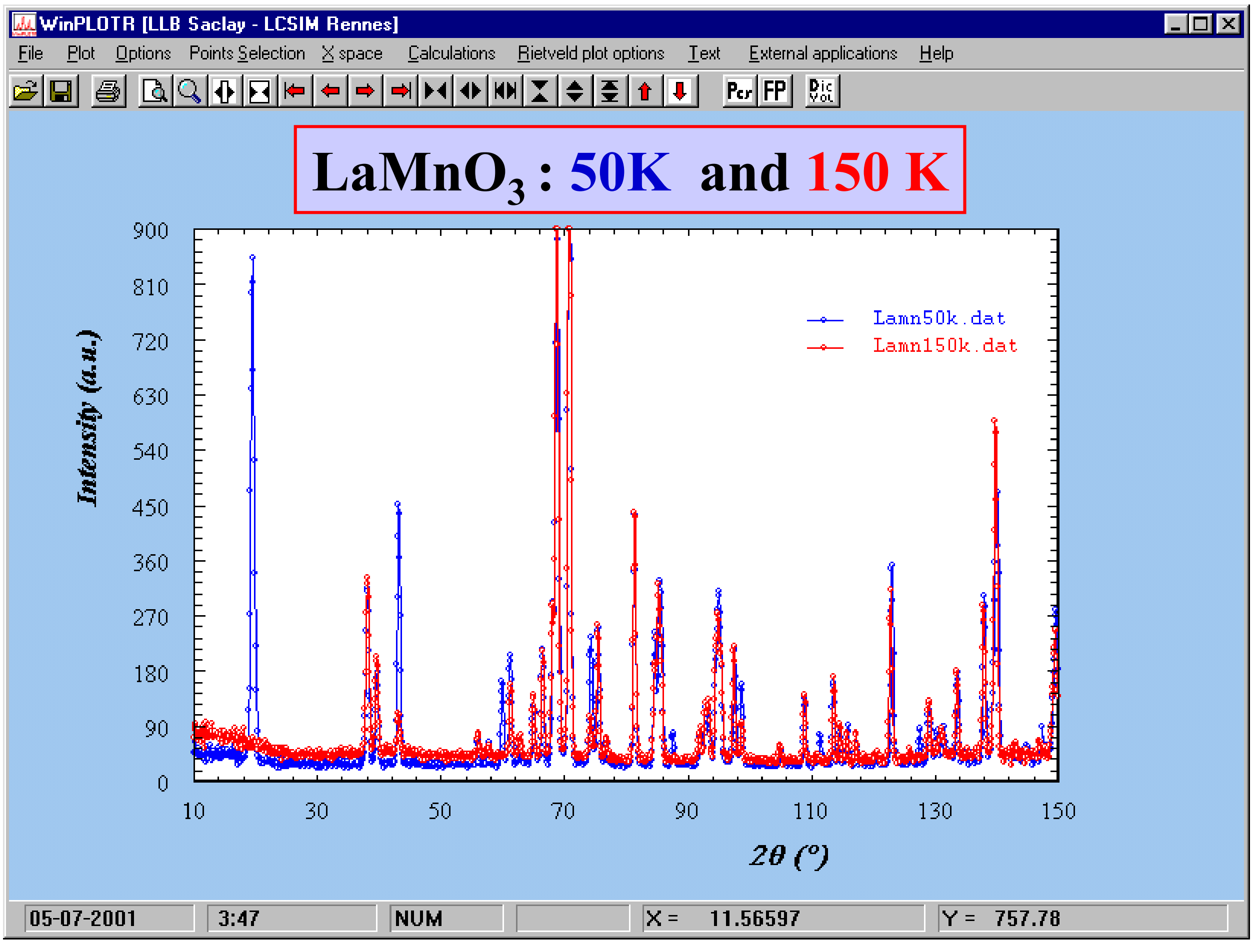

LaMnO$_3$: 50K and 150 K

05-07-2001 | 3:47 | NUM | X = 11.56597 | Y = 757.78

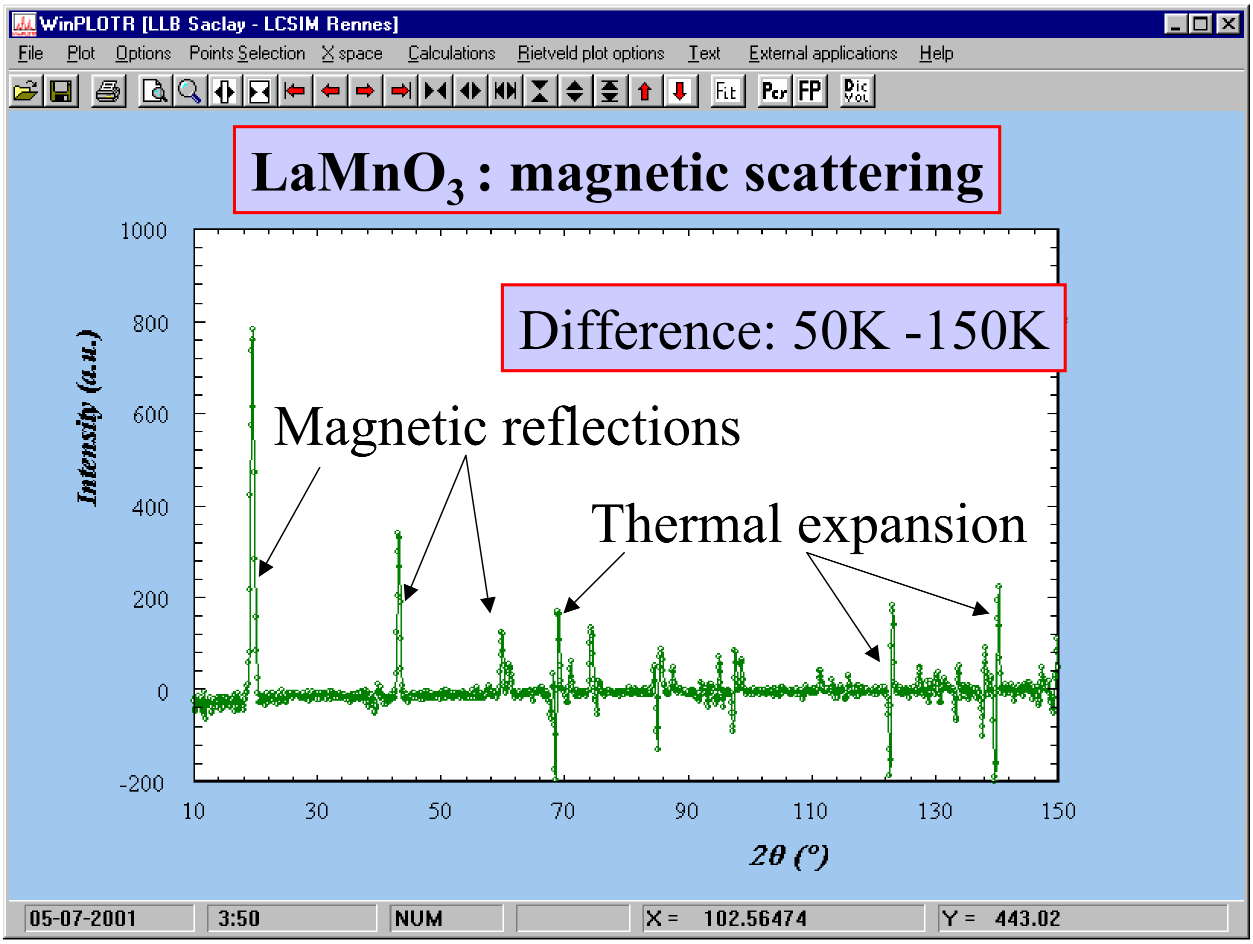

LaMnO$_3$: magnetic scattering

Difference: 50K -150K

Magnetic reflections

Thermal expansion

05-07-2001 | 3:50 | NUM | X = 102.56474 | Y = 443.02

Steps for Magnetic structure determination from Neutron Powder Diffraction

Propagation vector(s)
SuperCell

Peak positions of magnetic reflections
Cell parameters

Symmetry Analysis
BasIreps

Propagation vector
Space Group
Atom positions

Magnetic structure solution
***FullProf* (Simulated Annealing)**

Integrated intensities

Coefficients of the atomic components of basis functions

The Program *SuperCell*

(distributed within ***WinPLOTR***)

Program: ***SuperCell*** (J.Rodríguez-Carvajal, LLB-December-1998)

- This program can be used to index superstructure reflections from a powder diffraction pattern.
- The first approach consist in searching the best "magnetic unit cell" compatible with a set of observed SUPERSTRUCTURE lines in the powder diffraction pattern.
- If the first approach fails to give a suitable solution, the superstructure may be incommensurate and a direct search for the propagation vector and one of its harmonics have to be used.

LaMnO$_3$: Extraction of magnetic integrated intensities

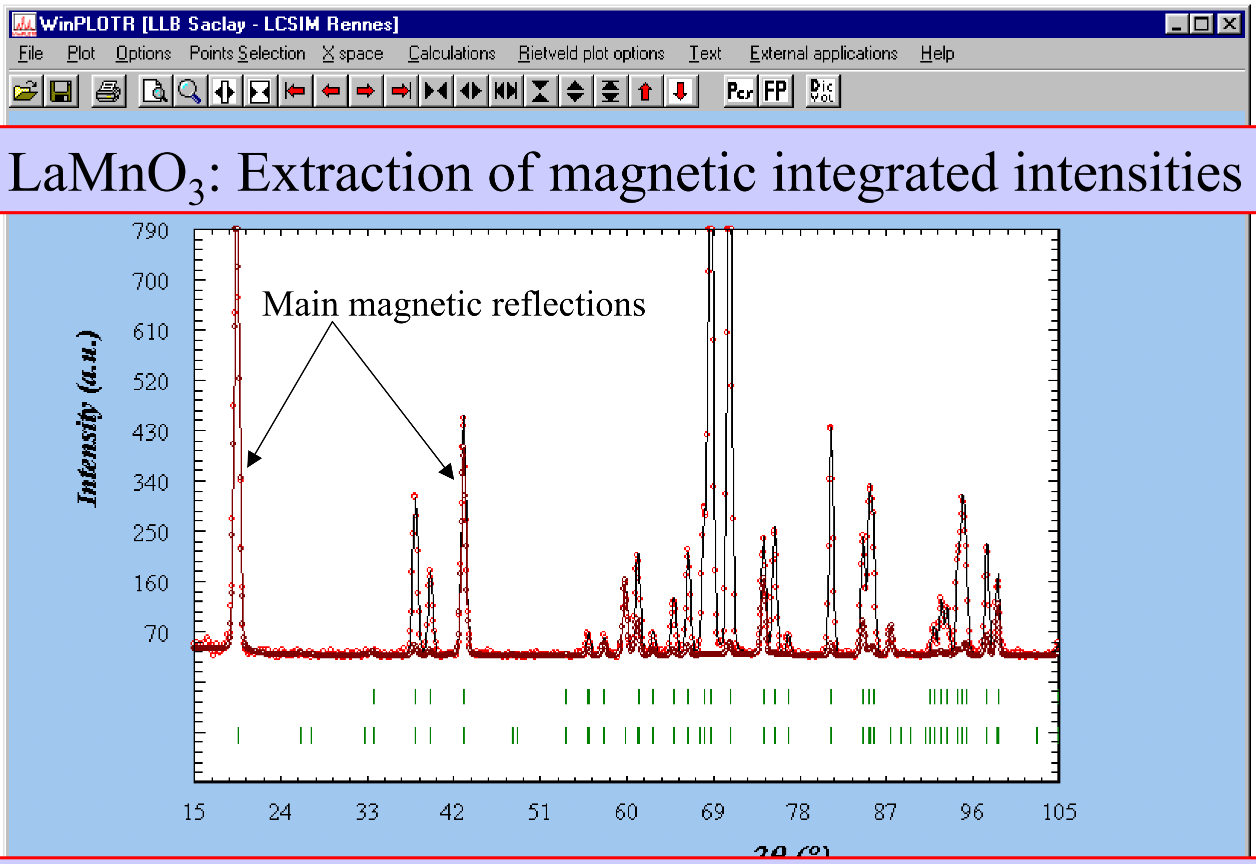

Propagation vector **k**=(0,0,0) ⇒ magnetic cell=crystal cell

---

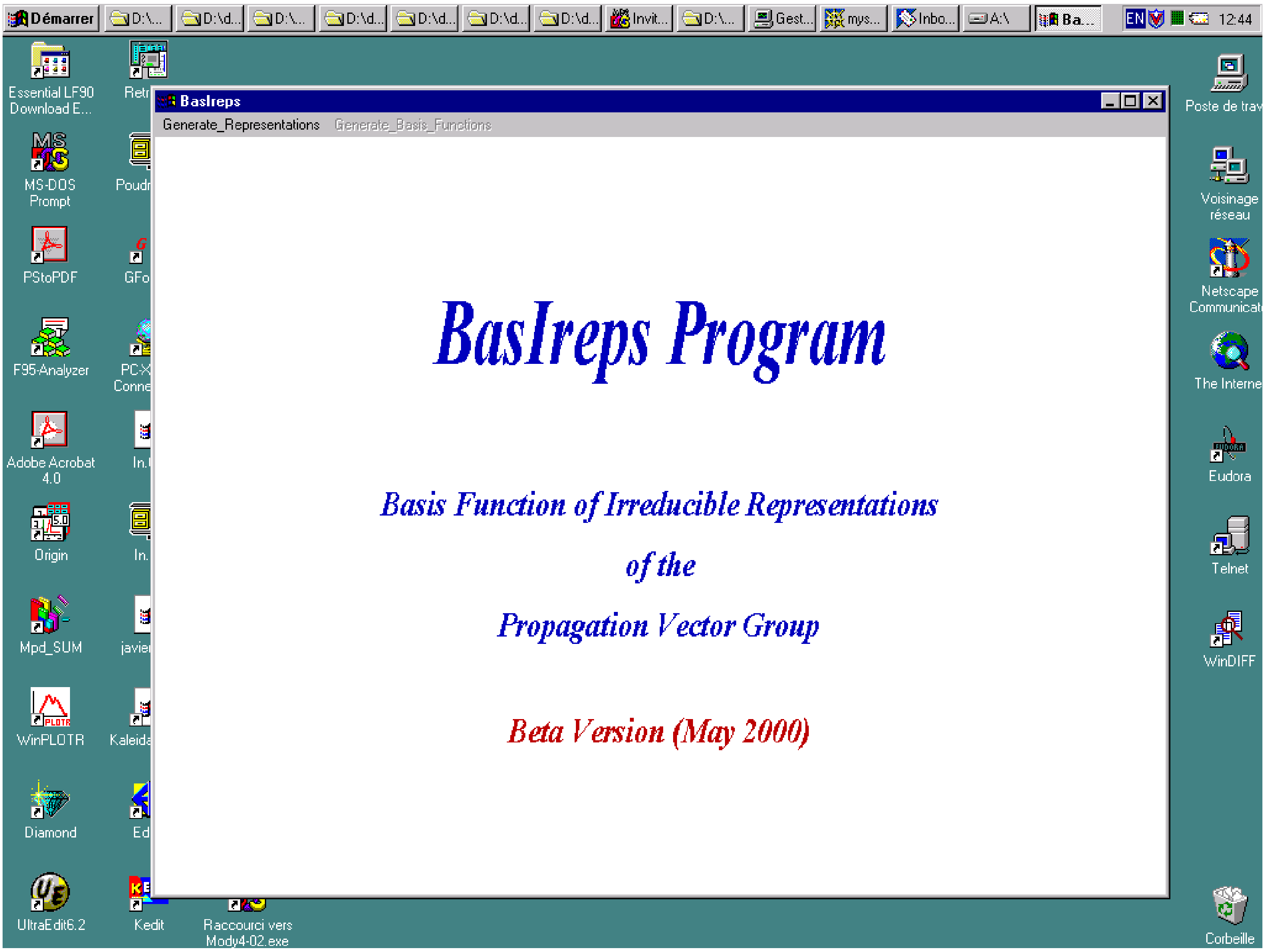

BasIreps Program

Basis Function of Irreducible Representations

of the

Propagation Vector Group

Beta Version (May 2000)

BasIreps provides the basis functions (normal modes) of the irreducible representations of the wave-vector group $\mathbf{G_k}$

$$\mathbf{m}_{ljs} = \sum_{\{\mathbf{k}\}} \mathbf{S}_{\mathbf{k}js} \; exp\{-2\pi i \mathbf{k}\mathbf{R}_l\}$$

$$\mathbf{S}_{\mathbf{k}js} = \sum_{n\lambda} C^{\nu}_{n\lambda} \mathbf{S}^{\mathbf{k}\,\nu}_{n\lambda}(js)$$

Basis Functions (constant vectors): $\mathbf{S}^{\mathbf{k}\,\nu}_{n\lambda}(js)$

December 2002 Workshop on Magnetic Structures (Abingdon)

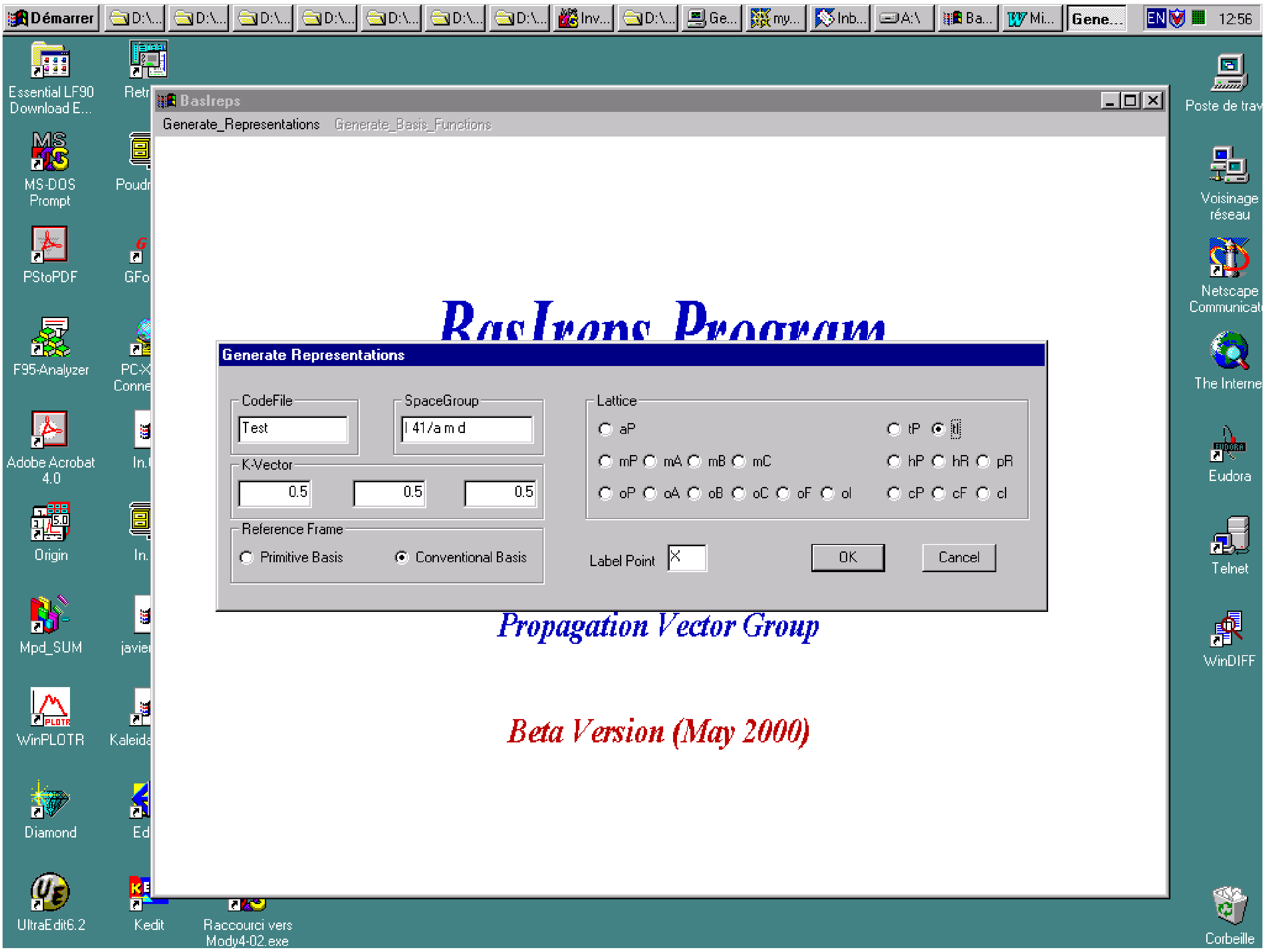

Generate Representations

CodeFile: Test

SpaceGroup: I 41/a m d

K-Vector: 0.5 0.5 0.5

Reference Frame: ○ Primitive Basis ● Conventional Basis

Lattice:
○ aP ○ tP ● tI
○ mP ○ mA ○ mB ○ mC ○ hP ○ hR ○ pR
○ oP ○ oA ○ oB ○ oC ○ oF ○ oI ○ cP ○ cF ○ cI

Label Point: X

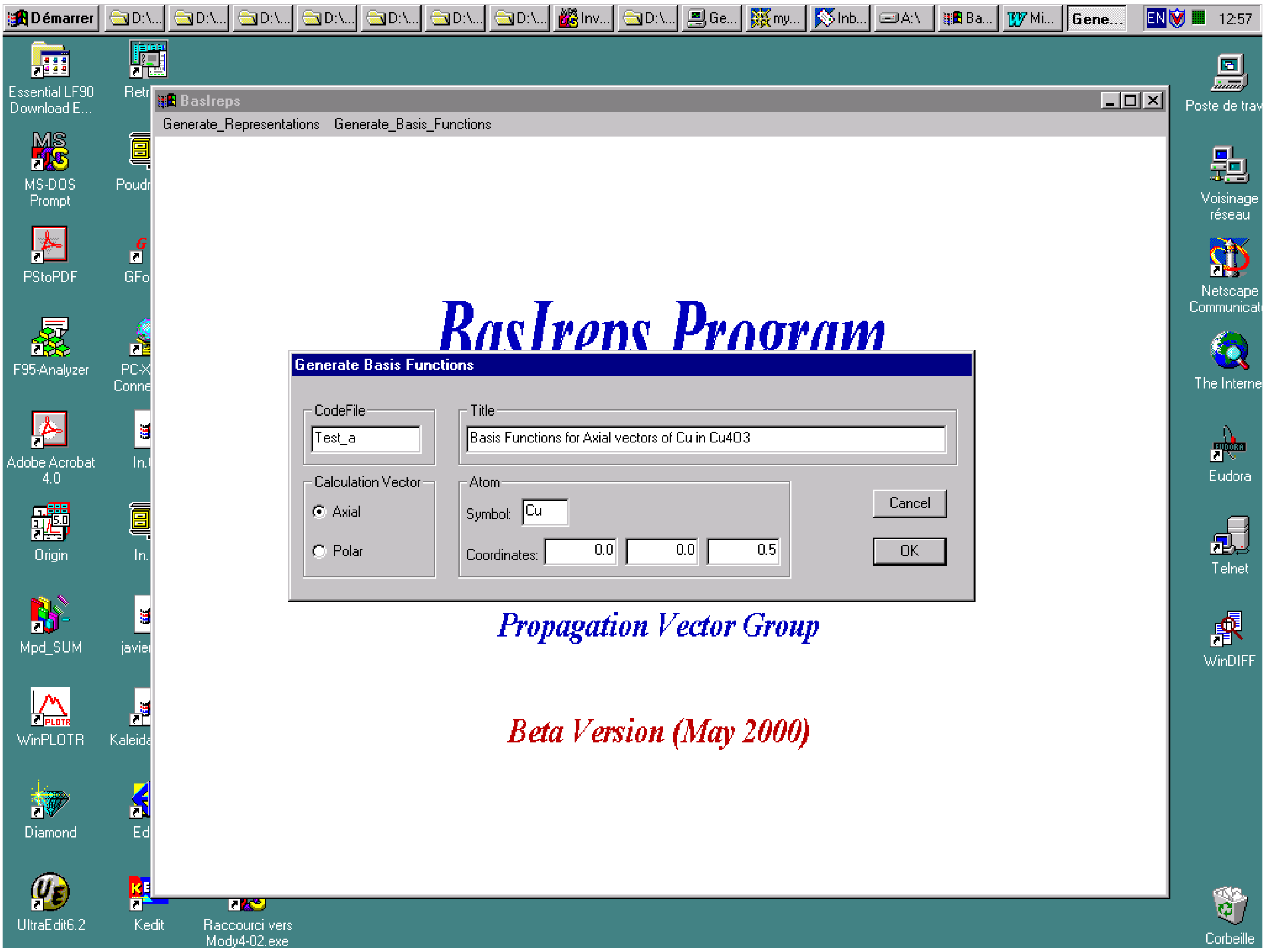

Generate Basis Functions

CodeFile: Test_a

Title: Basis Functions for Axial vectors of Cu in Cu4O3

Calculation Vector:
- ● Axial
- ○ Polar

Atom:
- Symbol: Cu
- Coordinates: 0.0 0.0 0.5

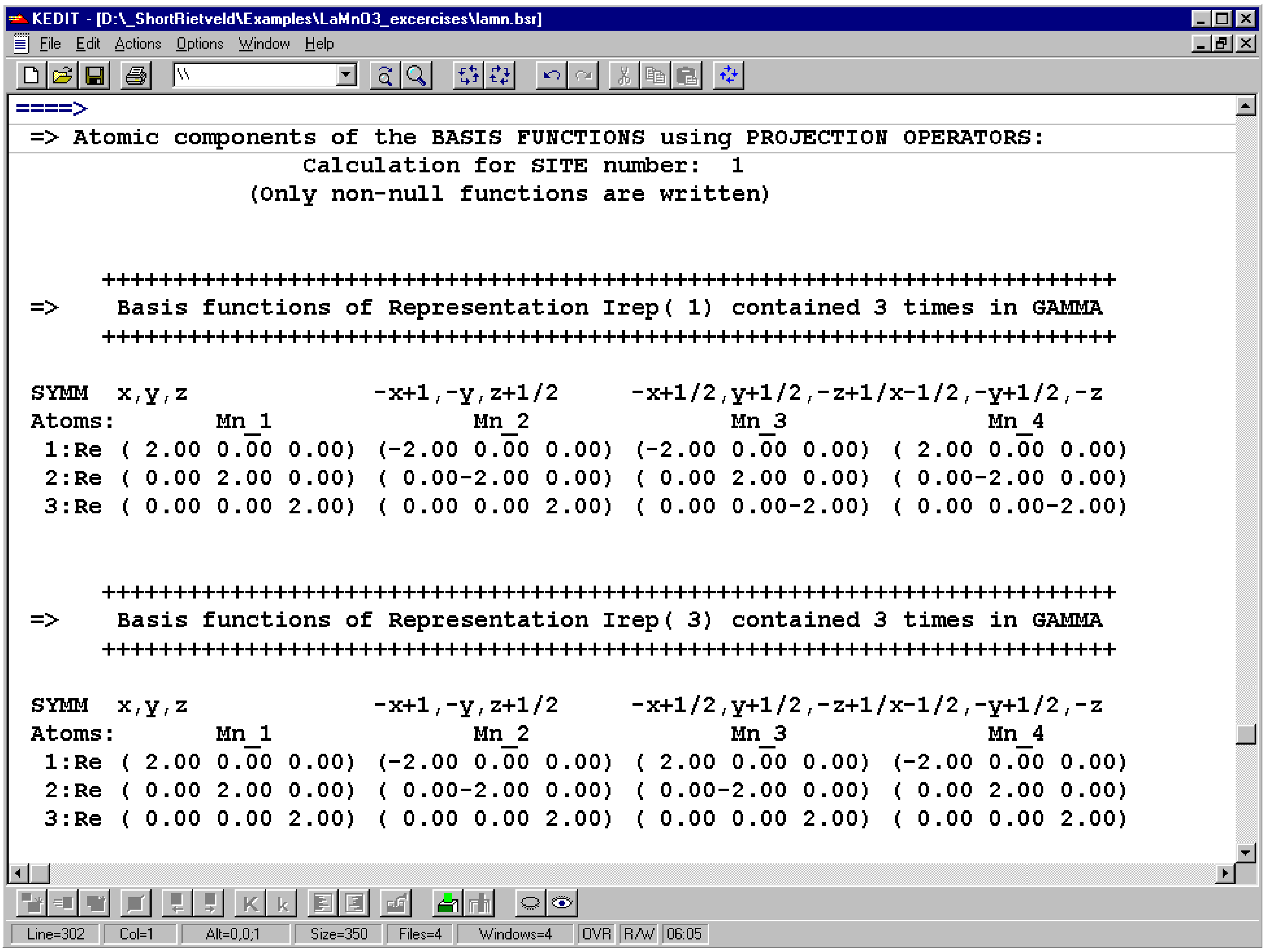

```
====>
 => Atomic components of the BASIS FUNCTIONS using PROJECTION OPERATORS:
                    Calculation for SITE number:   1
                (Only non-null functions are written)


      +++++++++++++++++++++++++++++++++++++++++++++++++++++++++++++++++++++++
 =>    Basis functions of Representation Irep( 1) contained 3 times in GAMMA
      +++++++++++++++++++++++++++++++++++++++++++++++++++++++++++++++++++++++

 SYMM  x,y,z              -x+1,-y,z+1/2     -x+1/2,y+1/2,-z+1/x-1/2,-y+1/2,-z
 Atoms:       Mn_1                Mn_2                Mn_3                Mn_4
  1:Re  ( 2.00 0.00 0.00) (-2.00 0.00 0.00) (-2.00 0.00 0.00) ( 2.00 0.00 0.00)
  2:Re  ( 0.00 2.00 0.00) ( 0.00-2.00 0.00) ( 0.00 2.00 0.00) ( 0.00-2.00 0.00)
  3:Re  ( 0.00 0.00 2.00) ( 0.00 0.00 2.00) ( 0.00 0.00-2.00) ( 0.00 0.00-2.00)


      +++++++++++++++++++++++++++++++++++++++++++++++++++++++++++++++++++++++
 =>    Basis functions of Representation Irep( 3) contained 3 times in GAMMA
      +++++++++++++++++++++++++++++++++++++++++++++++++++++++++++++++++++++++

 SYMM  x,y,z              -x+1,-y,z+1/2     -x+1/2,y+1/2,-z+1/x-1/2,-y+1/2,-z
 Atoms:       Mn_1                Mn_2                Mn_3                Mn_4
  1:Re  ( 2.00 0.00 0.00) (-2.00 0.00 0.00) ( 2.00 0.00 0.00) (-2.00 0.00 0.00)
  2:Re  ( 0.00 2.00 0.00) ( 0.00-2.00 0.00) ( 0.00-2.00 0.00) ( 0.00 2.00 0.00)
  3:Re  ( 0.00 0.00 2.00) ( 0.00 0.00 2.00) ( 0.00 0.00 2.00) ( 0.00 0.00 2.00)
```

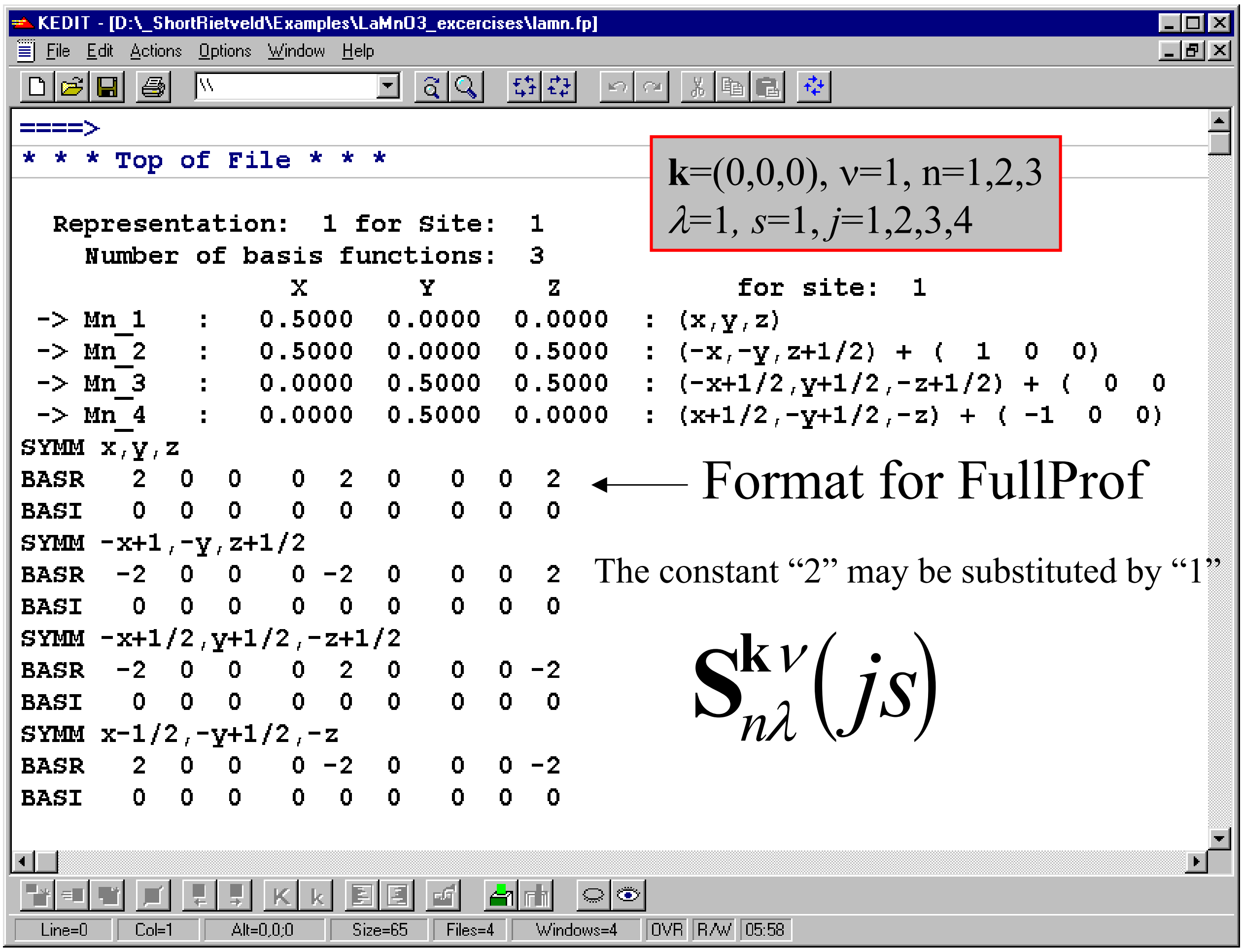

```
====>
* * * Top of File * * *

  Representation:  1 for Site:  1
    Number of basis functions:  3
                         X         Y         Z              for site:  1
 -> Mn_1    :   0.5000  0.0000  0.0000  : (x,y,z)
 -> Mn_2    :   0.5000  0.0000  0.5000  : (-x,-y,z+1/2) + (  1   0   0)
 -> Mn_3    :   0.0000  0.5000  0.5000  : (-x+1/2,y+1/2,-z+1/2) + (   0   0
 -> Mn_4    :   0.0000  0.5000  0.0000  : (x+1/2,-y+1/2,-z) + ( -1   0   0)
SYMM x,y,z
BASR    2  0  0    0  2  0    0  0  2
BASI    0  0  0    0  0  0    0  0  0
SYMM -x+1,-y,z+1/2
BASR   -2  0  0    0 -2  0    0  0  2
BASI    0  0  0    0  0  0    0  0  0
SYMM -x+1/2,y+1/2,-z+1/2
BASR   -2  0  0    0  2  0    0  0 -2
BASI    0  0  0    0  0  0    0  0  0
SYMM x-1/2,-y+1/2,-z
BASR    2  0  0    0 -2  0    0  0 -2
BASI    0  0  0    0  0  0    0  0  0
```

$\mathbf{k}=(0,0,0)$, $\nu=1$, $n=1,2,3$
$\lambda=1$, $s=1$, $j=1,2,3,4$

← Format for FullProf

The constant “2” may be substituted by “1”

$$\mathbf{S}^{\mathbf{k}\nu}_{n\lambda}(js)$$

Example of magnetic structure in terms of basis functions of the irreducible representations of the propagation vector group (1)

$$\mathbf{S}_{\mathbf{k}js} = \sum_{n\lambda} C^{\nu}_{n\lambda} \mathbf{S}^{\mathbf{k}\nu}_{n\lambda}(js)$$

For $\mathrm{LaMnO_3}$ this sum is reduced to three terms for each representation to be tested. Example, for representation $\nu=1$, dropping the superfluous indices $\mathbf{k}$, s, λ :

$$\mathbf{S}_j = \sum_{n=1,2,3} C^1_n \mathbf{S}^1_n(j)$$

$$\mathbf{S}_1 = C^1_1\mathbf{S}^1_1(1) + C^1_2\mathbf{S}^1_2(1) + C^1_3\mathbf{S}^1_3(1)$$

$$\mathbf{S}_2 = C^1_1\mathbf{S}^1_1(2) + C^1_2\mathbf{S}^1_2(2) + C^1_3\mathbf{S}^1_3(2)$$

....

Example of magnetic structure in terms of basis functions of the irreducible representations of the propagation vector group (2)

$$\mathbf{S}_j = \sum_{n=1,2,3} C_n^1 \mathbf{S}_n^1(j)$$

$$\mathbf{S}_1 = C_1^1(1,0,0) + C_2^1(0,1,0) + C_3^1(0,0,1) = (C_1^1, C_2^1, C_3^1)$$

$$\mathbf{S}_2 = C_1^1(-1,0,0) + C_2^1(0,-1,0) + C_3^1(0,0,1) = (-C_1^1, -C_2^1, C_3^1)$$

$$\mathbf{S}_3 = C_1^1(-1,0,0) + C_2^1(0,1,0) + C_3^1(0,0,-1) = (-C_1^1, C_2^1, -C_3^1)$$

$$\mathbf{S}_4 = C_1^1(1,0,0) + C_2^1(0,-1,0) + C_3^1(0,0,-1) = (C_1^1, -C_2^1, -C_3^1)$$

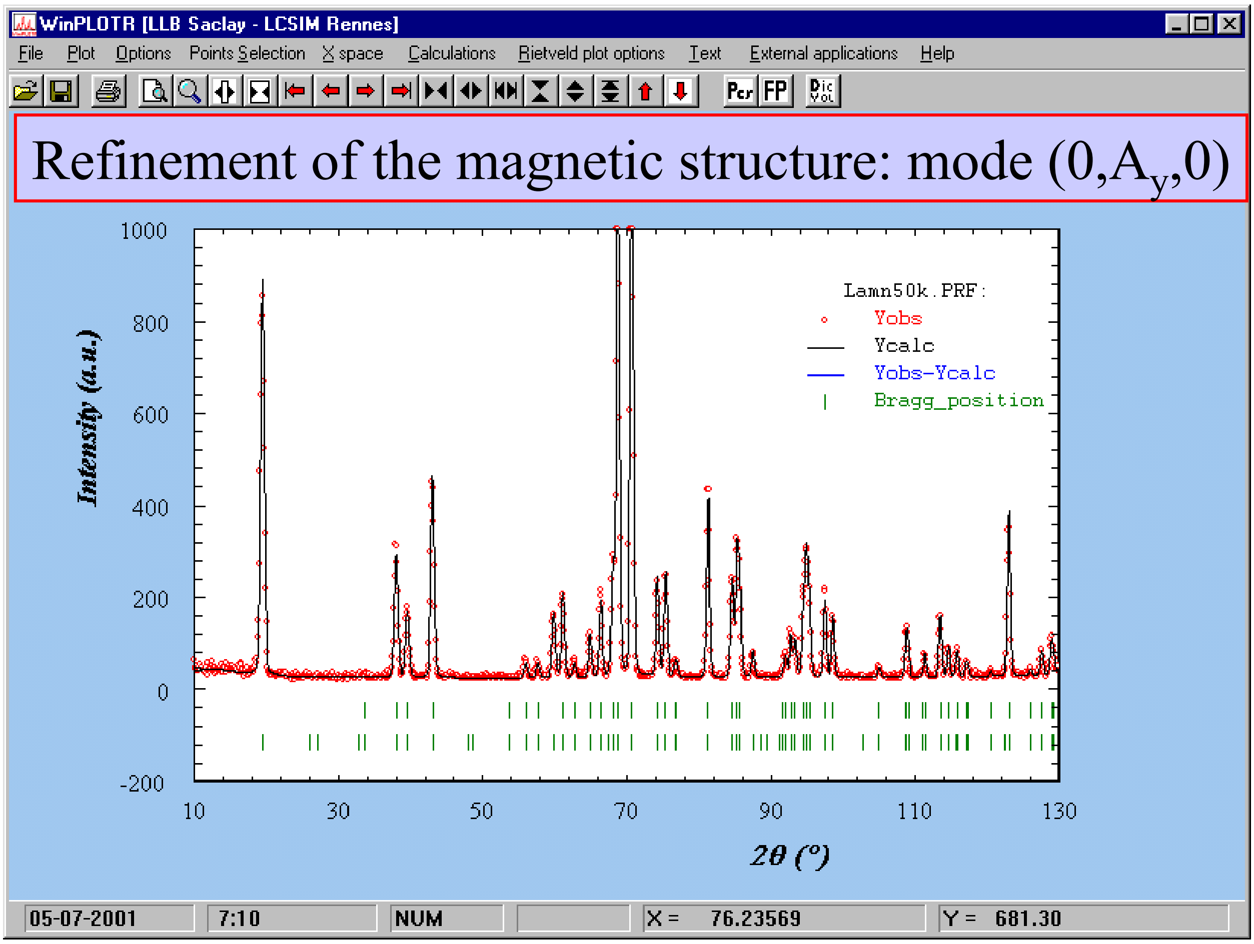

Refinement of the magnetic structure: mode $(0,A_y,0)$

05-07-2001 | 7:10 | NUM | X = 76.23569 | Y = 681.30

Magnetic structure determination in complex systems: Simulating Annealing

---

Direct space methods:

- Look directly for coefficients of the expansion:

$$\mathbf{S}_{\mathbf{k}js} = \sum_{n\lambda} C^{\nu}_{n\lambda} \mathbf{S}^{\mathbf{k}\,\nu}_{n\lambda}(js)$$

or components of S_{k} and phases, explaining the experimental data

- Minimize a reliability factor with respect to the "configuration vector"

$$\boxed{\varpi = \left| C_1, C_2, C_3, C_4, C_5, \ldots C_m \right\rangle}$$

$$\boxed{R_m(\varpi) = c \sum_{r=1}^{N} \left| G^2_{obs}(\mathbf{h}_r) - G^2_{calc}(\mathbf{h}_r, \varpi) \right|}$$

Behavior of parameters in Simulated Annealing runs

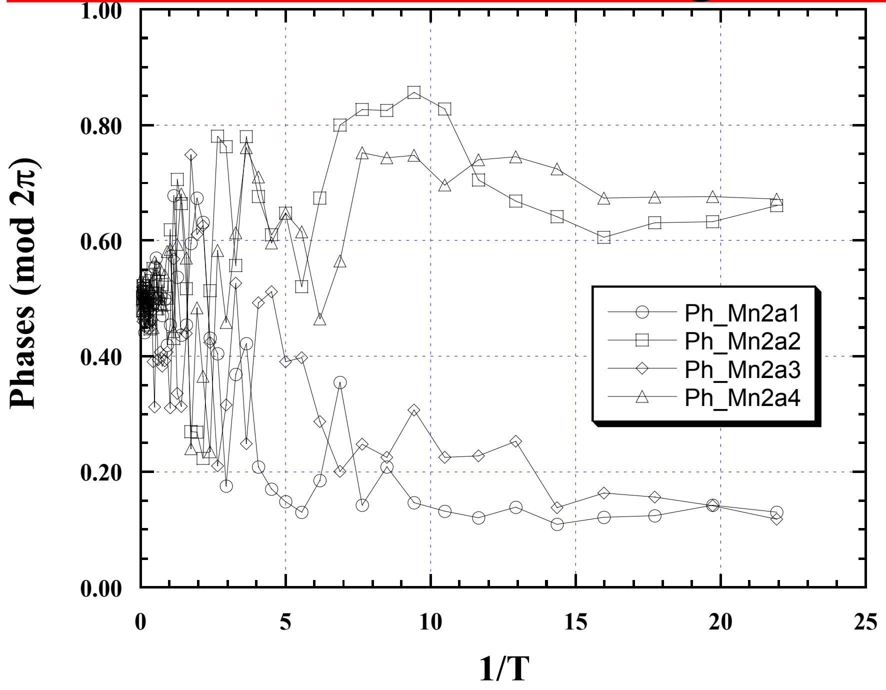

Average step …
Corana algorithm

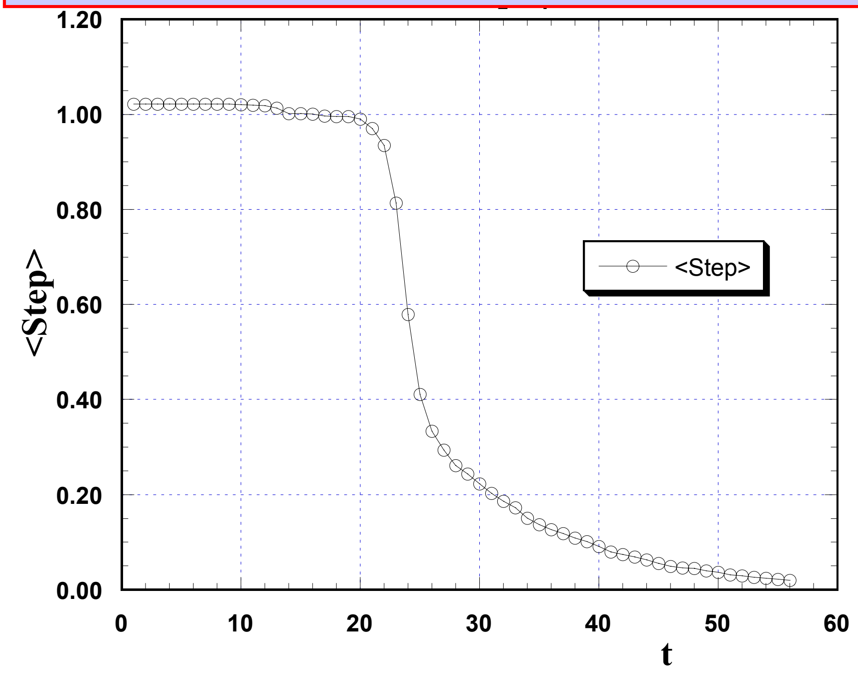

Interpretation of the magnetic structure as the ground state (first ordered state) of a classical spin system

Classical magnetic energy: $E = -\sum_{\langle ij\rangle} J_{ij}\,\mathbf{S}_i\,\mathbf{S}_j$

First ordered state corresponds to the lowest eigenvalue of the Fourier matrix of the exchange interactions:

$$\boxed{\xi_{ij}(\mathbf{k}) = -\sum\nolimits_{\mathrm{m}} J_{ij}(\mathbf{R}_{\mathrm{m}}).\exp\{-2\pi i\,\mathbf{k}\,\mathbf{R}_{\mathrm{m}}\}}$$

Crystal structure of R_2BaNiO_5 (R: Pr, Nd, Tb, Dy…)

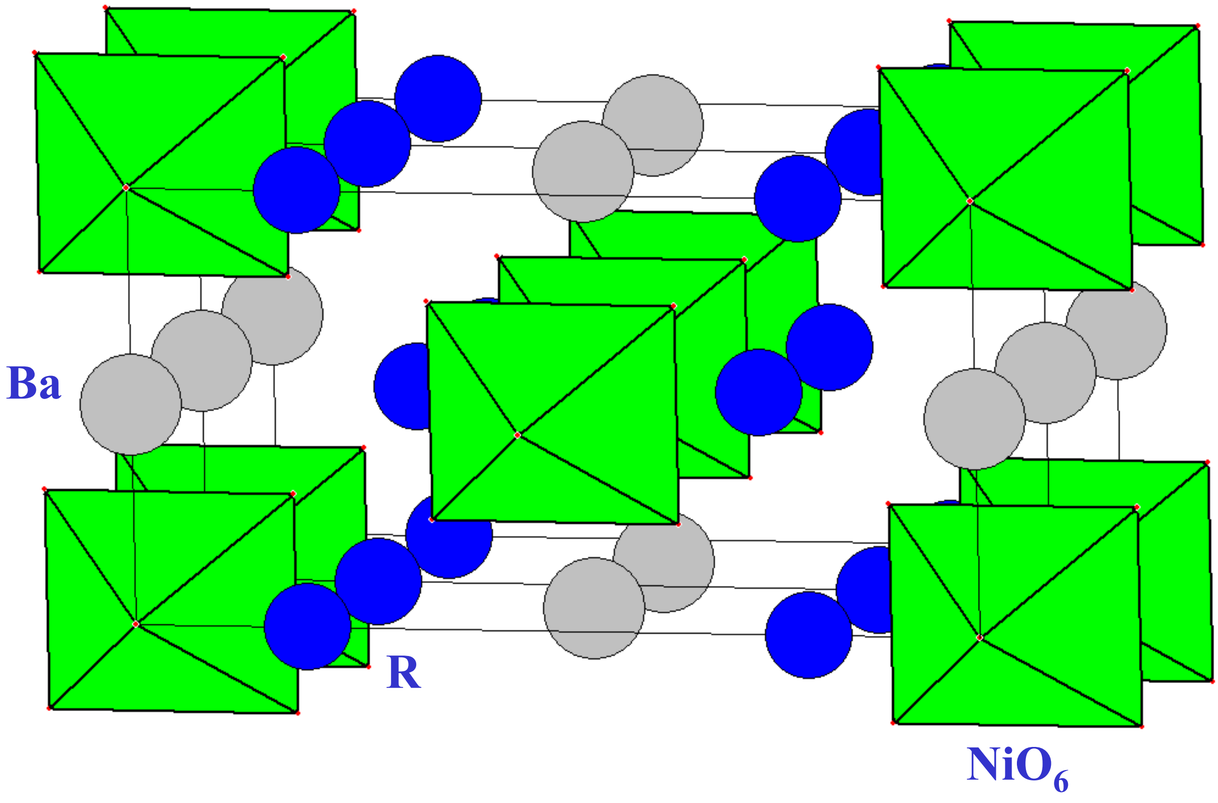

Neutron powder diffraction pattern of Dy_2BaNiO_5 at 1.5K

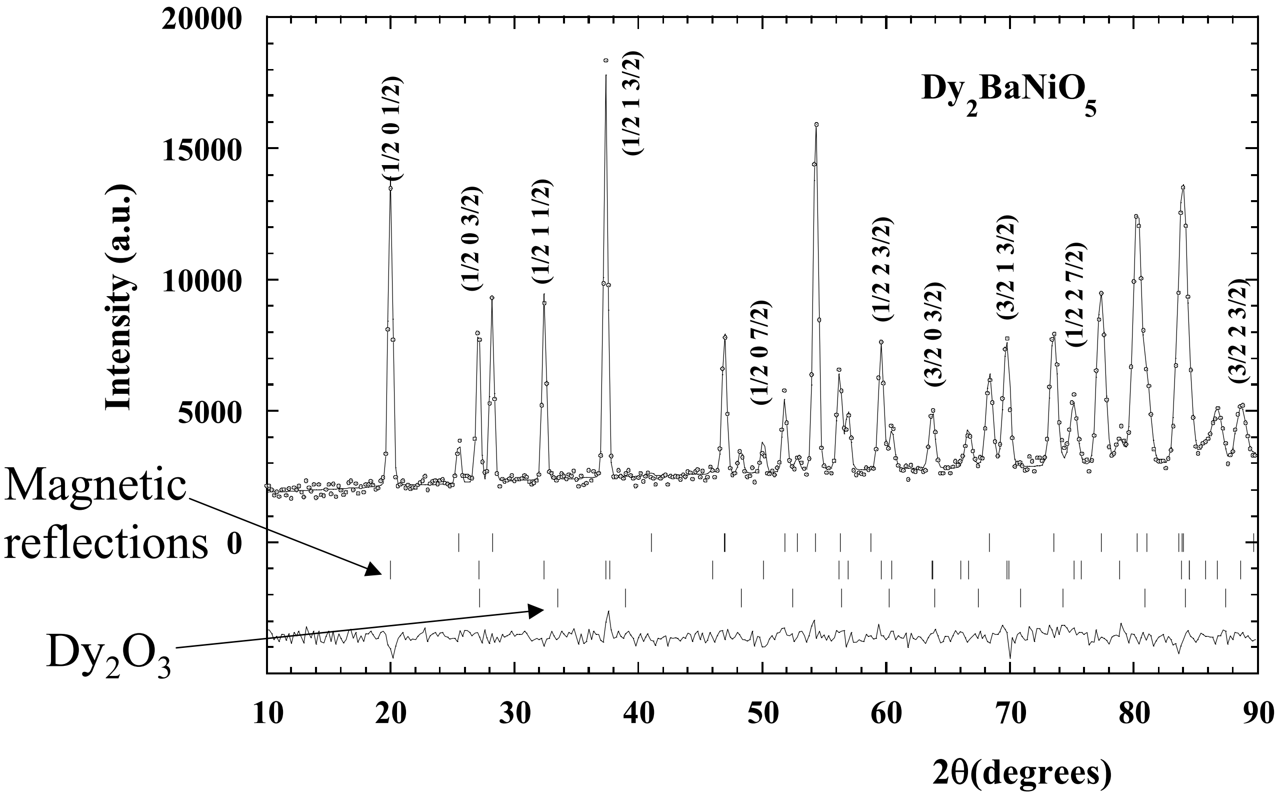

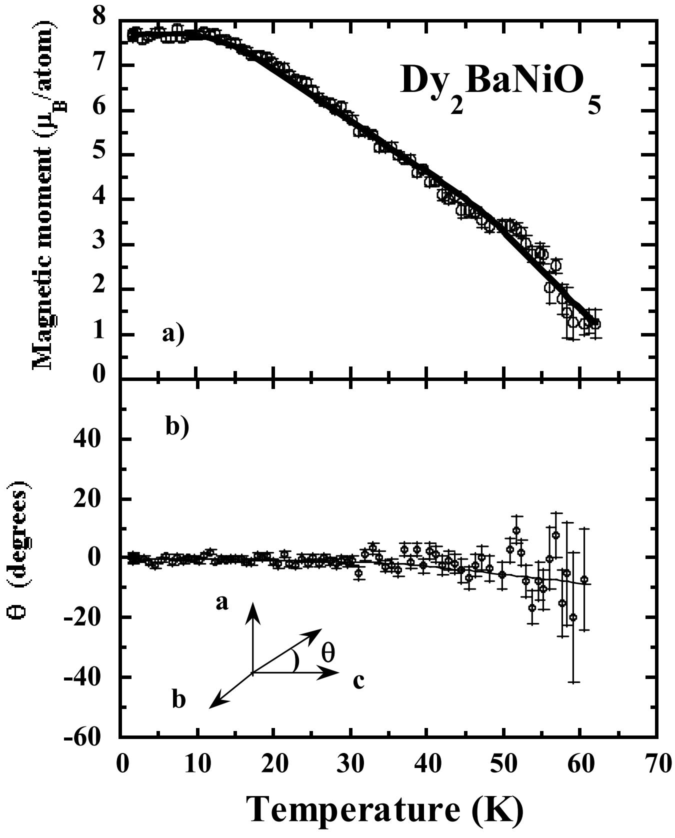

Space group: *Immm*

The magnetic structure of all members of the family R_2BaNiO_5 has the propagation vector **k**=(1/2,0,1/2)

- Ni ions are in a single Bravais sublattice at (000)(2a) site.

- The rare earth site (4j) generates two sublattices 1: (1/2, 0, z) and 2: (-1/2, 0, -z) in a primitive unit cell

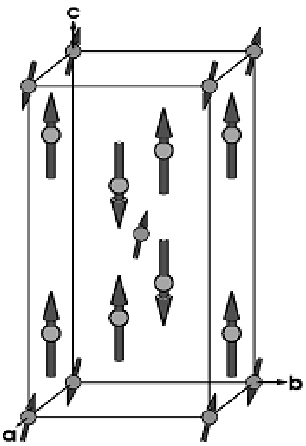

Nd_2BaNiO_5

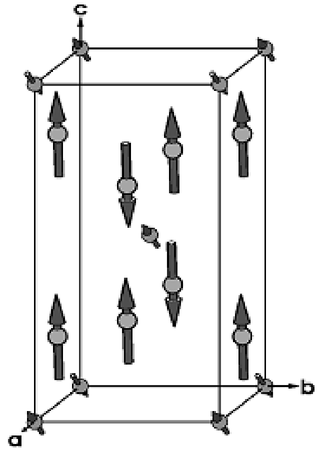

Tb_2BaNiO_5

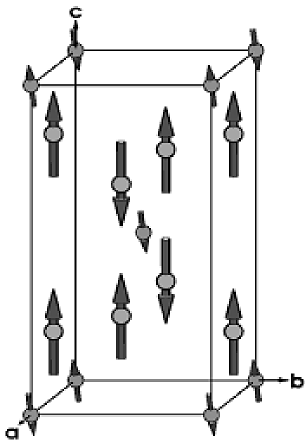

Dy_2BaNiO_5

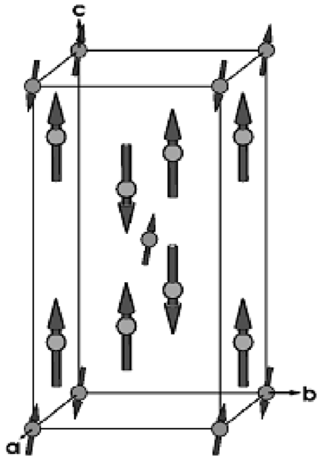

Ho_2BaNiO_5

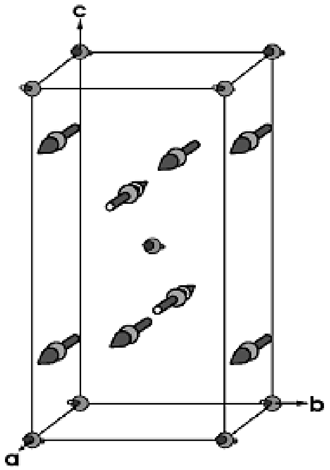

Er_2BaNiO_5

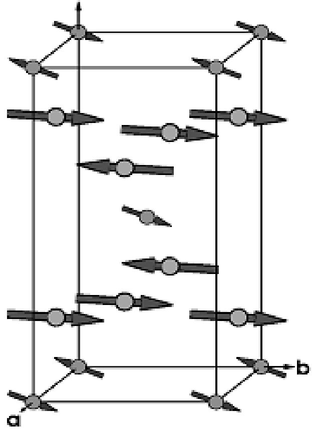

Tm_2BaNiO_5

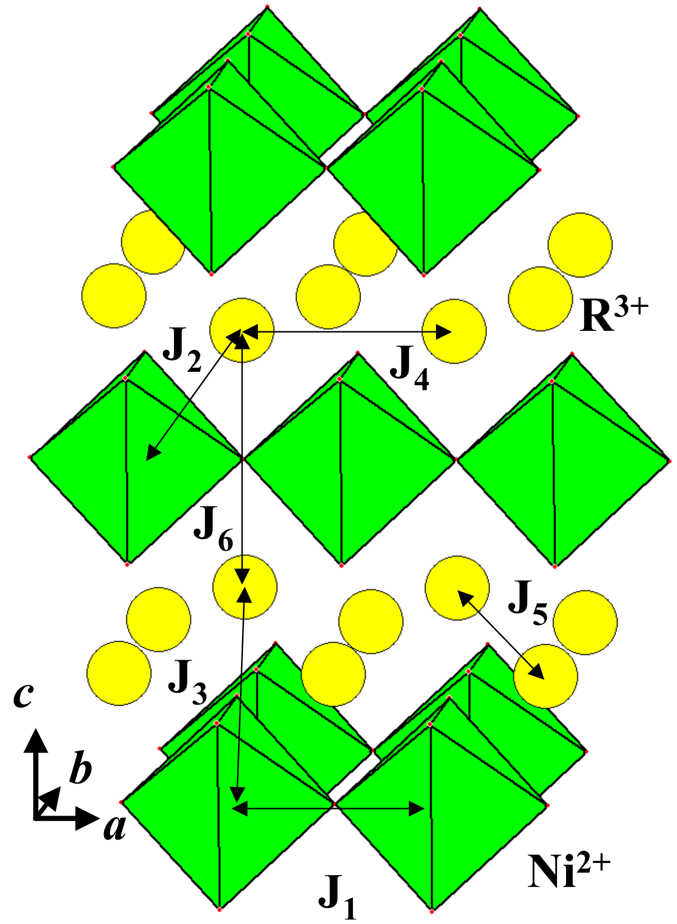

R_2BaNiO_5: 1 Ni and 2 R ions in the primitive cell
Exchange Fourier matrix 3 x 3, $\mathbf{k}=(X, Y, Z)$

$$J_{11}(\mathbf{k}) = 2J_1 \cos 2\pi X$$
$$J_{12}(\mathbf{k}) = J_{21}(\mathbf{k})^* = J_2(1+ \exp\{2\pi iX\}) + 2J_3 \cos \pi Y \exp\{\pi i(X+Z)\}$$
$$J_{13}(\mathbf{k}) = J_{31}(\mathbf{k})^* = J_2\,(1+\exp\{2\pi iX\}) \exp\{2\pi iZ\}+2J_3 \cos\pi k \exp\{\pi i(X+Z)\}$$
$$J_{22}(\mathbf{k}) = J_{33}(\mathbf{k}) = 2J_4 \cos 2\pi X$$
$$J_{23}(\mathbf{k}) = J_{32}(\mathbf{k})^* = 4J_5 \cos\pi X \cos\pi Y \exp\{\pi iZ\} + J_6 \exp\{2\pi iZ\}$$

If we neglect R-R interactions ($J_4=J_5=J_6=0$) the eigenvalues are:
$\lambda_1(\mathbf{k})=0$,
$\lambda_{2,3}(\mathbf{k})= 2J_1 \cos 2\pi X \pm (J_1^2\cos^2 2\pi X + 4\, J_3^2\{1+\cos^2 2\pi Y\})^{1/2}$

The energy is independent of Z, so no 3D order is possible with isotropic exchange neglecting R-R interactions.

Phase diagram for the topology of $MFePO_5$

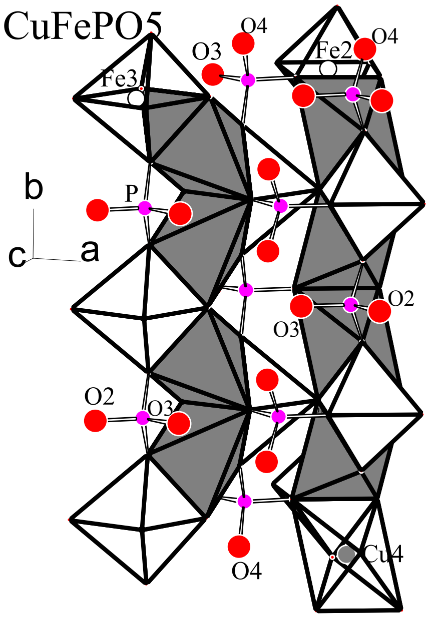

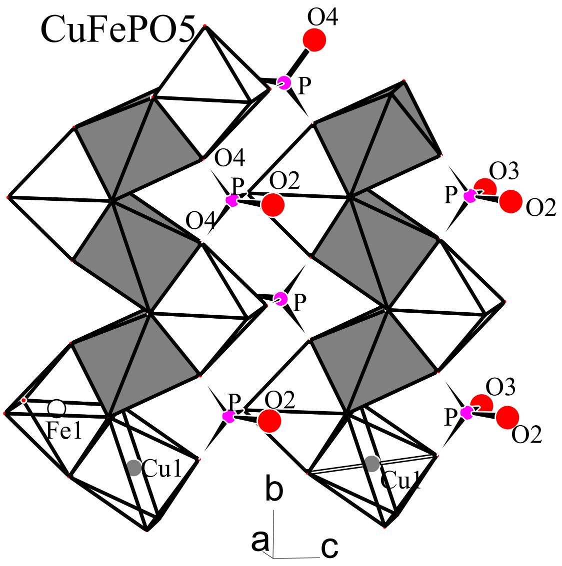

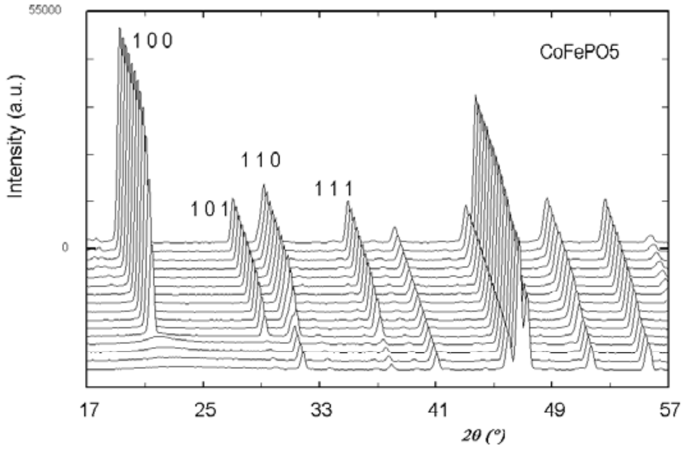

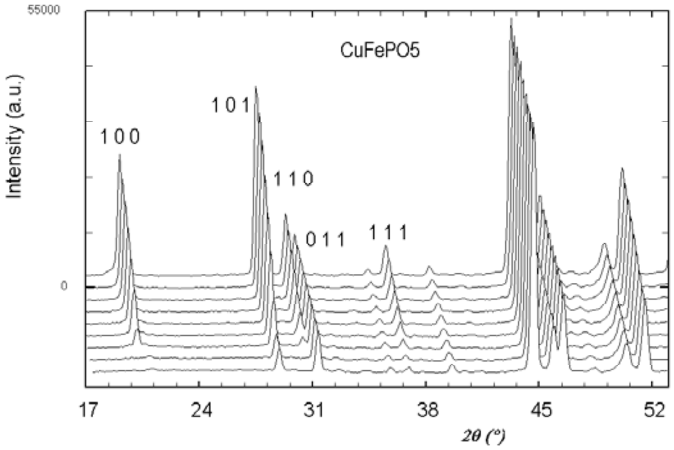

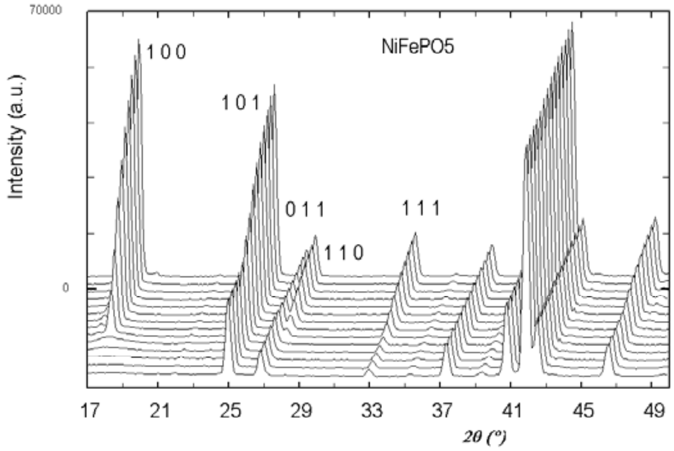

Similar magnetic structures **k**=(0,0,0), two sites M and Fe of four sublattices

$G_M+G_{Fe} = (+ - + - ; + - + -)$

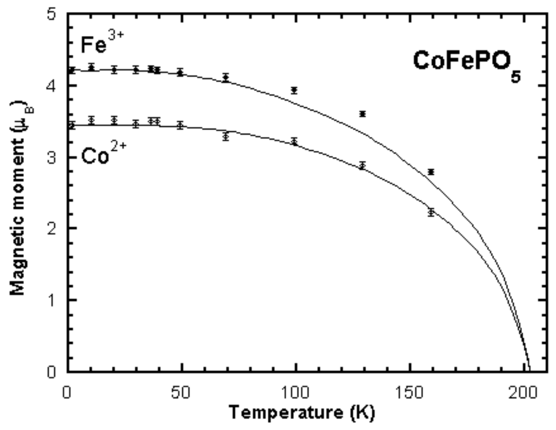

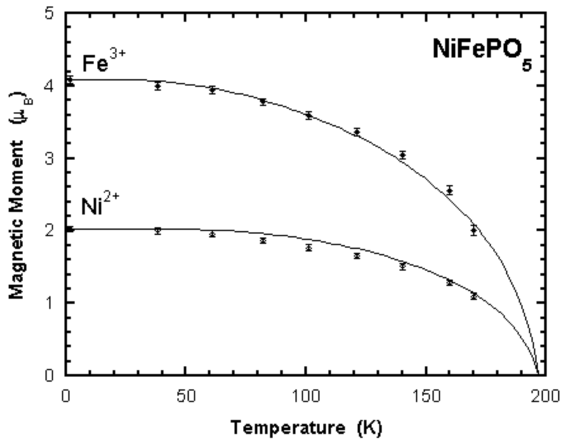

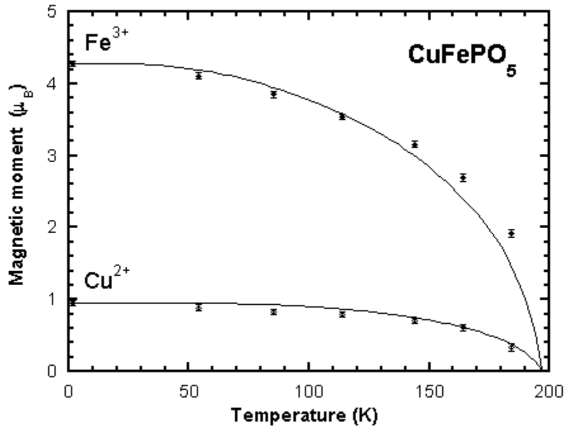

Sublattice magnetization of three members of the family $MFePO_5$

Continuous curves: Adjusted by self-consistent Brillouin functions

The program SIMBO

- Geometrical analysis of the exchange paths for ionic structures (input: cell parameters, space group, atom positions in the asymmetric unit, magnetic moments)
- Automatic generation of the formal expression of the Fourier matrix of the exchange integrals
- Output file for ENERMAG

$$\xi(\vec{k}) = \begin{pmatrix} 0 & 0 & J_2(1+e^{2\pi i(Y)}) & 0 & J_1e^{2\pi i(Z)} & J_3e^{2\pi i(X+Z)} & J_1e^{2\pi i(X+Y)} & J_3e^{2\pi i(Y)} \\ 0 & 0 & 0 & J_2(1+e^{-2\pi i(Y)}) & J_3 & J_1 & J_3 & J_1 \\ J_2(1+e^{-2\pi i(Y)}) & 0 & 0 & 0 & J_1e^{2\pi i(Z)} & J_3e^{2\pi i(X+Z)} & J_1e^{2\pi i(X)} & J_3 \\ 0 & J_2(1+e^{2\pi i(Y)}) & 0 & 0 & J_3 & J_1 & J_3e^{2\pi i(Y)} & J_1e^{2\pi i(Y)} \\ J_1e^{-2\pi i(Z)} & J_3 & J_1e^{-2\pi i(Z)} & J_3 & 0 & J_4(1+e^{2\pi i(X)}) & 0 & 0 \\ J_3e^{-2\pi i(X+Z)} & J_1 & J_3e^{-2\pi i(X+Z)} & J_1 & J_4(1+e^{-2\pi i(X)}) & 0 & 0 & 0 \\ J_1e^{-2\pi i(X+Y)} & J_3 & J_1e^{-2\pi i(X)} & J_3e^{-2\pi i(Y)} & 0 & 0 & 0 & J_4(1+e^{-2\pi i(X)}) \\ J_3e^{-2\pi i(Y)} & J_1 & J_3 & J_1e^{-2\pi i(Y)} & 0 & 0 & J_4(1+e^{2\pi i(X)}) & 0 \end{pmatrix}$$

The program ENERMAG

$$\xi_{ij}(\mathbf{k}) = -\sum_{\mathrm{m}} J_{ij}(\mathbf{R}_{\mathrm{m}}).\exp\{-2\pi i\ \mathbf{k}\ \mathbf{R}_{\mathrm{m}}\}$$

The program handles the diagonalization of the Fourier matrix solving the parametric equation:

$$\xi(\mathbf{k, J})\ \mathbf{v}(\mathbf{k, J}) = \lambda(\mathbf{k, J})\ \mathbf{v}(\mathbf{k, J})$$

- For a given set $\mathbf{J} = \{J_{ij}\}$, and no degeneracy, the lowest eigenvalue $\lambda_{\mathrm{min}}(\mathbf{k}_0, \mathbf{J})$ occurs for a particular $\mathbf{k}_0$.
- The corresponding eigenvector $\mathbf{v}_{\mathrm{min}}(\mathbf{k}_0, \mathbf{J})$ (that may be complex for incommensurate structures), describes the spin configuration of the first ordered state

The compounds of formula $MFePO_5$ can be modelled with four exchange interactions:

- J_1 corresponds to the exchange between M^{2+} and Fe^{3+} nearest neighbours.
- J_2 corresponds to the exchange between two M^{2+} cations (double oxygen bridge).
- J_3 corresponds to the exchange between next nearest neighbours M^{2+} and Fe^{3+} cations (single oxygen bridge).
- J_4 exchange between nearest neighbours Fe^{3+} cations (single oxygen bridge), taken here as J_4=-1

J_2=-6.7

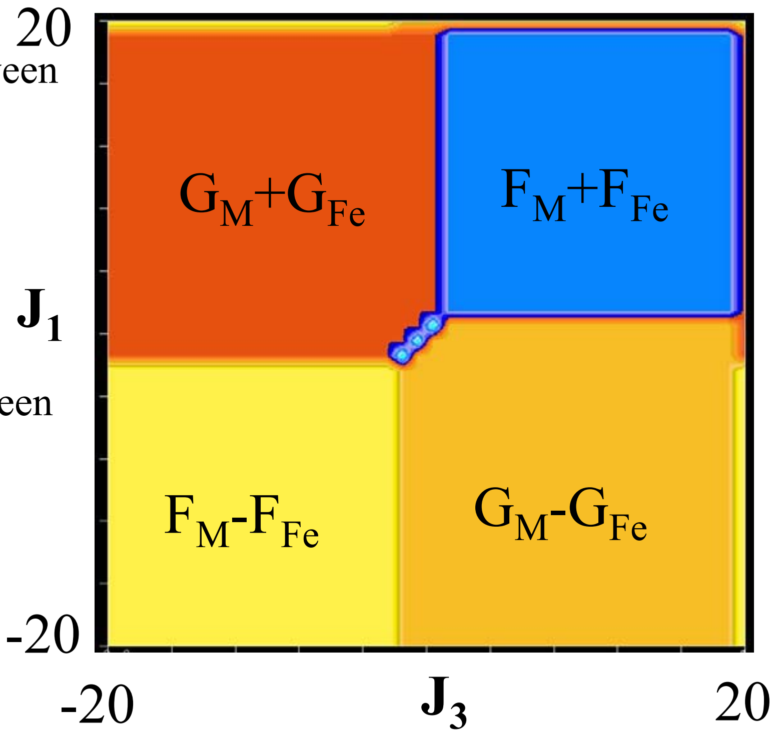

J_2 = -15

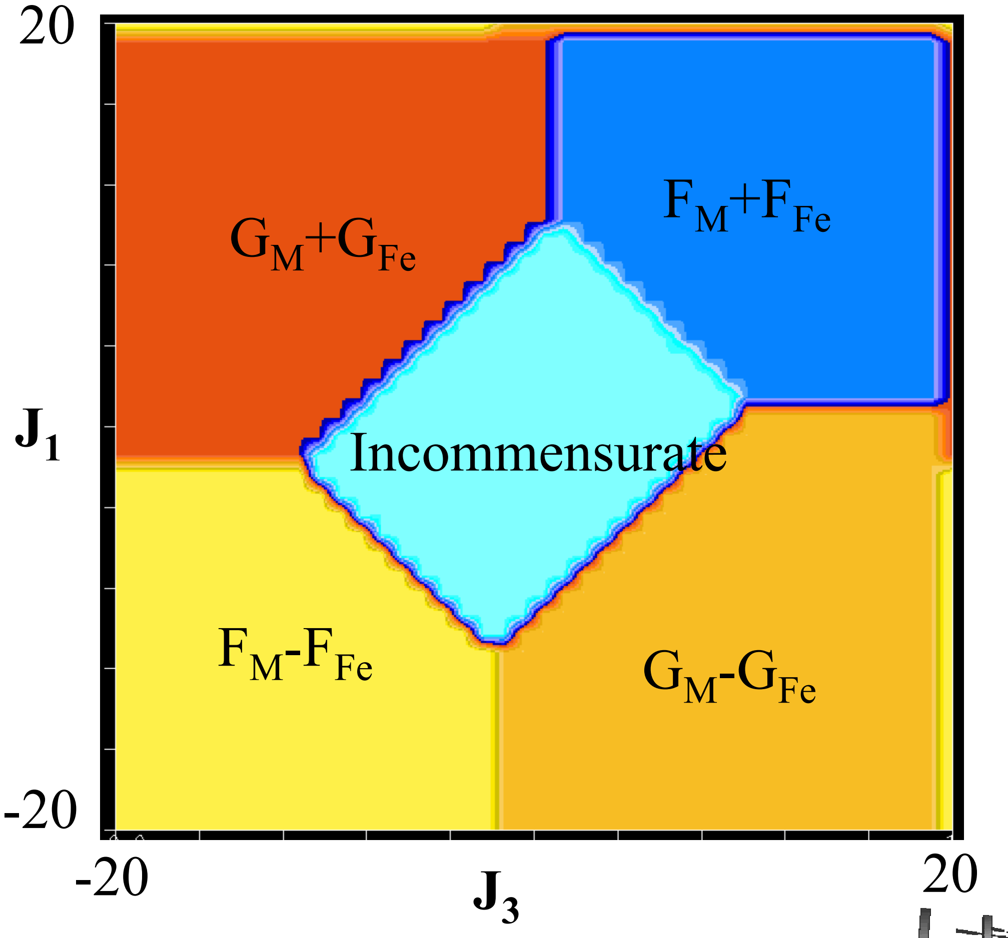

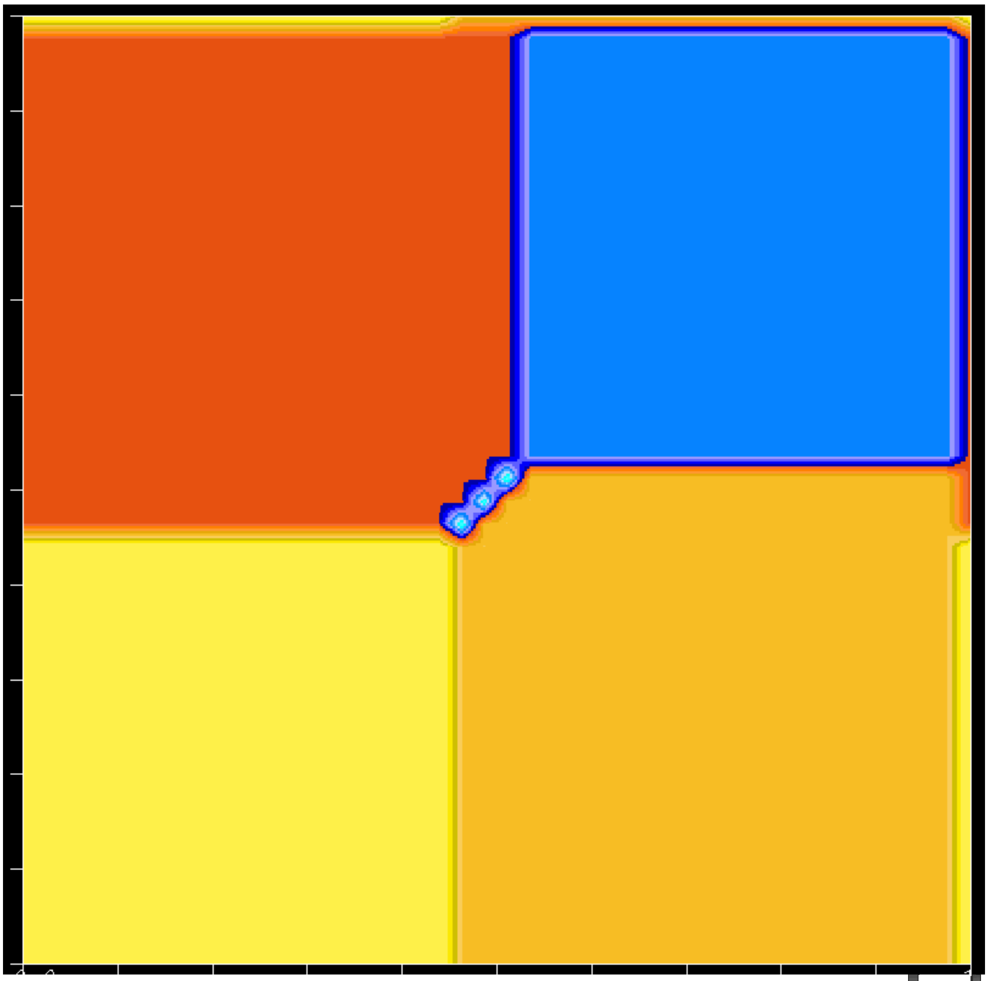

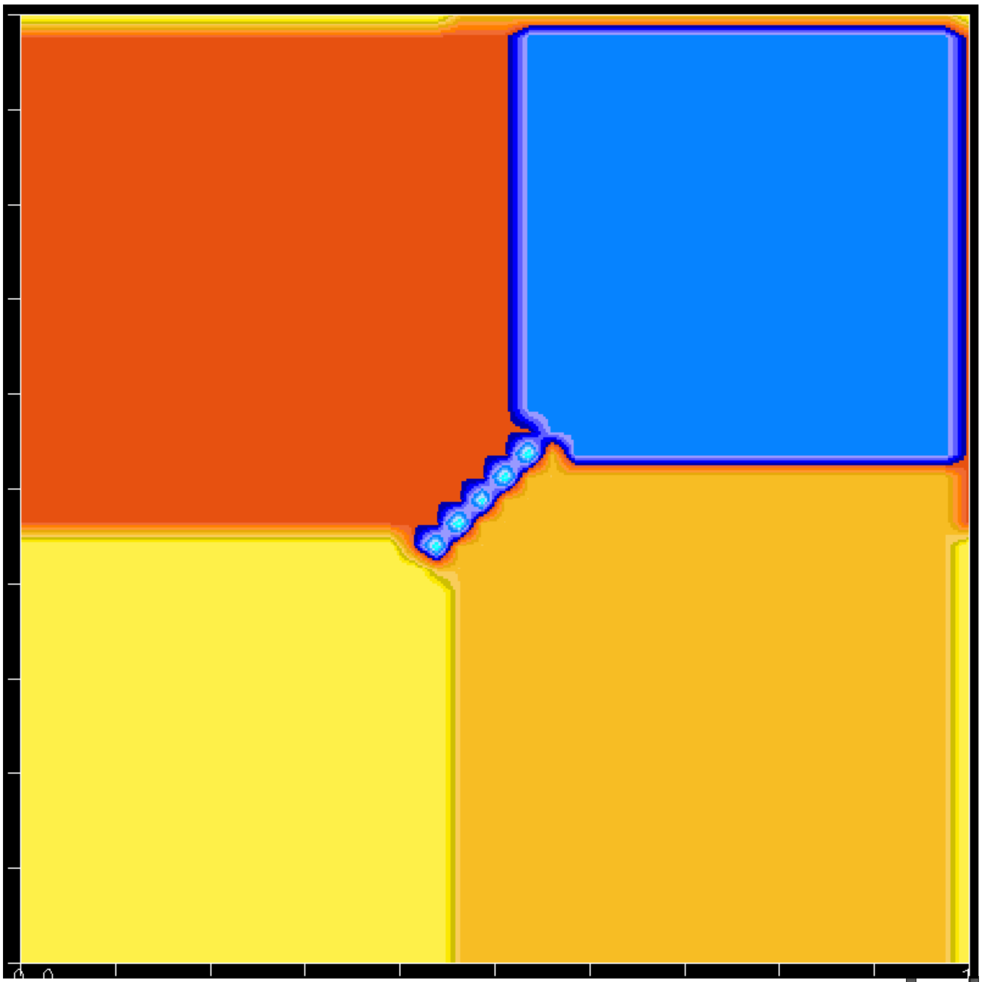

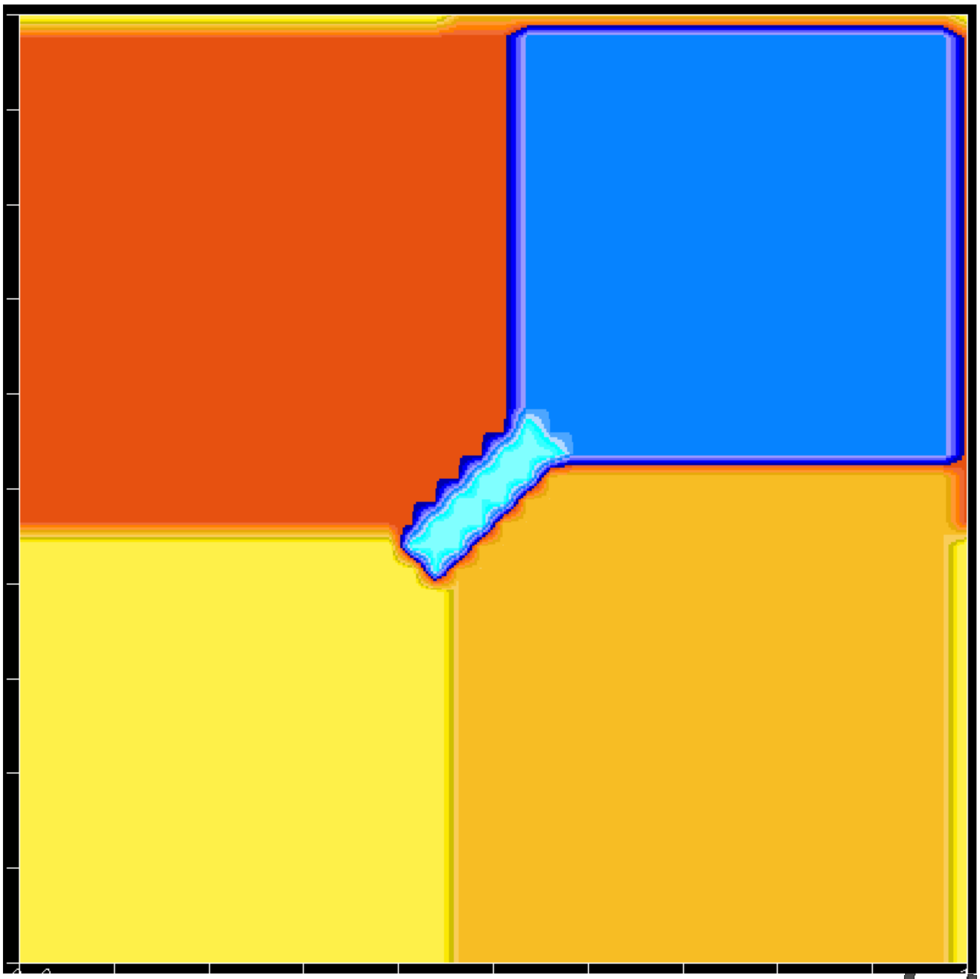

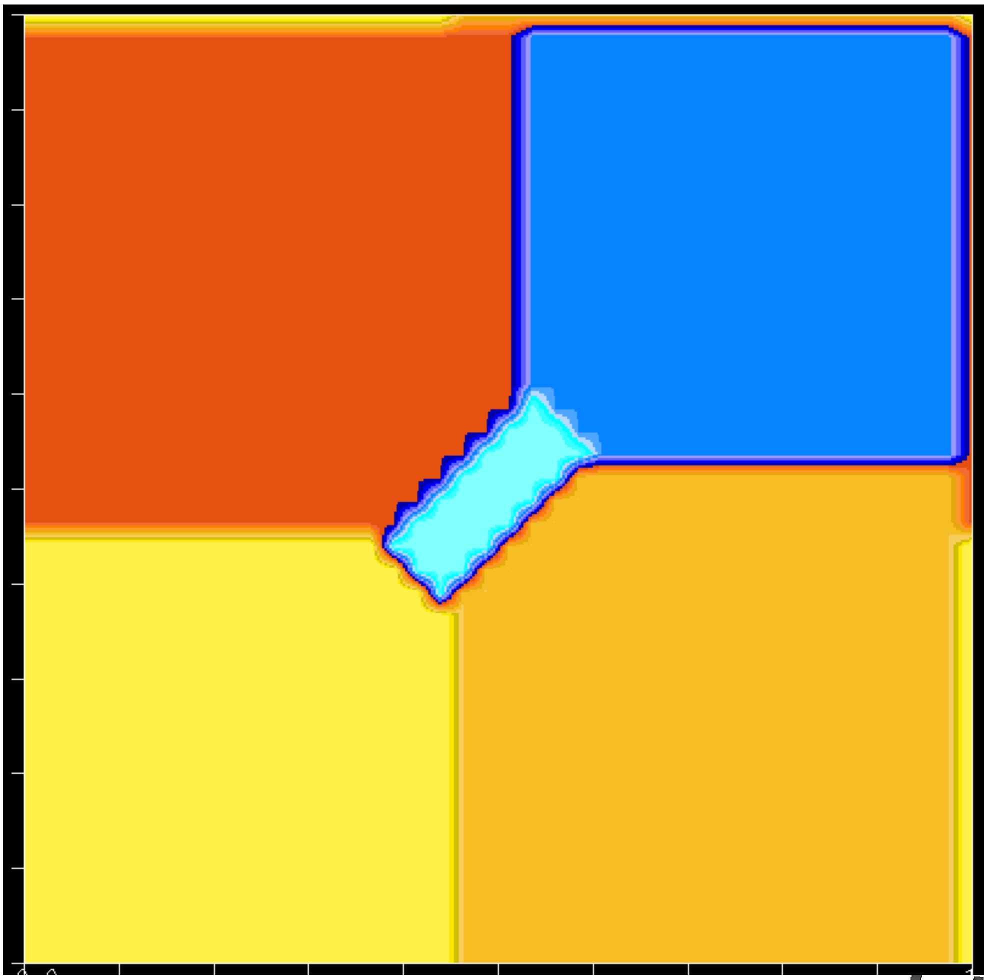

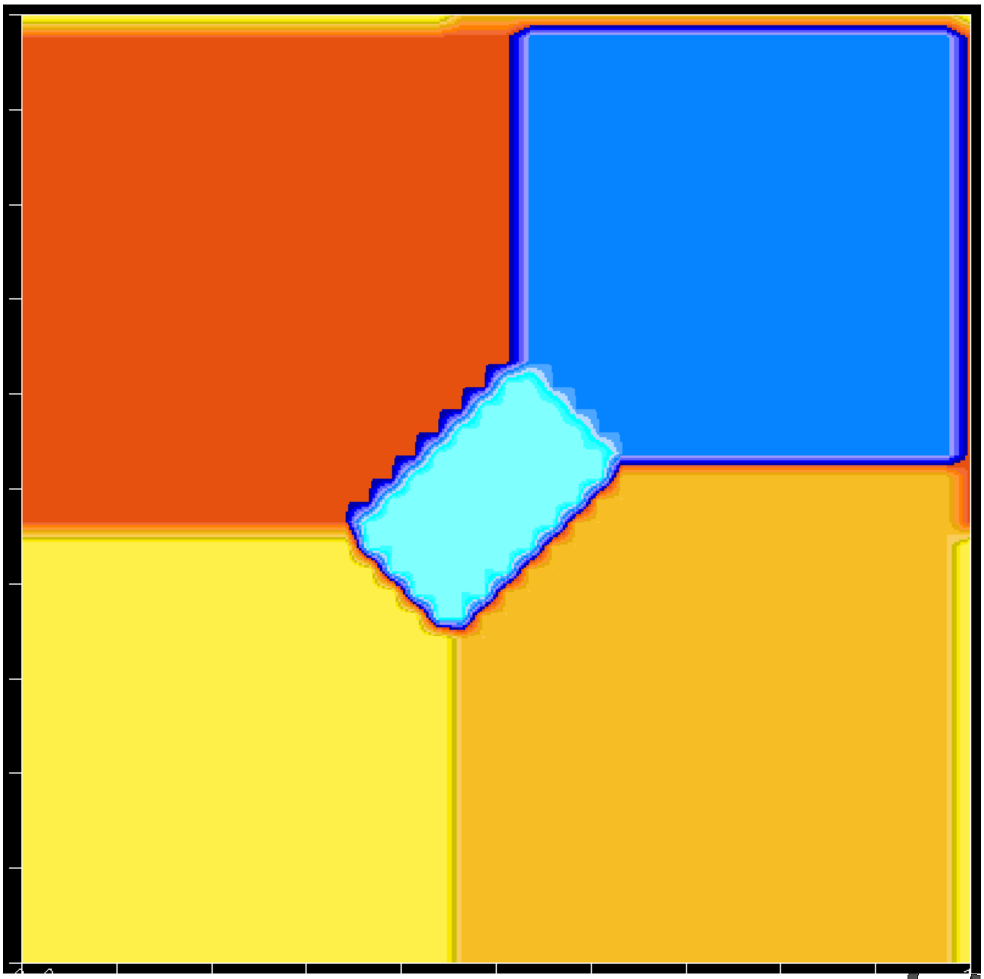

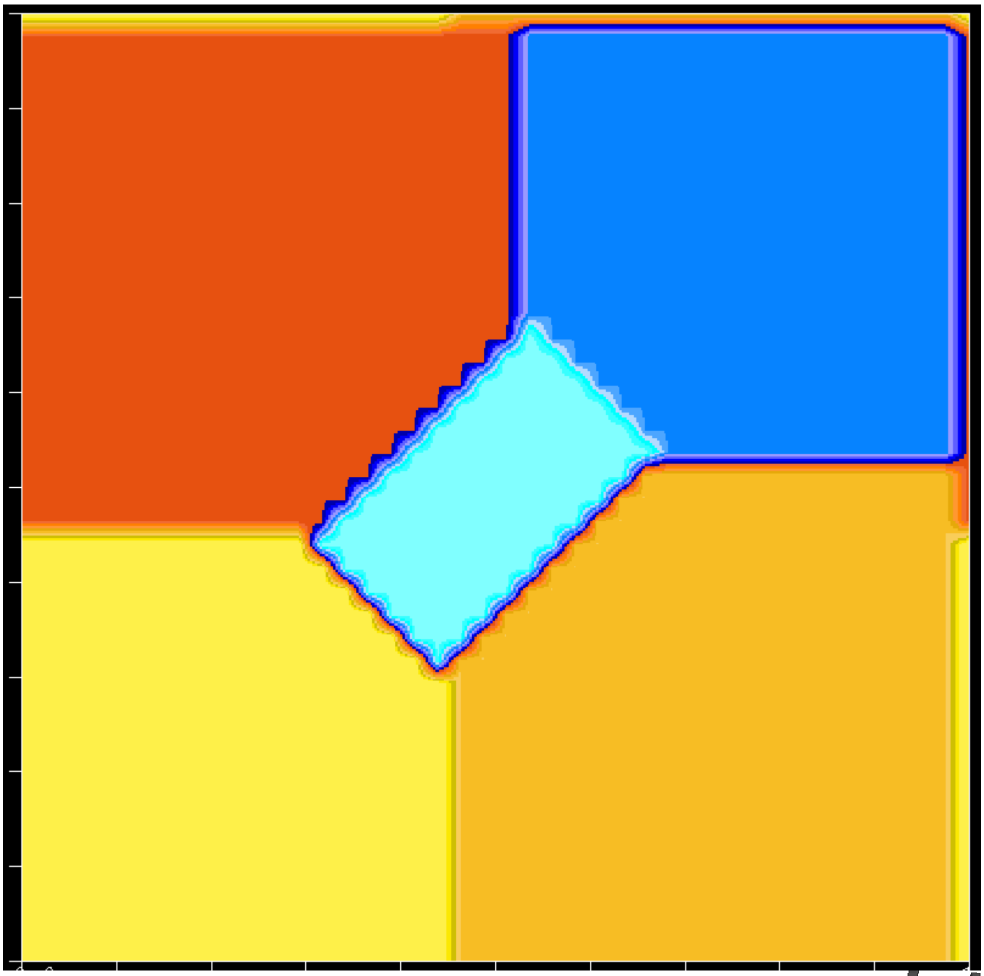

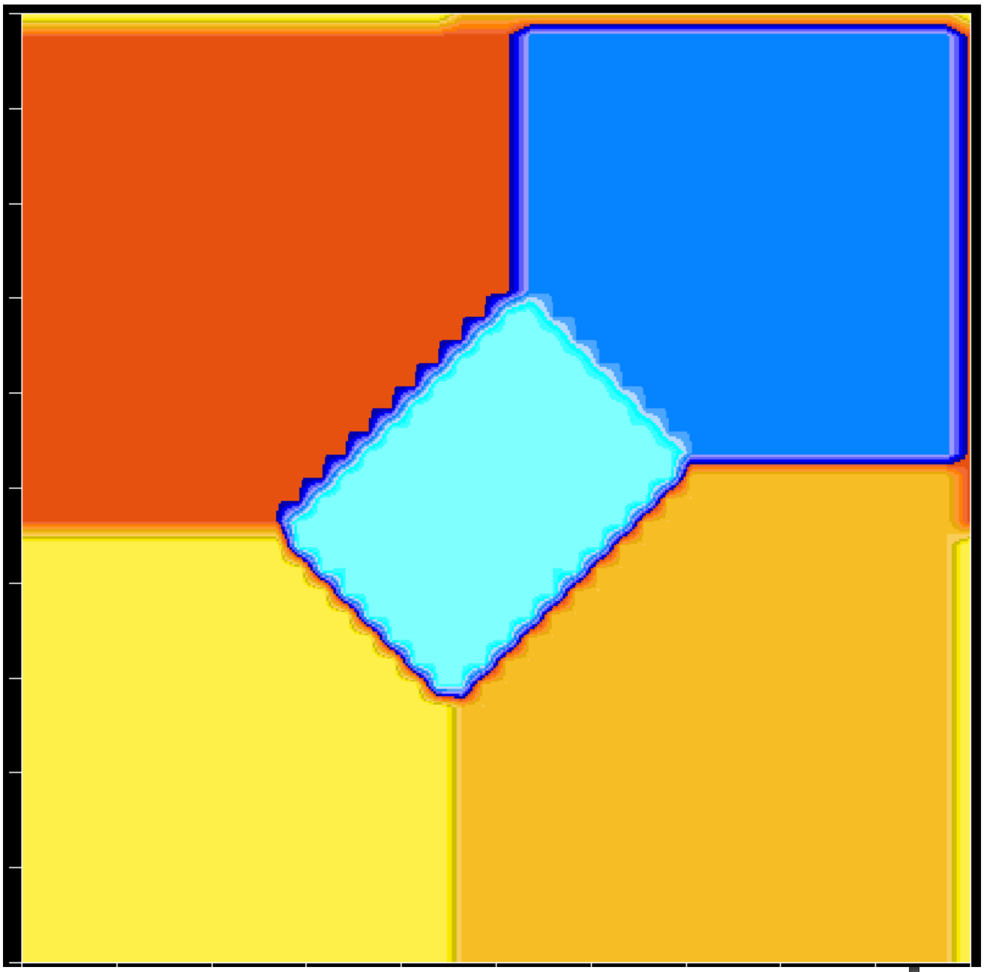

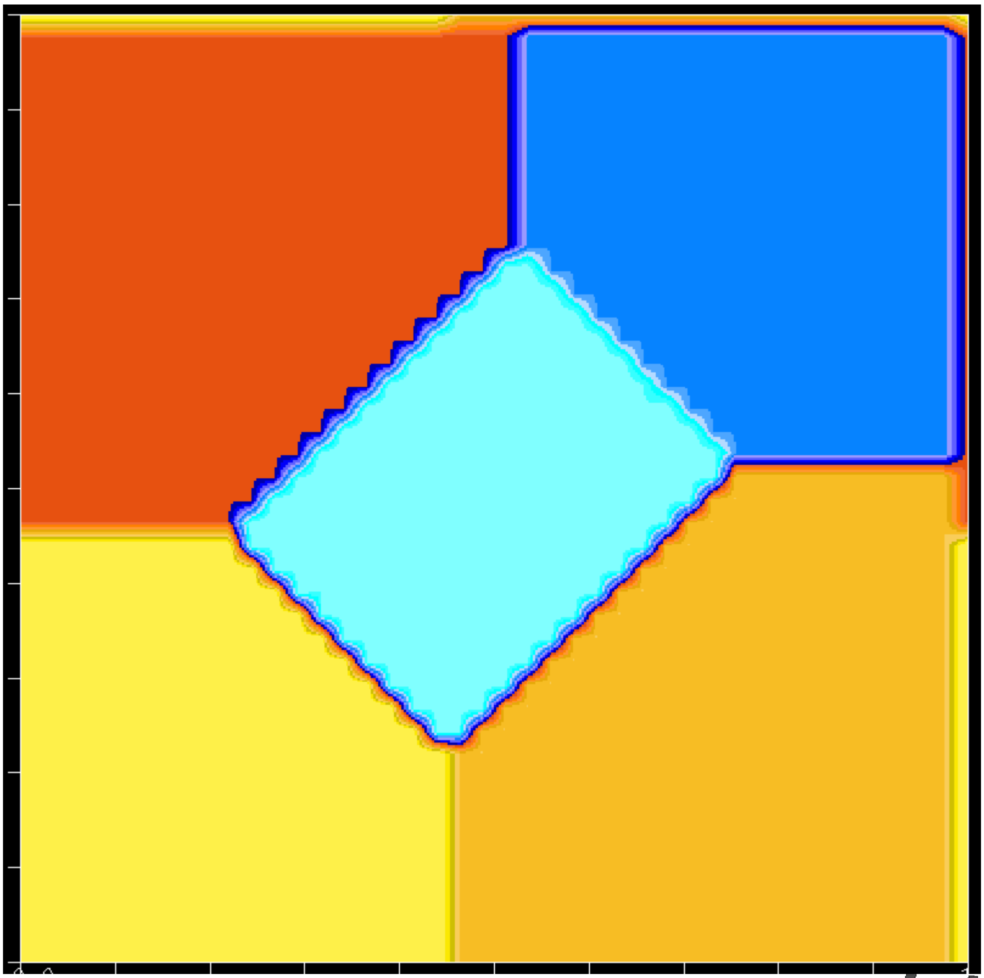

Conclusions

- Magnetic Powder diffraction is the primary technique for determining magnetic structures.
- Sometimes diffraction alone is not sufficient to determine without ambiguities a unique solution, even using single crystals.
- The Rietveld method extended for incommensurate structures has powered the powder method, providing not only the average structure but also the correlation lengths along different crystallographic directions.
- The analysis of exchange paths and the use of classical models for studying the magnetic ordering gives a first estimation of the relative exchange interactions.

THE PHASE PROBLEM OF MAGNETIC STRUCTURES WITH NON SYMMETRY-RELATED PROPAGATION VECTORS

Juan Rodríguez-Carvajal

Laboratoire Léon Brillouin, C.E.A./C.N.R.S., F-91191-Gif-sur-Yvette CEDEX, France

ABSTRACT

In these notes the limitations of neutron diffraction for determining the *true magnetic structure* of some compounds are discussed. The analytical expressions linking the measurable quantities to the model of a magnetic structure do not contain a crucial parameter: the phase factor between two Fourier coefficients not related by symmetry. The impossibility to obtain this parameter by conventional methods precludes the access to the true spin arrangement in the solid. The problem is first formulated analytically and illustrated by some simple examples, secondly we shall present some real examples concerning incommensurate-to-commensurate magnetic phase transitions and, finally, some conclusions are stated

1. Introduction

It is frequent the discovery of magnetic compounds that exhibit more than one propagation vector. The typical case is the so called multi-**k** structures, observed in some intermetallic compounds of high crystallographic symmetry [1]. Multi-**k** structures refers to a magnetic structure in which more than one arm of the star of **k** participates into the actual spin arrangement [*]. That is, the *transition chanel*, in terms of the Izyumov's school [2], has more than one propagation vector. Symmetry relations between the Fourier coefficients of the magnetic structure, when all the propagation vectors belong to a single star, can be obtained by group theory using the *geometrical* method of Bertaut [3] or the *algebraic* straightforward expressions that have been given by Izyumov and collaborators [2]. The practical determination of the transition chanel could be difficult because the magnetic phase transition, and the concommitant domain formation, produces satellites (in a single crystal diffraction pattern) which are not distinguishable (in usual conditions) from those of a true multi-**k** structure. External fields have to be applied to decide what is the actual situation. More unusual is the case showing two propagation vectors not belonging to the same star. However, a well known case is particularly common: the conical structures. Nagamiya [4] has given the conditions for two independent propagation vectors to describe *constant moment* (CM) magnetic structures. Nagamiya treated combinations of propagation vectors of the form $\mathbf{k}_1 = 1/2\mathbf{H}$ (or $\mathbf{k}_1 = 1/4\mathbf{H}$, $\mathbf{k}_1 = 3\mathbf{q}$) and $\mathbf{k}_2 = \mathbf{q}$ at the interior of the Brillouin Zone ($\mathbf{k}_2 \in IBZ$), so that the relative orientation of the Fourier coefficients is fixed and the relative phase is irrelevant. In this paper we shall formulate the problem in its full generality in relation with the practical structure determination. For that a summary of the most important scattering formulas is first given.

2. Neutron Scattering Cross Sections and Magnetic Structure Factor

For polarized neutrons the total scattered intensity and the final polarisation of scattered neutrons for the scattering vector **h** is given by the Blume's equations [5]. The scattered intensity is:

$$I_{\mathbf{h}} = N_{\mathbf{h}}N^*_{\mathbf{h}} + N_{\mathbf{h}}\{\mathbf{P}\cdot\mathbf{M}^*_{\perp\mathbf{h}}\} + N^*_{\mathbf{h}}\{\mathbf{P}\cdot\mathbf{M}_{\perp\mathbf{h}}\} + \mathbf{M}_{\perp\mathbf{h}}\cdot\mathbf{M}^*_{\perp\mathbf{h}} + i\mathbf{P}\cdot\{\mathbf{M}_{\perp\mathbf{h}}\times\mathbf{M}^*_{\perp\mathbf{h}}\} \qquad (1)$$

---

[*] In this paper we use the terms *spin* and *magnetic moment* indistinctly. The term *spin arrangement* is also used as synonymous of *magnetic structure*

The equation defining the scattered polarisation is:

$$\begin{aligned} \mathbf{P}_s I_{\mathbf{h}} &= \mathbf{P} N_{\mathbf{h}} N_{\mathbf{h}}^* + N_{\mathbf{h}} \mathbf{M}_{\perp\mathbf{h}}^* + N_{\mathbf{h}}^* \mathbf{M}_{\perp\mathbf{h}} + i\mathbf{P} \times \{\mathbf{M}_{\perp\mathbf{h}} N_{\mathbf{h}}^* - \mathbf{M}_{\perp\mathbf{h}}^* N_{\mathbf{h}}\} + \mathbf{M}_{\perp\mathbf{h}}\{\mathbf{P} \cdot \mathbf{M}_{\perp\mathbf{h}}^*\} \\ &+ \mathbf{M}_{\perp\mathbf{h}}^*\{\mathbf{P} \cdot \mathbf{M}_{\perp\mathbf{h}}\} - \mathbf{P}\{\mathbf{M}_{\perp\mathbf{h}} \cdot \mathbf{M}_{\perp\mathbf{h}}^*\} + i\{\mathbf{M}_{\perp\mathbf{h}} \times \mathbf{M}_{\perp\mathbf{h}}^*\} \qquad (2) \end{aligned}$$

Where $\mathbf{P}$ and $\mathbf{P}_s$ are the incident and scattered neutron polarisation, $N_{\mathbf{h}}$ is the nuclear structure factor and $\mathbf{M}_{\perp\mathbf{h}}$ is the magnetic interaction vector defined as:

$$\mathbf{M}_{\perp\mathbf{h}} = \mathbf{e} \times (\mathbf{M}(\mathbf{h}) \times \mathbf{e}) = \mathbf{M}(\mathbf{h}) - (\mathbf{e} \cdot \mathbf{M}(\mathbf{h}))\mathbf{e} \qquad (3)$$

$\mathbf{M}(\mathbf{h})$ is the magnetic structure factor, and $\mathbf{e}$ is the unit vector along the scattering vector $\mathbf{h}$. The scattering vector is $\mathbf{h}$=$\mathbf{H}$+$\mathbf{k}$ where $\mathbf{H}$ is a reciprocal lattice vector of the crystal structure and $\mathbf{k}$ the propagation vector corresponding to the current magnetic reflection. For a pure magnetic reflection $N_{\mathbf{h}} = 0$

The magnetic structures that we are considering have a distribution of magnetic moments that can be expanded as a Fourier series:

$$\mathbf{m}_{lj} = \sum_{\{\mathbf{k}\}} \mathbf{S}_{\mathbf{k}j} \exp\{-2\pi i \mathbf{k}\mathbf{R}_l\} \qquad (4)$$

The sum is extended to all propagation vectors that could belong to different stars. The Fourier coefficients $\mathbf{S}_{\mathbf{k}j}$ are, in general, complex vectors. The magnetic structure factor can be written as:

$$\mathbf{M}(\mathbf{H}+\mathbf{k}) = p \sum_{j=1}^{n_c} f_j(\mathbf{H}+\mathbf{k}) \mathbf{S}_{\mathbf{k}j} \exp\{2\pi i(\mathbf{H}+\mathbf{k})\mathbf{r}_j\} \qquad (5)$$

The sum is over *all the magnetic atoms* in the crystallographic cell. The constant $p(= r_e\gamma/2)$ is 0.2695 and allows the conversion of the Fourier components of magnetic moments, given in Bohr magnetons (μ_B) to scattering lengths units of 10^{-12}cm. $f_j(\mathbf{H}+\mathbf{k})$ is the magnetic form factor and $\mathbf{r}_j$ is the vector position of atom j. In the above expression the atoms have been considered at rest. If thermal motion is considered and if symmetry relations are established for coupling the different Fourier components, we obtain the general expression of the magnetic structure factor:

$$\mathbf{M}(\mathbf{h}) = p \sum_{j=1}^{n} O_j f_j(\mathbf{h}) T_j(iso) \sum_s M_{js} \mathbf{S}_{\mathbf{k}j} T_{js} \exp\{2\pi i[(\mathbf{H}+\mathbf{k})\{S \mid \mathbf{t}\}_s \mathbf{r}_j - \psi_{\mathbf{k}js}]\} \qquad (6)$$

The sum over j concerns the atoms of the magnetic asymmetric unit for the wavevector $\mathbf{k}$ (the Fourier component with index $\mathbf{k}$ contributes only to the $\mathbf{k}$-satellite). So that j labels different sites. The anisotropic temperature factor, T_{js}, is not generally necessary to be used in magnetic refinements($T_{js} = 1$). The sum over s concerns the different symmetry operators of the crystal space group that belong to the wave vector group. The matrix M_{js} transform the components of the Fourier term $\mathbf{S}_{\mathbf{k}j} = \mathbf{S}_{\mathbf{k}j1}$ of the starting atom $j1$ to that numbered as js in the orbit of j. The phase factor $\psi_{\mathbf{k}js}$ has two components:

$$\psi_{\mathbf{k}js} = \Phi_{\mathbf{k}j} + \phi_{\mathbf{k}js} \qquad (7)$$

$\Phi_{\mathbf{k}j}$ is a phase factor which is not determined by symmetry. It is a refinable parameter and it is significant only for an independent set of magnetic atoms (one orbit) which respect to another one. $\phi_{\mathbf{k}js}$ is a phase factor determined by symmetry. The Fourier component $\mathbf{k}$ of the magnetic moment of atom $j1$, $\mathbf{S}_{\mathbf{k}j}$, is transformed to

$$\mathbf{S}_{\mathbf{k}js} = M_{js} \mathbf{S}_{\mathbf{k}j} \exp\{-2\pi i \phi_{\mathbf{k}js}\} \qquad (8)$$

The matrices M_{js} and phases $\phi_{\mathbf{k}js}$ can be deduced from the atomic basis functions, obtained by applying projection operator formulas, corresponding to the active representation(s) participating in the definition of the actual magnetic structure. The sign of $\phi_{\mathbf{k}js}$ changes for -**k**.

In the general case $\mathbf{S}_{\mathbf{k}j}$ is a complex vector with six components. These six components per magnetic orbit constitute the parameters that have to be refined from the diffraction data. Symmetry reduces the number of free parameters per orbit to be refined. An alternative expression of the magnetic structure factor can be written as a function of *mixing coefficients* (parameters to be refined) and the atomic components of the basis functions of the relevant representation(s) [2]. In the case of a commensurate magnetic structure one can calculate the magnetic structure factor in the magnetic unit cell. In such a case $\mathbf{S}_{\mathbf{k}j}$ are real vectors corresponding to the magnetic moment of the atom j, the matrices M_{js} are real and all phases verify $\phi_{\mathbf{k}js} = 0$. The crystallographic magnetic groups theory can be fully applied in such a case [6].

If the magnetic structure represents an helical order the Fourier coefficients are of the form:

$$\mathbf{S}_{\mathbf{k}j} = \frac{1}{2}[m_{1j}\mathbf{u}_j + im_{2j}\mathbf{v}_j]\exp\{-2\pi i\phi_{\mathbf{k}j}\} \tag{9}$$

where $\mathbf{u}_j$ and $\mathbf{v}_j$ are orthogonal unit vectors. If $m_{1j} = m_{2j} = m_0$ the magnetic structure for the sublattice j corresponds to a classical helix (or spiral) of cylindrical envelope. All j atoms have a magnetic moment equal to m_0. If $m_{1j} \neq m_{2j}$ the helix has an elliptical envelope and the moments have values between $\min(m_{1j}, m_{2j})$ and $\max(m_{1j}, m_{2j})$. If $m_{2j} = 0$ the magnetic structure corresponds to a modulated sinusoid of amplitude m_{1j}.

3. The phase between independent k-vectors

When more than two independent propagation vectors appears in the diffraction pattern, the analysis of the data is unable to give a unique answer to the problem of the magnetic structure. In general is not possible to discriminate between the presence of two magnetic phases co-existing in the crystal and a coherent superposition of these two magnetic structures. We shall be concerned only with the latter picture. Even from this hypothesis it is not possible to get uniqueness. This can be seen adding a phase factor, depending only on **k**, to the Fourier series equation (4):

$$\mathbf{m}_{lj} = \sum_{\{\mathbf{k}\}} \mathbf{S}_{\mathbf{k}j}\exp\{-2\pi i(\mathbf{k}\mathbf{R}_l + \Psi_{\mathbf{k}})\} \tag{10}$$

The magnetic structure factor [equation (5)] transforms to:

$$\mathbf{M}(\mathbf{H}+\mathbf{k}) = p\exp\{2\pi i\Psi_{\mathbf{k}}\}\sum_{j=1}^{n_c} f_j(\mathbf{H}+\mathbf{k})\mathbf{S}_{\mathbf{k}j}\exp\{2\pi i(\mathbf{H}+\mathbf{k})\mathbf{r}_j\} \tag{11}$$

The phase $\Psi_{\mathbf{k}}$ appears in the expresion of the magnetic structure factor as a multiplicative phase factor that does not change the intensity of equation (1) or the scattered polarisation of (2) for a pure magnetic reflection. The phases $\Psi_{\mathbf{k}}$ are not accesible experimentally, so the real magnetic structure cannot be obtained from diffraction measurements alone.

The most simple case in which the phase plays an important role is the sinusoidally modulated structure in a simple Bravais lattice (a single magnetic atom per primitive cell) when the propagation vector takes special values. The Fourier coefficient and the corresponding magnetic moment at cell l are:

$$\mathbf{S}_{\mathbf{k}} = \frac{1}{2}m_o\mathbf{u}\exp\{-2\pi i\Psi_{\mathbf{k}}\} \qquad \mathbf{m}_l = m_o\mathbf{u}\cos 2\pi(\mathbf{k}\mathbf{R}_l + \Psi_{\mathbf{k}})$$

The phase $\Psi_{\mathbf{k}}$ plays no role when $\mathbf{k} \in IBZ$ and has no rational components. A change in the phase has the same effect as a change of the origin in the whole crystal. All magnetic moments between $-m_o\mathbf{u}$ and $m_o\mathbf{u}$ are realized somewhere in the lattice. However, if $\mathbf{k} = 1/4\mathbf{H}$ and $\Psi_{\mathbf{k}} = 1/8$ the magnetic structure is a CM-structure with the sequence $\{++--++--...\}$. This structure is indistinguishable of the sinusoidally modulated structure obtained with an arbitrary value of $\Psi_{\mathbf{k}}$. If all the components of $\mathbf{k}$ are rational the selection of the phase can have important consequences for the spin arrangement. This is the simplest case in which the physical picture depends on the election of a parameter ($\Psi_{\mathbf{k}}$) that is not accessible by diffraction methods. Physical considerations lead us to prefer one model among several other. For instance, CM-structures are normally expected at vey low temperatures when magnetic atoms have an intrinsic magnetic moment. This condition reduces the number of ways to combine non symmetry-related propagation vectors to several specific cases that have been discussed by Nagamiya [4]. Let us discuss some unusual simple cases that will be illustrated with real examples.

4. Fluctuating magnetic structures

The magnetic structures with more than one pair ($\mathbf{k}$,-$\mathbf{k}$) of propagation vectors not satisfying the Nagamiya's conditions are, as is the sinusoidally modulated magnetic structure, general non-constant moment structures. We shall call these spin configurations: *fluctuating structures* [†]

Fluctuating Structures with irrelevant phase-factors

This case corresponds to the combination of $\mathbf{k} = 1/2\mathbf{H}$ and $\mathbf{q} \in IBZ$ vectors. To simplify the notation we shall treat only one of the atoms of a particular Wyckoff site and we drop the reference index. The propagation vector $\mathbf{q}$ describes a helical configuration, and $\mathbf{k}$ corresponds to a uniaxial antiferromagnetic configuration, so that the Fourier coefficients of the atom are:

$$\mathbf{S}_{\mathbf{q}} = \frac{1}{2}m_1[\mathbf{u} + i\mathbf{v}]\exp\{-2\pi i\Psi_{\mathbf{q}}\} \qquad \mathbf{S}_{\mathbf{k}} = m_2\mathbf{n}$$

where, as above, $\mathbf{u}$ and $\mathbf{v}$ are orthogonal unit vectors defining the plane of the spiral of axis $\mathbf{w} = \mathbf{u} \times \mathbf{v}$, and $\mathbf{n}$ is a unit vector defining the axis of the spin configuration related to propagation vector $\mathbf{k} = 1/2\mathbf{H}$. The director cosines of $\mathbf{n}$ with respect to the axes ($\mathbf{u}, \mathbf{v}, \mathbf{w}$) are (n_1, n_2, n_3). The magnetic moment distribution of a coherent superposition of the two types of Fourier coefficients is given by the following formula (notice that $\Phi_l = 2\pi(\mathbf{q}\mathbf{R}_l + \Psi_{\mathbf{q}})$ and $l_h = \mathbf{H}\mathbf{R}_l$):

$$\begin{aligned}
\mathbf{m}_l &= m_1 \cos 2\pi(\mathbf{q}\mathbf{R}_l + \Psi_{\mathbf{q}})\mathbf{u} + m_1 \sin 2\pi(\mathbf{q}\mathbf{R}_l + \Psi_{\mathbf{q}})\mathbf{v} + m_2 \exp\{-\pi i\mathbf{H}\mathbf{R}_l\}\mathbf{n} \\
&= m_1 \cos \Phi_l\mathbf{u} + m_1 \sin \Phi_l\mathbf{v} + m_2(-1)^{l_h}\mathbf{n} \\
&= (m_1 \cos \Phi_l + (-1)^{l_h}m_2n_1)\mathbf{u} + (m_1 \sin \Phi_l + (-1)^{l_h}m_2n_2)\mathbf{v} + (-1)^{l_h}m_2n_3\mathbf{w} \qquad (12)
\end{aligned}$$

The modulus of the magnetic moment can be calculated by taking the square of equation (12):

$$\begin{aligned}
m_l^2 &= m_1^2 + m_2^2 + 2m_1m_2(-1)^{l_h}(n_1 \cos \Phi_l + n_2 \sin \Phi_l) \\
&= m_1^2 + m_2^2 + 2m_1m_2(-1)^{l_h} \cos \alpha_l \qquad (13)
\end{aligned}$$

If $\mathbf{n}$ is parallel to $\mathbf{w}$ the moment is constant and we obtain an antiferromagnetic conical structure (if $\mathbf{H}$= 0, we obtain the classical ferromagnetic conical structure). For the

---

[†] The term *fluctuating* has no dynamic content in the present context

general orientation of $\mathbf{n}$ (non vanishing components in the $\mathbf{u}$-$\mathbf{v}$ plane) the modulus of this distribution is not constant. The amplitude varies between the two extreme values $\sqrt{m_1^2 + m_2^2 + 2m_1m_2 \sin\theta}$ and $\sqrt{m_1^2 + m_2^2 - 2m_1m_2 \sin\theta}$, being θ the angle of $\mathbf{n}$ with $\mathbf{w}$. A real system in which this behaviour seems to take place is the compound $\mathrm{CsMnF_4}$ [7]. Another interesting system is $\mathrm{TbMn_6Ge_6}$ [8] [‡] The second wave vector, in this case, is $\mathbf{k} = 0$ and the associated magnetic moment lies within the $\mathbf{u}$-$\mathbf{v}$ plane defining the spiral plane of the first propagation vector. This gives rise to a distorted spiral structure.

In all these cases, the selection of the phase factor $\Psi_\mathbf{q}$ is completely irrelevant. That is, the physical picture obtained after using the equation (10) is not changed by varying the phase factor.

Fluctuating Structures Approaching CM-structures

We shall now consider the case of two pairs of propagation vectors ($\mathbf{k}$,-$\mathbf{k}$) and ($\mathbf{q}$,-$\mathbf{q}$) verifying $\mathbf{k}, \mathbf{q} \in IBZ$. Such a magnetic structure has as Fourier coefficients:

$$\mathbf{S_k} = \frac{1}{2}(\mathbf{R_k} + i\mathbf{I_k}) \qquad \mathbf{S_q} = \frac{1}{2}(\mathbf{R_q} + i\mathbf{I_q}) \exp\{-i\Psi\}$$

Using the notation $\Phi_{\mathbf{k}l} = 2\pi\mathbf{k}\mathbf{R}_l$ the magnetic moment distribution is given by:

$$\mathbf{m}_l = \mathbf{R_k} \cos\Phi_{\mathbf{k}l} + \mathbf{I_k} \sin\Phi_{\mathbf{k}l} + \mathbf{R_q} \cos(\Phi_{\mathbf{q}l} + \Psi) + \mathbf{I_q} \sin(\Phi_{\mathbf{q}l} + \Psi) \tag{14}$$

This moment distribution is generally a non-CM structure and the change of the phase factor Ψ can modify the physical picture if both vectors $\mathbf{k}$ and $\mathbf{q}$ have rational components. This last case is interesting when the components are simple integer fractions because one can treat the problem using the magnetic cell and search for a magnetic space group that fix automatically the phase. The finding of such a commensurate magnetic structure does not eliminate the problem of uniqueness of the magnetic moment distribution compatible with the experimental results. However, the possibility to have a simple spin arrangement with magnetic moments of atoms approaching the expected intrinsic moment is more satisfying form the physical point of view.

If a CM-structure can be found refining the magnetic structure using the magnetic cell, a particular set of equations (14) can be established for atoms inside the magnetic cell and the phase factor Ψ can be obtained solving these equations. Of course, to get a set of compatible equations the vectors $\mathbf{R}$ and $\mathbf{I}$ cannot be arbitrary. An example can be readily shown if we consider only *real* Fourier coefficients in equation (14). We can write for the α-component:

$$R^\alpha_\mathbf{q} \cos(\Phi_{\mathbf{q}l} + \Psi) = m^\alpha_l - R^\alpha_\mathbf{k} \cos\Phi_{\mathbf{k}l} \quad \Longrightarrow \quad \Psi = \cos^{-1} \frac{m^\alpha_l - R^\alpha_\mathbf{k} \cos\Phi_{\mathbf{k}l}}{R^\alpha_\mathbf{q}} - \Phi_{\mathbf{q}l}$$

The above equations must be verified for the set of points l inside the magnetic cell and for all components simultaneously. This indicates that only very special relationships between Fourier coefficients must be verified to have a single Ψ to connect the two descriptions.

An interesting example is the magnetic ordering of $\mathrm{TbGe_3}$ [9]. This compound crystallizes in the space group $Cmcm$, ($a = 4.07, b = 20.8, c = 3.92$ Å), with Tb-atoms in positions ($4c$) $\pm(0, y, 1/4)$. Below the Néel temperature ($T_N = 40$K) the magnetic order is characterized by two independent propagations vectors $\mathbf{k} = (k_x, 0, 0)$ and $\mathbf{q} = (q_x, 0, q_z)$ with $k_x \approx q_x \approx \frac{1}{2}$ and $q_z \approx \frac{1}{3}$. Below $T_{ic} = 24$K the propagation vectors lock-in to commensurate values. Both vectors verify $\mathbf{k}, \mathbf{q} \in IBZ$ with a two-arm star for $\mathbf{k}$

[‡] See also the article: *Magnetic Spiral Structures in the Hexagonal RMn_6Ge_6 Compounds*, by P. Schobinger-Papamantellos, J. Rodríguez-Carvajal, G. André and K.H.J. Buschow, in these proceedings

($G_{\mathbf{k}} = C2cm$) and a four-arm star for $\mathbf{q}$ ($G_{\mathbf{q}} = Cc$). The refinement of the magnetic structure at low temperature in the magnetic unit cell using powder diffraction data provides a quasi-collinear structure with two types of Tb-atoms having similar moments ($m(Tb_1) = 9.2\mu_B, m(Tb_2) = 8.8\mu_B$). The refinement using real Fourier coefficients for all propagation vectors (including the second pair of the star of $\mathbf{q}$) gave similar agreement. A systematic search of the phase factors using a computer program [10] allows the finding of a consistent set of phases that produces fluctuations of $m(Tb)$ between $9.4\mu_B$ and $7.0\mu_B$. The spin arrangement is similar to that observed in the magnetic cell refinement. For the incommensurate phase we suppose that the spin arrangement does not change dramatically, so that the phases found for the lock-in phase are still valid.
Symmetry analysis can be applied to each wave vector separately. There is no interference terms between reflections belonging to different sets of satellites, so that we can proceed as if two magnetic different phases co-exist and only at the end of the analysis we can think in the coherent superposition of both phases. The computer program [10] we have written can be used as a general tool for searching phase factors between Fourier coefficients belonging to non-symmetry related wave vectors giving the lowest fluctuation between m_{min} and m_{max}.

5. Conclusions

The physical origin of the stabilization of two propagation vectors belonging to different stars is not yet clear in the absence of external fields. In Bravais lattices we have to think in the action of higher order terms (biquadratic) in the spin hamiltonian to stabilize two propagation vectors. In complex crystal structures the nature of the ground state is not known in the general case and, probably, it is not necessary to invoke higher order terms to stabilize two non-related propagation vectors. Only the case of conical structures ($\mathbf{k} = 0$ and $\mathbf{q} \in IBZ$) has been studied with some detail [11] for the spinel lattice. We can conclude that only a physical model based in the microscopic spin-spin interactions is able to fix completely the phases appearing in the Fourier expansion of the magnetic moment distribution in the solid. Experimentally, other techniques (like Mössbauer spectroscopy, neutron or X-ray topography, μ-SR, etc...) may help, in some cases, to distinguish between several models. Unfortunately there is no general method to overcome this *phase problem.*

References

1. J.Rossat-Mignod, *Magnetic Structures*, in *Methods of Experimental Physics*: Neutron Scattering, Vol 3, Academic Press (1987).
2. Y.A. Izyumov, V.E. Naish, *J.Magn.Magn.Mat.* **12**, 239 (1979); Y.A. Izyumov, V.E. Naish and V.N. Syromiatnikov, *J.Magn.Magn.Mat.* **12**, 249 (1979); Y.A. Izyumov, V.E. Naish and S.B. Petrov, *J.Magn.Magn.Mat.* **13**, 267(1979); *ibidem* **13**, 275 (1979)
3. E.F. Bertaut, *Spin Configurations of Ionic Structures. Theory and Practice*, in *Magnetism* (G.T. Rado and H. Shul, eds.), Vol III, Ch. 4, 149 Academic Press, New York. (1963); see also *Acta Cryst* **A24**, 217 (1968), *J. de Physique*, Coll. C1, sup. n-3,32, C1-462 (1971) and *J.Magn.Magn.Mat.* **24**, 267 (1981).
4. T. Nagamiya, *Solid State Physics* **20**, 305-411 (1967)
5. M. Blume, *Phys Rev* **130**(5), 1670 (1963)
6. W. Opechowski and R. Guccione, *Magnetic Symmetry*, in *Magnetism* (G.T. Rado and H. Shull, eds.), Vol II A, Ch. 3, 105 Academic Press, New York. (1965).
7. J. Rodríguez-Carvajal, *Physica B* **192**, 55 (1993)
8. P. Schobinger-Papamantellos, J. Rodríguez-Carvajal, G. André and K.H.J. Buschow, *J.Magn.Magn.Mat.* **150**, 311 (1995)
9. P. Schobinger-Papamantellos, J. Rodríguez-Carvajal, T. Janssen and K.H.J. Buschow, *Proc.Int.Conf Aperiodic Crystals*, p. 311 (1994). Ed. G. Chapuis, W. Paciorěk, World Scientific, Singapore.
10. J. Rodríguez-Carvajal, *Program* MOMENT (1994), (unpublished).
11. D.H. Lyons, T.A. Kaplan, K. Dwight and.N. Menyuk *Phys Rev* **126**(2), 540 (1962).

MAGNETIC STRUCTURE DETERMINATION FROM POWDER DIFFRACTION USING THE PROGRAM *FullProf*

JUAN RODRIGUEZ-CARVAJAL

Laboratoire Léon Brillouin, (CEA-CNRS), CEA/Saclay, 91191 Gif sur Yvette Cedex, FRANCE
E-mail: juan@llb.saclay.cea.fr

In this paper the techniques for magnetic structure determination from neutron powder diffraction (NPD) data as implemented in the program *FullProf* are reviewed. In the general case the magnetic moment of an atom in the crystal is given as a Fourier series. The Fourier coefficients are complex vectors constituting the "unknowns" to be determined. These vectors define the magnetic structure and they correspond to the "atom positions" of an unknown crystal structure. The use of group theoretical methods for the symmetry analysis is needed to find the smallest set of free parameters. In general the Fourier coefficients are linear combinations of the basis functions of the irreducible representations of the wave vector group. The coefficients of the linear combinations can be determined by the simulated annealing (SA) technique comparing the calculated versus the observed magnetic intensities. The SA method has been improved and extended to the case of incommensurate magnetic structures within *FullProf*.

1 Introduction

In the last years the Rietveld Method (RM) has allowed great progress in the analysis of powder diffraction data. The RM is not designed for structure determination, it is just a least squares optimisation of an initial model of the crystal and magnetic structure supposed to describe approximately the experimental powder diffraction pattern. It is important to start with a "good" initial model in order to succeed the refinement procedure. In this paper we shall be concerned with the problem of getting the initial model of a magnetic structure in order to refine it from powder diffraction data. We shall describe the basis of the technique and the way the magnetic structure determination is implemented in the program *FullProf*.

2 The formalism of propagation vectors for describing magnetic structures.

The reader interested in the basis of the elastic magnetic scattering in relation with magnetic structures may consult the references [1, 2]. Here we will follow the reference [3] but using a different convention for the sign of phases and a somewhat different notation. The intensity of a Bragg reflection (we neglect here the geometrical factors) for non polarised neutrons is given by:

$$I_{\mathbf{h}} = N_{\mathbf{h}} N_{\mathbf{h}}^{*} + \mathbf{M}_{\perp\mathbf{h}} \cdot \mathbf{M}_{\perp\mathbf{h}}^{*} \qquad (1)$$

where $N_{\mathbf{h}}$ is the nuclear structure factor and the magnetic interaction vector $\mathbf{M}_{\perp\mathbf{h}}$ is defined as:

$$\mathbf{M}_{\perp\mathbf{h}} = \mathbf{e} \times (\mathbf{M}(\mathbf{h}) \times \mathbf{e}) = \mathbf{M}(\mathbf{h}) - \mathbf{e}(\mathbf{e} \cdot \mathbf{M}(\mathbf{h})) \qquad (2)$$

$\mathbf{M}(\mathbf{h})$ is the magnetic structure factor, and $\mathbf{e}$ is the unit vector along the scattering vector $\mathbf{h}=\mathbf{H}+\mathbf{k}$, where $\mathbf{H}$ is a reciprocal lattice vector of the crystal structure and $\mathbf{k}$ the propagation vector corresponding to the current magnetic reflection. The magnetic structures that we are considering have a distribution of magnetic moments that can be expanded as a Fourier series:

$$\mathbf{m}_{lj} = \sum_{\{\mathbf{k}\}} \mathbf{S}_{\mathbf{k}j}\; exp\{-2\pi\, i\mathbf{k}\mathbf{R}_l\} \qquad (3)$$

The sum is extended to all propagation vectors that could belong to different stars. The Fourier coefficients $\mathbf{S}_{\mathbf{k}j}$ are, in general, complex vectors. The magnetic structure factor corresponding to such a magnetic structure can be written as:

$$\mathbf{M}(\mathbf{h}) = p\sum_{j=1}^{n} O_j f_j(\mathbf{h}) T_j^{iso} \sum_{s} M_{js}\mathbf{S}_{\mathbf{k}j} exp\left\{2\pi i\left[(\mathbf{H}+\mathbf{k})\{S|\mathbf{t}\}_s \mathbf{r}_j - \psi_{\mathbf{k}js}\right]\right\} \qquad (4)$$

The sum over j concerns the atoms of the magnetic asymmetric unit for the wave vector **k**. We are concerned only with magnetic atoms within the crystallographic unit cell, so that j label different sites: $f_j(\mathbf{h})$ is the magnetic form factor and $\mathbf{r}_j$ is the vector position of atom j. The constant $p = r_e\, \gamma/2 = 0.2695$ allows the conversion of the Fourier components of magnetic moments, given in Bohr magnetons to scattering lengths units of 10^{-12} cm. The sum over s concerns the different symmetry operators of the crystal space group that belong to the wave vector group $G_\mathbf{k}$ (subgroup of the crystallographic space group formed by the operators leaving invariant the propagation vector). The matrix M_{js} transform the components of the Fourier term $\mathbf{S}_{\mathbf{k}j}$ of the starting atom j to that numbered as js in the orbit of j. The phase factor $\psi_{\mathbf{k}js}$ has two components:

$$\psi_{\mathbf{k}js} = \Phi_{\mathbf{k}j} + \phi_{\mathbf{k}js} \qquad (5)$$

$\Phi_{\mathbf{k}j}$ is a phase factor that is not determined by symmetry. It is a free parameter and it is significant only for an independent set of magnetic atoms (one orbit) which respect to another one. $\phi_{\mathbf{k}js}$ is a phase factor determined by symmetry. The Fourier component $\mathbf{S}_{\mathbf{k}j}$ of the representative starting atom j is transformed to

$$\mathbf{S}_{\mathbf{k}js} = M_{js}\mathbf{S}_{\mathbf{k}j}\; exp\{-2\pi\, i\phi_{\mathbf{k}js}\} \qquad (6)$$

The matrices M_{js} and phases $\phi_{\mathbf{k}js}$ can be deduced from the atomic basis functions, obtained by applying projection operator formulas, corresponding to the active representation(s) participating in the definition of the actual magnetic structure. The sign of $\phi_{\mathbf{k}js}$ changes for **-k**. In the general case $\mathbf{S}_{\mathbf{k}j}$ is a complex vector with six components. These six components per magnetic orbit constitute the parameters that have to be refined from the diffraction data. Symmetry reduces the number of free parameters to be refined. In some cases, transformations like expression (6) cannot be obtained from the basis functions of the irreducible representations of the propagation vector group; for those cases an alternative expression of the magnetic structure factor can be written as a function of "mixing coefficients" (parameters to be refined) and the atomic components of the basis functions of the relevant representation [4]. The expression of the Fourier coefficients in terms of the atomic components of the basis functions is given as:

$$\mathbf{S}_{\mathbf{k}js} = \sum_{m\lambda} C_{jm\lambda}^{\nu}\mathbf{S}_{m\lambda}^{\mathbf{k}\,\nu}(js) \qquad (7)$$

The formula of the magnetic structure factor is then transformed to:

$$\mathbf{M}(\mathbf{h}) = p\sum_{j=1}^{n} O_j f_j(\mathbf{h}) T_j^{iso} \sum_{m\lambda} C_{jm\lambda}^{\nu} \sum_{s} \mathbf{S}_{m\lambda}^{\mathbf{k}\,\nu}(js) exp\left\{2\pi i\left[\mathbf{h}_s\mathbf{r}_j - \Phi_{\mathbf{k}j}\right]\right\} \qquad (8)$$

In the above expressions, ν labels the active irreducible representation, Γ_ν, of the of the propagation vector group $G_\mathbf{k}$, λ labels the component corresponding to the dimension of the representation Γ_ν, m is an index running between one and the number of times the representation Γ_ν is contained in the global magnetic representation Γ_M. Finally $\mathbf{S}_{n\lambda}^{\mathbf{k}\,\nu}(js)$

are constant vectors obtained by the application of the projection operator formula to unit vectors along the directions of the unit cell basis. An addition sum over ν is sometimes necessary when more than one irreducible representation is involved in the magnetic phase transition. See reference [4] for details.

If the magnetic structure has several propagation vectors **k**, it is not possible in general to determine unambiguously the spin configuration, because the phase between the different Fourier components cannot be determined. Fortunately, nature often selects simple solutions and many magnetic structures have a single propagation vector, or display some symmetry constraints that reduce the complexity of the periodic magnetic structure given by Eq.3. Solving a magnetic structure consist of finding a set of propagation vectors indexing the whole set of magnetic reflections and a set of "mixing coefficients" (or, equivalently, the components of the Fourier coefficients and phases) providing a good agreement between the intensities of the observed and calculated (using the above expressions) magnetic reflections. In some cases the search for a good starting model may be formulated in terms of other set of parameters. For instance, in cases of conical/helical structures involving magnetic atoms with a common cone-axis, the magnetic structure factor can be written in terms of the module of the magnetic moments, the angle between the moments and the cone-axis, and phases between the different atoms. This description in real space gives a more intuitive picture of the magnetic structure.

3 The search for the propagation vector and symmetry analysis.

The first problem to be solved before attempting the resolution of the magnetic structure is the determination of the propagation vector(s), i.e. its "periodicity". To find **k** is necessary to index the magnetic reflections appearing below the ordering temperature. With a single crystal the task is somewhat easy, but is tedious for a powder because only the module of reciprocal vectors is available. We have developed a method for searching the propagation vector of a commensurate or incommensurate structure implemented in the program *SuperCell* [5]. Once an approximate propagation vector is obtained the symmetry analysis according to references [4] can be started. The program *BasIreps* may be used for obtaining the vectors $\mathbf{S}_{n\lambda}^{\mathbf{k}\,\nu}\left(js\right)$ in Eq.7 for each crystallographic site occupied by magnetic atoms.

To solve the magnetic structure, the integrated intensities of the magnetic reflections may be obtained using the method of "profile matching", simultaneously with the Rietveld method, implemented in the program *FullProf* [3, 5]. This mixed procedure has to be used with caution: no structural parameter of the known phase must be refined. This is the usual case of neutron diffraction patterns of magnetically ordered compounds, where the nuclear reflections coexist with the magnetic reflections. For illustration purposes we show in Fig.1 the plot of the observed versus calculated pattern of a portion of the simulated diffraction pattern of $DyMn_6Ge_6$ at low temperature after performing the extraction procedure. The magnetic structure has two propagation vectors $\mathbf{k}_1=(0,0,0)$ and $\mathbf{k}_2=(0,0,\delta)$, with $\delta \approx 0.165$ with respect to the reciprocal lattice of the crystallographic unit cell. All satellite reflections are indexed with $\mathbf{h}=\mathbf{H}\pm\mathbf{k}_2$. There are also contributions to the same positions of the nuclear reflections, $\mathbf{h}=\mathbf{H}$ ($\mathbf{k}_1=0$), accounting for a ferromagnetic component. The spin arrangement corresponds to a double cone magnetic structure.

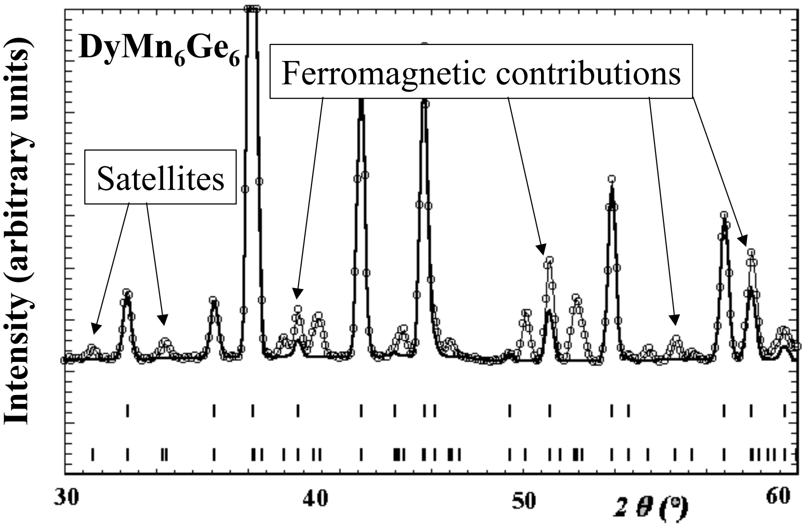

Figure 1. Profile matching refinement of the $DyMn_6Ge_6$ neutron diffraction pattern at low temperature. The profile of the calculated nuclear contribution (upper reflection marks) is also displayed as a thick continuous line. The second set of reflection markers corresponds to the magnetic peaks. Markers at the same positions as the nuclear (first set) reflections correspond to $\mathbf{k}_1=(0,0,0)$, the extra markers are the position of the satellites corresponding to $\mathbf{k}_2=(0,0,\delta)$.

4 The resolution of magnetic structures from powder data: the simulated annealing method

We shall describe the Simulated Annealing (SA) technique to solve the magnetic structure using clusters of overlapped reflections as single observations. The merging of clusters is automatically performed using the option “profile matching” of the program *FullProf* [5]. The SA method described below is also valid for the analysis of single crystal data where, except for domains, there is no reflection overlap.

The SA algorithm is a general-purpose optimisation technique for large combinatorial problems introduced in 1983 by Kirpatrick, Gelatt and Vecchi [6]. The function, $E(\boldsymbol{\omega})$ to be optimised with respect to the configuration described by the vector state $\boldsymbol{\omega}$ is called the “cost” function. In the context of magnetic structures the configuration $\boldsymbol{\omega}$ is the list of all the components of the Fourier coefficients of magnetic atoms existing in the chemical unit cell and this list is obtained from the independent parameters $\boldsymbol{\beta}$ that are those really participating in the annealing procedure. The most general case of parameters constituting the vector $\boldsymbol{\beta}$ corresponds to the set of mixing coefficients of the linear combination given by Eq.8, but, as stated above, another set of parameters in real space (moment amplitudes, angles, …) may also be used. First we select an initial configuration, $\boldsymbol{\omega}_{old}$, then each step of SA method consists of a slight change of the old configuration to a new one, $\boldsymbol{\omega}_{new}$. If $\Delta=E(\boldsymbol{\omega}_{new})-E(\boldsymbol{\omega}_{old}) \leq 0$ the new configuration serves as old configuration for the next step. If Δ is positive, $\boldsymbol{\omega}_{new}$ is accepted as current configuration only with certain probability that depends on the so-called “temperature”, T, parameter and Δ. The probability, given by the Boltzman factor $\exp(-\Delta/T)$, that a worse configuration is accepted is slowly decreased on “cooling”.

For magnetic structure determination, the cost function can be chosen as the conventional crystallographic R-factor, or some function related to it. In the new version of *FullProf* [5] the following expression is used:

$$E[\omega(\beta)]= R[\omega(\beta)] = c \sum_k \left| I_{obs}(k) - S\sum_{j(k)} I_{calc}(j)[\omega(\beta)] \right|$$

The sum over *k* is extended for all the "observations" (clusters of overlapped reflections), and that over j(*k*) for all the reflections contributing to the observation *k*. The constant factor *c* is given by: $1/c = I_T = \Sigma_k I_{obs}(k)$. *S* is a scale factor.

To start solving a magnetic structure with the SA method one has to create the intensity file where the indices of each reflection and its intensity are written. This is performed automatically within *FullProf* by using profile matching modes and the option that outputs the overlapped reflection clusters in a file that can be used as input for the SA method. The usual PCR file [5] of *FullProf* is then used for controlling the algorithm. A pseudo-code describing the SA procedure was given in reference [3]. The SA parameters are those defining the limits of loops in the algorithm described in [3]: *T_ini* = initial temperature, *N* = maximum number of temperatures, *NcyclM* = number of Montecarlo cycles per temperature, *Accept*=Minimum percentage of accepted configurations; and the "cooling" schedule *T(t+1)=qT(t)* ($q<1$, $q \approx 0.9$). The user may select either a fixed step for each variable (that are defined within a simulation box of hard or periodic limits) or a variable step (Corana's algorithm) that is dynamically adapted in order to have an adequate rate of accepted configurations for each temperature [7].

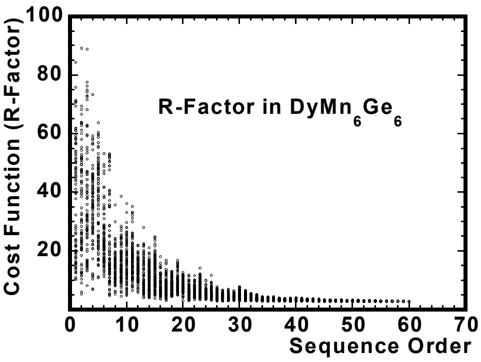

Figure 2. Evolution of the cost function for accepted configuration in the resolution of the magnetic structure of $DyMn_6Ge_6$ by simulated annealing as a function of the sequential order of temperatures. For a single temperature on can see the dispersion of the R-factor, corresponding to the different configurations, that is reducing as temperature decreases.

The starting point may be an arbitrary configuration or a given one. At variance with least-squares optimisation methods, the SA algorithm never diverges. Always the algorithm proceeds roughly in two steps. The first step, at high temperatures, the algorithm is searching for the "basin of attraction" of the minimum in the configuration space, this part constitutes the "magnetic structure determination". Once the region is attained, a more or less sharp drop in the average "energy" (R-factor) occurs. Then, the second step starts when the average R-factor is low enough, the algorithm enters in its phase of "refinement", where the good configuration has already been found, and performs a progressive improvement of the solution. This is clearly seen in the behaviour of the cost function versus the ordinal number of the temperature parameter in Fig.2, illustrating the case of $DyMn_6Ge_6$. In figure 3 it is shown the behavior of the amplitude of the magnetic moments of Dy and Mn atoms. The plot shows that there are a large dispersion at the stage of “magnetic structure solution” (starting phase of the algorithm) and a progress toward definite values within the “refinement” region.

For a given set of constraints the final average R–factor should be reasonably good (below 20%) except for contradictory or false constraints. False minima are encountered when the number of free parameters is of the same order of magnitude than the number of observations and/or the observations are of bad quality (very weak magnetic reflections and large errors associated to them). Ambiguities can be easily discovered. When the intensity data do not depend on a parameter, this shows an anomalous behaviour: in a plot similar to that of Fig. 3, large oscillations persist even at low temperature.

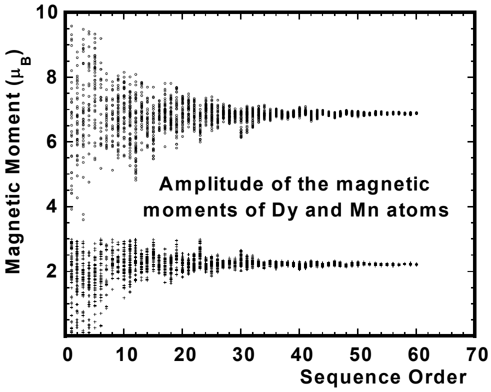

Figure 3. Evolution of the magnetic moment of Dy and Mn versus the number of sequential temperature. Similar plots can be observed for other magnetic parameters (cone angles and magnetic phase angles).

In conclusion, we have shown that the SA algorithm can be used for the magnetic structure determination even in the case of complex incommensurate magnetic structures. The method is straightforward and is fully implemented in the program *FullProf* that is publicly available [5].

References

1. J.Rossat-Mignod, “Magnetic Structures”, in *Methods of Experimental Physics: Neutron Scattering* (1987), Vol 3, Academic Press, New York.
2. P.J. Brown, “Magnetic Structure”, in *Frontiers of Neutron Scattering* , (1986), p. 31, (R.J. Birgeneau, D.E. Moncton & A. Zeilinger eds.). Elsevier Science Publishers, North-Holland Amsterdam.
3. J. Rodríguez-Carvajal, *Physica* **B 192** (1993), p. 55.
4. Y.A. Izyumov, V.E. Naish, *J Magn.Magn.Mat.* **12** (1979), p. 239; Y.A. Izyumov, V.E. Naish and V.N. Syromiatnikov *J Magn.Magn.Mat.* **12** (1979), p. 249; Y.A. Izyumov, V.E. Naish and S.B. Petrov, *J Magn.Magn.Mat.* **13** (1979), p. 267; *ibid.* 13 (1979), p. 275;Y.A. Izyumov, *J Magn.Magn.Mat.* **21** (1980), p. 33
5. J. Rodríguez-Carvajal and T. Roisnel (1999). *FullProf*, *WinPLOTR* and accompanying programs at http://www-llb.cea.fr/fullweb/powder.htm
6. S. Kirpatrick, C.D. Gelatt and M.P. Vecchi, *Science* **220** (1983), p 671.
7. A. Corana, M. Marchesi, C. Martini and S. Ridella, *ACM Trans. Math. Software* **13** (1987), p 262

Flow Chart of Magnetic Structure Determination

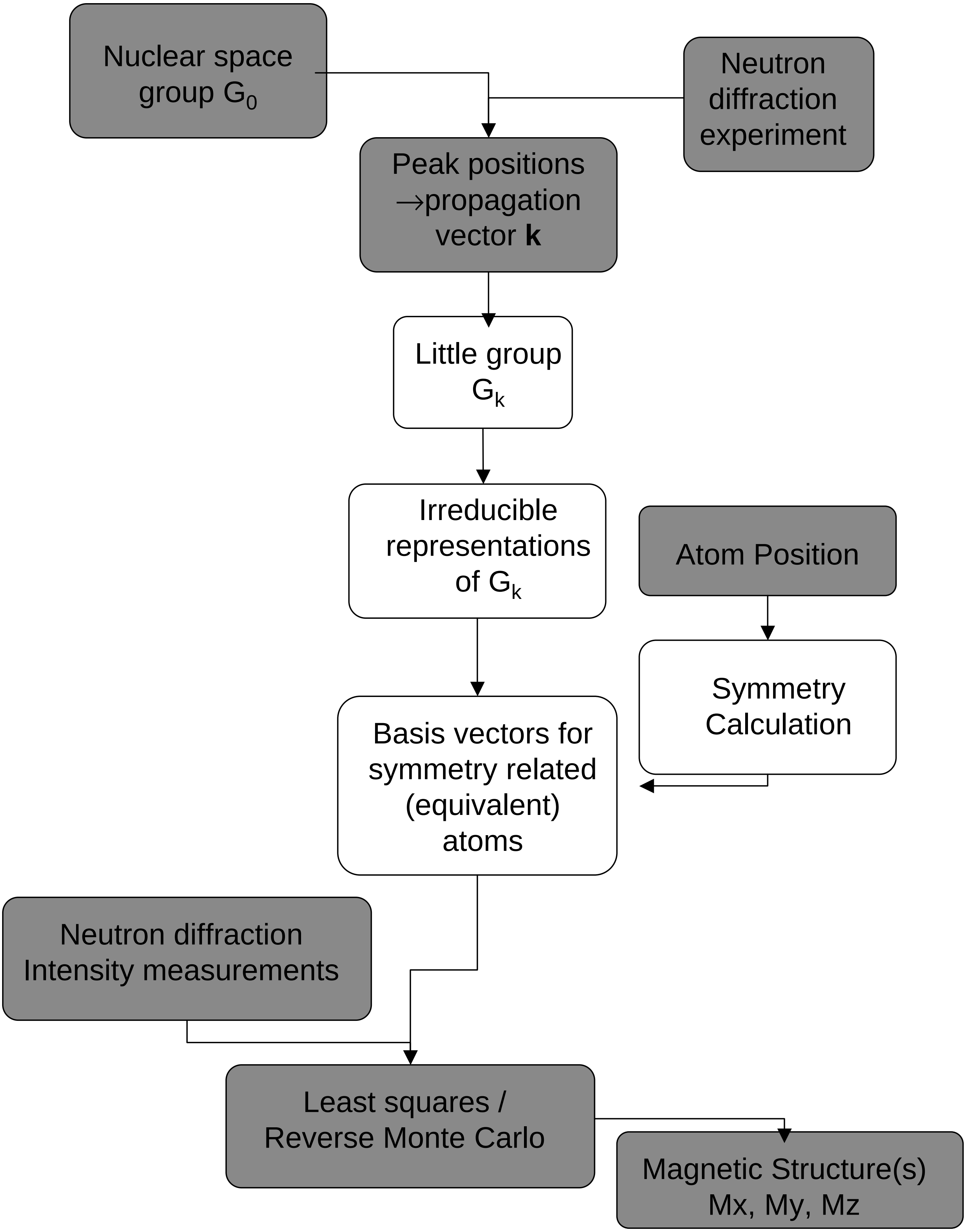

Magnetic Structure – Group Theory

Andrew S. Wills

Magnetic structures and their determination using Group Theory

A. S. Wills[*]
Departement of Chemistry, Christopher-Ingold Laboratories
University College London, 20 Gordon Street,
London, WH1H 0AJ.

based on the JDN9 Ecole Magnétisme et Neutrons, 22-23 May 2000, published in *J. Phys. IV France* **11**, Pr9-133 (2001).

1 Introduction

The determination of magnetic structures is a special area of condensed matter research. While being fundamental to the understanding of electronic structures and properties, it remains a subject that is treated with difficulty and is full of incorrect solutions. This article is based around two goals:

- The explanation of the different possible types of magnetic structure.
- The demonstration of how symmetry leads to their proper description, and can aid their solution.

In content, the first part of this article is based on the practicalities of what an experimenter *should* know in order to understand and describe a magnetic structure. In the second part, symmetry arguments will be shown to reduce the otherwise arduous task of determining a magnetic structure, to the investigation of a handful of possible structures.

---

[*] email: a.s.wills@ucl.ac.uk

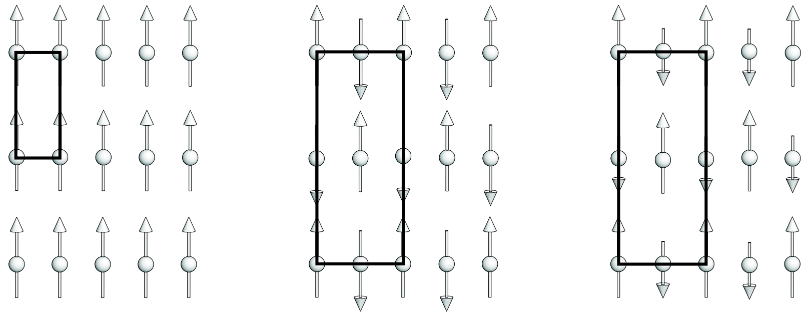

a) ferromagnetic b) antiferromagnetic c) ferrimagnetic

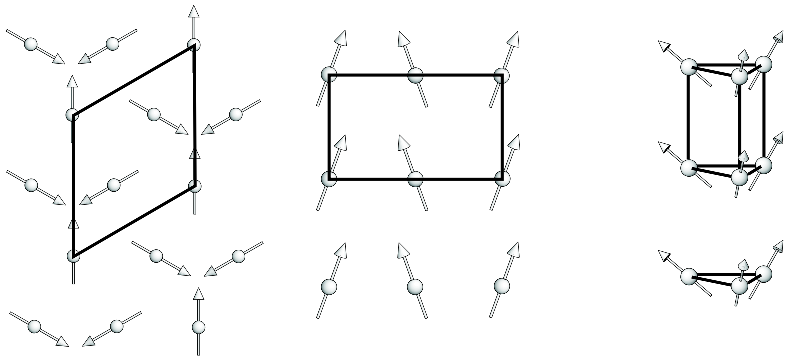

d) triangular e) canted f) umbrella

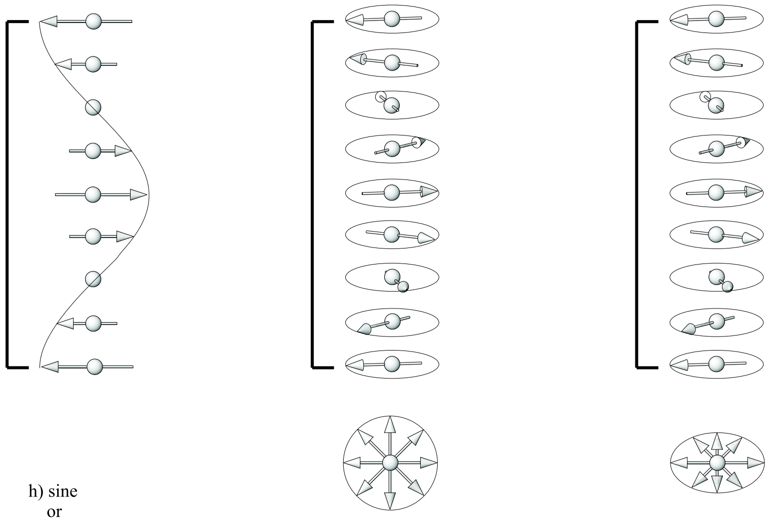

h) sine
or
cosine
i) circular helix
j) elliptical helix

Figure 1: Some different types of magnetic structures.

2 Basic crystallography

2.1 Nuclear crystal structures

A nuclear crystal structure can be described in terms of lattice translations of a unit cell. If the unit cell contains only one atom it is said to be a primitive cell; if it contains several atoms it is said to be a non-primitive lattice. The atomic positions of an arbitrary atom in the lth unit cell is given by

$$\mathbf{R_{tj}} = \mathbf{t} + \mathbf{r_j} \tag{1}$$

where

$$\mathbf{t} = n_1\mathbf{a} + n_2\mathbf{b} + n_3\mathbf{c} \tag{2}$$

and

$$\mathbf{r}_j = x\mathbf{a} + y\mathbf{b} + z\mathbf{c} \tag{3}$$

Here a, b, c are unit vectors of the nuclear cell defined according to the International Tables; n_1, n_2, n_3 are integers and x, y, z have values that are less than unity.

2.2 Reciprocal lattice

In crystallography a useful and much used construction is the ‘reciprocal lattice’- this can be defined as:

$$\mathbf{a}^* = \frac{2\pi}{v_0}\mathbf{b} \wedge \mathbf{c} \tag{4}$$

$$\mathbf{b}^* = \frac{2\pi}{v_0}\mathbf{c} \wedge \mathbf{a} \tag{5}$$

$$\mathbf{c}^* = \frac{2\pi}{v_0}\mathbf{a} \wedge \mathbf{b} \tag{6}$$

Where v_0 is the volume of the unit cell, $v_0 = \mathbf{a} \cdot (\mathbf{b} \times \mathbf{c})$. A reciprocal lattice vector $\boldsymbol{\tau}$ connects the origin to a given node in reciprocal space

$$\boldsymbol{\tau} = h\mathbf{a}^* + k\mathbf{b}^* + l\mathbf{c}^* \tag{7}$$

when h, k, and l are integer numbers.

3 Propagation vector and its star

3.1 Description of moments

Before we detail what a magnetic structure is, we must begin with a description of the magnetic moment itself. There are of course a variety of ways and coordinate systems that can be used to describe a magnetic moment, e.g. Cartesian, polar or crystallographic coordinates. While it is of course preferable to describe the particular properties of the final structure in the most useful system (e.g. a rotation of a moment away from an axis is best described in terms of an angle), in the general case it is easiest to describe a moment in terms of projections along the crystallographic axes. Rather than say that a moment is of unit length and makes an angle of 0 ° with the *c*-axis, we will simply say that the projection of the moments along the crystallographic axes can be described by a 'basis vector' $\mathbf{\Psi}$ which has components along these axes. In this case, the basis vector is $\mathbf{\Psi} = (001)$. In fact, when the basis vector is real, it simply corresponds to the projection of the moment along the different crystallographic axes, and so :

$$\mathbf{m}_j = \mathbf{\Psi}_j \tag{8}$$

Often, however, the projections of the moment are described not just by one basis vector, but by the summation of several (see Section 5) :

$$\mathbf{\Psi}_j = \sum_{\nu} C_{\nu} \boldsymbol{\psi}_{\nu} \tag{9}$$

In this work we will use $\boldsymbol{\psi}_{\nu}$ to represent the ν components of $\mathbf{\Psi}_j$ for a given propagation vector $\mathbf{k}$. The values of $\mathbf{\Psi}_j$ will be taken as being those of atom j in the *zero*th unit cell (*i.e.* the crystallographic cell) .

3.2 Formalism of a propagation vector k

Magnetic structures can be described by the periodic repetition of a magnetic unit cell, just as crystal structures are described by translation of a nuclear unit cell. For convenience, rather than building a complete magnetic unit cell (which could contain thousands of magnetic atoms) we use a description based on the nuclear unit cell and a 'propagation vector', $\mathbf{k}$, that describes the relation between moment orientations of equivalent magnetic atoms in different nuclear unit cells. This provides a simple and a general formalism for the description of a magnetic structure.

We illustrate this for the moment distribution m_j associated with the atom j of a magnetic structure. This can be Fourier expanded, whatever the nature of the ordering, according to:

$$\mathbf{m}_j = \sum_k \mathbf{\Psi}_j^{\mathbf{k}} e^{-2\pi i \mathbf{k}\cdot\mathbf{t}} \tag{10}$$

That the summation is made over several wave vectors that are confined to the first Brillouin zone of the Bravais lattice of the nuclear cell is explained in detail in Section 3.4. If only one wave vector is involved, this simplifies to:

$$\mathbf{m}_j = \mathbf{\Psi}_j^{\mathbf{k}} e^{-2\pi i \mathbf{k}\cdot\mathbf{t}} \tag{11}$$

This equation describes the translation properties in real space of the basis vector $\mathbf{\Psi}_j$, which at present we can think of as the projections of the magnetic moment along the a, b, c crystallographic axes with relation to the atomic site in the *zero*th (nuclear) cell. At another atomic site (of the same type) in the crystal that is related by a lattice translation vector $\mathbf{t}$, the projections of the moment on the 3 crystallographic axes are related to those in the nuclear cell by Equation 11. An example of this is shown in Figure 2. Here the magnetic unit cell is 2 times larger along the c-axis than the nuclear unit cell and the propagation vector is $\mathbf{k}=00\frac{1}{2}$. The moment in the *zero*th cell is described by the basis vector $\mathbf{\Psi}_j$=(0 1 0), that is to say the moment is pointing along the b-axis. When we move to the cell above (*i.e.* to a site that is related by the translation vector[1] $\mathbf{t}$=(0 0 1) the moment is rotated by 180 ° and now points along the (0 -1 0) direction. As we move up the structure we find that the moment turns by 180 ° for each nuclear cell translation until at $\mathbf{t}$=(0 0 2) it is the same as in the *zero*th cell. In this way, if we know the basis vector that describes the moment orientation in the *zero*th cell and the propagation vector, we can use Equation 11 to calculate the basis vector and moment orientation, of any equivalent atom in the crystal structure.

3.3 Stability of magnetic structures

When the sample is cooled and condenses into a state with magnetic order, the magnetic structure that results must leave the Hamiltonian invariant to lattice translations, *i.e.* the magnetic Hamiltonian of different unit cells must be the same. The minimisation in the magnetic energy of the system results in three possible situations:

---

[1] Remember that a lattice translation vector in real space is given the symbol $\mathbf{t}$, while one in reciprocal space has the symbol $\boldsymbol{\tau}$.

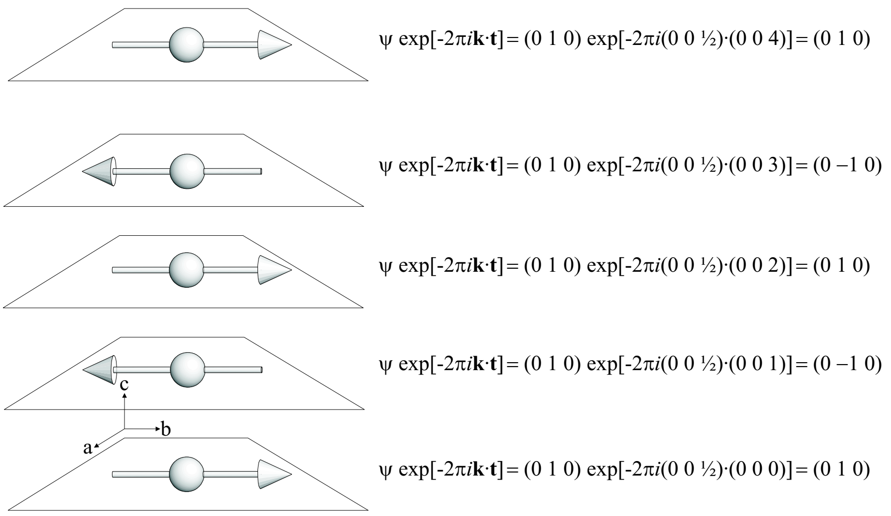

Figure 2: Description of translational properties with the propagation vector **k**. In this example the basis vector for the moment in the *zero*th cell is $\mathbf{\Psi}$ =(0 1 0), **k**=$00\frac{1}{2}$ and each plane corresponds to a lattice translation of **t**=001

- one **k** vector is more favourable than the others and the system chooses a ground state configuration that is described by:

$$\mathbf{m}_j = \mathbf{\Psi}_j^{\mathbf{k}} e^{-2\pi i \mathbf{k}\cdot\mathbf{t}} \tag{12}$$

  This is the most common situation and most of this work will be devoted to single **k** structures.

- several **k** vectors of the star are involved. The ground state is then described by:

$$\mathbf{m}_j = \sum_{\mathbf{k}} \mathbf{\Psi}_j^{\mathbf{k}} e^{-2\pi i \mathbf{k}\cdot\mathbf{t}} \tag{13}$$

  This is termed a 'multi-**k**' configuration.

- One **k** vector and its harmonics are involved, e.g. $\frac{\mathbf{k}}{2}$. The ground state is then described by:

$$\mathbf{m}_j = \sum_{\text{harmonics of } \mathbf{k}} \mathbf{\Psi}_j^{\mathbf{k}} e^{-2\pi i \mathbf{k}\cdot\mathbf{t}} \tag{14}$$

If the transition involves several arms of the star of propagation vector $\mathbf{k}$ and their harmonic terms, we have the possibility of *crossed* harmonics that are sometimes referred to as intermodulations.

3.4 Star of the propagation vector -k

We will now consider the effects of the space group, G_0, of our crystal structure on the propagation vector $\mathbf{k}$. For ease we will separate each symmetry element $g = \{h, \boldsymbol{\tau}\}$ into rotation and translation parts, these are h and $\boldsymbol{\tau}$ respectively. The action of the rotation part h on the reciprocal vector $\mathbf{k}$, results either in leaving $\mathbf{k}$ unchanged, or the generation of an unequivalent wave vector $\mathbf{k}'$:

$$\mathbf{k}' = \mathbf{k}h \tag{15}$$

where,

$$\mathbf{k}' = \mathbf{k} \quad \text{or} \quad \mathbf{k}' \neq \mathbf{k} \tag{16}$$

In the general case, a number of distinct propagation vectors will result from the operations of the rotational elements of the space group G_0 on the propagation vector $\mathbf{k}$. The symmetry elements of G_0 may then be classed into *cosets*, where the first coset $\mathrm{G}_{\mathbf{k}}$ is made up of elements that do not change the vector $\mathbf{k}$, the second coset (given the symbol g_2) transform it into the unequivalent vector $\mathbf{k}_2$, and so on. If g_L represents the elements of the coset L, we can write this relation as

$$\mathbf{k}_L = \mathbf{k}g_L \tag{17}$$

In this way, we find that the rotation elements of the space group G_0 gives rise to a set of unequivalent wave vectors. These we describe as being the 'star' of the propagation vector $\mathbf{k}$;[1] each wave vector is an 'arm' of the star (and example of a star is given in Figure 3). The number of arms, $l_{\mathbf{k}}$, that make up a star is of course equal to the number of cosets and cannot exceed the number of elements in G_0.

If Crystal Electric Field (*CEF*) or higher-order exchange interactions (e.g. quadrupolar-type) are appropriate, several arms of a star can be involved in the structure, it is then said to be a 'multi-$\mathbf{k}$' structure (this notion will be expanded upon in Section 4). More often, the magnetic structure is the result of only the first $\mathbf{k}$ vector. For this reason, we will now focus on the rotation elements that leave $\mathbf{k}$ invariant.

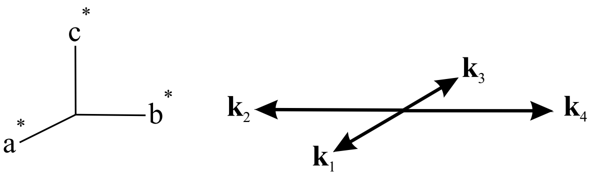

Figure 3: The star of the propagation vector **k**=(x 0 0) in the tetragonal space group I4/mmm (point group D^{17}_{4h}). The arms of the star are: $\mathbf{k}_1$=(x 0 0), $\mathbf{k}_2$=(0 -x 0), $\mathbf{k}_3$=(-x 0 0) and $\mathbf{k}_4$=(0 x 0)

3.5 The little group of the propagation vector -k

The symmetry elements of G_0 that leave the **k** vector invariant are of particular importance in the determination of a magnetic structure. For this reason the elements of the first coset are given a special name- they make up the 'little group' $G_\mathbf{k}$, and it is on these that all the Group Theory arguments that follow in Sections 7 and 8 are based. The little group will be discussed in greater detail in Section 8.

4 Multi-domain and multi-k structures

While the majority of magnetic structures that we come across involve only a single propagation vector **k**, it is useful to see how the different types of propagation vectors can take part in a magnetic structure. Experimentally, these situations are revealed by the appearance of more than a single reflection around a reciprocal lattice point.

4.1 Multi-domain structures

The first magnetic neutron diffraction pattern collected was that of MnO, published by Shull and Smart[2]. The period of the magnetic unit cell was found to be doubled along each of the cubic axes of the FCC structure , and so its volume is 8 times that of the crystallographic cell.

We now know that the structure in fact involves domains that order according to the 4 different arms of the propagation vector. The four **k** vectors involved are:

$$\mathbf{k}_1 = \left(\frac{1}{2}, \frac{1}{2}, \frac{1}{2}\right) \mathbf{k}_2 = \left(\frac{\bar{1}}{2}, \frac{1}{2}, \frac{1}{2}\right) \mathbf{k}_3 = \left(\frac{1}{2}, \frac{\bar{1}}{2}, \frac{1}{2}\right) \mathbf{k}_4 = \left(\frac{1}{2}, \frac{1}{2}, \frac{\bar{1}}{2}\right) \qquad (18)$$

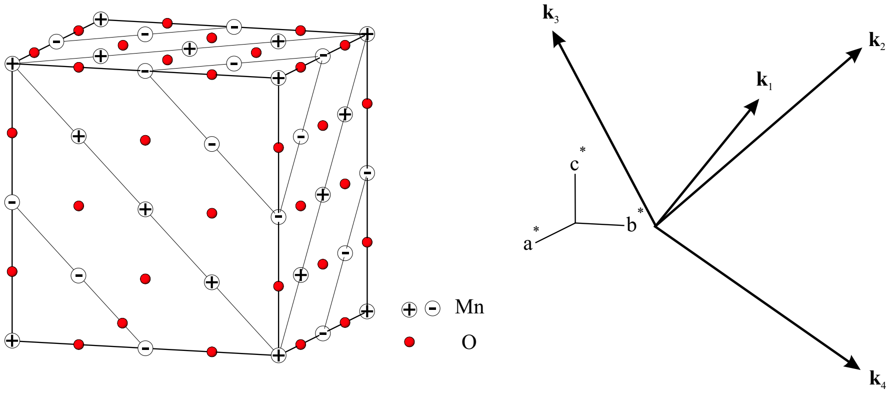

Figure 4: a) The magnetic motif of MnO made up of ferromagnetic planes of moments that are coupled antiferromagnetically. b) The star of **k** in reciprocal space is made up of the four propagation vectors related by the rotation elements of the space group G_0: $\mathbf{k}_1 = \left(\frac{1}{2}, \frac{1}{2}, \frac{1}{2}\right)$, $\mathbf{k}_2 = \left(\frac{\bar{1}}{2}, \frac{1}{2}, \frac{1}{2}\right)$, $\mathbf{k}_3 = \left(\frac{1}{2}, \frac{\bar{1}}{2}, \frac{1}{2}\right)$ and $\mathbf{k}_4 = \left(\frac{1}{2}, \frac{1}{2}, \frac{\bar{1}}{2}\right)$. Domains are found that correspond to each of these **k**-vectors.

As there are domains that order according to vector $\mathbf{k}_1$, others to $\mathbf{k}_2$,..., $\mathbf{k}_4$, this is termed a 'multi-domain' structure.

Experimentally, different **k** domains will lead to different magnetic reflections, just as in multi-**k** structures. In fact, the diffraction patterns of multiple domain and multi-**k** structures are identical and it is impossible to distinguish them without the application of an external constraint that breaks the symmetry on a macroscopic scale, and favours the population of one **k** domain over another.

4.2 k and -k structures

Structures that involve contributions from the two arms **k** and -**k** do not fall simply into the class of multi-**k** structures because, as we will show in Section 5, the requirement of a contribution from the -**k** arm can simply be the result of the form of the basis vectors, or the value of **k**. Typically, the contribution of these two components gives rise to modulated magnetic structures, e.g. sine and ellipse structures.

4.3 Multi -k structures

As we have already seen, multi-**k** structures can involve different arms of the star of the propagation vector **k**. This is a situation favoured by higher terms in the exchange Hamiltonian of the magnetic system. Also possible are structures that involve an 'accidental' degeneracy between the stars of unrelated propagation vectors. A magnetic transition that involves several stars does not necessarily follow the Landau theory for a second-order transition (Sections 7.3 and 7.2), but if suitable degeneracies occur the resulting structure may still order under a single Irreducible Representation.

4.4 Structures that involve the harmonics of k

Addition of components of the harmonics of **k** to a structure will lead to a squaring up of the modulation, that is to say the magnitudes of the moments on the atoms becomes equal. This situation can be driven by CEF effects that disfavour any reduction in the amplitude of magnetic moment, or an instability of the modulated structure because of the large entropy associated with it. This is exemplified by a sine structure, where decreasing temperature leads to the structure becoming unstable and may lead to a squaring up of the modulation of the moments. Examples of this are the metals Er and Tm (see Figure 5) where third, fifth and higher order harmonics progressively appear with decreasing temperature.[3]

5 Translation properties of magnetic structures

Now that we will return to the situations that involve only a single propagation vector **k**, and perhaps its inverse -**k**. We have already shown how basis vectors and propagation vectors can be used in the description of magnetic structures. In this Section we will examine the different types of magnetic structures demonstrated in Figure 1. In the general case, the **k** vector may refer to any point within or on the surface of the first Brillouin zone. This gives rise to two general classes of magnetic structures:

- *Commensurate*- the magnetic cell that is a simple multiple of the nuclear cell. It is in this group that are found the majority of known magnetic structures: simple ferromagnets, antiferromagnets and ferrimagnets.

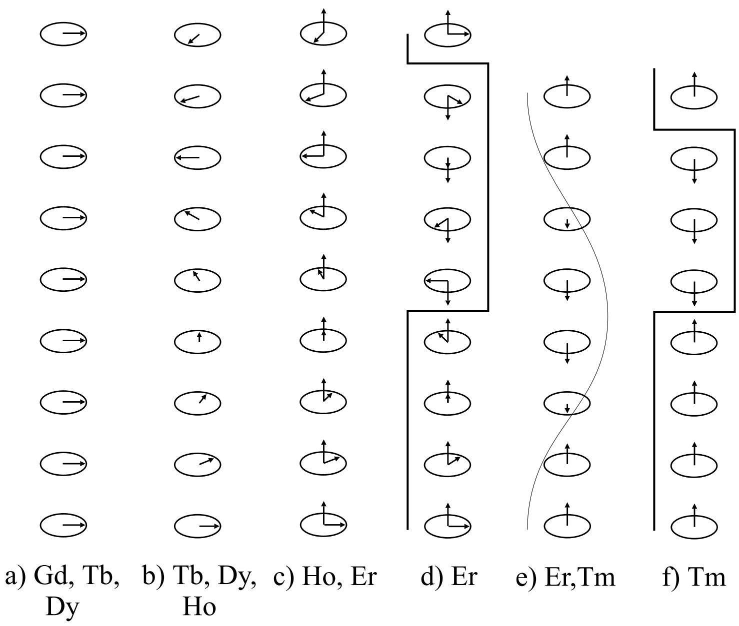

Figure 5: The magnetic structures of the heavy rare earth metals.

- *Incommensurate*- there is no simple relation between the structural and magnetic cells.

It is important to note that these classifications describe only the propagation vector; the magnetic structure itself is the result of the propagation vector **k** *and* the basis vector $\boldsymbol{\Psi_j}$. It is the combination of *both* of these that gives rise to the different possible structures[1, 4, 5, 6].

5.1 Simple structures and Sine structures

As we have seen, the translation properties of a magnetic structure may be described by:

$$\mathbf{m}_j = \boldsymbol{\Psi}_j^{\mathbf{k}} e^{-2\pi i \mathbf{k}\cdot\mathbf{t}} \tag{19}$$

Let us now expand the exponential:

$$\mathbf{m}_j = \boldsymbol{\Psi}_j^{\mathbf{k}} \left[\cos(-2\pi\mathbf{k}\cdot\mathbf{t}) + i\sin(-2\pi\mathbf{k}\cdot\mathbf{t})\right] \tag{20}$$

and consider various possibilities for the basis vector $\boldsymbol{\Psi_j}$ and the propagation vector **k**.

5.1.1 Ψ is real and the sine component is null

The simplest situation occurs when $\mathbf{\Psi}_j^{\mathbf{k}}$ is a real basis vector. The condition that $\mathbf{m}_j$ is real requires that the sine component is zero- this occurs only for certain values of **k**. Equation 20 then reduces to

$$\mathbf{m}_j = \mathrm{Re}(\mathbf{\Psi}_j^{\mathbf{k}}\cos(-2\pi\mathbf{k}\cdot\mathbf{t})) \tag{21}$$

As the sine component is null, the cosine component is necessarily of maximal magnitude and so translation to another unit cell results only in some rotation of the moment, and does not change its magnitude. This is the situation in many simple ferromagnetic, ferrimagnetic, and antiferromagnetic structures (examples are given in Figure 1a-f).)

5.1.2 Ψ is real and the sine component is non-zero

If the basis vector is real and the sine component is non-zero, Equation 20 leads to a magnetic moment that is complex- an impossible situation as the magnetic moment is a real entity. We are therefore left with the problem of how to relate our complex basis vector to the projections of a real moment. This in fact turns out to be very simple: the moment here cannot be described by a single propagation vector, but rather is described by contributions from 2 propagation vectors. The second propagation vector that is required in order to describe the magnetic moment distribution is the propagation vector -**k**.

The atomic vector for an atom in the *n*th cell related to that in the *zero*th cell by translation **t** is then given by:[4]

$$\mathbf{m}_j = \mathbf{\Psi}_j^{\mathbf{k}} e^{-2\pi i\mathbf{k}\cdot\mathbf{t}} + \mathbf{\Psi}_j^{-\mathbf{k}} e^{2\pi i\mathbf{k}\cdot\mathbf{t}}, \tag{22}$$

Where [4],

$$\mathbf{\Psi}_{\boldsymbol{j}}^{-\boldsymbol{k}} = \mathbf{\Psi}_j^{\mathbf{k}^*} \tag{23}$$

Insertion of this relation into Equation 22 and expansion of the exponential leads to

$$\mathbf{m}_j = 2\mathrm{Re}(\mathbf{\Psi}_j^{\mathbf{k}})\cos(-2\pi\mathbf{k}\cdot\mathbf{t}) + 2\mathrm{Im}(\mathbf{\Psi}_j^{\mathbf{k}})\sin(-2\pi\mathbf{k}\cdot\mathbf{t}) \tag{24}$$

As we are considering real basis vectors, the imaginary component in Equation 24 is zero and this reduces to

$$\mathbf{m}_j = 2\mathrm{Re}(\mathbf{\Psi}_j^{\mathbf{k}})\cos(-2\pi\mathbf{k}\cdot\mathbf{t}) \tag{25}$$

We therefore see that if the propagation vector **k** leads a non-zero sine component in Equation 20, the magnetic structure involves both the wave vectors

k and -**k**. A non-zero sine component requires also that the magnitude of the moment changes with translation through the crystal. The resulting structure has a sine modulation and an example is shown in Figure 1h.

5.2 Helical structures

5.2.1 Ψ is complex and Re(Ψ)=Im(Ψ)

A complex basis vector associated with the vector **k** requires also a contribution from the -**k**. Therefore, we begin again from Equation 24:

$$\mathbf{m}_j = 2\mathrm{Re}(\mathbf{\Psi}_j^{\mathbf{k}})\mathrm{cos}(-2\pi\mathbf{k}\cdot\mathbf{t}) + 2\mathrm{Im}(\mathbf{\Psi}_j^{\mathbf{k}})\mathrm{sin}(-2\pi\mathbf{k}\cdot\mathbf{t}) \tag{26}$$

If the real and imaginary components of $\mathbf{\Psi}$ are equal we find that this simplifies to:

$$\mathbf{m}_j = 2\mathrm{Re}(\mathbf{\Psi}_j^{\mathbf{k}})\left[\cos(-2\pi\mathbf{k}\cdot\mathbf{t}) + \sin(-2\pi\mathbf{k}\cdot\mathbf{t})\right] \tag{27}$$

As the sine and cosine components define the points on a circle, the resulting structure is said to be a ‘circular helix’, *i.e.* one in which the magnitude of the moment is constant, but its orientation changes (Figure 1i).

5.2.2 Ψ is complex and Re(Ψ)$\neq$Im(Ψ)

As the real and imaginary components are of different size, the equation

$$\mathbf{m}_j = 2\mathrm{Re}(\mathbf{\Psi}_j^{\mathbf{k}})\mathrm{cos}(-2\pi\mathbf{k}\cdot\mathbf{t}) + 2\mathrm{Im}(\mathbf{\Psi}_j^{\mathbf{k}})\mathrm{sin}(-2\pi\mathbf{k}\cdot\mathbf{t}) \tag{28}$$

describes an ellipse rather than a circle. The resulting structure is referred to as an ‘elliptical helix’ (Figure 1j).

5.3 Summary of structures and basis vectors

In this Section we have shown that the class of a magnetic structure is the result of both the propagation vector and the form of the basis vectors involved. Sine structures and simple structures arise from real basis vectors, while helices involve complex basis vectors. The key equations are

$$\mathbf{m}_j = \mathbf{\Psi}_j^{\mathbf{k}} e^{-2\pi i\mathbf{k}\cdot\mathbf{t}} \tag{29}$$

and

$$\mathbf{m}_j = 2\mathrm{Re}(\mathbf{\Psi}_j^{\mathbf{k}})\mathrm{cos}(-2\pi\mathbf{k}\cdot\mathbf{t}) + 2\mathrm{Im}(\mathbf{\Psi}_j^{\mathbf{k}})\mathrm{sin}(-2\pi\mathbf{k}\cdot\mathbf{t}) \tag{30}$$

The calculation of these basis vectors will be detailed later in the section on Group Theory calculations (Section 8).

6 Location of magnetic reflections

6.1 k=0 ferromagnetic (ferri- antiferromagnetic)

As the magnetic and crystallographic unit cells are of the same size, the magnetic reflections occur at the nodes of the nuclear reciprocal lattice and their intensities therefore add to those of the nuclear reflections. Assuming an unpolarised incident beam, the magnetic cross section[7, 8] is then given in barns by:

$$\left(\frac{d\sigma}{d\Omega}\right)_{mag} = \sum_{\boldsymbol{\tau}} |\mathbf{M}_{\perp}(\mathbf{Q})|^2 \, \delta(\mathbf{Q} - \boldsymbol{\tau}) \tag{31}$$

Where $\boldsymbol{\tau}$ is a reciprocal space vector as defined by Equation 7 and $\mathbf{M}_{\perp}(\mathbf{Q})$ is the magnetic interaction vector (the component of the magnetic structure factor perpendicular to the scattering vector $\mathbf{Q}$, in units of 10^{-12} cm):

$$\mathbf{M}_{\perp}(\mathbf{Q}) = 0.2695 \; 10^{-12} \, \mathbf{F}_{M\perp}(\mathbf{Q}), \tag{32}$$

where $\mathbf{F}_{M\perp}(\mathbf{Q})$ has units of Bohr magnetons.

6.2 k≠0 antiferromagnetic- commensurate

The example shown in Figure 6b is of the propagation vector $\mathbf{k}$=($\frac{1}{2}$00). As the magnetic unit cell is 2 times larger in the a direction than the nuclear cell, the reflections will occur at half-integer positions ($\frac{h}{2}kl$).

6.3 k≠0 antiferromagnetic- incommensurate

We know that due to the form of Equation 11, contributions from the basis vectors of both **k** and -**k** are required. Reflections will therefore be at positions associated with both of these propagation vectors, and pairs of Bragg reflections will surround each reciprocal lattice point. As demonstrated in Figure 6c, magnetic reflections will be observed at:

1. For **k**

   $\mathbf{Q} = \boldsymbol{\tau} + \mathbf{k}$: reflection $\boldsymbol{\tau}^{+}$ or (hkl)$^{+}$

2. For -**k**

   $\mathbf{Q} = \boldsymbol{\tau} - \mathbf{k}$: reflection $\boldsymbol{\tau}^-$ or $(\mathrm{hkl})^-$

6.4 Multi-k

Figure 6d demonstrates the diffraction pattern of a structure described by two incommensurate propagation vectors. We see that there is a pair of reflections for each propagation vector about the reciprocal lattice points. This magnetic pattern is exactly the same as that from a structure with two equally populated **k** domains and only the application of a suitable external constraint can allow the distinction of these situations.

6.5 Harmonics of k

Contributions from the harmonics of **k** lead to the occurrence of reflections at positions that correspond to fractions of **k**. The example given in Figure 6 is of an incommensurate propagation vector and its harmonic $\frac{1}{2}\mathbf{k}$.

7 Symmetry in magnetic structures

7.1 The little group $\mathrm{G}_\mathbf{k}$ and its irreducible representations

As we have already stated, the little group $\mathrm{G}_\mathbf{k}$ that is made up of all the symmetry elements that leave **k** invariant, is a central concept in the symmetry analysis of magnetic structures. For a magnetic structure to be possible, it must be compatible with all of the symmetry operations of $\mathrm{G}_\mathbf{k}$ simultaneously. The set of matrices that describes how the moments transform under all of the operations of $\mathrm{G}_\mathbf{k}$ makes up a 'representation'. It is useful to separate these representations into orthogonal *Irreducible Representations*[9] (IRs), just as we separate the vibrations of a molecule into *normal* modes.

7.2 Landau Theory and its application to magnetic phase transitions and structures

The power and utility of Group Theory calculations with regards to the determination of magnetic structures comes from the Landau theory of a second-order phase transition. In the simplest of terms, this states that a

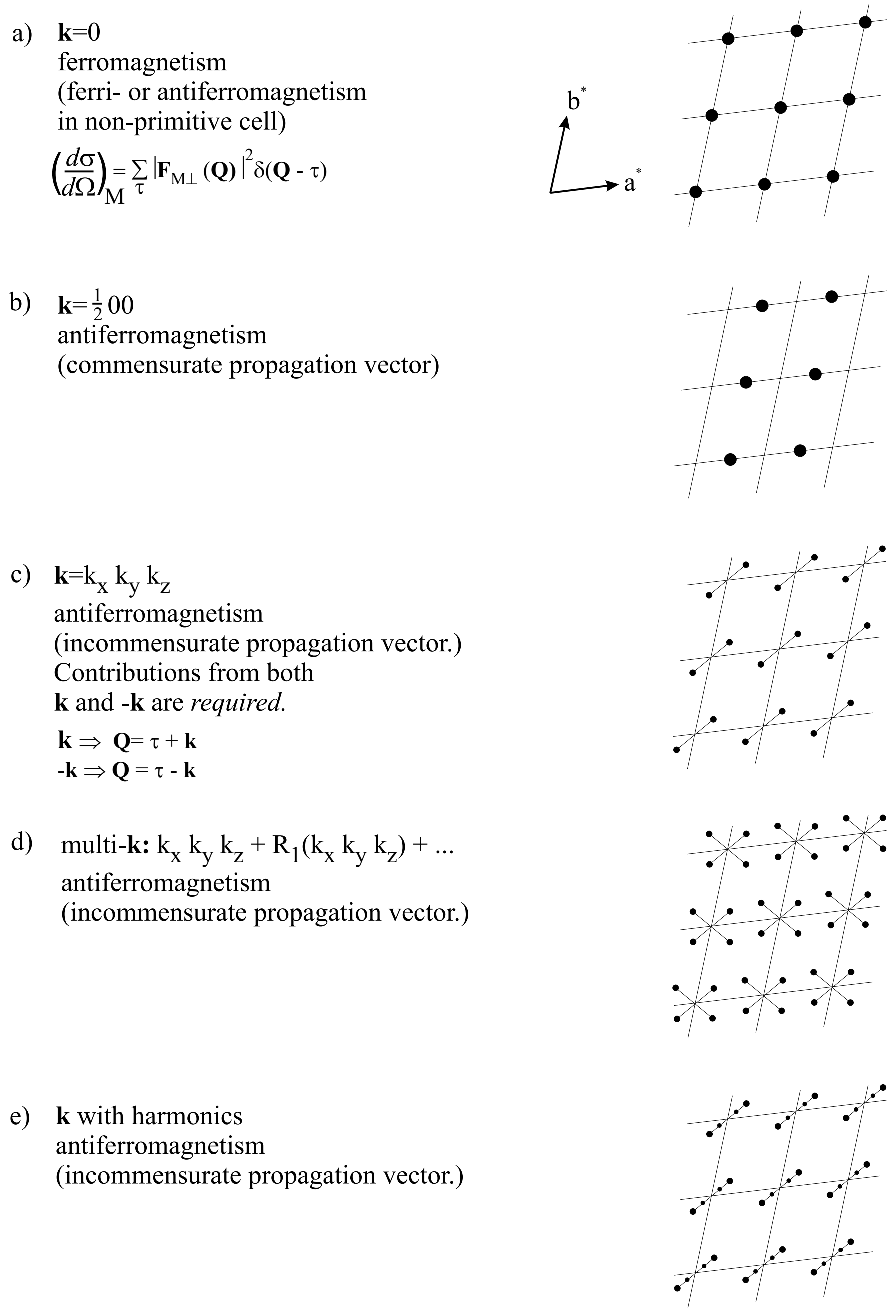

Figure 6: Cross-sections and graphs in reciprocal space for a variety of magnetic structure classes

second-order transition can involve the build up of magnetic fluctuations that have the symmetry of only one Irreducible Representation (in this case an Irreducible Representation describes the symmetry properties of a magnetic moment under all the symmetry operations of the little group $G_{\mathbf{k}}$)[4, 6, 9]. Because of this, the resulting magnetic structure can be described by the basis vectors associated with only that Irreducible Representation and the basis vectors associated with the Irreducible Representations not involved in the transition are necessarily zero. This greatly limits the number of possible magnetic models and the number of parameters that are involved in their refinement

Even in the cases where the transition is not second-order, nature is often kind to us and the structures that result are often the same as would be predicted for a second-order transition.The calculations detailed in Section 8 therefore continue to constitute a useful step in the determination, and description, of a magnetic structure.

7.3 Application to structures with several magnetic sites

If the unit cell of interest has several magnetic sites we have to consider how they will behave. If there are two types of site, A and B, there are 3 limiting cases and we will consider each separately[4]:

- The two intra-site interactions are dominant: $I_A > I_B > I_{AB}$.
  Here the coupling between the sites is small and so the sites behave independently. Each will therefore have its own ordering transition and no relation between the different Irreducible Representations involved is necessary.

- The inter-site interactions are dominant: $I_{AB} > I_A > I_B$.
  The strong coupling between the sites leads to a single critical temperature. The basis vectors that are associated with both sites must belong to the same Irreducible Representation. This places a great restriction on the number of possible structures.

- One intra-site interaction is dominant: $I_A > I_{AB} > I_B$.
  Upon cooling 2 distinct phase transitions will occur. The first involves the moments on the A sites. The inter-site coupling will lead to this structure polarising the B moments. These will then display the same magnetic structure as the A atoms. At a lower temperature, the B

> moments will undergo a symmetry-breaking transition and order cooperatively. The strong coupling between the A and B sites requires that these two orderings involve the same Irreducible Representation.

As an example, let us consider a system where there are 4 possible Irreducible Representations:

- Site A: $1\Gamma_1 + 0\Gamma_2 + 1\Gamma_3 + 1\Gamma_4$
- Site B: $1\Gamma_1 + 1\Gamma_2 + 0\Gamma_3 + 0\Gamma_4$

We know that only non-zero Irreducible Representations (labelled Γ) can be responsible for a magnetic structure. We see immediately that not all the Irreducible Representations occur on the two sites, *i.e.* on site A, Γ_2 is not involved. If site A orders separately, the resulting structure will correspond to either that of Γ_1, Γ_3 or Γ_4, that is to say there are 3 possible magnetic 'models'. Similarly site B could order according to Γ_1 or Γ_2. If there is no coupling between the sites and each orders separately, there are no symmetry restrictions on the possible Irreducible Representations involved. The sites can therefore order according to any of their allowed Irreducible Representations. However, if the situation is such that both order together, the two sites must order under the same Irreducible Representation, and only the Irreducible Representation Γ_1 can lead to a magnetic structure. The determination of the magnetic structure is therefore greatly simplified, as it can only involve the basis vectors associated with Γ_1.

8 Representational Analysis

8.1 Group Theory and magnetic structures

In non-primitive cells we must also determine the relation between the different magnetic moments in the cell. This relation can be very difficult to derive and is often found by comparison with known magnetic structures, or by trial and error. Group Theory arguments allow us to calculate symmetry-allowed relations between the moments and to greatly simplify this process. The results of these calculations are precisely the basis vectors, that we have been using to describe the magnetic structures.

The technique that will be presented in this work involving the application of Group Theory to magnetic structures is termed *Representational Analysis*[10, 1, 11]. The only pieces of information that are required for these calculations are the propagation vector **k**, the crystallographic space group and the atomic coordinates of the magnetic atoms *before* the magnetic phase transition. Rather than simply detailing the calculations involved, their application to an example problem will be used.

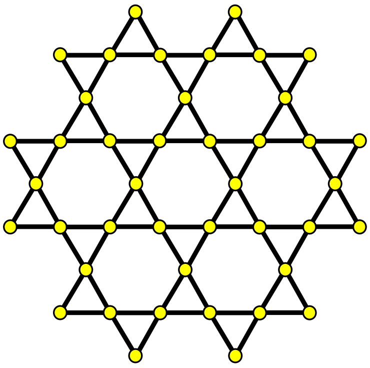

Figure 7: The *kagomé* lattice.

8.2 Computer programs

A number of computer programs exist that perform the calculations that make up magnetic symmetry analysis. Irreducible Representations can be calculated using KAREP[12], MODY[13], BASIREPS[14], and SARA*h*[15]. Basis vectors for the symmetry-allowed magnetic structures can be calculated using MODY, BASIREPS, or SARA*h*. All the Group Theory calculations and refinements presented here have been made using the program SARA*h*.

8.3 Example: of $\mathbf{AgFe_3(SO_4)_2(OH)_6}$ with $\mathbf{k} = 00\frac{3}{2}$

The jarosites are described in the space group $R\bar{3}$m (point group D_{3d}^{5}) and their crystal structure is displayed in Figure 8. All the calculations that follow will refer to the hexagonal non-primative setting of this space group, the symmetry elements of which are given in Table 1. As the cell is hexagonal there are three kagomé layers in the crystal structure and these have the stacking sequence ...ABC... The magnetic Fe^{3+} ions make up a 2-dimensional geometry called a *kagomé* lattice (Figure 7). In the mineral argento-jarosite, $AgFe_3(SO_4)_2(OH)_6$, the exchange is antiferromagnetic and magnetic ordering with a propagation vector $\mathbf{k} = 00\frac{3}{2}$ (with respect to the hexagonal axes) has been found at low temperature.[16, 17, 18] In this section we will calculate the symmetry-allowed magnetic structures using Representational Analysis. These calculations are also detailed in Ref. [17].

Element number	IT notation	Jones symbol	Rotation matrix
g1	$\{1 \mid 0\ 0\ 0\}$	x, y, z	$\begin{pmatrix} 1 & 0 & 0 \\ 0 & 1 & 0 \\ 0 & 0 & 1 \end{pmatrix}$
g2	$\{3^{+} \mid 0\ 0\ 0\}$	$\bar{y}, x-y, z$	$\begin{pmatrix} 0 & \bar{1} & 0 \\ 1 & \bar{1} & 0 \\ 0 & 0 & 1 \end{pmatrix}$
g3	$\{3^{-} \mid 0\ 0\ 0\}$	$y-x, \bar{x}, z$	$\begin{pmatrix} \bar{1} & 1 & 0 \\ \bar{1} & 0 & 0 \\ 0 & 0 & 1 \end{pmatrix}$
g4	$\{2 \mid 0\ 0\ 0\}$	$y, x, \bar{z}$	$\begin{pmatrix} 0 & 1 & 0 \\ 1 & 0 & 0 \\ 0 & 0 & \bar{1} \end{pmatrix}$
g5	$\{2 \mid 0\ 0\ 0\}$	$x-y, \bar{y}, \bar{z}$	$\begin{pmatrix} 1 & \bar{1} & 0 \\ 0 & \bar{1} & 0 \\ 0 & 0 & \bar{1} \end{pmatrix}$
g6	$\{2 \mid 0\ 0\ 0\}$	$-x, y-x, \bar{z}$	$\begin{pmatrix} \bar{1} & 0 & 0 \\ \bar{1} & 1 & 0 \\ 0 & 0 & \bar{1} \end{pmatrix}$
g7	$\{\bar{1} \mid 0\ 0\ 0\}$	$\bar{x}, \bar{y}, \bar{z}$	$\begin{pmatrix} \bar{1} & 0 & 0 \\ 0 & \bar{1} & 0 \\ 0 & 0 & \bar{1} \end{pmatrix}$
g8	$\{\bar{3}^{+} \mid 0\ 0\ 0\}$	$y, y-x, \bar{z}$	$\begin{pmatrix} 0 & 1 & 0 \\ \bar{1} & 1 & 0 \\ 0 & 0 & \bar{1} \end{pmatrix}$
g9	$\{\bar{3} \mid 0\ 0\ 0\}$	$x-y, x, \bar{z}$	$\begin{pmatrix} 1 & \bar{1} & 0 \\ 1 & 0 & 0 \\ 0 & 0 & \bar{1} \end{pmatrix}$
g10	$\{\mathrm{m} \mid 0\ 0\ 0\}$	$\bar{y}, \bar{x}, z$	$\begin{pmatrix} 0 & \bar{1} & 0 \\ \bar{1} & 0 & 0 \\ 0 & 0 & 1 \end{pmatrix}$
g11	$\{\mathrm{m} \mid 0\ 0\ 0\}$	$y-x, y, z$	$\begin{pmatrix} \bar{1} & 1 & 0 \\ 0 & 1 & 0 \\ 0 & 0 & 1 \end{pmatrix}$
g12	$\{\mathrm{m} \mid 0\ 0\ 0\}$	$x, x-y, z$	$\begin{pmatrix} 1 & 0 & 0 \\ 1 & \bar{1} & 0 \\ 0 & 0 & 1 \end{pmatrix}$

Table 1: Symmetry elements of the space group $R\bar{3}$m. The notations used are of the International Tables, where the elements are separated into rotation and translation components, and the *Jones faithful representations* of the rotation parts. The latter corresponds to the vector formed from the operation of the rotation part of the element on (x, y, z).

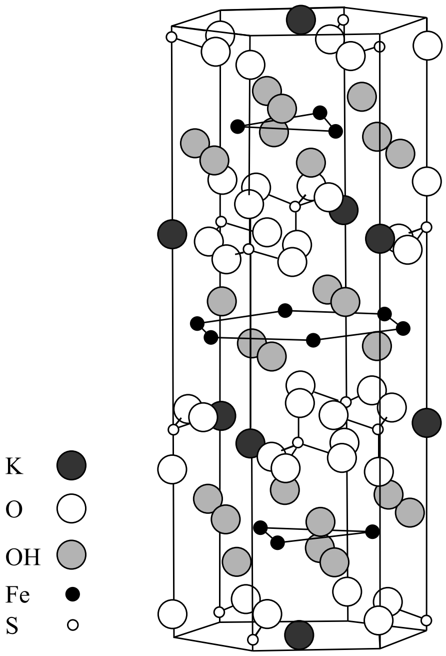

Figure 8: The jarosite crystal structure in the space group $R\bar{3}$m .

8.4 The group $\mathrm{G}_{\mathbf{k}}$ and its Irreducible Representations

As we have already explained in Section 3.4, for a given propagation vector **k**, some of the operators of the space group G_0, $g = \{h|\boldsymbol{\tau}\}$, leave it invariant while others transform it into an equivalent vector that differs by some arbitrary translation of the reciprocal lattice, $\boldsymbol{\tau}$, according to:

$$\mathbf{k}h = \mathbf{k} + \boldsymbol{\tau} \tag{33}$$

This set of elements makes up the so-called little group, $\mathrm{G}_{\mathbf{k}}$, which is a subgroup of G_0. The Irreducible Representations of this little group are given by the symbol Γ_ν, where ν is the label of the irreducible representation, and the matrix that corresponds to the symmetry element g is labelled by $d_\nu^{\mathbf{k}}(g)$

Looking at the example of $\mathrm{AgFe_3(SO_4)_2(OH)_6}$ with $\mathbf{k} = 00\frac{3}{2}$, we find that the little group contains all of the 12 symmetry operators of the space group $R\bar{3}$m. The Irreducible Representations of these are given in Tables 2 and 3. One sees immediately that the second-order representations Γ_5 and Γ_6 have the same elements for symmetry operations 1-6 and are related by a factor of (-1) for the operations 7-12.

These Irreducible Representations may be verified against tabulated val-

	g1	g2	g3	g4	g5	g6	g7	g8	g9	g10	g11	g12
Γ_1	1	1	1	1	1	1	1	1	1	1	1	1
Γ_2	1	1	1	1	1	1	-1	-1	-1	-1	-1	-1
Γ_3	1	1	1	-1	-1	-1	1	1	1	-1	-1	-1
Γ_4	1	1	1	-1	-1	-1	-1	-1	-1	1	1	1

Table 2: First-order Irreducible Representations for the group D_{3d}^5 for the vector **k**= $00\frac{3}{2}$.

	g1	g2	g3	g4	g5	g6
Γ_5, Γ_6	$\begin{matrix}1 & 0\\0 & 1\end{matrix}$	$\begin{matrix}\epsilon & 0\\0 & \epsilon^2\end{matrix}$	$\begin{matrix}\epsilon^2 & 0\\0 & \epsilon\end{matrix}$	$\begin{matrix}0 & 1\\1 & 0\end{matrix}$	$\begin{matrix}0 & \epsilon^2\\\epsilon & 0\end{matrix}$	$\begin{matrix}0 & \epsilon\\\epsilon^2 & 0\end{matrix}$
	g7	g8	g9	g10	g11	g12
Γ_5	$\begin{matrix}-1 & 0\\0 & -1\end{matrix}$	$\begin{matrix}-\epsilon & 0\\0 & -\epsilon^2\end{matrix}$	$\begin{matrix}-\epsilon^2 & 0\\0 & -\epsilon\end{matrix}$	$\begin{matrix}0 & -1\\-1 & 0\end{matrix}$	$\begin{matrix}0 & -\epsilon^2\\-\epsilon & 0\end{matrix}$	$\begin{matrix}0 & -\epsilon\\-\epsilon^2 & 0\end{matrix}$
Γ_6	$\begin{matrix}1 & 0\\0 & 1\end{matrix}$	$\begin{matrix}\epsilon & 0\\0 & \epsilon^2\end{matrix}$	$\begin{matrix}\epsilon^2 & 0\\0 & \epsilon\end{matrix}$	$\begin{matrix}0 & 1\\1 & 0\end{matrix}$	$\begin{matrix}0 & \epsilon^2\\\epsilon & 0\end{matrix}$	$\begin{matrix}0 & \epsilon\\\epsilon^2 & 0\end{matrix}$

Table 3: Second-order Irreducible Representations for the group D_{3d}^5 for the vector **k**= $00\frac{3}{2}$. ϵ=exp(-$\frac{2\pi}{3}$) .

ues of the projective (or 'loaded') representations, d_ν^{pr}, given in works such as Bradley and Cracknell[9] and Kovalev[19]. The tabulated representations are given for the various point group symmetries and can be converted into the Irreducible Representations of the little group $\mathrm{G}_{\mathbf{k}}$ of the propagation vector **k** by multiplicating them with a phase factor:

$$d_\nu = d_\nu^{pr} \cdot \mathrm{e}^{-2\pi\mathbf{k}\cdot\boldsymbol{\tau}} \tag{34}$$

Where $\boldsymbol{\tau}$ represents the translation part of the symmetry operator to which d_ν is associated.

8.5 Effect of symmetry element on a moment bearing atom

The effect of a symmetry element is two-fold: it will act to change the position of an atom, and reorientate the magnetic moment, e.g. atom 1 moves to the position of atom 2, and its moment is reversed. The combination of these two results are described by the magnetic representation, Γ. We will examine these two effects separately:

8.5.1 Effect of symmetry element on atom positions: the permutation representation

A symmetry operator $g = \{h|\boldsymbol{\tau}\}$ acts on both the position r_j of the atom and on the components α of the axial vector that describes the moment. The operation that sends r_j in the *zero*th cell to r_i in the pth cell can be symbolically stated as

$$g(j0) \rightarrow (ia_p) \tag{35}$$

In other terms, the effect of a symmetry operation g is to permute the column matrix of atom labels, **P**:

$$g(\mathbf{P}) \rightarrow \mathbf{P}' \tag{36}$$

This operation is governed by a permutation representation, Γ_{perm}, which has matrices of order N_A, where N_A is the number of equivalent positions of the crystallographic site. It is important to note that when a symmetry operation results in an atomic position that is outside the *zero*th cell, a phase factor must be included that relates the generated position to that in the *zero*th cell. This phase is simply given by:

$$\theta = -2\pi\mathbf{k}\cdot\mathbf{T} \tag{37}$$

Where **T** is the translation vector, that relates the original and generated atoms.

As an example, from Table 4 we see that the permutation equation for the atoms of the three Bravais sublattices under the g=$\{3^+ \mid 0\ 0\ 0\}$ operation is:

$$\begin{pmatrix} 2\cdot\exp(\theta_a) \\ 3\cdot\exp(\theta_b) \\ 1\cdot\exp(\theta_c) \end{pmatrix} = \Gamma_{perm}\begin{pmatrix} 1 \\ 2 \\ 3 \end{pmatrix} \tag{38}$$

Where the atomic positions follow the labelling: 1=$(\frac{1}{2}\ \ \frac{1}{2}\ \ \frac{1}{2})$, 2=$(\frac{1}{2}\ \ 0\ \ \frac{1}{2})$, 3=$(0\ \ \frac{1}{2}\ \ \frac{1}{2})$. For the operation g=$\{3^+ \mid 0\ 0\ 0\}$, $\theta_a = \theta_b = \theta_c = 0$ for **k**= $00\frac{3}{2}$.

The permutation representation is therefore given by

$$\Gamma_{perm}^{\{3^+|000\}} = \begin{pmatrix} 0 & 1 & 0 \\ 0 & 0 & 1 \\ 1 & 0 & 0 \end{pmatrix} \tag{39}$$

The character of this representation, χ_{perm}, for each symmetry operator is then simply the sum of the phases $\theta(g)$ for the atoms that are transformed into an equivalent atom under a symmetry operation, and so for both the propagation vectors, $\chi_{perm}^{\{3^{+}|000\}}= 0$.

8.5.2 Effect of symmetry element on moment vectors: the axial vector representation

The second effect of this symmetry operation is to transform the spin components with index α, $(\alpha = x, y, z)$ of the reference spin j into the index α' of the atom at r_i.[10, 1, 11] These transformations are described by the axial vector representation, $\tilde{V}$, the character of which is given by

$$\chi_{\tilde{V}}^{h} = \sum_{a=b} R_{ab}^{h} det(h), \tag{40}$$

Where R_{ab}^{h} refers to a specific element a,b of the rotation matrix h, and $det(h)$ represents the determinant of the rotation matrix R^{h},and has the value of +1 for a proper and -1 for an improper rotation. This is exemplified for the 3^{+} rotation, where the operation of h(3^{+}) on the moment vector $\vec{M}$=(m$_x$ m$_y$ m$_z$) gives:

$$R(3^{+})\vec{M} = det(h) \begin{pmatrix} 0 & \bar{1} & 0 \\ 1 & \bar{1} & 0 \\ 0 & 0 & 1 \end{pmatrix} \begin{pmatrix} m_x \\ m_y \\ m_z \end{pmatrix} \tag{41}$$

$$= 1 \begin{pmatrix} -m_y \\ m_x - m_y \\ m_z \end{pmatrix} \tag{42}$$

As 3^{+} is a proper rotation, $det(3^{+}) = 1$ and the character of $\tilde{V}$ for h(3^{+}) is therefore $\chi_{\tilde{V}}^{3^{+}}$=0.

8.6 Magnetic representation

As we have already stated, the magnetic representation, Γ, describes both the result of the symmetry operation on the atomic positions, and on the axial vectors that describe the magnetic moments. As these effects are independent, the magnetic representation is given by their direct product[10, 11, 1]:

$$\Gamma = \tilde{V} \times \Gamma_{Perm} \tag{43}$$

Or, in terms of the matrices for the representations themselves

	Atoms				Axial vector components			
$g = \{h \mid \boldsymbol{\tau}\}$	1	2	3	χ_{perm}	m_x	m_y	m_z	$\chi_{\tilde{V}}$
$\{1 \mid 0\ 0\ 0\}$	1	2	3	3	m_x	m_y	m_z	3
$\{3^+ \mid 0\ 0\ 0\}$	2	3	1	0	-m_y	m_x-m_y	m_z	0
$\{3^- \mid 0\ 0\ 0\}$	3	1	2	0	-m_x+m_y	-m_x	m_z	0
$\{2 \mid 0\ 0\ 0\}$	-1	-3	-2	-1	m_y	m_x	-m_z	-1
$\{2 \mid 0\ 0\ 0\}$	-3	-2	-1	-1	m_x-m_y	-m_y	-m_z	-1
$\{2 \mid 0\ 0\ 0\}$	-2	-1	-3	-1	-m_x	-m_x+m_y	-m_z	-1
$\{\bar{1} \mid 0\ 0\ 0\}$	-1	-2	-3	-3	m_x	m_y	m_z	-3
$\{\bar{3}^+ \mid 0\ 0\ 0\}$	-2	-3	-1	0	-m_y	m_x-m_y	m_z	0
$\{\bar{3} \mid 0\ 0\ 0\}$	-3	-1	-2	0	-m_x+m_y	-m_x	m_z	0
$\{\mathrm{m} \mid 0\ 0\ 0\}$	1	3	2	1	m_y	m_x	-m_z	-1
$\{\mathrm{m} \mid 0\ 0\ 0\}$	3	2	1	1	m_x-m_y	-m_y	-m_z	-1
$\{\mathrm{m} \mid 0\ 0\ 0\}$	2	1	3	1	-m_x	-m_x+m_y	-m_z	-1

Table 4: The permutation of B^{3+} atoms (at position 9d) and the transformation of the axial components of the moment under the different symmetry operators of the $R\bar{3}$m space group (point group D^5_{3d}) for $\mathbf{k} = 00\frac{3}{2}$. The characters of the representations Γ_{perm} and $\tilde{V}$ are given.

$$D^{\Gamma}_{(h,\boldsymbol{\tau}_h)} = D^{\tilde{V}}_{(h)} \times D^{\Gamma_{Perm}}_{(h,\boldsymbol{\tau}_h)} \tag{44}$$

The characters of these representations are related according to:

$$\chi_{\Gamma} = \chi_{\tilde{V}} \times \chi_{perm} \tag{45}$$

8.7 Reduction of the Representation Γ

The magnetic representation for a particular site can be decomposed into contributions from the Irreducible Representations of the little group:

$$\Gamma = \sum_{\nu} n_{\nu} \Gamma_{\nu} \tag{46}$$

where n_{ν} is the number of times the irreducible representation Γ_{ν} appears in the magnetic representation Γ. n_{ν} is given by:

$$n_{\nu} = \frac{1}{n(G_k)} \sum_{h \in G_k} \chi_{\Gamma}(h) \chi_{\Gamma^*_{\nu}}(h) \tag{47}$$

Here, χ_{Γ} is the character of the magnetic space group and $\chi_{\Gamma^*_{\nu}}$ is the complex conjugate of the character of the irreducible representation with index ν.

8.8 Calculation of the basis vectors Ψ

The basis vectors, $\boldsymbol{\psi}_n$, that transform according to the μ dimensional irreducible representation $\Gamma_\nu^{(\mu)}$ are projected out of the representation matrix D_ν using a series of test functions $\boldsymbol{\phi}^\beta$, where $\boldsymbol{\phi}^1 = (100)$, $\boldsymbol{\phi}^2 = (010)$, and $\boldsymbol{\phi}^3 = (001)$. This is carried out by the projection operator formula:

$$\boldsymbol{\psi}_n^{i\lambda} = \sum_{g \in G_\mathbf{k}} D_\nu^{*\lambda}(g) \delta_{i,gi} \; \mathrm{e}^{-2\pi i \mathbf{k}\cdot(\mathbf{r}_{gi}-\mathbf{r}_i)} det(h) R^h \boldsymbol{\phi}^\beta, \tag{48}$$

The summation is over the symmetry elements of the little group $\mathrm{G}_\mathbf{k}$. $\boldsymbol{\psi}$ is a spin component that we represent by a column matrix $\boldsymbol{\psi}(\mathbf{r})$. $\delta_{i,gi}$ is unity if the atoms i and gi are equivalent positions of the crystallographic site that are related by a primitive lattice translation, *i.e.* they are of the same sublattice of the Wyckoff site. Equation 48 is applied sequentially to each element λ of the matrix D_ν, for each equivalent position i of the crystallographic site. The row of the matrices D_ν is fixed during the examination of a given IR.

In our calculations the μ elements are those that correspond to the first row of the matrix of D_ν. As for each element, labelled $\lambda = 1...\mu$, three components β are projected out, there are in total 3μ projected components. Of these, the number of non-zero unique projected components for a representation is of course the same as calculated using Equation (47).

8.9 Refinement of basis vectors mixing coefficients

Any linear combination of basis vectors within one representation is necessarily a symmetry-allowed basis vector. The atomic moment on a particular atom,$\mathbf{m}_j$, is therefore most generally given by the sum of the basis vectors for a particular irreducible representation:

$$\mathbf{m}_j = \sum_\nu C_\nu \boldsymbol{\psi}_\nu, \tag{49}$$

where C_ν is the mixing coefficient of the basis vector ν. In refining the orientation of an atomic moment, we are in effect refining the mixing coefficients C_ν of the basis vectors within the irreducible representation being examined. The number of variables in our refinement is simply the number of unique basis vectors that transform according to a given representation, *i.e.* $n_\nu \mu$.

8.10 Refinement of complex basis vectors

The refinement of the mixing coefficients that relate complex basis vectors will be dealt with in detail, to demonstrate how an ordered array of magnetic moments, which are necessarily real entities, can be described by complex basis vectors.

8.11 Decomposition of the magnetic representation and the basis vectors of $AgFe_3(SO_4)_2(OH)_6$

In the hexagonal setting the magnetic Fe^{3+} ions are found on the 9d sites. For these sites the decomposition of the magnetic representation according to Equation 47 is:

$$\Gamma = 0\Gamma_1^{(1)} + 2\Gamma_2^{(1)} + 0\Gamma_3^{(1)} + 1\Gamma_4^{(2)} + 3\Gamma_5^{(2)} + 0\Gamma_6^{(2)} \tag{50}$$

The Landau theory of a second-order phase transition, requires that only one representation is involved, and so for this **k** there are only three possible magnetic structures. These correspond to representations Γ_2, Γ_4 and Γ_5.

The basis vectors for these representations calculated according to Equation 48 are given in Table 5. The atomic sites are labelled following the convention given in Section 8.5.1. The basis vectors have varied forms and we will now explain in detail the types of magnetic structures that they correspond to.

IR	b-v	Atom 1			Atom 2			Atom 3		
		m_x	m_y	m_z	m_x	m_y	m_z	m_x	m_y	m_z
Γ_2	ψ_1	1	-1	0	1	2	0	-2	-1	0
	ψ_2	0	0	1	0	0	1	0	0	1
Γ_4	ψ_3	1	1	0	-1	0	0	0	-1	0
Γ_5	ψ_4	1	0	0	0	$-\frac{1}{2} - \frac{\sqrt{3}}{2}\mathrm{i}$	0	$\frac{1}{2} - \frac{\sqrt{3}}{2}\mathrm{i}$	$\frac{1}{2} - \frac{\sqrt{3}}{2}\mathrm{i}$	0
	ψ_5	0	1	0	$\frac{1}{2} + \frac{\sqrt{3}}{2}\mathrm{i}$	$\frac{1}{2} + \frac{\sqrt{3}}{2}\mathrm{i}$	0	$-\frac{1}{2} + \frac{\sqrt{3}}{2}\mathrm{i}$	0	0
	ψ_6	0	0	1	0	0	$-\frac{1}{2} - \frac{\sqrt{3}}{2}\mathrm{i}$	0	0	$-\frac{1}{2} + \frac{\sqrt{3}}{2}\mathrm{i}$
	ψ_7	0	1	0	$\frac{1}{2} - \frac{\sqrt{3}}{2}\mathrm{i}$	$\frac{1}{2} - \frac{\sqrt{3}}{2}\mathrm{i}$	0	$-\frac{1}{2} - \frac{\sqrt{3}}{2}\mathrm{i}$	0	0
	ψ_8	1	0	0	0	$-\frac{1}{2} + \frac{\sqrt{3}}{2}\mathrm{i}$	0	$\frac{1}{2} + \frac{\sqrt{3}}{2}\mathrm{i}$	$\frac{1}{2} + \frac{\sqrt{3}}{2}\mathrm{i}$	0
	ψ_9	0	0	-1	0	0	$\frac{1}{2} - \frac{\sqrt{3}}{2}\mathrm{i}$	0	0	$\frac{1}{2} + \frac{\sqrt{3}}{2}\mathrm{i}$

Table 5: The basis vectors of the Irreducible Group Representations of the space group $R\bar{3}$m (point group D_{3d}^5) appearing in the magnetic representation with $\mathbf{k} = 00\frac{3}{2}$

Representations Γ_2 and Γ_4 are one dimensional. They therefore correspond to simple magnetic structures in which the atomic moments are orientated along particular crystallographic axes. It is noteworthy that both $\boldsymbol{\psi}_1$ and $\boldsymbol{\psi}_2$ correspond to 120° spin structures, with the total spin on any given triangle plaquette being $\sum_i \mathbf{S}_i$=0. While, the two spin structures are in fact related by a global rotation of spins, the two representations differ in that Γ_2 allows the introduction of an out-of-plane component, which corresponds to $\boldsymbol{\psi}_2$. The combination of the 2 basis functions $\boldsymbol{\psi}_1$ and $\boldsymbol{\psi}_2$ creates a so-called 'umbrella structure' (of the type shown in Figure 1f) in which the degree of out-of-plane canting is a refinement variable.

Representation Γ_5 is two dimensional and is repeated 3 times. It therefore corresponds to a 6 basis vector magnetic structure. As the general solution involves any linear combination of these 6 basis vectors we can not ascribe to this representation a simple structure. We do note however, that there are relations between the basis vectors and these will simplify the refinement of the mixing coefficients: $\boldsymbol{\psi}_4^*$=$\boldsymbol{\psi}_8$, $\boldsymbol{\psi}_5^*$=$\boldsymbol{\psi}_7$ and $\boldsymbol{\psi}_6^*$=-$\boldsymbol{\psi}_9$.

For pedagogical reasons we will ignore these relations and continue as if Γ_5 involved six untelated complex basis vectors. In this case, as the atomic spins are real entities, it is necessary to introduce the corresponding basis vectors of the propagation vector -**k** in order to make the summation of the two components real (Section 5). A description of the translation properties of this structures begins as normal from:

$$\mathbf{m}_j = \boldsymbol{\Psi}_j^{\mathbf{k}} e^{-2\pi i \mathbf{k}\cdot\mathbf{t}} + \boldsymbol{\Psi}_j^{-\mathbf{k}} e^{2\pi i \mathbf{k}\cdot\mathbf{t}}, \tag{51}$$

However, as for $\mathbf{k} = 00\frac{3}{2}$ the vectors **k** and -**k** are equivalent, we have $-\mathbf{k} = \mathbf{k}$ and so

$$e^{-2\pi i \mathbf{k}\cdot\mathbf{t}} = e^{2\pi i \mathbf{k}\cdot\mathbf{t}} \tag{52}$$

and

$$\mathbf{m}_j = (\boldsymbol{\Psi}_j^{\mathbf{k}} + \boldsymbol{\Psi}_j^{-\mathbf{k}}) e^{2\pi i \mathbf{k}\cdot\mathbf{t}} \tag{53}$$

A further simplification arises from the fact that the addition of the -**k** contribution corresponds to the addition of the conjugate of the basis vector of **k**, *i.e.*

$$\boldsymbol{\Psi}_j^{-\mathbf{k}} = \boldsymbol{\Psi}_j^{\mathbf{k}^*} \tag{54}$$

We therefore obtain

$$\mathbf{m}_j = 2\mathrm{Re}(\boldsymbol{\Psi}_j^{\mathbf{k}}) \left[\cos(2\pi \mathbf{k}\cdot\mathbf{t}_n) + i\sin(2\pi \mathbf{k}\cdot\mathbf{t})\right] \tag{55}$$

For both $\mathbf{k} = 00\frac{3}{2}$ the sine component vanishes under the centring translations of the non-primitive cell, or integer translations of the crystallographic cell, and so Equation 55 reduces to

$$\mathbf{m}_j = 2\mathrm{R}e(\mathbf{\Psi}_j^{\mathbf{k}})\cos(2\pi\mathbf{k}\cdot\mathbf{t}) \tag{56}$$

As in general, the basis vectors associated with Γ_5 that are to be tested against the magnetic structure are complex, when considering the translational properties of the magnetic moments it is sufficient just to add their complex conjugate in order to arrive at real values for the atomic moments. In these two cases this leads to Equation 56. The astute reader will have noted that while this procedure began with six basis vectors, it finished with only three: we have apparently halved the dimensionality of the basis vector space. In order to determine the remaining three basis vectors we must look at the imaginary part of $\boldsymbol{\psi}$ in Equation 53. This is done by first multiplying the basis vector $\boldsymbol{\psi}$ by the imaginary number i. Equation 53 would then read

$$\mathbf{m}_j = (i\mathbf{\Psi}_j^{\mathbf{k}} + i\mathbf{\Psi}_j^{-\mathbf{k}})e^{2\pi i\mathbf{k}\cdot\mathbf{t}} \tag{57}$$

and Equation 56 would become

$$\mathbf{m}_j = 2\mathrm{I}m(\mathbf{\Psi}_j^{\mathbf{k}})\cos(2\pi\mathbf{k}\cdot\mathbf{t}) \tag{58}$$

As the basis vectors on Γ_5 are themselves related by complex conjugation, we do not need in fact need to resort to this addition of the components associated with -**k**. Instead, we can simply equate the mixing coeffients of the conjugate pairs, *i.e.*, $C(\boldsymbol{\psi}_4^*)$=$C(\boldsymbol{\psi}_8)$,*etc.*.

There is an alternative way of dealing with complex basis vectors. Instead of combinining the complex basis vectors with their conjugates as described above, we can use the properties of irreducible representations. In some cases[2] unitary rotations can be applied to the Irredicible Representations that make them real. These two techniques are equivalent.

8.12 Refinement of the magnetic structure of $\mathbf{AgFe_3(SO_4)_2(OD)_6}$

The collected neutron diffraction data were found to be compatible only with a magnetic structure described by the representation Γ_4. Figure 9 displays the value of χ^2 as a function of the mixing coefficients $C(\boldsymbol{\psi}_1)$ and $C(\boldsymbol{\psi}_2)$; the only refinement variable in the least-squares matrix was the magnitude of the magnetic moment. In all cases the sum of the mixing coefficients was adjusted to be unity, and a trivial factor was then used to separately scale the magnitudes of moments described. The best value of χ^2 corresponds to the

---

[2] this criteria for this transformation is that the Coirreducible Representation (CIR) derived from the Irreducible Representation is real

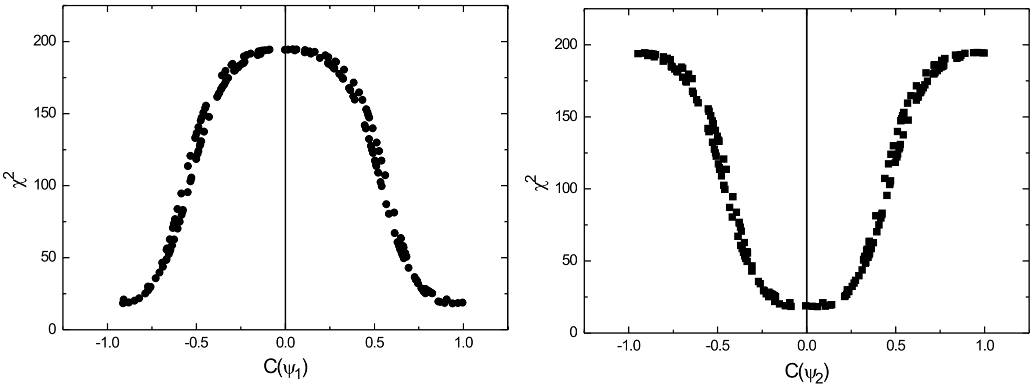

Figure 9: χ^2 as a function of the basis vector coefficients $C(\psi_1)$ and $C(\psi_2)$ during the refinement of the magnetic structure of $AgFe_3(SO_4)_2(OD)_6$ at 1.5K.

coefficients $C(\psi_1)$=0.99 (5) and $C(\psi_2)$=0.01 (5), that is to say the refined structure is coplanar and the contribution from out-of-plane canting is zero within the error of these data. The final refined profile is presented in Figure 10 and the final magnetic structure in Figure 11.

8.13 Discussion of the magnetic structure of $AgFe_3(SO_4)_2(OD)_6$

The magnetic structure that is refined is a triangular structure, that is to say the neighbouring moments are related by 120°. This is what we would naïvely expect for a triangular array of antiferromagnetically coupled spins. The Group Theory arguments we have used indicate that only particular orientations are possible for this configuration. As we will show in the practicals that accompany this course, the out-of-plane component that is only allowed in Γ_2 is important at higher temperatures and leads to the formation of an umbrella structure.

9 Summary of course

As stated in the introduction, this course was intended to explain how to describe a magnetic structure in terms of a propagation vector and some of its associated basis vectors. The examples given show how the different possible types of magnetic structure lead directly from this description. The second part of this text has been devoted to magnetic symmetry analysis-

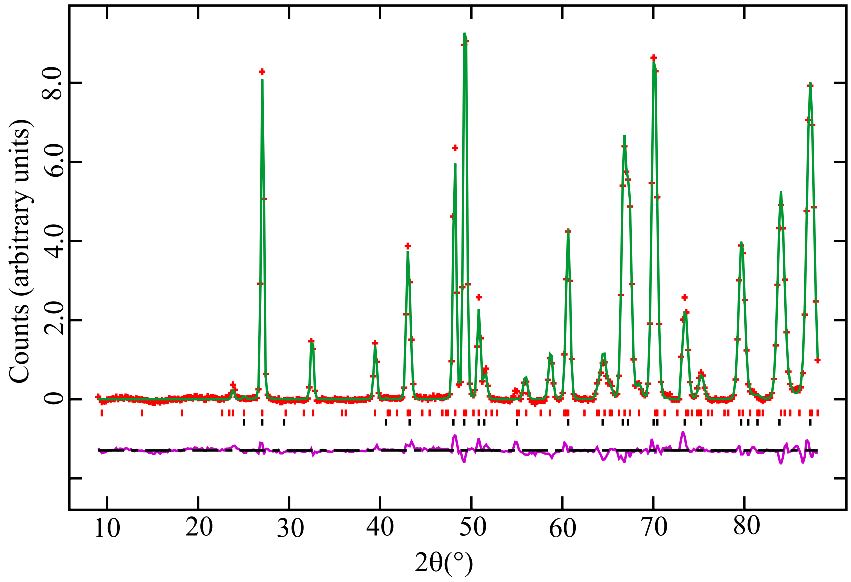

Figure 10: Experimental and calculated diffraction patterns for $AgFe_3(SO_4)_2(OD)_6$ at 1.5K. Magnetic and crystallographic reflections are indicated by the upper and lower tick marks respectively.

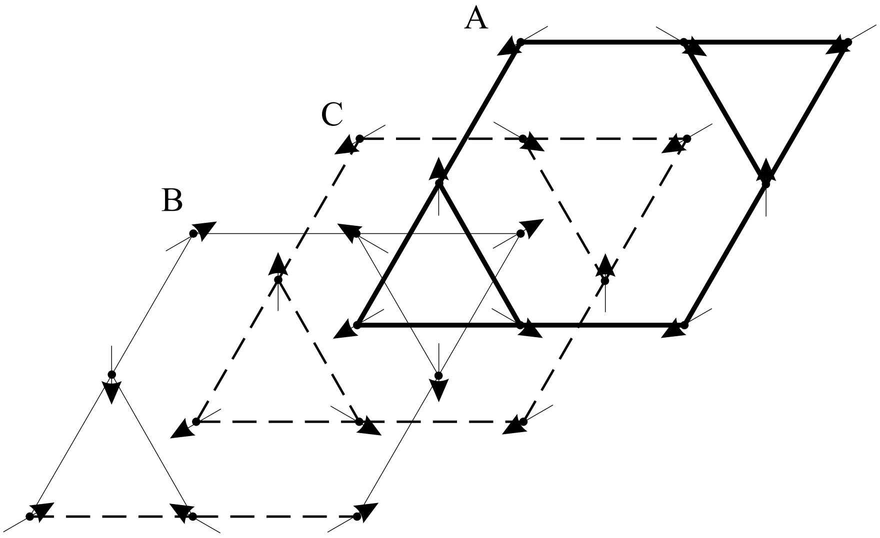

Figure 11: Magnetic structure of $AgFe_3(SO_4)_2(OD)_6$.

Representational Analysis. The Group Theory calculations that this involves are tedious, but now computer programs exist that perform these calculations in seconds. The basis vectors that result simplify greatly the processes of finding a magnetic structure, and can facilitate their correct description.

10 Further reading

Much inspiration, of varying levels, has been taken from a number of works on magnetic structures and magnetic symmetry analysis. For a first step into these subjects the References [1, 4, 5, 6, 7] are particular suitable. Reference [7] presents a clear introduction into the technical aspects of magnetic neutron scattering.

11 Acknowledgements

ASW would like to thank the Marie-Curie project of the EC for support and the Grenoble school of magnetism for their tuition, encouragement, and patience.

References

[1] Yu.A. Izymov, V.E. Naish and R.P. Ozerov, 'Neutron Diffraction of Magnetic Materials', Consultants Bureau, New York, 1991.

[2] C.G. Shull and J.S. Smart, Phys. Rev. **76**, 1256 (1949).

[3] D. Gignoux, J.C. Gomez Sal, J. Magn. Magn. Mat. **1**, 203 (1976).

[4] J. Rossat-Mignod in: 'Methods in Experimental Physics', ed. K. Sköld and D.L. Price (Academic Press, 1987). J. Rossat-Mignod in 'Systematics and the Propeties of the Lanthanides', Ed. S.P. Sinha, D. Reidel Publishing (1983).

[5] P.J. Brown, Physica B **137**, 31 (1986).

[6] J. Schweizer, in: 'Hercules- Neutron and Synchrotron Radiation for Condensed Matter Research', Springer Verlag, Berlin (1994).

[7] F. Tasset, *Recent developments in neutron scattering* Proceedings of Les Houches École de Physique 2000.

[8] F. Tasset, *Structures magnétiques et polarimétrie neutronique* Proceedings of ‘l’Ecole Magnétisme et Neutrons’ de la Société Française de la Neutronique, a French Translation of Ref. [7] to appear in J. de Physique (2001).

[9] C.J. Bradley and A.P. Cracknell, ‘The Mathematical Theory of Symmetry in Solids’, Clarendon Press (Oxford, 1972).

[10] E.F. Bertaut, J. Appl. Phys. **33**, 1138 (1962). E.F. Bertaut, Acta. Cryst. **A24**, 217 (1968) E.F. Bertaut, J. de Physique, Colloque C1, 462 (1971). E.F. Bertaut, J. Magn. Magn. Mat. **24**, 267 (1981).

[11] Yu.A. Izyumov and V.E. Naish, J. Magn, Magn. Mat.**12**, 239 (1979); Yu.A. Izyumov and V.E. Naish, J. Magn, Magn. Mat.**12**, 249 (1979); Yu.A. Izyumov and V.E. Naish, J. Magn, Magn. Mat.**13**, 267 (1979).

[12] E.R. Hovestreydt, M.I. Aroyo and H. Wondratschek, J. Appl. Cryst. **25**, 544 (1992).

[13] P. Czapnik and W. Sikora, *unpublished work.*

[14] J. Rodriguez-Carvajal, *unpublished work.*

[15] A.S. Wills, Physica B **276-278**(2000), 680. Program available from ftp://ftp.ill.fr/pub/dif/sarah/

[16] A.S. Wills, A. Harrison, C. Ritter and R.I. Smith, Phys. Rev. B **61**, 6156 (2000).

[17] A.S. Wills, Phys. Rev. B, **63**, 064430 (2001).

[18] A.S. Wills, Proceedings of Highly Frustrated Magnetism 2000 Conference, to appear in Can. J. Phys. (2001).

[19] O.V. Kovalev, ‘Irreducibe Representations of the Space Groups’, Gordon and Breach (New York, 1961).

Proceedings on the International Conference on Neutron Scattering, Munich 2001.
(PROOF COPY)

Applied Physics A
Materials
Science & Processing

Symmetry and magnetic structure determination: developments in refinement techniques and examples

A.S. Wills[*]

Institut Laue-Langevin, 6 Rue Jules Horowitz, BP 156, 38042 Grenoble Cedex 9, France

Received: 12 July 2001/Accepted: 24 October 2001 –

Abstract. Group-theory techniques can aid greatly the determination of magnetic structures. The integration of their calculations into new and existing refinement programs is an ongoing development that will simplify and make more rigorous the analysis of experimental data. This paper presents an overview of the practical application of symmetry analysis to the determination of magnetic structures. Details are given of the different programs that perform these calculations and how refinements can be carried out using their results. Examples are presented that show how such analysis can be important in the interpretation of magnetic diffraction data, and to our reasoning of the causes for the observed ordering.

PACS: 75.10.-b; 75.25.+z

Despite immense technical progress since the first magnetic neutron diffraction experiments of Shull and Smart [1], the determination of magnetic structures remains a subject that is typically limited by the data-analysis strategy: structures are generally determined by intuition or simple trial and error refinement. As a consequence, the literature is full of incorrect magnetic structures and incomplete refinements. While group-theory techniques can be applied to limit the number of trial structures, or to determine along which directions the spin components can lie, their calculations when carried out by hand are arduous. This has led to their being applied only when a problem warrants their use or, more commonly, when it is sufficiently close to an example already in the literature. Recently, a number of computer programs have been developed that allow the unspecialised user to perform these calculations automatically. Their integration with common refinement codes allow for the first time the simple and rigorous examination of which symmetry-allowed magnetic structures are compatible with collected data.

In this article a brief overview is made of the practical application of using group theory to aid the determination of magnetic structures from both powder and single-crystal samples. Examples are given that demonstrate the importance of symmetry information for the correct analysis of magnetic diffraction data, and concomitantly to the understanding of the physical reasons for the formation of a long-range magnetic order.

1 Representational analysis calculations

The calculations can be separated into two parts. The first is a grouping according to symmetry of the possible magnetic structures that are compatible with both the space group of the crystal structure and the propagation vector $\boldsymbol{k}$ of the magnetic ordering. The second part involves the application of Landau theory as a tool to simplify which of these are possible as a result of a continuous second-order phase transition. While the grouping and the labelling of the different magnetic structures by their symmetry properties is completely general, the assumptions made that involve the Landau theory are subject to its limitations.

The application of group theory to the determination of magnetic structures is termed representational analysis [2–6] and is based on the calculation of the Fourier components of an ordered magnetic structure that are compatible with the symmetry of the crystal space group before the phase transition and the propagation vector.

The first step in the analysis is the identification of the propagation vector $\boldsymbol{k}$ associated with the phase transition, and which space-group symmetry operations leave it invariant. These operations form the little group $\mathrm{G}_{\boldsymbol{k}}$. The symmetry elements of $\mathrm{G}_{\boldsymbol{k}}$ and the value of $\boldsymbol{k}$ are then used to determine the different irreducible representations (IRs) of $\mathrm{G}_{\boldsymbol{k}}$. The different basis vectors (Fourier components of the magnetic structure), BVs, that are projected out from an irreducible representation define a basis-vector space that may be termed a ‘symmetry-allowed’ model. The different IRs define orthogonal basis-vector spaces that can be used to conveniently classify the different possible magnetic structures.

---

[*] E-mail: a.s.wills@ill.fr

2 Application of Landau theory

The Landau theory of a second-order phase transition requires that the Hamiltonian of the system is invariant under the symmetry operations of $G_{\boldsymbol{k}}$. This leads to the requirement that for a second-order phase transition an ordered structure can be the result of only a single IR becoming critical. This typically reduces the number of trial structures and the variables that each involve.

When the assumptions of Landau theory are not valid, for instance when the Hamiltonian possesses odd-powered terms, the mixing of components from different IRs becomes possible. Continuing with this logic, the observation of a magnetic structure that involves different IRs is suggestive of either successive ordering transitions for each IR, or additional terms in the magnetic Hamiltonian that relax the single-IR rule, e.g. crystal-field terms at sites with certain point symmetries.

3 Programs that perform these calculations

While tabulated values of the IRs of the space groups have existed for many years [7, 8], they are prone to inaccuracies[1] and their laborious use in calculations carried out by hand is perhaps the major reason for their restricted use. Preferable to many are the programs that have been written that calculate these IRs, or use files of tabulated values such as: KAREP [10] (calculated), MODY [11] (unverified tabulated values), BasiReps [12] (based on KAREP), and SARA*h* [13] (with the choice of KAREP-based and computer-verified tabulated values). MODY, BasiReps, and SARA*h* also use these values to calculate directly the basis vectors associated with the different IRs, and so allow the rapid and simple calculation of the possible symmetry-allowed structures.

4 Refinement using the results of symmetry analysis

The simplest and most general mathematical description of a magnetic structure is in terms of Fourier components: the basis vectors that result from the group theory. The panoply of different possible commensurate and modulated incommensurate structures can be simply understood in terms of the form of the basis vector(s) for a site and the value(s) of $\boldsymbol{k}$. To simplify the refinement process, SARA*h* and BasiReps have been written to integrate with the standard refinement codes FullProf 2000 [14] (BasiReps and SARA*h*) and GSAS [15] (SARA*h*). The applicability of the technique is now limited principally by the choice of refinement codes[2].

The reduction in data due to the magnetic form factor and the observation of only the component of the magnetisation perpendicular to the scattering vector result in instabilities and limitations when using conventional least-squares refinements. These can be overcome by the reverse-Monte Carlo-based algorithms which allow the automatic exploration of the degrees of freedom associated with a given magnetic structure and the identification of additional minima in the refinement [13]. In more complex cases the technique of simulated annealing can be employed: this uses a decreasing criterion to allow the more controlled evolution of the system that is required to bypass the false minima commonly associated with larger numbers of variables.

5 Ongoing development of refinement codes

Due to the difficulties in magnetic structure refinement being greatest for data from powders, development of these new magnetic structure refinement codes has concentrated on their analysis. As part of a collaboration between the Institut Laue-Langevin, the Commissariat à lÉnergie Atomique, and the Laboratoire Léon Brillouin we are at present working on the extension of the FullProf package not only towards the refinement of unpolarised and polarised neutron-diffraction data collected from single crystals, but also towards data collected by the technique of spherical neutron polarimetry. After these developments the data collected by any technique, from conventional powder diffraction to even the most complex collection techniques, will be refinable in terms of symmetry-generated basis vectors.

6 Canted antiferromagnetism in $M_2[Ni(CN_2)]$ (where $M = Mn$ and Fe)

The first example of the application of these techniques is taken from the $M_2[NiCN_2]$ (where $M = Mn$ and Fe) molecular solids [16]. These binary metal–dicyanide molecular materials crystallise in the space group P*nnm*. Below second-order transitions at $T \sim 16\,K$ for the Mn and $T \sim 19\,K$ for the Fe compounds, these display long-range magnetic order with the propagation vector $\boldsymbol{k} = (0\,0\,0)$. Symmetry analysis of the magnetic M atom at the 2*a* position indicates that there are four symmetry-allowed models; these correspond to the IRs Γ_1, Γ_3, Γ_5, and Γ_7 in the notation of Kovalev [8, 9] and their basis vectors are given in Table 1. While data collected using powder neutron diffraction can be well fitted by a simple model of antiparallel spins ($M1 = -M2$) that were free to rotate in the *ab* plane, this spin structure is not allowed by symmetry. Investigation of the symmetry-allowed models found that the data could only be well fitted by Γ_5.

IR	BV	M1	M2
Γ_1	ψ_1	(0 0 1)	$(0\ 0\ \bar{1})$
Γ_3	ψ_2	(1 0 0)	(1 0 0)
	ψ_3	(0 1 0)	$(0\ \bar{1}\ 0)$
Γ_5	ψ_4	(1 0 0)	$(\bar{1}\ 0\ 0)$
	ψ_5	(0 1 0)	(0 1 0)
Γ_7	ψ_6	(0 0 1)	(0 0 1)

Table 1. Magnetic basis vectors, BVs, for the 2*a* site of the space group P*nmm* with the propagation vector $\boldsymbol{k} = (0\,0\,0)$. M1 and M2 are the atomic positions $(0\,0\,0)$ and $(\frac{1}{2}\ \frac{1}{2}\ \frac{1}{2})$

---

[1] The exception to this is likely to be those presented in [9] as these have been subject to computer verification.

[2] Perhaps the most important restriction arises from the absence of a propagation vector in GSAS – it is consequently limited to only simple commensurate structures.

Inspection of the associated basis vectors (ψ_4 and ψ_5) shows that while the moments are antiferromagnetically aligned along *a*, an uncompensated magnetisation can exist along *b*. The presence of such a ferromagnetic spin canting has been confirmed by dc susceptibility data.

7 Rare-earth nickel borocarbides

Very recently, symmetry analysis has provided important new information about the variety of magnetic orderings that are observed in the rare-earth nickel borocarbides RNi_2B_2C (R = Gd–Lu, Y) [17]. In these materials Fermi surface nesting effects propagated via the RKKY interactions create a strong tendency for these materials to order magnetically with the propagation vector $\boldsymbol{k} = (0.55\ 0\ 0)$. Despite this, a large number of different magnetic structures are observed for the series.

The key to understanding the magnetism of these materials was the single-ion anisotropies of the rare earths. These are typically well defined and possess a characteristic energy scale that is far greater than that of the exchange interactions. Their effect is to force the magnetisation to point along specific crystallographic directions. Symmetry analysis of the different magnetic structures that are possible for the propagation vector $\boldsymbol{k} = (0.55\ 0\ 0)$ in this system indicated that when the single-ion effects were incompatible with the symmetry-allowed directions for this propagation vector, the system orders according to another propagation vector that *does* allow the single-ion effects of the rare earth in question to be satisfied.

8 The jarosites

The jarosites $(AFe_3(SO_4)_2(OD)_6$, where $A = Na^+, K^+, Rb^+, Ag^+, ND_4^+, \frac{1}{2}Pb^{+2})$, are the most studied examples of kagomé antiferromagnets. They have been the object of much scrutiny as the magnetic sublattice makes up a geometry of vertex-sharing triangles. This results in their having an infinite number of classical ground states in the presence of only nearest-neighbour antiferromagnetic exchange interactions. Further-neighbour interactions can raise this degeneracy and cause one particular ordered spin configuration to be favoured from the degenerate manifold. Unfortunately, the experimental determination of which occurs is strongly hindered by an ignorance of the particular degeneracy-breaking interaction. Not only did symmetry analysis provide a particularly effective tool for the reduction in the number of trial structures, but it also helped to understand them in terms of the different terms in the exchange Hamiltonian [18].

9 Conclusion

The tools are now available that allow the unspecialised researcher to use symmetry analysis to make simpler and more rigorous the refinement of magnetic neutron diffraction data. As demonstrated here, their application to even the simplest structures is important, as physically unreasonable models still often fit experimental data.

References

1. C.G. Shull, J.S. Smart: Phys. Rev. **76**, 1256 (1949)
2. E.F. Bertaut: J. Appl. Phys. **33**, 1138 (1962)
3. E.F. Bertaut: Acta Crystallogr. A **24**, 217 (1968)
4. E.F. Bertaut: J. Phys. Colloq. **C1**, 462 (1971)
5. E.F. Bertaut: J. Magn. Magn. Mater. **24**, 267 (1981)
6. Y.A. Izyumov, V.E. Naish, R.P. Ozerov: *Neutron Diffraction of Magnetic Materials* (Consultants Bureau, New York 1991)
7. C.J. Bradley, A.P. Cracknell: *The Mathematical Theory of Symmetry in Solids* (Clarendon, Oxford 1972)
8. O.V. Kovalev: *Irreducible Representations of the Space Groups* (Gordon and Breach, New York 1965)
9. O.V. Kovalev: *Representations of the Crystallographic Space Groups*, 2nd edn. (Gordon and Breach, Switzerland, 1993)
10. E.R. Hovestreydt, M.I. Aroyo, H. Wondratschek: J. Appl. Crystallogr. **25**, 544 (1992)
11. P. Czapnik, W. Sikora: program available from www.ftj.agh.edu.pl/zffs/staff/sikora/program/mody.zip
12. J. Rodríguez-Carvajal: program available from juan@llb.saclay.cea.fr
13. A.S. Wills: Physica B **276**, 680 (2000). Program available from ftp://ftp.ill.fr/pub/dif/sarah/
14. J. Rodríguez-Carvajal: Physica B **192**, 55 (1993)
15. A.C. Larsen, R.B. von Dreele: program available from ftp://ftp.lanl.gov/public/gsas/
16. A. Lappas, A.S. Wills, M.A. Green, M. Kurmoo, K. Prassides: Phys. Rev. B (2002), submitted
17. A.S. Wills, C. Detlefs, P.C. Canfield: Eur. Phys. J. B (2001) submitted
18. A.S. Wills: Phys. Rev. B **63**, 064430 (2001)

Magnetic Refinements in GSAS

Paolo G. Radaelli

GSAS magnetic options

- The approach of GSAS to magnetic structures is loosely based on Shubnikov groups.
- However, for each space group, not all Shubnicov groups generated from it are possible. The only possible ones are those corresponding to subgroups of index 2 of types I and IIa. In other words, the *conventional* unit cell must be in common between the parent group and the subgroup.
- In GSAS there is a straight implementation of the OG formalism, where ‘primed’ operators (or lattices) correspond to ‘red’ operators.
- Alternatively, one can always generate an additional magnetic phase with appropriate constraints.

GSAS magnetic entries

- **Phase**: in the “phase” menu (keystrokes **k-p-p**), one has the option of selecting (**m**) whether the phase is nuclear, nuclear *and* magnetic or purely magnetic (**a**, **b**, **c**, respectively).
- **Form factor**: in the form factor editing menu (**k-p-f**) there is an option (**m**) to edit magnetic form factors. One can use the default values (warning! They are different for different oxidation states) or input user values (see ITC, volume C).
- **Atoms**: in the atom editing menu (**k-l-a**) there is an option (**m**) to assign magnetic moments to individual atoms. Within that menu, there is an option (**s**) to ‘prime’ the group generators. GSAS automatically determines if the magnetic point group of the site is admissible, and, if so, for which spin directions. One can change colours with the **c** option. Once out of the **s** menu, one can change the spin components with the **m** option.

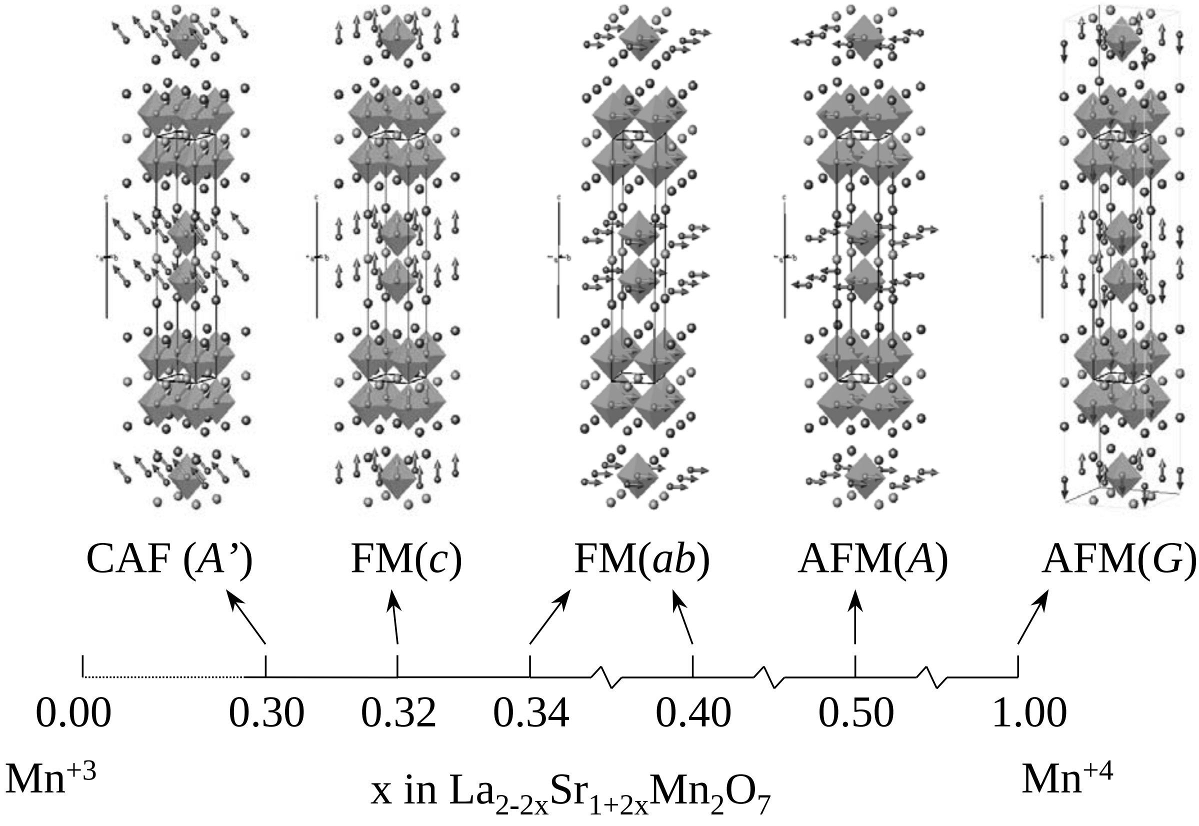

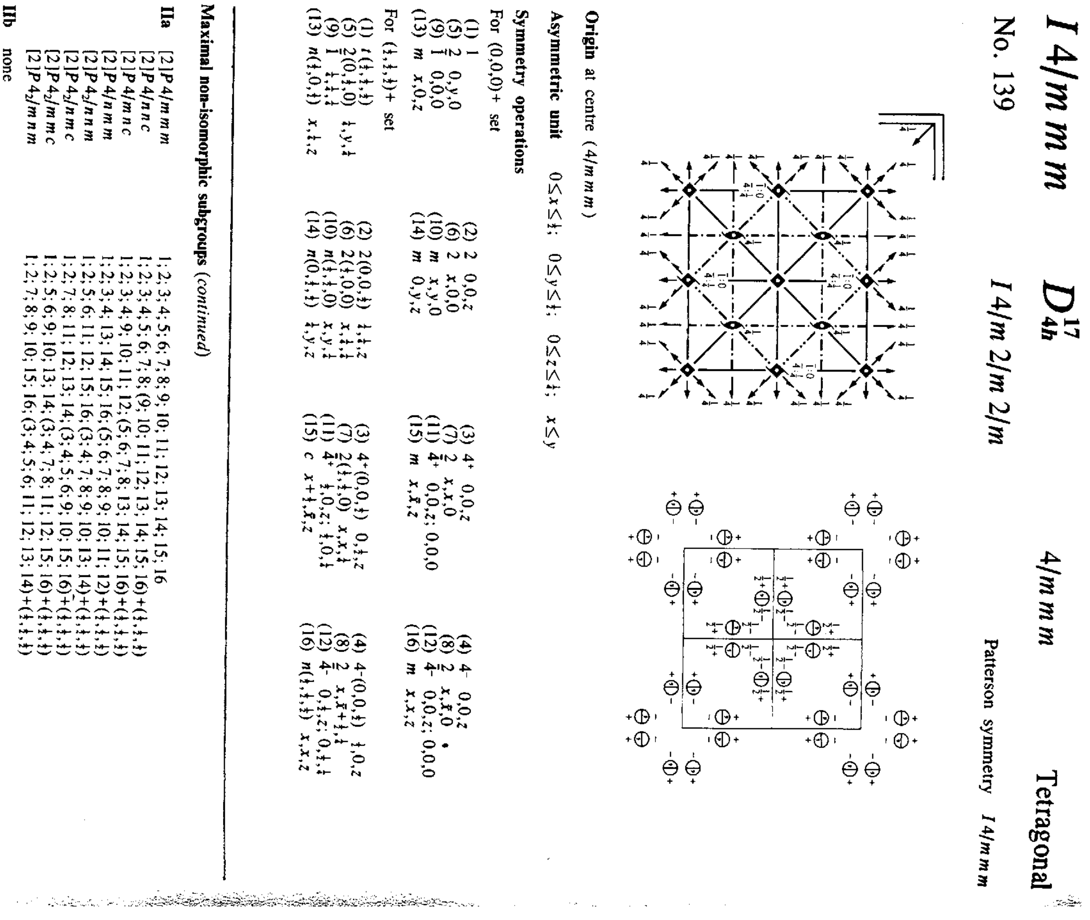

I 4/*m m m* D_{4h}^{17} 4/*m m m* Tetragonal

No. 139 *I* 4/*m* 2/*m* 2/*m* Patterson symmetry *I* 4/*m m m*

Origin at centre (4/*m m m*)

Asymmetric unit $0 \leq x \leq \frac{1}{2}$; $0 \leq y \leq \frac{1}{2}$; $0 \leq z \leq \frac{1}{4}$; $x \leq y$

Symmetry operations

For (0,0,0)+ set

(1) 1	(2) 2 0,0,*z*	(3) 4^+ 0,0,*z*	(4) 4^- 0,0,*z*
(5) 2 0,*y*,0	(6) 2 *x*,0,0	(7) 2 *x*,*x*,0	(8) 2 $x,\bar{x},0$ •
(9) $\bar{1}$ 0,0,0	(10) *m* *x*,*y*,0	(11) $\bar{4}^+$ 0,0,*z*; 0,0,0	(12) $\bar{4}^-$ 0,0,*z*; 0,0,0
(13) *m* *x*,0,*z*	(14) *m* 0,*y*,*z*	(15) *m* $x,\bar{x},z$	(16) *m* *x*,*x*,*z*

For $(\frac{1}{2},\frac{1}{2},\frac{1}{2})$+ set

(1) $t(\frac{1}{2},\frac{1}{2},\frac{1}{2})$	(2) $2(0,0,\frac{1}{2})$ $\frac{1}{4},\frac{1}{4},z$	(3) $4^+(0,0,\frac{1}{2})$ $0,\frac{1}{2},z$	(4) $4^-(0,0,\frac{1}{2})$ $\frac{1}{2},0,z$
(5) $2(0,\frac{1}{2},0)$ $\frac{1}{4},y,\frac{1}{4}$	(6) $2(\frac{1}{2},0,0)$ $x,\frac{1}{4},\frac{1}{4}$	(7) $2(\frac{1}{2},\frac{1}{2},0)$ $x,x,\frac{1}{4}$	(8) 2 $x,\bar{x}+\frac{1}{2},\frac{1}{4}$
(9) $\bar{1}$ $\frac{1}{4},\frac{1}{4},\frac{1}{4}$	(10) $n(\frac{1}{2},\frac{1}{2},0)$ $x,y,\frac{1}{4}$	(11) $\bar{4}^+$ $\frac{1}{2},0,z$; $\frac{1}{2},0,\frac{1}{4}$	(12) $\bar{4}^-$ $0,\frac{1}{2},z$; $0,\frac{1}{2},\frac{1}{4}$
(13) $n(\frac{1}{2},0,\frac{1}{2})$ $x,\frac{1}{4},z$	(14) $n(0,\frac{1}{2},\frac{1}{2})$ $\frac{1}{4},y,z$	(15) *c* $x+\frac{1}{2},\bar{x},z$	(16) $n(\frac{1}{2},\frac{1}{2},\frac{1}{2})$ *x*,*x*,*z*

Maximal non-isomorphic subgroups (*continued*)

IIa	[2]*P* 4/*m m m*	1; 2; 3; 4; 5; 6; 7; 8; 9; 10; 11; 12; 13; 14; 15; 16
	[2]*P* 4/*n n c*	1; 2; 3; 4; 5; 6; 7; 8; (9; 10; 11; 12; 13; 14; 15; 16)+$(\frac{1}{2},\frac{1}{2},\frac{1}{2})$
	[2]*P* 4/*m n c*	1; 2; 3; 4; 9; 10; 11; 12; (5; 6; 7; 8; 13; 14; 15; 16)+$(\frac{1}{2},\frac{1}{2},\frac{1}{2})$
	[2]*P* 4/*n m m*	1; 2; 3; 4; 13; 14; 15; 16; (5; 6; 7; 8; 9; 10; 11; 12)+$(\frac{1}{2},\frac{1}{2},\frac{1}{2})$
	[2]$P4_2/nnm$	1; 2; 5; 6; 11; 12; 15; 16; (3; 4; 7; 8; 9; 10; 13; 14)+$(\frac{1}{2},\frac{1}{2},\frac{1}{2})$
	[2]$P4_2/nmc$	1; 2; 7; 8; 11; 12; 13; 14; (3; 4; 5; 6; 9; 10; 15; 16)+$(\frac{1}{2},\frac{1}{2},\frac{1}{2})$
	[2]$P4_2/mmc$	1; 2; 5; 6; 9; 10; 13; 14; (3; 4; 7; 8; 11; 12; 15; 16)+$(\frac{1}{2},\frac{1}{2},\frac{1}{2})$
	[2]$P4_2/mnm$	1; 2; 7; 8; 9; 10; 15; 16; (3; 4; 5; 6; 11; 12; 13; 14)+$(\frac{1}{2},\frac{1}{2},\frac{1}{2})$
IIb	none	

Maximal isomorphic subgroups of lowest index

IIc [3]*I* 4/*m m m* ($\mathbf{c}' = 3\mathbf{c}$); [9]*I* 4/*m m m* ($\mathbf{a}' = 3\mathbf{a}$, $\mathbf{b}' = 3\mathbf{b}$)

Minimal non-isomorphic supergroups

I [3]$Fm\bar{3}m$; [3]$Im\bar{3}m$

II [2]*C* 4/*m m m* ($2\mathbf{c}' = \mathbf{c}$)(*P* 4/*m m m*)

468

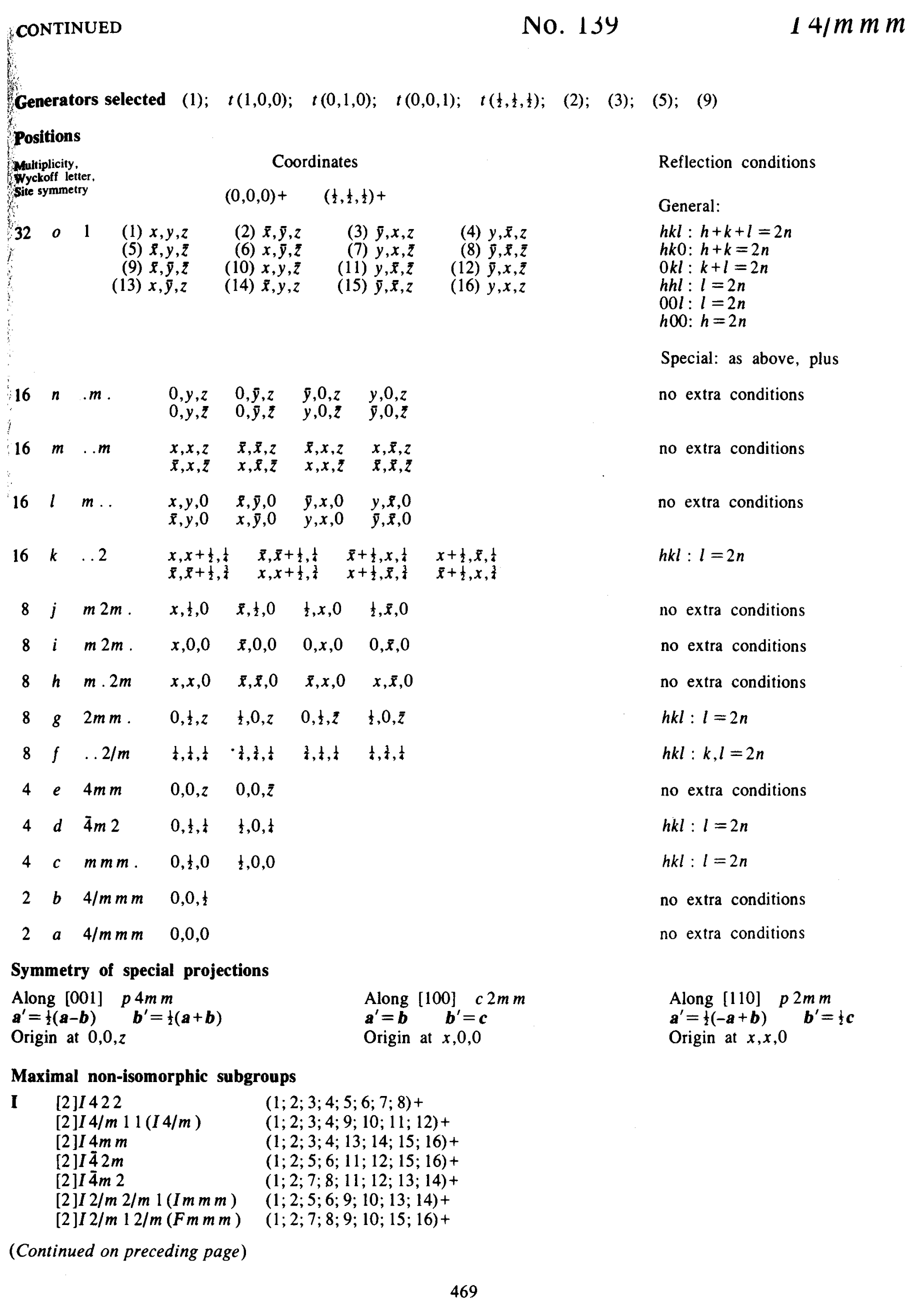

CONTINUED No. 139 $I\,4/m\,m\,m$

Generators selected (1); $t(1,0,0)$; $t(0,1,0)$; $t(0,0,1)$; $t(\frac{1}{2},\frac{1}{2},\frac{1}{2})$; (2); (3); (5); (9)

Positions

Multiplicity, Wyckoff letter, Site symmetry			Coordinates $(0,0,0)+ \quad (\frac{1}{2},\frac{1}{2},\frac{1}{2})+$	Reflection conditions
				General:
32	*o*	1	(1) x,y,z (2) $\bar{x},\bar{y},z$ (3) $\bar{y},x,z$ (4) $y,\bar{x},z$ (5) $\bar{x},y,\bar{z}$ (6) $x,\bar{y},\bar{z}$ (7) $y,x,\bar{z}$ (8) $\bar{y},\bar{x},\bar{z}$ (9) $\bar{x},\bar{y},\bar{z}$ (10) $x,y,\bar{z}$ (11) $y,\bar{x},\bar{z}$ (12) $\bar{y},x,\bar{z}$ (13) $x,\bar{y},z$ (14) $\bar{x},y,z$ (15) $\bar{y},\bar{x},z$ (16) y,x,z	hkl: $h+k+l=2n$ $hk0$: $h+k=2n$ $0kl$: $k+l=2n$ hhl: $l=2n$ $00l$: $l=2n$ $h00$: $h=2n$
				Special: as above, plus
16	*n*	$.m.$	$0,y,z$ $\quad 0,\bar{y},z$ $\quad \bar{y},0,z$ $\quad y,0,z$ $0,y,\bar{z}$ $\quad 0,\bar{y},\bar{z}$ $\quad y,0,\bar{z}$ $\quad \bar{y},0,\bar{z}$	no extra conditions
16	*m*	$..m$	x,x,z $\quad \bar{x},\bar{x},z$ $\quad \bar{x},x,z$ $\quad x,\bar{x},z$ $\bar{x},x,\bar{z}$ $\quad x,\bar{x},\bar{z}$ $\quad x,x,\bar{z}$ $\quad \bar{x},\bar{x},\bar{z}$	no extra conditions
16	*l*	$m..$	$x,y,0$ $\quad \bar{x},\bar{y},0$ $\quad \bar{y},x,0$ $\quad y,\bar{x},0$ $\bar{x},y,0$ $\quad x,\bar{y},0$ $\quad y,x,0$ $\quad \bar{y},\bar{x},0$	no extra conditions
16	*k*	$..2$	$x,x+\frac{1}{2},\frac{1}{4}$ $\quad \bar{x},\bar{x}+\frac{1}{2},\frac{1}{4}$ $\quad \bar{x}+\frac{1}{2},x,\frac{1}{4}$ $\quad x+\frac{1}{2},\bar{x},\frac{1}{4}$ $\bar{x},\bar{x}+\frac{1}{2},\frac{3}{4}$ $\quad x,x+\frac{1}{2},\frac{3}{4}$ $\quad x+\frac{1}{2},\bar{x},\frac{3}{4}$ $\quad \bar{x}+\frac{1}{2},x,\frac{3}{4}$	hkl: $l=2n$
8	*j*	$m2m.$	$x,\frac{1}{2},0$ $\quad \bar{x},\frac{1}{2},0$ $\quad \frac{1}{2},x,0$ $\quad \frac{1}{2},\bar{x},0$	no extra conditions
8	*i*	$m2m.$	$x,0,0$ $\quad \bar{x},0,0$ $\quad 0,x,0$ $\quad 0,\bar{x},0$	no extra conditions
8	*h*	$m.2m$	$x,x,0$ $\quad \bar{x},\bar{x},0$ $\quad \bar{x},x,0$ $\quad x,\bar{x},0$	no extra conditions
8	*g*	$2mm.$	$0,\frac{1}{2},z$ $\quad \frac{1}{2},0,z$ $\quad 0,\frac{1}{2},\bar{z}$ $\quad \frac{1}{2},0,\bar{z}$	hkl: $l=2n$
8	*f*	$..2/m$	$\frac{1}{4},\frac{1}{4},\frac{1}{4}$ $\quad \frac{3}{4},\frac{3}{4},\frac{1}{4}$ $\quad \frac{3}{4},\frac{1}{4},\frac{1}{4}$ $\quad \frac{1}{4},\frac{3}{4},\frac{1}{4}$	hkl: $k,l=2n$
4	*e*	$4mm$	$0,0,z$ $\quad 0,0,\bar{z}$	no extra conditions
4	*d*	$\bar{4}m2$	$0,\frac{1}{2},\frac{1}{4}$ $\quad \frac{1}{2},0,\frac{1}{4}$	hkl: $l=2n$
4	*c*	$mmm.$	$0,\frac{1}{2},0$ $\quad \frac{1}{2},0,0$	hkl: $l=2n$
2	*b*	$4/mmm$	$0,0,\frac{1}{2}$	no extra conditions
2	*a*	$4/mmm$	$0,0,0$	no extra conditions

Symmetry of special projections

Along [001] $p\,4mm$	Along [100] $c\,2mm$	Along [110] $p\,2mm$
$\mathbf{a}'=\frac{1}{2}(\mathbf{a}-\mathbf{b})$ $\quad \mathbf{b}'=\frac{1}{2}(\mathbf{a}+\mathbf{b})$	$\mathbf{a}'=\mathbf{b}$ $\quad \mathbf{b}'=\mathbf{c}$	$\mathbf{a}'=\frac{1}{2}(-\mathbf{a}+\mathbf{b})$ $\quad \mathbf{b}'=\frac{1}{2}\mathbf{c}$
Origin at $0,0,z$	Origin at $x,0,0$	Origin at $x,x,0$

Maximal non-isomorphic subgroups

I	$[2]I\,422$	(1; 2; 3; 4; 5; 6; 7; 8)+
	$[2]I\,4/m\,1\,1\,(I\,4/m)$	(1; 2; 3; 4; 9; 10; 11; 12)+
	$[2]I\,4mm$	(1; 2; 3; 4; 13; 14; 15; 16)+
	$[2]I\,\bar{4}\,2m$	(1; 2; 5; 6; 11; 12; 15; 16)+
	$[2]I\,\bar{4}m\,2$	(1; 2; 7; 8; 11; 12; 13; 14)+
	$[2]I\,2/m\,2/m\,1\,(I\,mmm)$	(1; 2; 5; 6; 9; 10; 13; 14)+
	$[2]I\,2/m\,1\,2/m\,(F\,mmm)$	(1; 2; 7; 8; 9; 10; 15; 16)+

(Continued on preceding page)

469

Notes on the Layered Manganite example

- The manganite site is 4e [4mm]. Of the magnetic subgroups of [4mm], the only admissible one is 4m’m’. Consequently, the only possible magnetic space groups are *I4/mm’m’ I4/m’m’m’, $\mathrm{I_P}$4/mm’m’ and $\mathrm{I_P}$4/m’m’m’. Note that the first one is a ferromagnetic group.
- An immediate consequence of the site symmetry of the Mn site is that the spin *has* to be directed along the 4-fold axis.
- There are therefore only 4 magnetic structures generated with the Shubnikov approach. The layers are *always* FM, with the intra- and inter-bilayer coupling being FM or AFM.
- Note the significant number of magnetic structures which are observed, but cannot be generated with the Shubnikov approach.

Magnetic refinements - multi-phase approach

Should the Shubnikov approach be insufficient to describe the magnetic structure, one can resort to introducing a second *purely magnetic* phase with appropriate constraints but lower symmetry This enables one to deal with any kind of commensurate structure, including the representation analysis. Here are a few tips:

1. If the magnetic phase has the same conventional cell as the nuclear one, the lattice and phase fraction constraints are straightforward.
2. If the magnetic cell is *larger* than the nuclear one, one has to remember that the phase fraction is proportional to the number of unit cells in the sample. So, if the the volume of the MP is doubled, its phase fraction must be halved.
3. One can also set constraints on the lattice when the two cells are different. However, remember that the constraints are on the reciprocal metric tensor, *not* on lattice parameters. Consult a crystallography book to see how they are related for the various lattices.

Shubnikov Groups:
a GSAS application

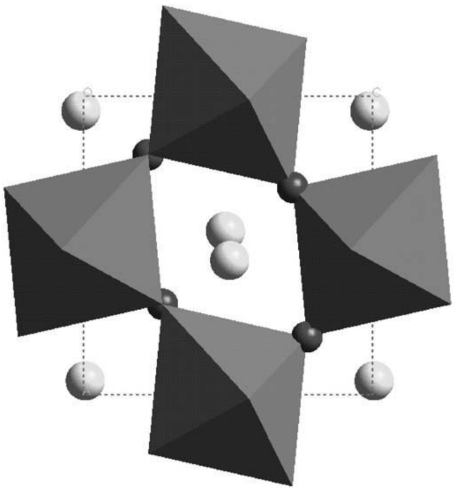

Pnma

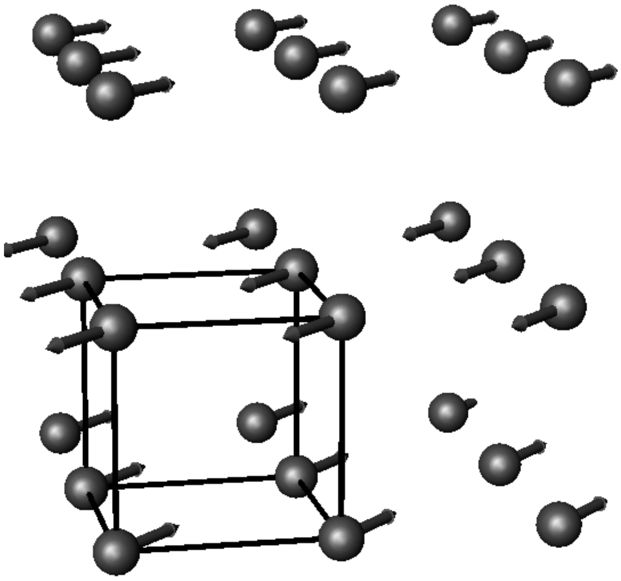

Magnetic powder diffraction and instrumentation

Paolo G. Radaelli

Spin Density

Unit-Cell Spin Density (localised and isotropic approx.):

$$\mathbf{M}_u(\mathbf{r}) = \sum_{j=1}^{\mathbf{n\ atoms}} \hat{\mathbf{m}}_j \mu_j G_j\left(\left|\mathbf{r}-\mathbf{r}_j\right|\right) \qquad \tilde{\mathbf{M}}_u(\mathbf{k}) = \sum_{j=1}^{\mathbf{n\ atoms}} \hat{\mathbf{m}}_j \mu_j f_j(k) \mathrm{e}^{-i\mathbf{k}\cdot\mathbf{r}_j}$$

Lattice Spin Density (simple translational symmetry):

$$\mathbf{M}(\mathbf{r}) = \sum_{\mathbf{r}_n} \mathbf{M}_u\left(\mathbf{r}-\mathbf{r}_n\right) \qquad \tilde{\mathbf{M}}(\mathbf{k}) = \sum_{\boldsymbol{\kappa}\in\Gamma^*} \delta\left(\boldsymbol{\kappa}-\mathbf{k}\right) \sum_{j=1}^{\mathbf{n\ atoms}} \hat{\mathbf{m}}_j \mu_j f_j(k) \mathrm{e}^{-i\boldsymbol{\kappa}\cdot\mathbf{r}_j}$$

Lattice Spin Density (1-dimensional modulation):

$$\mathbf{M}(\mathbf{r}) = \sum_{\mathbf{r}_n} \overline{\overline{P}}\left(\mathbf{r}_n\cdot\boldsymbol{\tau}\right)\cdot\mathbf{M}_u\left(\mathbf{r}-\mathbf{r}_n\right) \qquad \tilde{\mathbf{M}}(\mathbf{k}) = \sum_{\substack{\boldsymbol{\kappa}\in\Gamma^* \\ l=-\infty,+\infty}} \delta\left(\boldsymbol{\kappa}-l\boldsymbol{\tau}-\mathbf{k}\right) \sum_{j=1}^{\mathbf{n\ atoms}} \left(\overline{\overline{A}}_l\cdot\hat{\mathbf{m}}_j\right)\mu_j f_j(k) \mathrm{e}^{-i\boldsymbol{\kappa}\cdot\mathbf{r}_j}$$

where $\overline{\overline{P}}(x) = \sum_{l=-\infty}^{+\infty} \overline{\overline{A}}_l \, \mathrm{e}^{ilx}$ has a periodicity of 1.

Magnetic Scattering of Neutrons

Neutrons are strongly scattered from magnetic moments. The scattering amplitude from an ion is of the order of $\gamma r_e \mu$, where:

$\gamma = -1.91$ — Neutron magnetic moment in nuclear magnetons (spin + orbital).

$r_e = 0.282 \cdot 10^{-12}$ *cm* — Electron classical radius ($e^2/m_e c^2$)

μ = ion magnetic moment in Bohr magnetons.

For comparison, typical nuclear scattering amplitudes for neutrons are of the order of $0.5\text{-}1.0 \cdot 10^{-12}$ *cm*.

Magnetic Scattering of Neutrons- II

Let’s recall the formula for the lattice spin density and its Fourier transform:

$$\mathbf{M}(\mathbf{r}) = \sum_{\mathbf{r}_n} \mathbf{M}_u(\mathbf{r}-\mathbf{r}_n) \qquad \tilde{\mathbf{M}}(\mathbf{k}) = \sum_{\boldsymbol{\kappa}\in\Gamma^*} \delta(\boldsymbol{\kappa}-\mathbf{k}) \sum_{j=1}^{\textbf{n atoms}} \hat{\mathbf{m}}_j \mu_j f_j(k) \mathrm{e}^{-i\boldsymbol{\kappa}\cdot\mathbf{r}_j}$$

The Fourier transform $\tilde{\mathbf{M}}(\mathbf{k})$ is called <u>magnetic structure factor.</u> Unlike the nuclear structure factor, it is an <u>axial vector</u> quantity, and it has to be combined with the other vector quantity in the problem in order to obtain the <u>cross section</u>, which is a scalar. The other vector quantities are the momentum transfer **k** (a conventional vector) and the neutron spin $\mathbf{s}_\mathrm{n}$ (an axial vector).

The Magnetic Form Factor

$$f(\mathbf{k}) = \frac{\left\langle q \middle| \int \mathbf{M}(\mathbf{r}) \mathrm{e}^{i\mathbf{k}\cdot\mathbf{r}}\, dr^3 \middle| q \right\rangle}{\left\langle q \middle| \int \mathbf{M}(\mathbf{r}) dr^3 \middle| q \right\rangle} \textbf{ over a single atom}$$

In the isotropic case:

$$f(\mathbf{k}) = f(k) = \langle j_0(k) \rangle + \left(1 - {}^{2}\!/_{g}\right) \langle j_2(k) \rangle$$

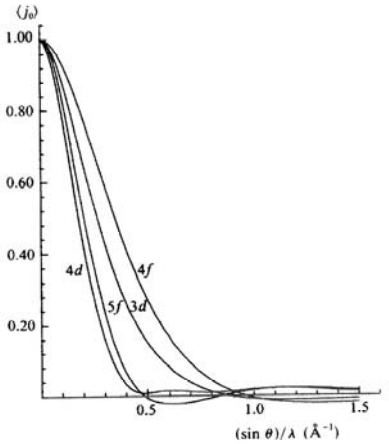

Fig. 6.1.2.2. Comparison of 3*d*, 4*d*, 4*f*, and 5*f* form factors. The 3 form factor is for Co, and the 4*d* for Rh, both calculated fron wavefunctions given by Clementi & Roetti (1974). The 4*f* forn factor is for Gd^{3+} calculated by Freeman & Desclaux (1972) anc the 5*f* is that for U^{3+} given by Desclaux & Freeman (1978).

From: International Tables of Crystallography, Volume C, ed. by AJC Wilson, Kluwer Ac. Pub., 1998, p. 513

Scattering of Neutrons from MS

It is useful to introduce the quantity **Q**(**k**), known as magnetic interaction vector, and defined as:

$$\mathbf{Q}(\mathbf{k}) = \hat{\mathbf{k}} \times \tilde{\mathbf{M}}(\mathbf{k}) \times \hat{\mathbf{k}}$$

Q(**k**) is the projection of the magnetic structure factor upon the plane perpendicular to the momentum transfer **k**. Magnetic neutron scattering cross sections only contain **Q**(**k**). In other words, scattering of neutrons through **k** is only determined by the components of the magnetic moments ⊥ to **k**. Note that **Q**(**k**) can be complex.

Magnetic Scattering Formulæ

Polarised neutrons - polarisation analysis

Non-flip

$$\left(\frac{\mathrm{d}\sigma}{\mathrm{d}\Omega}(\mathbf{k})\right)^{++} = (\gamma r_e)^2 \left\{ \left|\hat{\mathbf{s}}_n \cdot \mathbf{Q}(\mathbf{k})\right|^2 + \left|F'(\mathbf{k})\right|^2 + \hat{\mathbf{s}}_n \cdot \left[\mathbf{Q}^*(\mathbf{k}) F'(\mathbf{k}) + \mathbf{Q}(\mathbf{k}) F'^*(\mathbf{k})\right] \right\}$$

Flip

$$\left(\frac{\mathrm{d}\sigma}{\mathrm{d}\Omega}(\mathbf{k})\right)^{+-} = (\gamma r_e)^2 \left\{ \left[\hat{\mathbf{s}}_n \times \mathbf{Q}(\mathbf{k})\right] \cdot \left[\hat{\mathbf{s}}_n \times \mathbf{Q}^*(\mathbf{k})\right] + i\hat{\mathbf{s}}_n \cdot \left[\mathbf{Q}(\mathbf{k})^* \times \mathbf{Q}(\mathbf{k})\right] \right\}$$

Total

$$\left(\frac{\mathrm{d}\sigma}{\mathrm{d}\Omega}(\mathbf{k})\right)^{\uparrow} = (\gamma r_e)^2 \left\{ \left|\mathbf{Q}(\mathbf{k})\right|^2 + \left|F'(\mathbf{k})\right|^2 + \hat{\mathbf{s}}_n \cdot \left[\mathbf{Q}^*(\mathbf{k}) F'(\mathbf{k}) + \mathbf{Q}(\mathbf{k}) F'^*(\mathbf{k}) + i\mathbf{Q}(\mathbf{k})^* \times \mathbf{Q}(\mathbf{k})\right] \right.$$

Unpolarised neutrons

$$\left(\frac{\mathrm{d}\sigma}{\mathrm{d}\Omega}(\mathbf{k})\right)^{Unpol} = (\gamma r_e)^2 \left\{ \left|\mathbf{Q}(\mathbf{k})\right|^2 + \left|F'(\mathbf{k})\right|^2 \right\}$$

Formulæ Explained

Non-flip:	In addition to the nuclear scattering, it contains the components of **Q**(**k**) parallel to the neutron spin and a magneto-structural interference term.
Flip:	It contains the components of **Q**(**k**) perpendicular to the neutron spin, plus an additional term which is present only if **Q**(**k**) is complex.
Total:	It contains the nuclear term, the module square of **Q**(**k**) and the two terms which are linear in $\mathbf{s}_n$.
Unpolarised:	It contains only the nuclear term and the module square of **Q**(**k**), since the two terms which are linear in $\mathbf{s}_n$ cancel upon averaging.

Neutron beam polarisation

As we have seen, the scattering cross section depends on the initial spin direction $\mathbf{s}_i$. Also, in general, the final direction of the neutron spin $\mathbf{s}_f$ is not parallel to the initial one $\mathbf{s}_i$. Therefore, the population of spins in a neutron beam is generally altered by magnetic scattering. One defines the neutron beam polarisation as $\mathbf{P} = \langle \hat{\mathbf{s}}_n \rangle$, where $\hat{\mathbf{s}}_n$ is the neutron spin direction and the average is taken over all the neutrons in the beam. The transformation of the neutron polarisation upon scattering is given by:

$$\mathbf{P}_f = \overline{\overline{\mathbf{D}}}\mathbf{P}_i + \mathbf{P}_C$$

Where $\overline{\overline{\mathbf{D}}}$ is a tensor describing the effects of rotation and depolarisation and $\mathbf{P}_C$ describes the creation of new polarisation.

The simplest case-I

Scattering of unpolarised neutrons from a collinear unmodulated structure. Here, κ is a reciprocal lattice vector.

For collinear structures (all moments $/\!/\ \hat{\mathbf{m}}$)

$$|\mathbf{Q}(\boldsymbol{\kappa})|^2 = \sin^2(\alpha)\left|\sum_{j=1}^{\mathbf{n\ atoms}} \mu_j f_j(\kappa)\mathrm{e}^{-i\boldsymbol{\kappa}\cdot\mathbf{r}_j}\right|^2$$

where α is the angle between $\hat{\boldsymbol{\kappa}}$ and $\hat{\mathbf{m}}$

$$\left(\frac{\mathrm{d}\sigma}{\mathrm{d}\Omega}(\boldsymbol{\kappa})\right)^{Unpol} = (\gamma r_e)^2\left\{|\mathbf{Q}(\boldsymbol{\kappa})|^2 + |F'(\boldsymbol{\kappa})|^2\right\}$$

The simplest case-II

It looks like all the information is there to solve the structure even with unpolarised neutrons and powder diffraction. All the magnetic moment magnitudes are contained in $\mathbf{Q}(\boldsymbol{\kappa})$ with the appropriate phase factors and signs. Also, the information about the direction of the magnetic moments is there through the prefactor $\sin^2(\alpha)$. So, why bother with polarised neutrons and single-crystal techniques?

Magnetic Powder Diffraction

Averaging of the $\sin^2(\alpha)$ term over the (quasi)-degenerate reflections:

- For Uniaxial Groups (3-fold, 4-fold, 6-fold) we can only determine the angle ϕ:

$$\overline{\sin^2\alpha} = 1 - \tfrac{1}{2}\sin^2\psi\sin^2\varphi - \cos^2\psi\cos^2\varphi$$

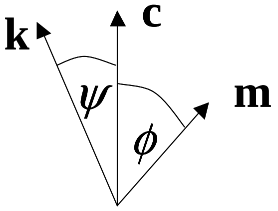

- For Cubic Structures, the direction of the magnetic moments is undetermined:

$$\overline{\sin^2\alpha} = 2/3$$

Magnetic Powder Diffractometers-I

- High-*k* range: For magnetic structure analysis, one rarely needs to go beyond $\sin(\theta)/\lambda = 0.5$. Wavelengths > 2 Å are ideal.
- Low-*k* range: It is essential to have good coverage at low *k*, as many helimagnetic structures have very long periodicity. $k = 0.5$ Å^{-1} is the minimum acceptable to do any sensible work. $k = 0.1$ Å^{-1} is ideal.
- Resolution: it is desirable especially in structure with low crystallographic symmetry, because it enables to reduce the accidental degeneracy.

CW Powder Diffractometers

- Most magnetic structure problems are first tackled using high-intensity CW powder diffractometers (e.g., D1B). The biggest advantages are the excellent coverage at low *k*, the high flux (that can be further enhanced through focussing) and the simplicity of the data structure. Resolution is generally quite poor.
- The use of high-resolution machines (e.g., D2B) is becoming more common, especially when the magnetic moments are large, the structure has low symmetry and there is an interplay between magnetism and structural properties.

The High-Intensity CW Powder diffractometer D1B at the ILL

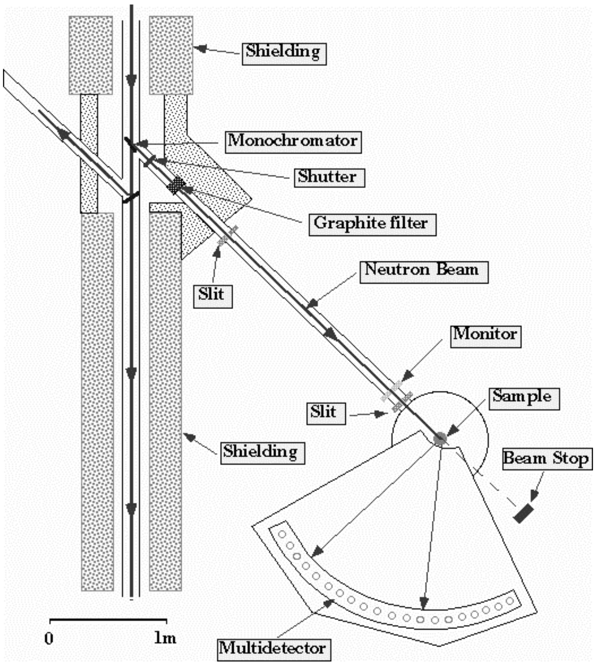

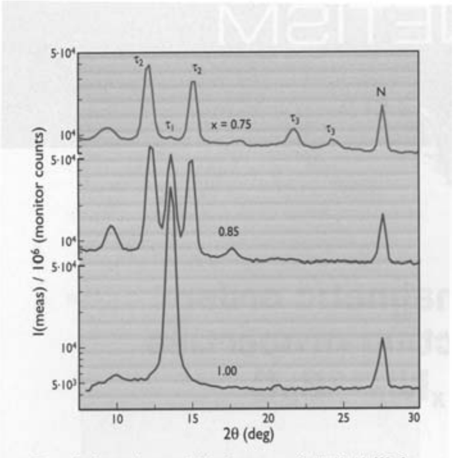

Figure 2: *Low-angle part of diffraction pattern for $Ho_xY_{1-x}Ni_2{}^{11}B_2C$ at 3 K with marked nuclear (N) and magnetic (τ_1, τ_2, τ_3) reflections.*

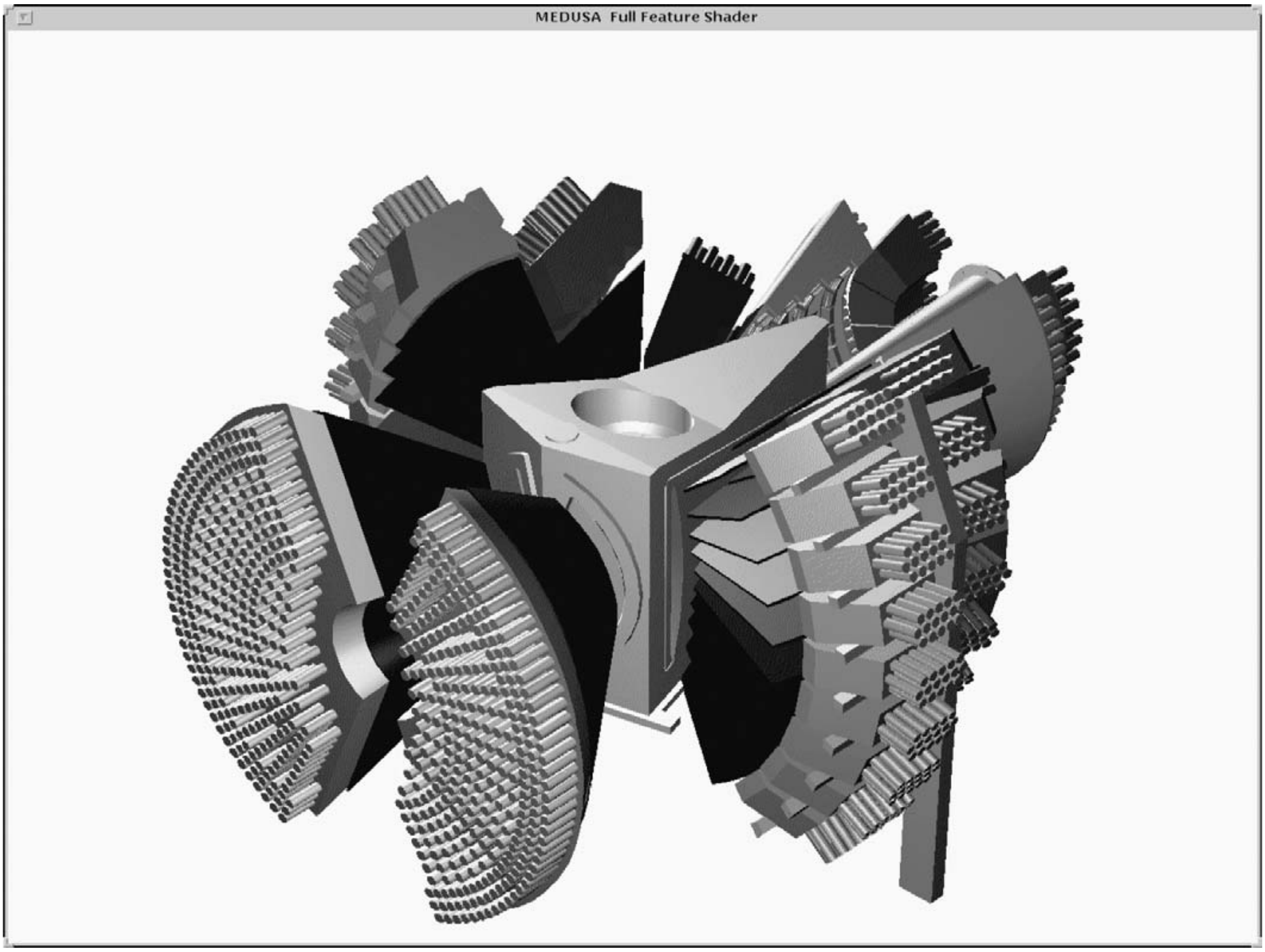
MEDUSA Full Feature Shader

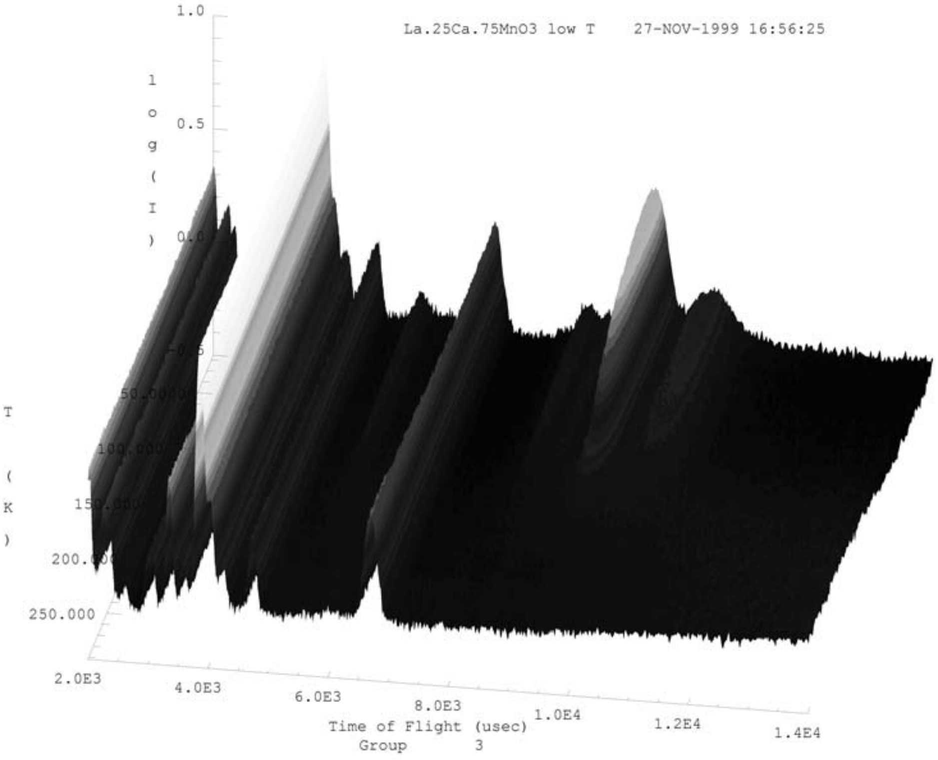
La.25Ca.75MnO3 low T 27-NOV-1999 16:56:25
log(I)
1.0
0.5
0.0
-0.5
T (K)
50.000
100.000
150.000
200.000
250.000
2.0E3
4.0E3
6.0E3
8.0E3
1.0E4
1.2E4
1.4E4
Time of Flight (usec)
Group 3

$Pr_{0.65}(Ca_y,Sr_{1-y})_{0.35}MnO_3$

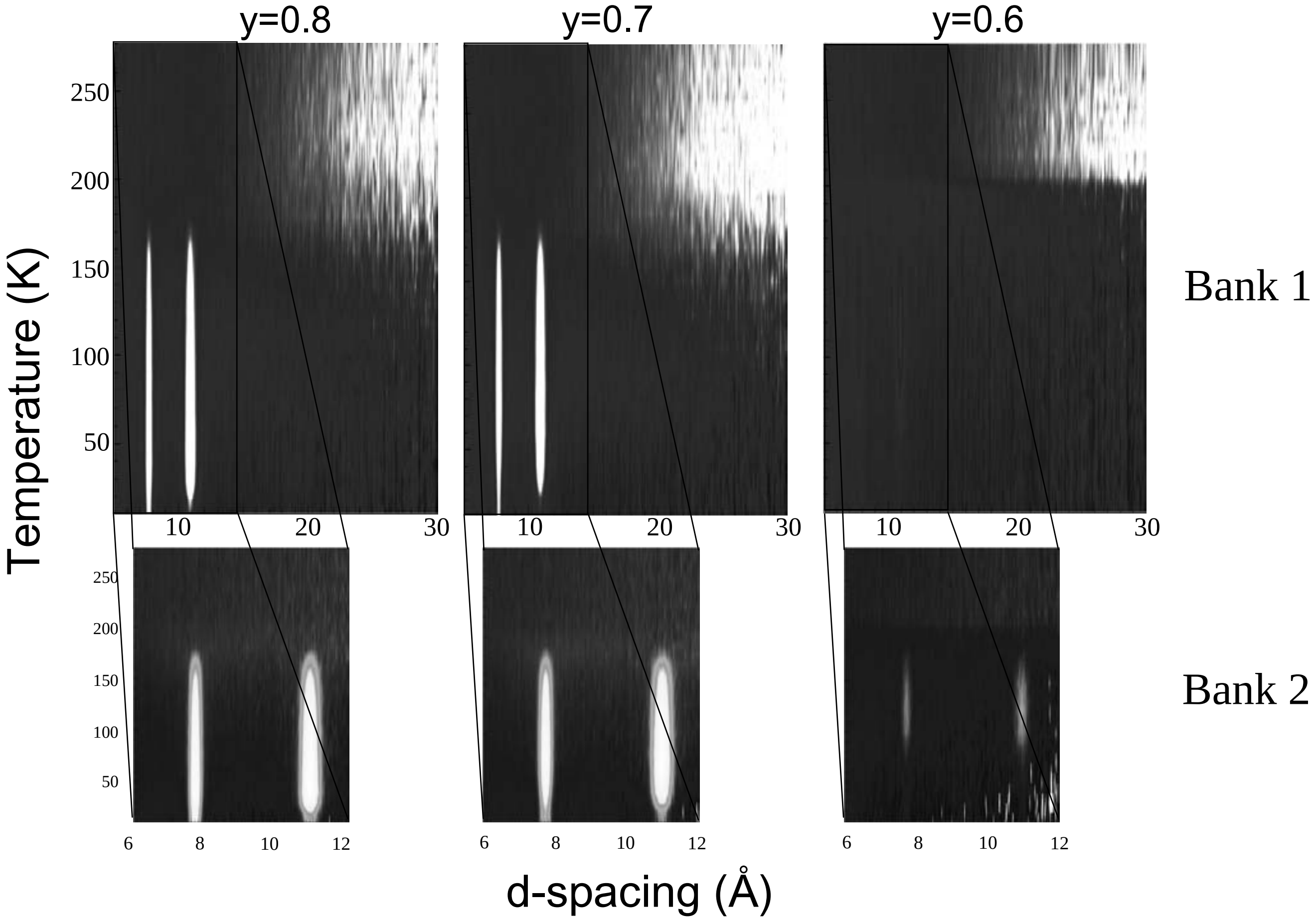

OSIRIS

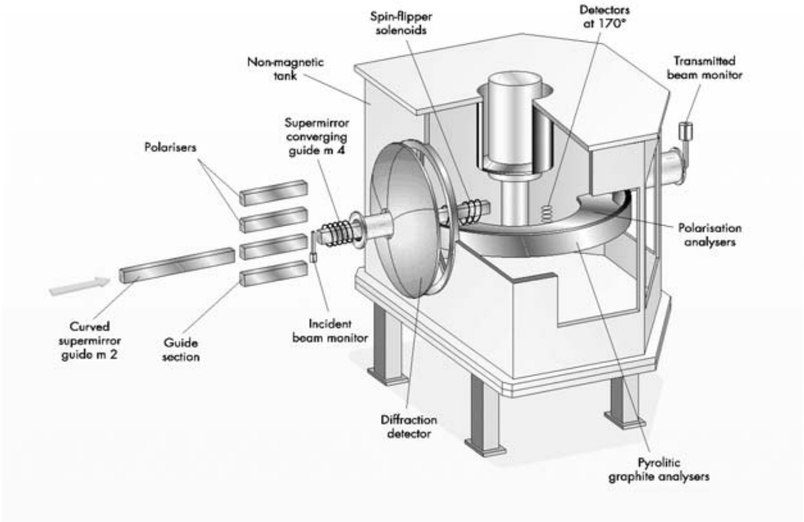

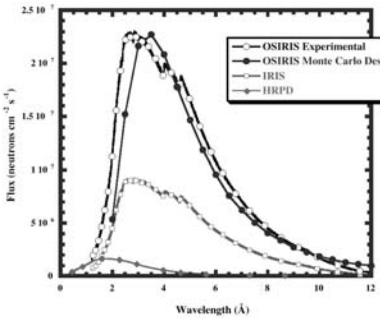

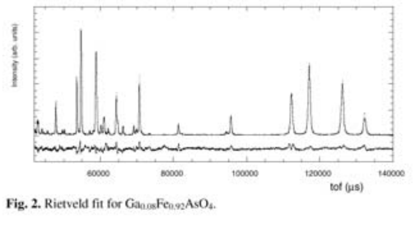

Fig. 2. Rietveld fit for $Ga_{0.08}Fe_{0.92}AsO_4$.

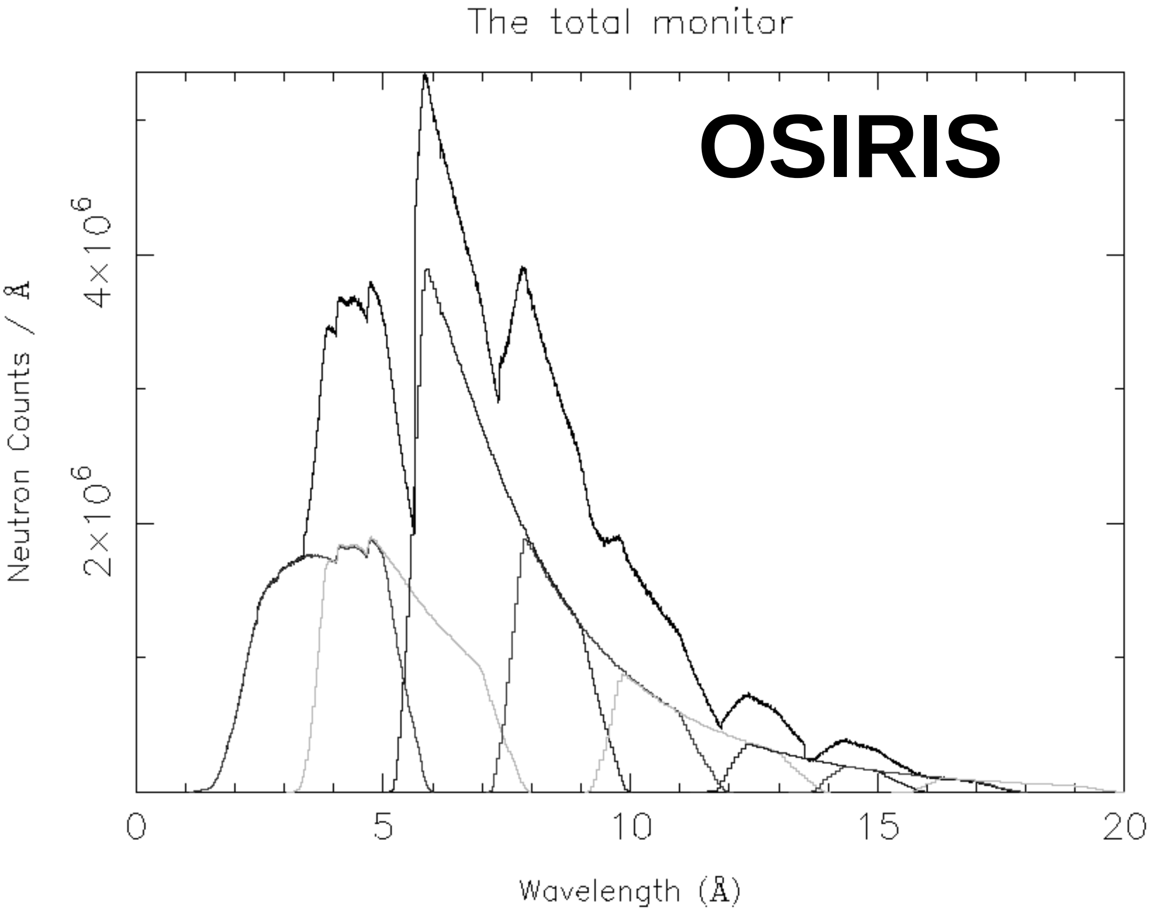

GEM-OSIRIS Comparison

Magnetic Diffraction

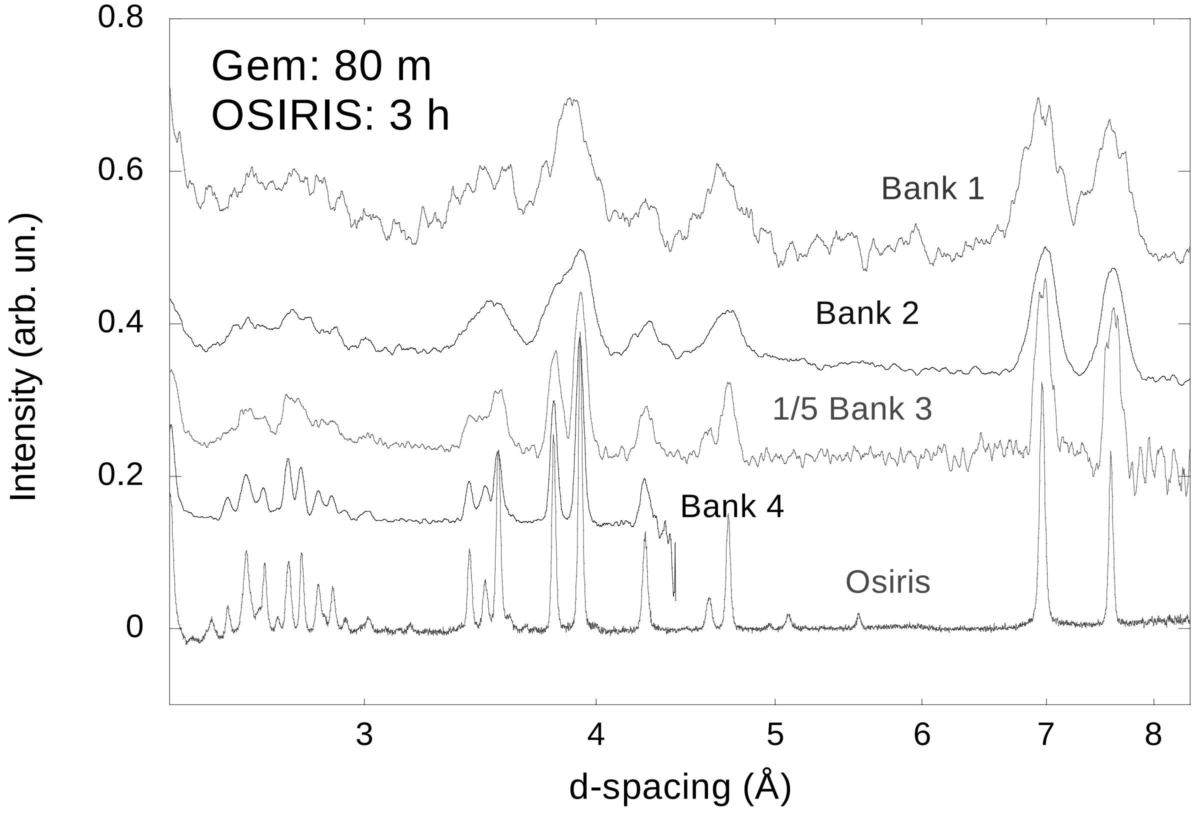

WISH Schematic drawing

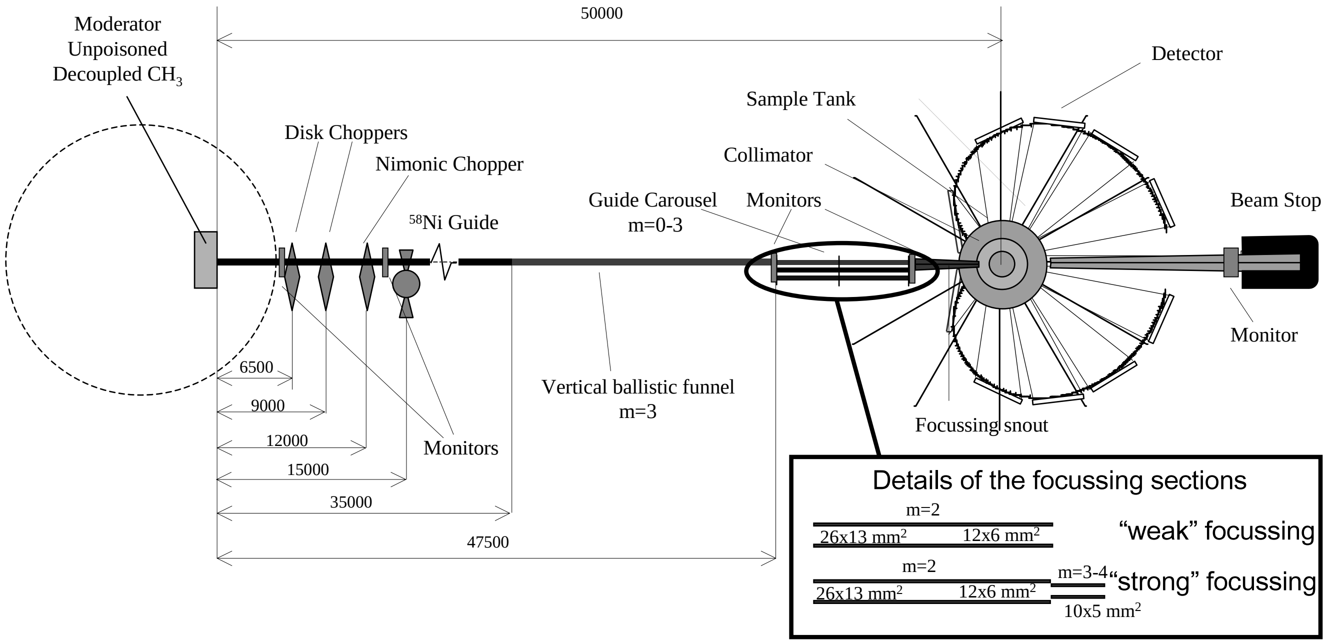

Magnetic peak height WISH @50m vs. GEM @17m

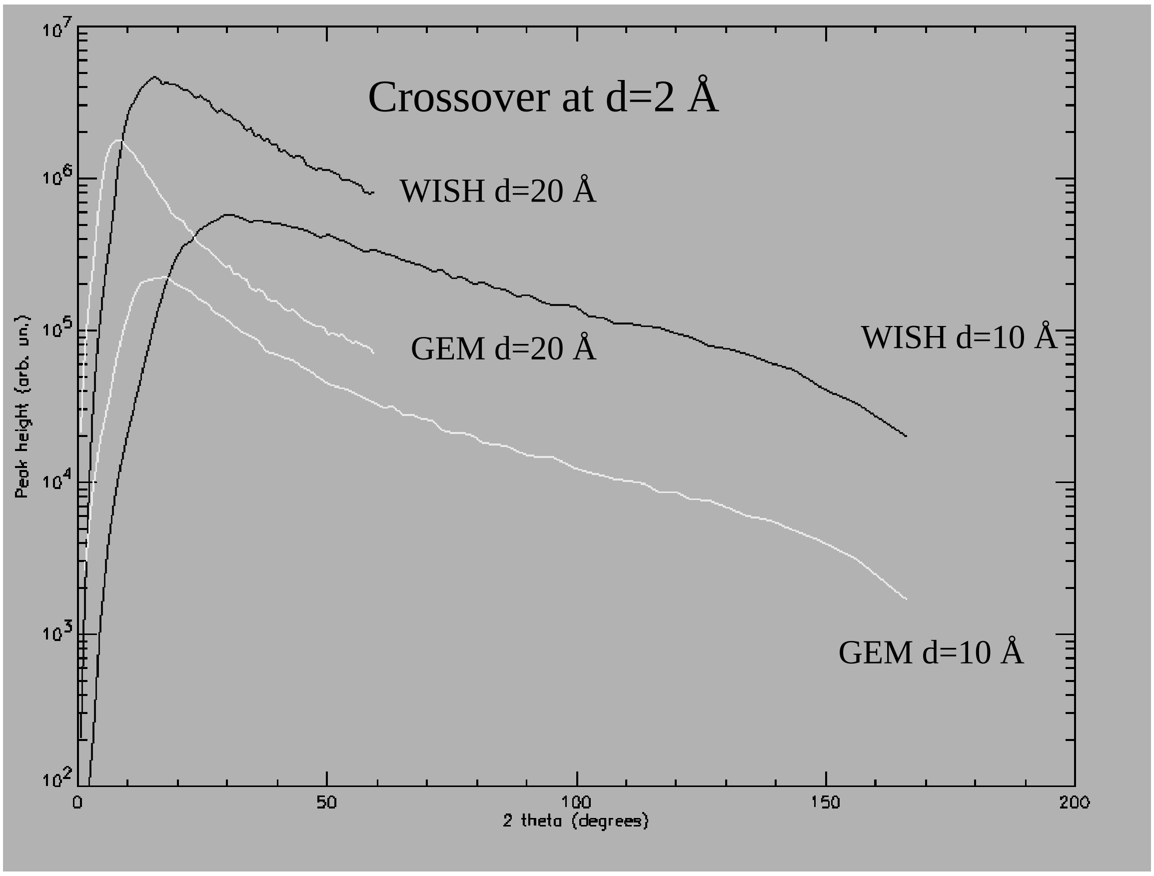

Means to obtain a polarised beam

- Scattering from a magnetic crystal (monochromatic): Cu_2MnAl (Heusler), (Co,Fe)

$$\left(\frac{\mathrm{d}\sigma}{\mathrm{d}\Omega}(\mathbf{k})\right)^{\uparrow} = (\gamma r_e)^2\left\{\left|\mathbf{Q}(\mathbf{k})\right|^2 + \left|F'(\mathbf{k})\right|^2 + 2\hat{\mathbf{s}}_n\cdot\left[\mathbf{Q}(\mathbf{k})F'(\mathbf{k})\right]\right\}$$

  cancels out for spins antiparallel to the magnetic interaction vector and $|\mathbf{Q}(\mathbf{k})|=F'(\mathbf{k})$

- Magnetic multilayers (white beam)

- ^{3}He polarising filters (white beam)

Uses of the neutron polarisation

Technique	**Materials**	**Method**	**Applications**	**Instruments (examples)**
Unpolarised neutrons	Powders and single crystals	Measure total cross section for unpolarised neutrons	Survey. Simple collinear structures	D1B, D20 (CWP) OSIRIS, GEM(TOFP) D10, D15 (CWSX)
Polarised neutrons	Usu. single crystals, typically FM.	Set **M**, measure with **P** parallel or antiparallel to **M**, to obtain "Flipping ratios"	Form factors, spin density distributions.	D3
Uniaxial polarimetry	Powders and single crystals	Set $\mathbf{P}_i$ along any direction and measure the projection of $\mathbf{P}_f$ onto $\mathbf{P}_i$.	Separate magnetic from nuclear scattering. Some non-collinear structures	D7 TAS + polariser + analyser. OSIRIS (future)
Spherical polarimetry.	Single crystals	Set $\mathbf{P}_i$ along any direction and measure the full $\mathbf{P}_f$.	Complex non-collinear AFM strcutures.	TAS + polariser + analyser +Cryopad

D3 (ILL)

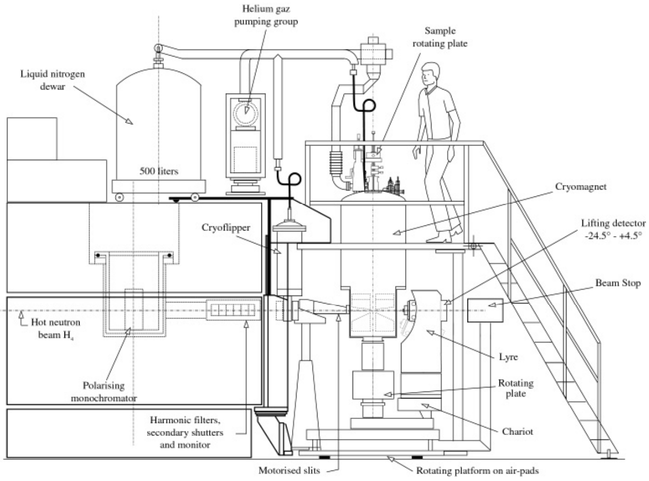

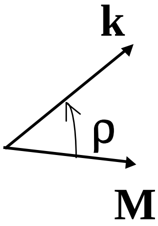

$$\left(\frac{\mathrm{d}\sigma}{\mathrm{d}\Omega}(\mathbf{k})\right)^{\uparrow} = (\gamma r_e)^2\left\{|\mathbf{Q}(\mathbf{k})|^2 + |F'(\mathbf{k})|^2 + 2\hat{\mathbf{s}}_n\cdot[\mathbf{Q}(\mathbf{k})F'(\mathbf{k})]\right\}$$

$$R = \frac{1+2Py\sin^2\rho + y^2\sin^2\rho}{1-2Py\sin^2\rho + y^2\sin^2\rho} \quad ; \; y = (\gamma r_e)M(\mathbf{k})/F(\mathbf{k})$$

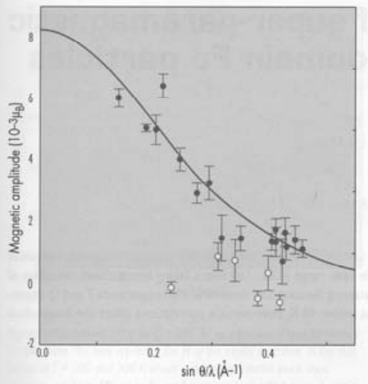

Figure 2: *The magnetic amplitude per V^{3+} ion induced in V_2O_3 by 4.6 T at 180 K. The points denoted by ● are for reflections with ℓ even and those marked ○ are for ℓ odd. The full curve is the V^{3+} 3d form factor normalised*

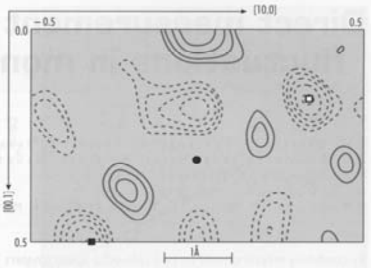

Figure 3: *The section, parallel to (01.0) passing through the origin, of the maximum entropy reconstruction of the difference between the observed magnetisation distribution and that due to spherically symmetric V^{3+} ions. The ● marks the position of the V^{3+} ion, the ■ that of the O^{2-} ion in the plane of the section and the □ that of the O^{2-} which is 0.1 Å below it. The contours are logarithmically spaced with a factor of two between successive levels. The highest contour is at $0.33\cdot10^{-3}\ \mu_B\ \text{Å}^{-3}$.*

Uniaxial Polarisation Analysis

- One-detector setup

	Non spin-flip	Spin-flip
$\vec{P}_i \parallel \mathbf{k}$	$\sigma_c + \frac{1}{3}\sigma_i$	$\frac{2}{3}\sigma_i + \sigma_m$
$\vec{P}_i \perp \mathbf{k}$	$\sigma_c + \frac{1}{3}\sigma_i + \frac{1}{2}\sigma_m$	$\frac{2}{3}\sigma_i + \frac{1}{2}\sigma_m$

σ_c:	Nuclear Coherent
σ_i:	Nuclear spin-incoherent
σ_m:	Magnetic (electrons)

- Multidetector setup

	Non spin-flip	Spin-flip
$\vec{P}_i \parallel \vec{x}$	$\sigma_c + \frac{1}{3}\sigma_i + \frac{1}{2}\sigma_m \sin^2\alpha$	$\frac{2}{3}\sigma_i + \frac{1}{2}\sigma_m(1+\cos^2\alpha)$
$\vec{P}_i \parallel \vec{y}$	$\sigma_c + \frac{1}{3}\sigma_i + \frac{1}{2}\sigma_m \cos^2\alpha$	$\frac{2}{3}\sigma_i + \frac{1}{2}\sigma_m(1+\sin^2\alpha)$
$\vec{P}_i \parallel \vec{z}$	$\sigma_c + \frac{1}{3}\sigma_i + \frac{1}{2}\sigma_m$	$\frac{2}{3}\sigma_i + \frac{1}{2}\sigma_m$

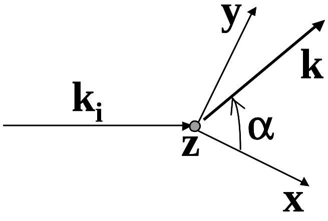

D7 (ILL)

- Diffuse scattering
- Cold neutrons
- Supermirror polarisers
- 32 detectors
- 1-directional polarisation analysis: Separation of coherent and incoherent scattering
- 3-directional polarisation analysis:Separation also of magnetic scattering
- Time-of-flight option

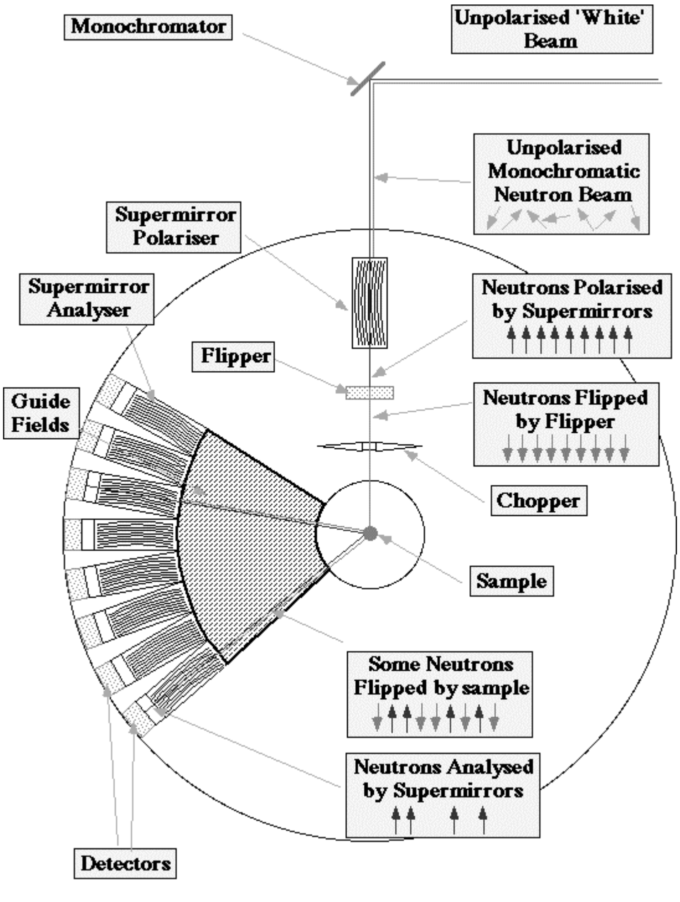

General Layout of D7 for Polarisation Analyses